Impacts of volcanic eruptions on the landscape evolution of Lombok Island, Indonesia

Mukhamad Ngainul Malawani

UNIVERSITÉ PARIS 1
PANTHÉON SORBONNE

ECOLE DOCTORALE DE GEOGRAPHIE DE PARIS (ED 434)

Laboratoire de Géographie Physique - UMR 8591

THÈSE

Doctoral Thesis

Présentée pour obtenir le grade de Docteur en Géographie

Presented to obtain a degree of Doctor in Geography

Mukhamad Ngainul MALAWANI

Impacts des éruptions volcaniques sur l'évolution du paysage de l'île de Lombok, Indonésie

Impacts of volcanic eruptions on the landscape evolution of Lombok Island, Indonesia

Soutenue publiquement le 30 Juin 2023

Defense on 30 June 2023

Franck LAVIGNE	Professeur, Université Paris 1 – Directeur de Thèse
Danang Sri HADMOKO,	Associate Professeur, Universitas Gadjah Mada – Co-directeur
Gilles ARNAUD-FASSETTA	Professeur, Université Paris Cité – Rapporteur
Armelle DECAULNE	Directrice de Recherche, CNRS LETG-Nantes – Rapporteuse
Eric FOUACHE	Professeur, Sorbonne Université – Examinateur
Aline GARNIER	MCF, Université Paris-Est Créteil – Examinatrice
Muh Aris MARFAI	Professeur, Geospatial Information Agency – Examinateur

Impacts des éruptions volcaniques sur l'évolution du paysage de l'île de Lombok, Indonésie

Résumé

En Indonésie, les études qui analysent de manière combinée les impacts physiques et sociétaux des éruptions passées sont encore limitées. Dans cette thèse, nous traîtons de cette thématique, principalement pour évaluer les impacts de l'éruption de 1257 CE et ceux d'une avalanche de débris d'âge Holocène du volcan Samalas à Lombok. Le premier objectif était de reconstruire la morphométrie du dépôt d'avalanche de débris (DAD) Kalibabak et de dater cet événement. Nous concluons que ce DAD se classe parmi les trois premières avalanches de débris volcaniques les plus volumineuses d'Indonésie, et se classe au huitième rang des plus volumineux DAD dans le monde. Sur la base d'une série de 10 nouvelles datations de paléosols, nous suggéronss que le DAD a été mis en place lors de l'éruption subplinienne qui a produit la « Propok pumice » entre 5000 et 2600 BCE. Le deuxième objectif était de reconstruire les impacts géomorphologiques de l'éruption du Samalas de 1257 CE dans la partie occidentale de Lombok. Les changements abrupts dans la partie amont de la zone d'étude ont été causés par des dépôts pyroclastiques (courants de densité pyroclastiques ou PDC) d'un volume total de $110 \pm 3 \times 10^6$ m^3. En revanche, la zone en aval a connu des changements graduels dus aux lahars post-éruptifs et à la sédimentation fluviale ($208 \pm 3 \times 10^6$ m^3). Le dernier objectif de la thèse était d'analyser la réponse des habitants suite à l'éruption de Samalas en 1257 CE. Une exégèse de trois sources indigènes (babad) de Lombok a été réalisée. Le contexte géographique mentionné dans les babad est l'une des caractéristiques uniques des textes, qui ont permis de reconstituer la période de crise jusqu'à la période de relèvement.

Mots clés : avalanche de débris ; géomorphologie volcanique ; éruption de Samalas ; évolution du paysage ; sources écrites ; Indonésie.

Impacts of volcanic eruptions on the landscape evolution of Lombok Island, Indonesia

Abstract

Volcanic eruptions in Indonesia and other parts of the world have had many impacts, both physical and social. However, only limited studies combine the investigation of physical and social impacts in a single eruption, especially for past events. The investigation of these issues is applied to Lombok Island, in this thesis, primarily assessing the impacts of the 1257 CE Samalas eruption and a Holocene debris avalanche. The first objective is to reconstruct the old sector collapse and the morphometry of the resulting debris avalanche deposit (Kalibabak DAD). The results show that Kalibabak DAD ranks among the top three DADs in Indonesia based on its volume (after Raung and Galunggung volcanoes), and ranks eighth among the largest DADs worldwide. This DAD was emplaced during the subplinian eruption that expelled the Propok pumice between 5,000 and 2,600 BCE. The second objective is to reconstruct the geomorphological impact of the 1257 CE Samalas eruption in western part of Lombok. The study area has undergone both abrupt and gradual changes. The abrupt changes in the upstream part were caused by the deposition of $110 \pm 3 \times 10^6$ m^3 of pyroclastic density current (PDC) during the eruption. In contrast, the downstream area experienced gradual changes by post-eruptive lahars and fluvial sedimentation ($208 \pm 3 \times 10^6 m^3$). The last objective is to analyze the inhabitant's response following the eruption of Samalas in 1257 CE. Exegesis of three indigenous written sources (*babad*) form Lombok was conducted. The geographical context mentioned in the *babad* is one of the unique features of the texts from Lombok, which helps reconstruct the emergency-crisis up to the recovery period.

Keywords: debris avalanche; volcanic geomorphology; Samalas volcano; landscape evolution; written sources; Indonesia.

Résumé Substantiel

Contexte de la recherche

L'Indonésie est située sur une plaque tectonique active, influencée par la subduction de la plaque indo-australienne sous la plaque eurasienne et la plaque Pacifique à l'est. Les chaînes volcaniques s'étendent d'ouest en est et s'incurvent vers le nord. Sumatra et Java comptent de nombreux volcans, tandis que d'autres îles, comme Bali, Lombok et Halmahera, ont été formées par un processus à dominante volcanique. Certains volcans ont connu des éruptions importantes (indice d'explosivité volcanique ou VEI>4), tandis que d'autres ont eu des impacts mineurs avec des éruptions fréquentes de plus faible magnitude. Plusieurs volcans considérés comme dormants depuis des siècles se sont soudainement réactivés, comme le Sinabung (Sumatra) en 2010. D'autres ont connu une éruption majeure dans leur histoire éruptive, comme le Merapi (2010), le Krakatau (1883), le Tambora (1815) et le Kelud (1919). Cependant, en 2013, le mystère d'une autre éruption volcanique majeure a été révélé, à savoir l'éruption du Samalas (1257 CE) à Lombok.

Les éruptions volcaniques en Indonésie et dans d'autres parties du monde ont eu de nombreux impacts directs et indirects, à la fois physiques et sociaux. Elles provoquent généralement des effets domino ou aléas en cascade tels que des lahars, des tsunamis et des perturbations climatiques à l'échelle mondiale. Les impacts démographiques et économiques des éruptions peuvent être catastrophiques et provoquer, outre une surmortalité souvent liée à des pertes de récoltes, des migrations massives, un chaos économique, et des perturbations des transports. L'interaction entre l'homme et les volcans en Indonésie a toujours existé, et les volcans sont devenus la source de subsistance de nombreuses générations. Les impacts des éruptions dans le passé ont été pires que lors de ces dernières décennies en raison d'une technologie moins avancée et d'une perception des risques différente de celle de l'ère moderne. Pourtant, des traditions locales ont permis aux générations passées de parfois gérer efficacement les risques volcaniques en évitant des dommages physiques trop importants et en minimisant les dommages sociaux.

L'étude des événements volcaniques passés et de leurs impacts en Indonésie est encore limitée, bien que ce pays dispose d'un grand nombre d'anciens documents écrits. Lombok est une région d'Indonésie qui possède un grand nombre de manuscrits anciens. Cette île a connu l'une des plus grosses éruptions volcaniques de l'Holocène, celle du Samalas en 1257 CE, qui a laissé dans les carottes glaciaires le plus grand pic de sulfate depuis 2500 ans. La plupart des dépôts de l'éruption de Samalas qui ont recouvert Lombok en 1257 CE ont été engendrés par des courants de densité pyroclastiques (*Pyroclastic Density Currents* ou PDC en anglais) provenant de la quatrième phase de l'éruption. Ces dépôts de PDC sont étrangement dispersés dans la partie sud. Une zone de collines d'environ 40 km de long orientée ouest-est dans le centre de l'île a servi de barrière topographique pour la direction des PDCs. Cependant, aucune étude géomorphologique ou géologique n'a été réalisée sur ce dépôt non daté jusqu'à présent.

L'étude de l'impact physique et social d'une éruption passée est appliquée à Lombok dans le cadre de cette thèse, en évaluant principalement les impacts de l'éruption de Samalas en 1257 CE et de l'éruption non datée qui a provoqué l'avalanche de débris. Les objectifs sont de démontrer les conséquences géomorphologiques des éruptions majeures et de reconstruire la mémoire sociale préservée des anciens habitants face aux éruptions volcaniques.

Questions de recherche

- La première série de questions de recherche est la suivante : Quelles sont les caractéristiques des avalanches de débris volcaniques à Lombok ? Quand l'avalanche de débris volcaniques du Lombok s'est-elle produite ? Quel était l'état du paysage avant et après cette avalanche ?

- La deuxième série de questions de recherche est la suivante : quel est l'effet de l'éruption de Samalas en 1257 CE sur le changement de paysage dans la région de Mataram ? Quelles étaient les conditions paléo-topographiques à Mataram avant l'éruption du Samalas ? Comment les processus de transformation se sont-ils déroulés ?

- La troisième série de questions de recherche est la suivante : Les caractéristiques des anciennes civilisations de Lombok peuvent-elles être retracées par des sources écrites ? Comment ont-elles réagi aux éruptions volcaniques ? Comment ont-elles reconstruit leurs civilisations après avoir été détruites par des éruptions volcaniques ?

Objectifs

Cette thèse en cotutelle (Université Paris 1 - Panthéon Sorbonne et Universitas Gadjah Mada) est cofinancée par le Ministère de l'éducation, de la culture et de la technologie de la République d'Indonésie et plusieurs programmes bilatéraux de recherche entre la France et l'Indonésie (PICS du CNRS, projet IUF, Science et Impact). Commencée en octobre 2019, elle s'inscrit dans la continuité des études sur le volcan Samalas de la dernière décennie. Cette thèse vise à démontrer l'utilité de l'approche géomorphologique pour étudier l'évolution du paysage causée par les éruptions volcaniques et évaluer le contexte géographique des sources écrites relatives au volcanisme passé à Lombok. Cette thèse a trois objectifs principaux :

a) etudier l'effondrement de flanc du volcan Samalas qui est responsable du dépôt d'avalanche de débris de grande ampleur qui a transformé la morphologie d'un quart de l'île de Lombok ;
b) reconstituer l'évolution du paysage de la partie ouest de l'île suite à l'éruption du Samalas en 1257 CE ;
c) analyser les impacts sociétaux, la réponse d'urgence, le relèvement post-catastrophe et les stratégies de résilience des habitants de Lombok suite à l'éruption de 1257 CE du Samalas.

Cadre géographique de Lombok

Lombok est située au sud-est de l'archipel indonésien, à l'est de l'île de Bali. Ses parties est et ouest sont limitées par deux détroits, celui d'Alas et de Lombok, tandis que la partie sud est limitée par l'océan Indien. Selon la dernière enquête du Bureau régional des statistiques, Lombok est entourée de 196 petites îles et îlots. Lombok est rattachée à

la province de Nusa Tenggara Barat (NTB), dont la capitale est la ville de Mataram, située dans la partie occidentale de l'île. Lombok présente un complexe volcanique qui est actuellement inscrit dans la liste des géoparcs mondiaux de l'UNESCO : le géoparc Rinjaniqui occupe principalement le nord de l'île. Ce géoparc se caractérise par la caldera de l'ancien Samalas, le nouveau cône actif (appelé Barujari) dans le lac Segara Anak et le sommet du volcan Rinjani, qui culmine à 3726 m.

Lombok est incluse dans les Petites îles de la Sonde, un archipel formé à partir du Miocène, qui est constitué de Lombok, Bali, Sumbawa, Flores, Timor, Alor, Wetar et d'autres petites îles. L'émergence d'arcs volcaniques sur Lombok n'est pas seulement influencée par un seul facteur, à savoir la subduction de la plaque indo-australienne sur la tranchée de Java (~350 km en direction du sud de l'île), mais aussi par la subduction moins importante de la croûte océanique de Flores dans la partie nord. Par conséquent, les arcs volcaniques Sunda et Banda sont responsables de plusieurs éruptions volcaniques majeures depuis l'Holocène. Dans cette zone se trouvent trois volcans qui ont connu un indice d'explosivité volcanique (VEI) 7 : le Batur à Bali (34,6 ka), le Samalas à Lombok (1257 CE) et le Tambora à Sumbawa (1815 CE).

La formation des volcans de Lombok a été précédée par une intrusion dacitique et basaltique. La région s'est élevée au-dessus du niveau de la mer pour la première fois au cours du Miocène supérieur. Les processus d'intrusion ont ensuite cessé et le premier volcan a commencé à s'élever dans la zone nord, entraînant la formation séquentielle de laves tertiaires et la formation de laves tertiaires secondaires. Au cours du Pléistocène, une intrusion magmatique quaternaire a été initiée. L'intrusion magmatique récente a conduit à la formation de la lave du deuxième Quaternaire à travers les nouvelles cheminées magmatiques de Samalas et Rinjani, et les anciens cratères (Sembalun, G. Pusuk, G. Nangi) se sont manifestés dans la zone géothermique.

Au pré-Holocène, trois chambres magmatiques alimentaient le Samalas, le Rinjani et le Propok. L'évolution s'est poursuivie jusqu'au processus de fusion des magmas, qui a abouti à une seule grande chambre magmatique alimentant uniquement le Samalas. Ce processus de fusion a duré au moins 2000 ans. Cette chambre magmatique est le principal réservoir qui a alimenté l'éruption plinienne du Samalas en 1257 CE. La

caldeira de Rinjani (Segara Anak) s'est formée lors de cette éruption. Dans le passé, deux montagnes existaient dans cette région, mais après l'éruption, cet endroit a souvent été appelé le complexe de Rinjani, qui comprend une caldeira, le lac Segara Anak, le volcan Barujari et le sommet de Rinjani. Aujourd'hui, la chambre magmatique est relativement petite et profonde. La chambre magmatique ne soutient que le cône Barujari, tandis que deux autres petits cônes sont inactifs : Anak Barujari et Rombongan.

Lombok se compose de diverses formations rocheuses comme des dépôts superficiels, des sédiments, des roches volcaniques et intrusives. Les formations rocheuses les plus anciennes, déposées à l'Oligocène, sont les formations de Kawangan et de Pengulung. Ces formations rocheuses occupaient la zone montagneuse de la partie sud de Lombok. Plusieurs dépôts ont été déposés pendant l'Holocène, notamment des roches volcaniques indifférenciées provenant de Rinjani et des Alluvions. Plus anciennes que ces deux formations, des formations rocheuses d'âge similaire se sont déposées au milieu de Lombok, à savoir les formations de Kalibabak et de Kalipalung. La formation la plus récente, la formation de Lekopilo, est supposée avoir été formée par le dépôt des PDCs de l'éruption de Samalas en 1257 CE.

Cadre de recherche

L'impact d'une éruption volcanique est prévisible à l'aide de l'échelle VEI. Plus l'échelle VEI est élevée, plus l'éruption est susceptible de provoquer des perturbations, en passant de l'échelle locale à l'échelle mondiale. Les impacts locaux des éruptions volcaniques sont plus complexes que les impacts globaux car ils impliquent des aspects géomorphologiques. À l'échelle mondiale, même les communautés mondiales peuvent être touchées par des volcans provenant de régions éloignées du monde, mais la fréquence d'occurrence est faible. Les impacts locaux sur la morphologie et les systèmes de drainage sont liés à des impacts physiques qui peuvent entraîner des changements dans le paysage (topographie). Les approches de modélisation de l'évolution du paysage sont diverses. Les conséquences environnementales et sociales des impacts localisés, ainsi que les impacts globaux, influencent les réponses de l'homme aux éruptions.

Dépôt de débris d'avalanche (DAD) à Lombok

Les avalanches de débris modifient la forme du volcan, laissant généralement une forme de fer à cheval dans un édifice volcanique et des changements morphologiques soudains dans les parties médianes et distales, par exemple une aggradation massive du terrain et la formation de petites collines. Ce processus est l'un des facteurs importants susceptibles de modifier rapidement le paysage. En Indonésie, les études sur la DAD sont limitées. Certaines études, comme celle du volcan Raung, ont identifié les caractéristiques géomorphologiques de la DAD. La litho-stratigraphie et l'analyse de l'âge ont également été réalisées sur l'avalanche de débris du volcan Galunggung. Cependant, la modélisation des processus de déclenchement des avalanches de débris manque en Indonésie. Diverses mesures et caractéristiques morphologiques sont largement appliquées pour caractériser les DAD, comme le nombre de hummock (collines), la distance de déplacement, la superficie, la pente, la hauteur et la direction. La description stratigraphique de la DAD ne s'étant jamais faite à Lombok, cette analyse pourrait être la première à être réalisée. L'analyse stratigraphique est également cruciale pour la caractérisation de la DAD. L'âge des formations rocheuses dans la zone DAD n'a pas encore été étudié, sauf l'âge indiqué par la carte géologique, à savoir le Pléistocène. Un autre paramètre important qui doit être révélé est le facteur de déclenchement de l'avalanche de débris, qu'il soit lié à l'éruption ou non.

Évolution du paysage de la plaine de Mataram

Les recherches sur les changements de paysage à grande échelle sont rarement menées en Indonésie, mais uniquement dans une zone limitée, par exemple les changements de la morphologie des rivières et les changements de la morphologie des dômes volcaniques. À Lombok, l'éruption du Samalas en 1257 CE a entraîné des modifications du paysage sur la quasi-totalité de l'île. Le déversement massif de coulées pyroclastiques est responsable de nombreux paysages enfouis. Le paysage enfoui est également présent dans plusieurs régions, qu'il soit directement ou indirectement lié aux éruptions volcaniques. Par exemple, en Pologne, la ville de Cracovie a connu des changements topographiques au cours du dernier millénaire, avec une augmentation moyenne de 2 à 6 mètres en raison des dépôts fluviaux et anthropogéniques. Les dépôts

anthropogéniques ont également enfoui le paysage préromain d'Achen, en Allemagne, d'environ 3 mètres. Ces exemples de recherche impliquent principalement deux paramètres, à savoir le paysage actuel et le paysage ancien/enfoui. Entre ces deux paramètres, il en existe un autre essentiel pour décrire les changements topographiques : le delta-haut de la topographie. Ce paramètre permet de reconstituer le degré de sédimentation et d'estimer le volume des dépôts entre deux périodes différentes (ancienne et actuelle). Une autre ville connue à la topographie enfouie est Pompéi, en Italie, qui a été affectée par des coulées pyroclastiques au cours de l'éruption du Vésuve en 79 CE. Cette région présente des processus de sédimentation similaires à ceux de Lombok. Les processus de dépôt et les caractéristiques morphologiques de Pompéi sont similaires aux caractéristiques de la région de Mataram.

Impacts sociaux et réponse des populations face à l'éruption du Samalas en 1257 CE

Les conséquences des éruptions volcaniques sur la société et l'environnement constituent un type d'impact local supplémentaire. Dans le cas de l'éruption du Samalas, l'impact local associé aux conditions sociétales et environnementales n'a pas encore été entièrement identifié. Les impacts sociaux et environnementaux de plusieurs éruptions historiques en Indonésie sont partiellement révélés par des sources historiques, par exemple les éruptions du Tambora, du Krakatoa, du Merapi et du Kelud. Dans d'autres parties du monde, comme en Europe, où la culture de l'écrit est très développée, les sources écrites sont largement utilisées pour étudier ce sujet, par exemple à l'Etna, à Eldgjá et à Pompéi. L'évaluation de la vulnérabilité des civilisations anciennes peut également être réalisée à l'aide de sources écrites. Ces études ont conclu que la culture de la civilisation déterminait la réponse développée par la communauté (connaissances, sagesse locale et expérience), ainsi que les phases d'urgence, de rétablissement et de résilience. En utilisant une approche similaire aux recherches précédentes, les impacts sociaux et environnementaux à Lombok seront révélés à travers les sources écrites indigènes de Lombok, par exemple *Babad Lombok, Suwung* et *Sembalun*. Les sources de Lombok présentent une valeur spécifique, à savoir les caractéristiques géographiques et notamment les toponymes.

Méthodologie

La zone d'intérêt de cette étude est divisée en trois zones en fonction des objectifs. Le premier objectif est focalisé sur la zone occupée par les dépôts d'avalanches de débris. Ces dépôts couvrent environ 500 km^2 dans la partie centrale de l'île de Lombok. Cette zone est administrativement incluse dans les préfectures de Lombok central et Lombok oriental. Le deuxième objectif est focalisé sur la zone située entre la plaine de Mataram et le volcan Rinjani. Dans la littérature scientifique, cette zone est considérée comme totalement occupée par les dépôts de PDC de l'éruption de Samalas de 1257 CE. Pour étudier le troisième objectif lié à la réaction des habitants à la suite de l'éruption, la zone concernée est l'ensemble de l'île de Lombok. Il est possible que certains d'entre eux aient migré vers l'île voisine de Sumbawa.

Analyse du dépôt de débris d'avalanche (DAD)

L'analyse de la structure du DAD a été réalisée grâce à des données stratigraphiques issues de carottages profonds réalisés dans le passéQuelques coupes dans des carrières ont permis de distinguer les différents faciès du DAD. Des données géoélectriques (résistivité) ont complété les profils stratigraphiques afin de décrire plus en détail la structure du DAD et d'évaluer l'épaisseur de ce dernier. Cette étude a également permis de caler l'âge du DAD par la méthode du radiocarbone (C14), en datant des paléosols ou des sédiments situés au-dessus et à la base du DAD. La modélisation de l'écoulement de cette avalanche de débris fut un défi, car toute trace de la cicatrice d'arrachement initiale (caldera d'avalanche) a totalement disparu lors de l'effondrement total du volcan pendant son éruption de 1257 CE. Afin de pallier cette lacune, nous avons reconstitué la morphologie initiale supposée du cône du Samalas à l'aide du programme ShapeVolc, développé par P. Lahitte (Université Paris-Sud). Cette reconstitution paléotopographique a permis demodéliser la dynamique d'écoulement de l'avalanche de débris, à l'aide du programme VolcFlow, développé par K. Kelfoun (Université de Clermont-Auvergne).

Analyse de l'évolution du paysage dans la plaine de Mataram

L'analyse de l'évolution du paysage par la reconstruction paléotopographique à Lombok a été réalisée à l'aide de la méthode dite descendante. Cette méthode nécessite deux principaux types de données, à savoir la topographie et la stratigraphie, afin de pouvoir calculer la position de la paléosurface ou le delta-h (Δh), qui représente la variation d'altitude au cours du temps. Ces données sont mesurées sur chaque point stratigraphique. Chaque point de Δh est ensuite interpolé pour générer le delta-DEM (*Digital Elevation Model*/Modèle Numérique de Terrain). Le modèle paléo-topographique est obtenu par soustraction des deux DEM, c'est-à-dire que le DEM actuel est soustrait du delta-DEM pour produire le paléo-DEM (PDEM). Le résultat du PDEM est ensuite validé à l'aide de l'erreur quadratique moyenne (RMSE). L'étape suivante consiste à construire la paléo-rivière à l'aide du modèle d'accumulation de flux dans ArcMap. Le PDEM est également utile pour la modélisation de l'ancien trait de côte, qui a été déterminé en reclassant le PDEM : la valeur < 0 mètre est classée comme zone marine.

Analyse des impacts sociaux de l'éruption du Samalas en 1257 CE

L'analyses de trois sources écrites de Lombok, appelées *babad* (*Babad Lombok, Babad Sembalun,* et *Babad Suwung*) a fourni de nouvelles informations sur les trois phases de l'éruption de 1257 CE (pré-éruptive, syn-éruptive et post-éruptive). L'approche géographique a été utilisée pour aider à l'interprétation des manuscrits du *babad*, comme la spatialisation des toponymes. La vérification par des experts en chroniques (philologues) et des linguistes a été bénéfique pour s'assurer que les traductions sont correctement orthographiées et éviter les erreurs d'interprétation. Ils ont également aidé à trouver la signification des toponymes, à analyser la possibilité de transformation d'un nom et sa localisation sur la carte actuelle.

En résumé, trois types de données furent essentiels dans cette recherche, les données géospatiales (par exemple, DEM, imagerie, cartes), les données de terrain (par exemple, échantillonage, résistivité électrique) et les données d'archives sédimentaires et historiques. La combinaison des perspectives géographiques (par exemple, l'espace, le temps, les environnements) et des perspectives historiques est un élément important dans l'analyse des données dans cette recherche.

Résultats

L'avalanche de débris Kalibabak, un produit du volcan Samalas

En Indonésie, un grand DAD non daté couvre un large secteur (>500 km^2) de l'île de Lombok. Malgré son étendue, les recherches étaient limitées et les études préliminaires n'ont fourni d'analyse détaillée, ni de sa morphologie, ni de sa lithologie, ni des mécanismes d'écoulement qui l'ont produit. Il a été démontré que c'est ce dépôt qui a contrôlé le courant de densité pyroclastique de 1257 CE, et ainsi joué un rôle essentiel dans l'évolution géomorphologique de l'île.

À Lombok, la carte géologique de l'Indonésie (1:100 000) indique un vaste dépôt volcanoclastique appelé formation de Kalibabak, qui se caractérise par des roches brèches volcaniques. Cette formation est située dans la partie sud du complexe volcanique Samalas-Rinjani. Ce dépôt présente des fragments de roches de forme angulaire, principalement composés de matériaux andésitiques, comme l'andésite porphyrique ou l'andésite basaltique et de basalte. Les observations d'affleurements le long des berges de la rivière et sur les bords de route montrent que la formation de Kalibabak est composée de fragments lithiques hétérogènes, dominés par des graviers et des petits blocs (5-50 cm) mais contenant aussi des blocs plus gros (jusqu'à 2,5 m). La granulométrie de 34 échantillons de matrices de brèches de la formation de Kalibabak montre que le dépôt est mal trié, avec une matrice de graviers sableux (71 %). La proportion d'argile est très faible (<5%), ce qui suggère que la quantité d'eau a été limitée au cours du processus de déposition. Les caractéristiques morphométriques de la formation de Kalibabak, sa structure de surface et de subsurface, indiquent clairement qu'il s'agit d'un DADoriginaire du volcan Samalas.

La caractérisation de ce DAD commence par l'identification de la morphométrie des hummocks. Sur les 1704 hummocks identifiés, ceux de forme globalement circulaire dominent la zone d'étude, avec un total de 771. Les hummocks allongés, qui indiquent la direction du transport de débris, constituent 16% du total (265 hummocks). La majorité de hummocks est répartie à environ 30-31 km du rebord sud de la caldera actuelle. Les

plus grands, d'une superficie >8 ha, sont répartis sur une distance de 22-23 km, tandis que ceux de taille moyenne (2 ha) sont répartis sur l'ensemble du DAD. Le hummock le plus éloigné, situé sur la plage de Kwang Wai, se trouve à 39,5 km de ce rebord, tandis que le plus proche est à 18,6 km. . Vingt-neuf kilomètres au sud du bord de la caldeira, on peut observer des structures DAD presque homogènes, avec de la lave en feuillets et des fissures en puzzle (*jigsaw cracks*) typiques des DADs. Un autre hummock situé à 28 km au sud du bord de la caldeira contient plus de 75 % de matrice sableuse. Les données de 10 carottes indiquent une épaisseur du dépôt variant de 12 m à 58 m. La corrélation entre les carottes dans la direction NS montre que l'épaisseur du DAD diminue significativement au fur et à mesure que l'on s'éloigne de la caldera, alors que dans la direction WE, l'épaisseur de la DAD augmente au centre et diminue près des marges.

Notre reconstruction morphologique à l'aide de ShapeVolc montre que le sommet pré-avalanche était situé à environ 3,6 km du sommet actuel du Rinjani et à proximité du nouveau cône actif appelé Barujari (~500 m). Le sommet reconstruit a une inclinaison moyenne de 35%. La meilleure estimation à l'aide de ShapeVolc indique que l'ancien Samalas (avant l'avalanche de débris) avait une hauteur maximale d'environ 4200 m, soit ~480 m de plus que le Rinjani actuel. Les profils topographiques pré-avalanche et actuel se croisent à environ 8 km de l'ancien sommet simulé. Nous en avons déduit que la longueur possible de la caldera d'avalanche de débris était de 7-8 km en horizontal et d'une profondeur maximale d'environ 1,5 km. La longueur (LD) du DAD est inférieure à sa largeur (WD), ce qui lui donne une forme en éventail. L'épaisseur moyenne du DAD est d'environ 28,5 m. En appliquant une formule géométrique classique, le volume du DAD est estimé à 15,3 km^3, à un rsultat très proche de celui acquis par la méthode de soustraction du MNT, qui donne 14,9 km^3. La moyenne de ces deux résultats donne 15,1 km^3. Comparé aux Philippines, Nouvelle-Zélande, Mélanésie et aux régions Kuriles-Kamachatka, le DAD de Kalibabak est significativement plus grand que tous les DAD de ces régions. Plusieurs DAD holocènes dans le monde sont comparables en volume à celui produit par Samalas, par exemple, Meru, Tanzanie (10-20 km^3), Feugo, Guatemala (15 km^3), et Antuco, Chili (15 km^3). Sur la base de cet inventaire, la DAD de Kalibabak du volcan Samalas pourrait se classer au huitième rang des plus grandes (>5 km^3) DAD de l'Holocène dans le monde.

L’analyse morphométrique montre que la « tête » du DAD en amont se trouve à une altitude de 685 m, tandis que le front a atteint une altitude de 114 m, soit un dénivelé (HD) de 581 m. En comparant les valeurs HD et LD, nous avons une pente moyenne de 2 %. La longueur (L) de l'avalanche de débris de la source au front est de 39,3 km, avec une hauteur de chute maximale de 4 km. La comparaison de ces deux mesures donne une valeur H/L de 0,1 pour l'avalanche de débris de Lombok.

L'avalanche de débris a ensuite été simulée à l'aide de VolcFlow. Nous avons effectué quatre simulations pour évaluer la propagation de cet écoulement. La première simulation a utilisé un volume d’environ 15 km^3 avec une limite d'élasticité standard qui est généralement appliquée pour simuler la propagation du DAD (50 kPa) pour déterminer la propagation de l'avalanche et la zone de couverture pour un matériau dense. Les résultats montrent que la surface recouverte par le dépôt simulé est bien inférieure à celle du dépôt réel. La deuxième simulation a été réalisée avec le même volume et une limite d'élasticité modérée (20 kPa). Le résultat de cette simulation présente un dépôt plus étendu et plus large, mais ne couvre pas encore la partie la plus distale du dépôt identifié sur le terrain. La troisième simulation a utilisé une valeur encore plus faible de la limite d'élasticité (7 kPa), suggérant que le matériau est moins compacté que lors des simulations précédentes. Le résultat de la troisième simulation est le plus similaire au DAD en termes de forme et de couverture. La dernière simulation a utilisé la limite d'élasticité standard de 50 kPa mais a utilisé un volume double du volume calculé (soit ~30 km^3), en simulant un effondrement de flanc initial plus volumineux. Le résultat montre que la propagation finale du DAD atteint la limite extérieure du DAD original, bien que la forme finale ne soit pas identique.

La contrainte d'âge maximale du DAD de Kalibabak est déterminée sur la base du matériel daté en dessous de cette formation. Les résultats sont plus diversifiés, avec des variations d'environ 10 000 ans. Sur la plage de Kwangwai, en bordure externe du DAD, deux matériaux situés sous un hummock côtier ont donné un âge calibré de 7 000 à 7 600 ans BCE. Le paléosol pris en sandwich entre le DAD et le matériel éruptif de 1257 présente des âges entre 2 600 et 470 CE. D'après nos datations, l'âge de la DAD de Kalibabak se situe donc dans une fourchette comprise entre 7 000 et 2 600 BCE. Il y a de

très forte chances qu'elle ait été engendrée par l'éruption subplinienne voire plinienne du Samalas qui déposa l'unité stratigraphique connue sous le nom de Propok pumice, préalablement datée entre 5000 et 800 BCE. Par conséquent, le DAD de Kalibabak a dû être mis en place entre 5000 BCE (âge maximum de l'éruption) et 2600 BCE (âge le plus jeune des paléosols recouvrant le DAD).

Évolution de la Plaine de Mataram suite à l'éruption du Samalas en 1257 CE

Cette étude vise à reconstruire les processus de sédimentation qui ont suivi l'éruption du Samalas en 1257 CE à Mataram et dans les environs (en direction du sud-ouest de la caldera actuelle). La présente étude fournit une reconstruction de la paléo-topographie et de la paléo-hydrographie dans la partie occidentale de Lombok, qui est le siège de la capitale de la province de Nusa Tenggara Barat. La chronologie de l'évolution du paysage et les processus géomorphologiques qui l'accompagnent sont donc d'un grand intérêt.

La plaine de Mataram est dominée par une morphologie plate qui est principalement occupée par des dépôts de PDC et de lahar selon les études précédentes. La morphologie de cette zone provoque la convergence de nombreux cours d'eau vers le sud-ouest à partir de la caldera actuelle. La plaine de Mataram est canalisée par trois cours d'eau principaux, la Meninting, la Jangkok et la Babak. Le DAD du centre de Lombok a également joué le rôle de barrière topographique, déviant les PDC vers le sud-ouest. Des études antérieures réalisées sur la base de mesures sismiques dans la région de Mataram ont montré que les dépôts pyroclastiques remplissaient plusieurs anciens bassins avec des épaisseurs différentes,. Selon la carte géologique de l'Indonésie, les matériaux de surface de la plaine de Mataram sont composés d'alluvions Holocène, avec des dépôts fluvio-marins le long de la zone côtière.

Le modèle stratigraphique de la plaine de Mataram n'a pas encore été étudié en détail. Dans cette étude, nous analysons les caractéristiques stratigraphiques de la plaine de Mataram afin de connaître les modèles de sédimentation pendant et après l'éruption du Salamas en 1257 CE. Sur la base des données collectées pour cette étude, la stratigraphie

de la plaine de Mataram peut être divisée en quatre grands ensembles : pré-éruption et paléosol, dépôt d'éruption, dépôt post-éruption, et sol récent. Comme les données stratigraphiques, l'état de la subsurface à partir des mesures de résistivité montre que la zone d'étude peut être divisée en deux niveaux : sables-ponces (matériel sec : >300 Ωm/humide : 30-300 Ωm) et d'autres matériaux plus fins tels que argiles et limons (<30 Ωm). Cette division est utile pour interpréter la limite de la strate ponceuse comme limite de la paléo-surface avant l'éruption de Samalas en 1257 CE. Sur tous les profils de résistivité, le niveau ponceux est latéralement continue près de la surface, présentant une limite distincte avec le matériau sous-jacent à diverses profondeurs, avec un maximum de 50 m.

Dans le site de forage de Sesela, les coraux sont présents à 11 m de profondeur et sont mélangés avec des fragments de ponce remaniés. De même, des fragments de coraux du site de forage de Karangpule ont été identifiés entre 8 et 12 m de profondeur. L'un d'entre eux, à une profondeur de 11 m dans cette stratigraphie, a été daté de 1646-1832 CE. Les dépôts ponceux qui ont enseveli les coraux sont mélangés à du sable, ce qui indique des matériaux post-Samalas remaniés. La ponce syn-éruptive peut également avoir atteint la mer mais ne peut pas ensevelir les coraux avec une aussi grosse épaisseur parce qu'elle peut être enlevée par les courants marins et flotter au lieu de couler et de recouvrir les coraux. Cette zone a été progressivement ensevelie par les matériaux remaniés ou les dépôts post-éruptifs pendant au moins trois siècles après l'éruption.

La reconstruction paléo-topographique de la zone d'étude a été réalisée par soustraction de MNT. L'ensemble de la zone d'étude a subi une aggradation depuis l'état antérieur à l'éruption jusqu'à l'état actuel. Cependant, les processus d'aggradation peuvent également avoir eu lieu dans la zone du complexe volcanique plus ancien dans le nord de la zone d'étude, en raison du dépôt des retombées (ponce). L'accumulation de sédiments est concentrée dans les zones de basse altitude (<15 m), qui sont également sujettes à des changements topographiques majeurs. L'épaisseur moyenne des sédiments enfouis dans la zone d'étude après l'éruption du Samalas est de 4,6 m, alors que le dépôt post-éruptif le plus épais mesuré dans les données stratigraphiques est de 14 m.

La comparaison entre les rivières anciennes et actuelles permet de détecter les changements hydrographiques dans la zone d'étude. La Meninting, au nord, a connu un changement important dans son tracé. Précédemment, ce cours d'eau avait un chenal rectiligne (rapport de sinuosité (SR) : 1,01). Après l'éruption du Samalas, le degré de sinuosité de cette rivière a augmenté (SR : 1,5), et l'embouchure de ce petit fleuve s'est déplacée vers le sud, en formantun petit delta. Ce dernier s'est progressivement agrandi et transformé en une vaste forme de dépôt fluvio-marin.

Dans la zone de basse altitude, le fleuve Jangkok a également enregistré des changements significatifs. Il avait auparavant un SR de 1,01, mais il est maintenant monté à 1,2. Son embouchure s'est quant à elle déplacée vers le nord, et son affluent a disparu. Notre reconstruction a également révélé que le trait de côte au moment de l'éruption de 1257 CE se situait en moyenne à 1,6 km) à l'intérieur des terres vers l'est, soit un taux de sédimentation moyen de 2,3 m/an.

Nous avons également calculé le volume de dépôt qui a enseveli la paléo-topographie de la plaine de Mataram à la suite de l'éruption du Samalas. Le volume total préservé dans la zone d'étude est de 318 x 10^6 m^3, composé de deux types : PDC qui change soudainement la topographie (110 $\pm$ 3 x 10^6 m^3), et dépôts fluvio-lacustres qui se sont déposés progressivement (208 $\pm$ 3 x 10^6 m^3). Ce volume total ne représente que la moitié du volume total préservé dans la direction SE. Cette différence s'explique par le fait que l'épaisseur moyenne des dépôts dans la direction SE est de 7,8 m avec une épaisseur maximale de 30 m, alors que dans la zone d'étude ces valeurs sont de 4,6 m et 14 m respectivement.

Les modèles de sédimentation dans la partie occidentale de Lombok après l'éruption de Samalas en 1257 CE ont été reconstitués efficacement grâce à l'analyse de la paléo-topographie et de la paléo-hydrographie, en utilisant diverses sources de données stratigraphiques et des mesures géophysiques. Le résultat du modèle paléo-topographique est considéré correct avec une erreur relativement faible. Depuis l'éruption du Samalas en 1257 CE, la zone d'étude a subi des changements parfois abrupts et parfois progressifs. Les changements abrupts causés par le dépôt de PDC se sont produits en amont de la zone d'étude, tandis que la zone en aval a connu des changements graduels par dépôt de lahars

post-éruptifs et sédimentation fluviale. L'évolution du paysage dans la zone d'étude s'est déroulée en trois étapes. La première étape correspond à la période précédant l'éruption, lorsque la zone côtière de la plaine de Mataram était constituée de baies et de caps qui étaient localement occupés par des récifs coralliens. La deuxième étape est celle de l'éruption, lorsque le PDC recouvrait partiellement la zone d'étude. Au cours de la dernière étape, la sédimentation s'est faite progressivement par des lahars et des processus fluviaux. En plus de modifier les limites estimées du dépôt du PDC par rapport aux suggestions précédentes, les résultats de notre modélisation seront utiles pour poursuivre les recherches sur l'hypothèse d'une ancienne cité perdue qui aurait été ensevelie par les dépôts pyroclastiques de l'éruption de Samalas en 1257 CE.

L'éruption cataclysmique du volcan Samalas en 1257 CE révélée par les sources écrites indigènes

L'impact local de l'éruption de Samalas est illustré dans trois *babad* originaires de Lombok (*Babad Lombok, Babad Sembalun* et *Babad Suwung*). Le *Babad Lombok* et le *Babad Sembalun* sont écrits en vieux javanais, tandis que le Babad Suwung est écrit en langue Sasak. Ces deux langues sont couramment utilisées dans la littérature des communautés de Lombok. Le *Babad Lombok* est le document historique de Lombok le plus connu du grand public, et il est utilisé comme référence principale dans les études locales sur l'histoire de Lombok. En revanche, le contenu du *Babad Suwung* est pratiquement inconnu. Bien que l'original sur feuille de palmier (*lontar*) soit conservé au musée de *Nusa Tenggara Barat* (NTB), seuls quelques historiens connaissent cette source écrite. La *Babad Sembalun* contient des récits qui sont familiers à de nombreux habitants de la vallée de Sembalun, mais qui sont inconnus en dehors de cette région.

En comparaison avec d'autres régions de l'est de l'Indonésie, Lombok possède un grand nombre de manuscrits historiques. Des chercheurs précédents ont suggéré que le *Babad Lombok* original pourrait avoir été écrite vers le quatorzième siècle. Cependant, la majorité des manuscrits historiques ont été recompilés et restructurés depuis l'arrivée de la culture islamique à Lombok autour des XVIe et XVIIe siècles, dans le cadre d'une

stratégie de diffusion de l'Islam. L'existence de modèles et de symboles culturels islamiques dans l'ensemble des textes *babad* en est la preuve.

L'exégèse des *babad* a été réalisée sous différents angles, tels que l'histoire, la linguistique et la géographie. La perspective historique a été obtenue en confirmant les récits chronologiques avec des historiens locaux de Lombok. Nous avons sélectionné les récits relatifs aux éruptions volcaniques. Nous nous sommes concentrés uniquement sur la chronologie des éruptions volcaniques pour la période précédant l'arrivée de l'Islam à Lombok, qui a eu lieu au début du XVIe siècle. L'approche linguistique a été utilisée pour confirmer les toponymes mentionnés dans les *babad*. Nous avons déterminé le caractère littéral des toponymes afin de faciliter leur localisation sur la carte actuelle et d'identifier d'éventuelles transformations de noms de lieux. Nous avons enfin utilisé une approche géographique pour déterminer le mouvement et la direction des personnes évacuées ou déplacées mentionnés dans le *babad*.

Les trois *babad* que nous avons analysés offrent des informations essentielles sur le paysage sociétal ancien de Lombok, à savoir l'existence de deux anciens royaumes, celui de Suwung et celui de Pamatan. Le royaume de Suwung a été étudié par le biais d'entretiens avec des spécialistes locaux de Lombok : l'emplacement possible de Suwung se situe dans les environs de Sambelia et de Sugian, à l'Est de l'île. Un autre lieu possible de Suwung est situé dans la partie nord de Perigi. Bien que seul Pamatan ait été associé à l'éruption de Samalas, le récit de *Babad Lombok* rappelle le patrimoine du royaume de Suwung. Plusieurs établissements mentionnés dans la *Babad Suwung* sont également cités dans *Babad Lombok* comme étant les lieux où les survivants de Pamatan se sont réfugiés. Par conséquent, l'illustration géographique de l'emplacement estimé de Suwung aide à interpréter l'endroit où Pamatan aurait pu se trouver.

Les critères géographiques qui permettent de déterminer la localisation possible de Pamatan sont les suivants : 1) situé dans la zone PDC ; 2) sur les pentes inférieures du volcan ; 3) à proximité des zones de montagne appropriées pour l'évacuation ; et 4) dans la zone côtière proche de la mer, ce qui permet l'évacuation par bateau. En l'absence de toponymes correspondant à Pamatan, nous suggérons que l'ancien royaume de Pamatan était situé dans la partie orientale, à proximité de Selaparang, un village apparu à l'époque

du royaume de Suwung. Cette localisation géographique correspond aux narrations de *Babad Lombok*.

Les trois *babad* illustrent le fait que les habitants de Lombok ont procédé à une évacuation et à un exode massifs des villages affectés. Les mesures d'urgence prises par les survivants de Samalas étaient orientées sur des réponses immédiates : éviter les dangers et chercher des zones sécurisées. Cette réaction est similaire à celle des survivants de l'éruption de l'Etna en Italie en 1669 CE, qui pensaient que la catastrophe était une punition de Dieu. En plus des influences religieuses, les institutions politiques (gouvernementales) ont fortement contribué au succès des opérations d'évacuation et de récupération. Ce type de réponse immédiate ou d'urgence a prévalu dans les stratégies de gestion des catastrophes indonésiennes et mondiales jusque dans les années 1960. Elle a ensuite été remplacée par le paradigme réactif-proactif (1970-1990), et la réduction des risques est le paradigme le plus récent.

Le processus de reconstruction post-catastrophe a été relativement lent. Il a peut-être fallu jusqu'à un siècle pour achever le processus de résilience, marqué par la présence d'un nouveau royaume au 14e siècle. Nous suggérons que l'histoire de l'éruption de 1257 CE n'a pas été oubliée au cours des siècles postérieurs à l'éruption, mais que les souvenirs ont simplement été incorporés dans des histoires qui sont plus centrées sur les conditions politiques. Nous espérons que ces reconstructions de la tradition orale à partir des *babad* serviront d'informations précieuses pour renforcer les stratégies de préparation et de récupération en cas d'éruption volcanique à Lombok et dans la communauté plus vaste. Les trois *babad* de Lombok ont également apporté des connaissances utiles sur les processus de rétablissement après une éruption volcanique, qui sont utiles dans le monde moderne, par exemple en matière de rétablissement physique, de gouvernance, de rétablissement institutionnel, et de rétablissement économique.

Limites et perspectives de l'étude

Les études sur les impacts physiques et sociaux d'une éruption volcanique passée sont relativement limitées. Plusieurs limitations ont conduit à la rareté de ce sujet, comme l'accès aux données de terrain et/ou aux données historiques si l'éruption s'est produite dans le passé. Dans cette thèse, une telle recherche a été menée de manière approfondie sur l'île de Lombok, en utilisant diverses données géospatiales, des mesures sur le terrain, la modélisation géographique et l'analyse de sources écrites. Les impacts de deux grandes éruptions du volcan Samalas qui se sont produites en 1257 CE et 5000-2600 BCE sont analysés. Ces éruptions ont entraîné une évolution significative du paysage dans les zones proximales et distales. La mémoire sociale documentée dans les textes écrits a également fourni un récit complet des phases d'urgence, de migration et de récupération d'une éruption majeure formant une caldeira.

L'identification des impacts physiques et sociaux d'une éruption ancienne est particulièrement compliquée, mais plusieurs approches permettent de la réaliser. Cette recherche présente cependant plusieurs limites :

1) L'étude du DAD à Lombok a uniquement utilisé un nombre limité de données structurales. L'abondance des données lithologiques aurait permis de calculer plus précisément le volume du dépôt et d'améliorer le cadre stratigraphique régional. Il est à espérer que les résultats de cette recherche inciteront les communautés géologiques et volcanologiques à explorer la grande DAD de Lombok.

2) Les données stratigraphiques archivées ou héritées de l'exploration géologique à Lombok sont limitées. Ces données auraient été précieuses pour cette recherche pour développer un meilleur cadre stratigraphique que celui déjà établi.

3) L'analyse des documents historiques a été effectuée sur seulement trois documents. De nombreux autres documents peuvent contenir des informations sur le même événement, à savoir l'éruption du volcan Samalas en 1257 CE. Actuellement, la numérisation des documents anciens de Lombok est en cours de réalisation pour assurer un catalogue plus complet et des données accessibles à un public plus large.

Lombok a un potentiel intéressant en tant que laboratoire naturel de volcans holocènes avec des géosites et des géohéritages exceptionnels. Depuis 2013, l'éruption de 1257 CE du Samalas a incité les sociétés de géologie et de volcanologie à faire des recherches à Lombok. En raison de l'impact de deux événements majeurs sur le paysage de Lombok, les études sur les ressources en matière de sol et d'eau seront également d'un grand intérêt. Les matériaux extraits des éruptions ont constitué la première ressource pour la formation des sols, et leur déposition a affecté la structure de l'aquifère sous la surface. L'histoire et l'archéologie sont également des sujets qu'il est fortement suggéré d'explorer à Lombok. Seulement quelques artefacts ou ruines ont été trouvés à Lombok. Il est possible que des ruines d'anciens villages enfouis sous le sol soient découvertes, ainsi que l’ancienne capitale du royaume de Pamatan, dont la localisation reste un mystère.

Acknowledgement

First of all, I would like to express my gratitude to Allah S.W.T. for giving me the strength to finish this thesis. I would like to thank all those who have put their trust in me, their assistance, and their support during my study in France and Indonesia. This thesis was conducted at the Laboratory of Physical Geography - CNRS UMR 8591, the University of Paris 1 Pantheon Sorbonne, with support from various parties:

1. Directorate General of Higher Education, Research, and Technology (DGHERT), Ministry of Education Culture, Research, and Technology Republic Indonesia (BPPLN Scholarship)
2. Universitas Gadjah Mada (UGM), Indonesia
3. Université Paris 1 Panthéon Sorbonne (Aide à la Mobilité Internationale)
4. Institut Français d'Indonésie – Science et Impact 2022 (SEMBALUN, project coordinated by Prof. F. Lavigne)
5. Institut Universitaire de France (IUF) of Prof. F. Lavigne
6. Franco-Indonesian Association for the Development of Science (AFIDES) - Prize "Mahar Schützenberger" 2021

To my supervisor, Prof. Franck Lavigne, I am very grateful for your mentorship and moral support, as well as for sharing a lot of new insights to me. I also thank Dr. Danang Sri Hadmoko, who has given me motivation, guidance, and support during my study. Many appreciations are also given to the members of the jury, Prof. Gilles Arnaud-Fassetta, Dr. Armelle Decaulne, Prof. Eric Fouache, Dr. Aline Garnier, and Prof. Muh Aris Marfai.

I would like to thank my home base institution in Indonesia, the Rector of Universitas Gadjah Mada, the Dean of the Faculty of Geography, and the Head of the Department of Environmental Geography, who have been very supportive of me. Thanks to Dyah Fitia Dewi for handling the administrative charge during the research.

Thanks to colleagues from UMRAM who helped during data collection, especially Syamsuddin and Alm. Hiden, and to colleagues from BRIN (National Research and Innovation Agency), Lina Handayani and Yayat Sudrajat who also helped with data collection and analysis. Thanks also go to colleagues from various institutions who helped in the data analysis of this research, Wayan Jarrah Sastrawan, Jamaluddin, Ahmad Sirulhaq, Clement Virmoux, Segolene Saulnier-Copard, Bachtiar Mutaqin, Christoper Gomez, Pierre Lahitte, Karim Kelfoun, Pattrick Wassmer, Benjamin van Wyk de Vries, and Kusnadi.

I would say thanks to Riha Ali, Asnan Bambang, Herlan Satya, Syafii, Hisyam Ramadhan, Fariq, Erna, Witari, Arief, and all the local people in Lombok who participated and helped me during fieldwork.

For all members of the Laboratory of Physical Geography UMR 8591 and the Laboratory of Environmental Geomorphology and Disaster Mitigation, UGM, thanks for assisting me in completing this thesis.

Special thanks to the Lavigne family (Emma, Axel, and Livia) for their helpfulness during my stay in France.

Finally, I would like to thank my whole family members, especially my wife, Tiara Handayani, and my daughters, Ainayya and Askanaziya, for their understanding, care, love, prayers, and encouragement.

Thank you, Merci beaucoup, dan Terimakasih…

TABLE OF CONTENTS

CHAPTER 1

This chapter briefly introduces the study, starting with the research context, which explains the background, the scientific gap, and the urgency of the research. The study area of Lombok Island is presented in regard to the geomorphological, geological and volcanological conditions. These subjects are essential because this thesis mentions various processes of a volcano and their impact on the surrounding landscape. The research questions and problems are described to formulate the objectives.

INTRODUCTION

1.1. Research Context

Indonesia is situated within the ring of fire, which was formed by the subduction of the Indo-Australian Plate with the Eurasian Plate and the Pacific Plate from the east (Hall, 2009). At least three plates influence this region: The Indo-Australian plate moves to the north beneath the Indonesian (Eurasian) plate creating a continuous sea trench and volcanic arc along Sumatera, Java, and the Lesser Sunda (Figure 1.1). The Pacific plate pushes westward causing a bending shape in the northeastern part of the Banda Arc, forming volcanic and non-volcanic island arcs such as Babar, Tanimbar, and Kai. Located at the junction of three tectonic plates, the Lesser Sunda Arc is also categorized as very active with an unusual geodynamic setting (Hall, 2009; 2012).

Volcanic ranges pattern from west to east and bend northward. Sumatra and Java have numerous volcanoes, while other islands, such as Bali, Lombok, and Halmahera, were formed by a volcanic-dominated process. Many volcanoes have had significant eruptions (Volcanological Explosivity Index or VEI>4), while some have had minor impacts with frequent eruptions (De Maisonneuve & Bergal-Kuvikas, 2020). Some of those considered dormant for centuries have suddenly reactivated, as happened in Sinabung (Sumatra) in 2010 (Gunawan et al., 2019). Some volcanoes have had a major eruption in their eruptive history, like Merapi (2010), Krakatau (1883), Tambora (1815), and Kelud (1919) (De Maisonneuve & Bergal-Kuvikas, 2020; Newhall et al., 2018; Siebert et al., 2015) (Figure 1.2). However, in 2013, the mystery of another major volcanic eruption was revealed, i.e. the eruption of Samalas (1257 CE) in Lombok (Lavigne et al., 2013). Other volcanoes that are currently considered as inactive have had significant eruptions, such as Telaga caldera in Maluku, (ca. 17 ka: Faral et al., 2022) and an undated event of Naira volcano (volcanic explosivity index >5 (Faral et al., 2022; Suhendro et al., 2022).

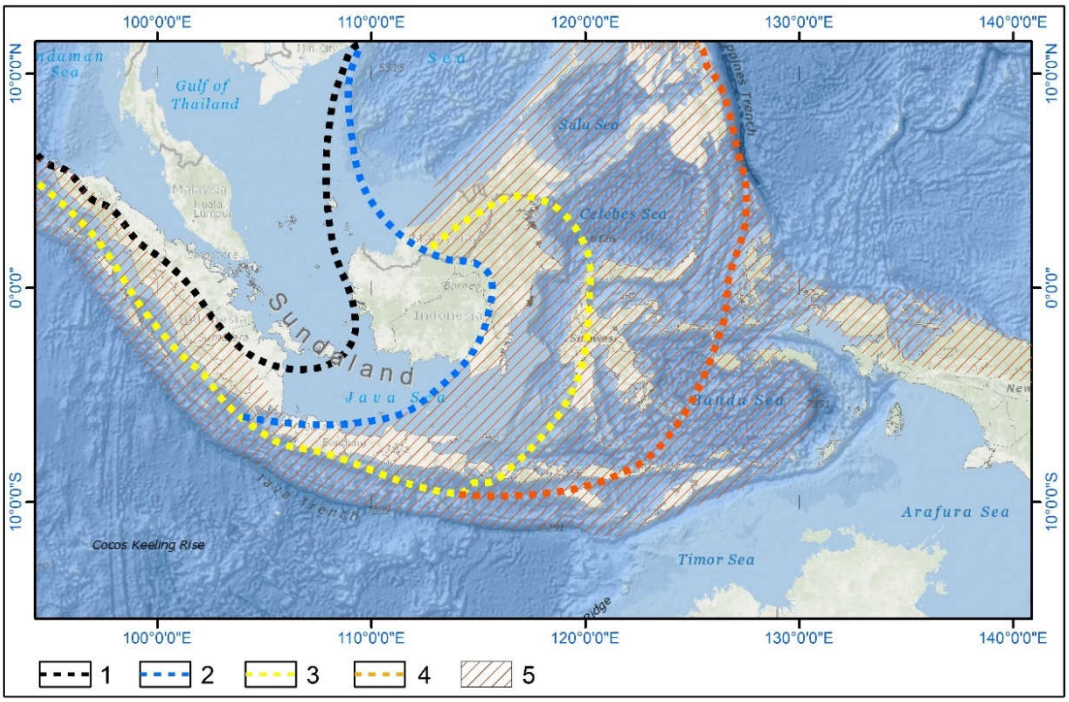

Figure 1.1. (1) Mesozoic sundaland-core (2) Early Cretaceous border (3) Late Cretaceous border (4) Early Miocene border (5) recent-continuous tectonic activity (Hall 2009, 2012).

Volcanic eruptions in Indonesia and other parts of the world have had many direct and indirect impacts (Biass et al., 2017; Brown et al., 2017), both physical and social. Volcanic eruptions generally cause domino or cascading effects such as lahars, tsunamis, and effects on the global climate (Aydin et al., 2013; Cooper et al., 2018). Direct social impacts, such as demographic and economic disturbance are also generally devastating as they cause mortality, migration, economic chaos, transport disruptions, and crop failures (Chester et al., 2015; Fei et al., 2007; Lechner et al., 2018).

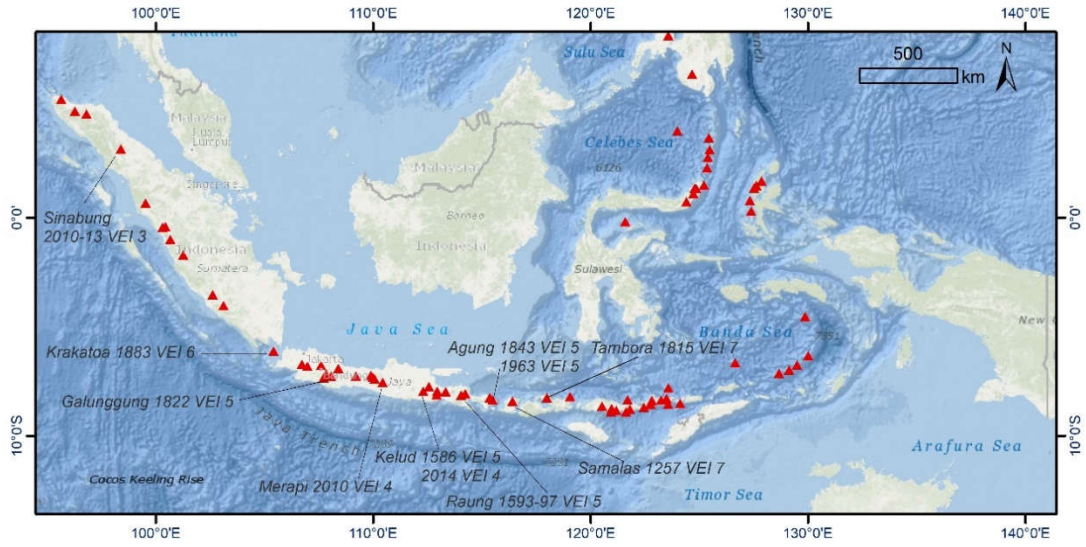

Figure 1.2. Distribution of active volcanoes in Indonesia. Several volcanoes create remarkable eruption by the range of volcanic explosivity index (VEI) 3-7 (Compiled from De Maisonneuve & Bergal-Kuvikas, 2020; Lavigne et al., 2013; Kasbani et al., 2019).

Considering that human interaction with volcanoes in Indonesia has a long history, volcanoes have become the source of livelihood for many generations (Reid, 2016; Sastrawan, 2022). Many ancient settlements developed on the slopes of volcanoes where adequate water resources and fertile soil are available (Gomez et al., 2010). The impact of eruptions in the past may have been worse due to less advanced technology and different risk perceptions from the modern era (Chester et al., 2012). Otherwise, as a result of long-term interaction, local wisdom has developed that allows past generations to manage volcanic hazards effectively in avoiding physical damage and minimize social damage (Lavigne et al., 2008; Troll et al., 2015). Since monitoring instruments and direct observations are available for recent events, the impacts of eruptions can be broadly identified and analyzed. In the case of past eruptions, this issue becomes very challenging due to the limited availability of archives and historical documents, either before, during, or after an eruption (Garrison et al., 2018; Tennant et al., 2021). The investigation of past volcanic events and their impacts in Indonesia is still limited, although Indonesia has a large number of ancient written documents and stone inscriptions (Sastrawan, 2022). These various ancient records are likely to contain stories of eruptions and information about their impacts. Three islands

in Indonesia have numerous resources of ancient written documents, namely Java, Bali, and Lombok (Hägerdal, 2015).

Several impacts of historical eruptions worldwide that have been identified through written sources include Vesuvius (79 CE) (Sigurdsson et al., 1982), Eldgjá (934–940 CE) (Brugnatelli and Tibaldi, 2020), Etna (1643 CE) (Branca and Vigliotti, 2015), Laki (1783-1784 CE) (Trigo et al., 2010), Tambora (1815 CE) (Oppenheimer, 2003), and Krakatoa (1883) (Verbeek, 1884). These multidisciplinary studies combine various approaches, such as volcanology, geology, geomorphology, history, and archaeology. The physical impact of past volcanic events such as climatic disruption is frequently emphasized due to potential global effects (Gao et al., 2008; Oppenheimer et al., 2018). However, the geomorphological impacts on volcano edifice and surrounding morphology are rarely addressed. For instance, the impact of Vesuvius eruption (79 CE) on the landscape evolution of the Sarno River Valley, Italy, has been investigated through geomorphological analysis (Vogel and Märker, 2010). Whereas, the societal impacts caused by past eruptions are widely highlighted (Campbell, 2017; Fei, Zhou, & Hou, 2007; Guillet et al., 2017). Only limited studies combine the investigation of both physical and social impact in a single eruption, especially on a past eruption event. This issue is of great interest in Indonesia, where historical records are numerous, although underexploited, and access to volcanological data in the field is accessible.

Lombok is the region with the largest number of ancient manuscripts in Indonesia (Hägerdal, 2015; Reid, 2016). This island also experienced one of the largest volcanic eruptions in modern human history. The 1257 CE eruption of Samalas is one of the most significant eruptions in the last 2000 years, having the highest sulfate spike in polar ice cores (Sigl et al., 2015). This eruption is also known as the biggest stratospheric eruption in the Common Era (Vidal et al., 2016). Most of the deposits of the Samalas eruption that mantled Lombok in 1257 CE are pyroclastic density currents (PDCs) from the fourth phase of the eruption (Vidal et al., 2015). These PDCs deposits have a strange dispersion in the southern part (Figure 1.3). The ~40 km wide hilly area in Central Lombok acted as a topographic barrier for the PDCs dispersion (Vidal et al., 2015). This deposit called Kalibabak formation on the geological map of Lombok has been interpreted as a debris avalanche by Vidal et al. (2015). However, neither

geomorphological nor geological investigations have been made on this deposit up to now. In addition to the 1257 CE event, older eruptions have significantly affected the evolution of landscape and maybe society in Lombok.

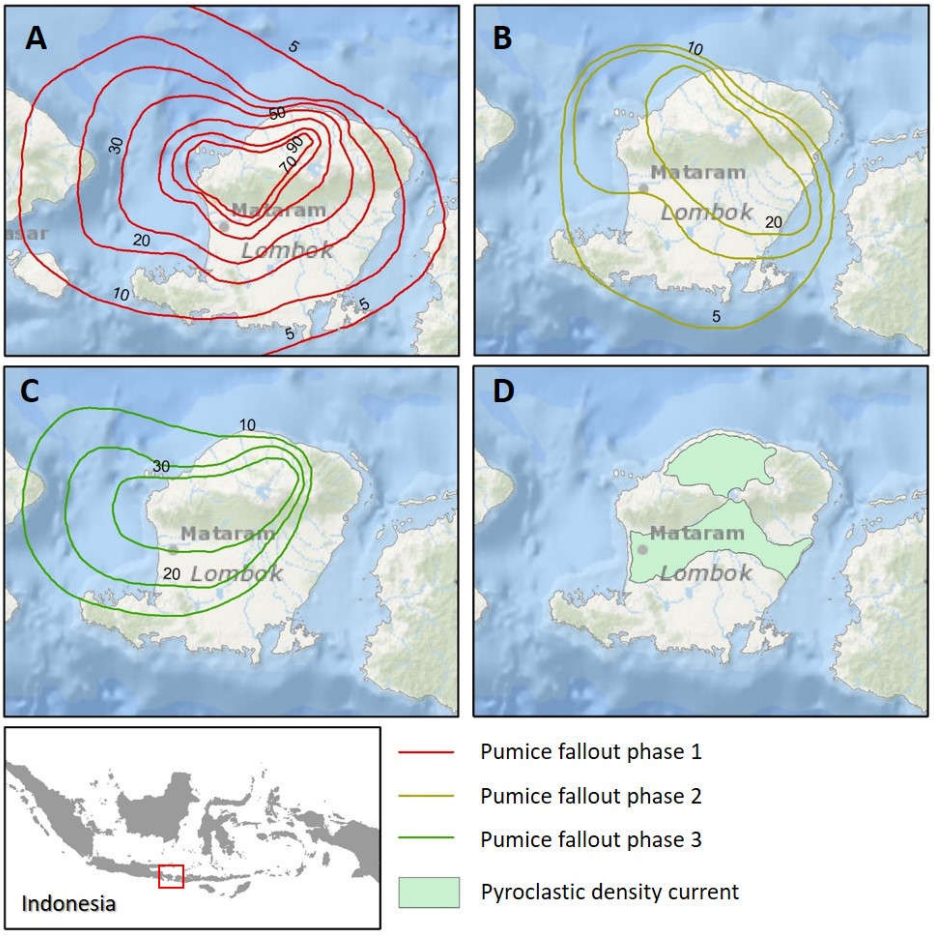

Figure 1.3. Widespread fallout deposits (A,B,C) and voluminous pyroclastic density currents (D) from the eruption of Samalas in 1257 CE (modified from Lavigne et al., 2013 and Vidal et al., 2015).

The investigation of physical and social impact of a past eruption event is applied in Lombok through this thesis, primarily evaluating the impacts of the 1257 CE Samalas eruption. This study is a continuation of the ten years ongoing study in Lombok. It aims to demonstrate the geomorphological consequences of major eruptions and reconstruct the preserved social memory of ancient inhabitants in dealing with volcanic eruptions.

1.2. Lombok Island

1.2.1. Geographic and Geologic Setting of Lombok

Lombok island, located at 8.565'S 116.351'E, is an island among 17,491 islands in the Indonesian archipelago. Lombok is located in the southeast of the Indonesian archipelago (UTC +8), east of Java island, and next to Bali island. Lombok island is similar in size to Bali. The geographic position of Lombok is adjacent to Bali Island and the Flores Sea in the northern part; the eastern and western parts are limited by two straits, Alas and Lombok strait respectively; while the southern part is limited by the Indian Ocean. According to the latest survey from the Bureau of Statistics, Lombok island is surrounded by 196 small islands (Statistic, 2020).

Lombok island is part of the Nusa Tenggara Barat (NTB) province. The capital of this province is Mataram city, in the western part of Lombok. On this island, there are five administrative municipalities: Mataram city as the capital province, Lombok Utara regency, Lombok Barat regency, Lombok Tengah regency, and Lombok Timur regency. Lombok displays a volcanic complex which is currently listed as a UNESCO global geopark: Rinjani Geopark. The area of this geopark occupies mostly the northern area of the island. The attractiveness of this geopark is the caldera of the former Samalas, the new active cone (called Barujari) within the Segara Anak lake, and the Rinjani summit. Several geo-sites are also scattered in the North and West, as well as geological, biological, and cultural sites.

Lombok is included in the Lesser Sunda Islands: a group of Miocene or younger islands located in the north west of Australia and immediately east of Java. Other than Lombok, this island group consists of Bali, Sumbawa, Flores, Timor, Alor, Wetar, and other small islands. This region is commonly divided into two zones due to the mechanism of magmatism processes, i.e., the East Sunda Arc, which includes Bali, Lombok, and Sumbawa, while the rest is the Banda Arc.

Lombok consists of various rock formations such as surficial deposits, sediment, volcanic, and intrusive rocks (Figure 1.4). The oldest rock formation deposited in Oligocene is Kawangan (Tomk) and Pengulung Formation (Tomp) (Mangga et al., 1994). These rock formations occupied the mountainous area in the eastern part of Lombok. Recent deposits were emplaced during the Holocene, namely

undifferentiated volcanic rock from Rinjani (Qhv) and alluvium (Qa). Older than these two formations, two identical rock formations were deposited in the middle of Lombok, i.e., Kalibabak (TQb) and Kalipalung Formation (TQp). Based on Maryanto (2009), these two formations of rock were deposited through flow or laharic processes. Using grainsize analysis, the Lekopilo Formation (Qvl) was suggested due to epiclastic flows (Maryanto, 2009). This suggestion also corresponds to the latest finding that this formation formed from the pyroclastic density current (PDC) deposit of Samalas eruption in 1257 CE (Lavigne et al., 2013; Vidal et al., 2015). A simplified classification of surficial sediments in Lombok was also conducted by Metrich et al. (2017), especially for volcanic rocks. Lombok is divided into three different formations, i.e. (1) Rinjani complex, Propok, and Punikan, (2) undifferentiated volcanic rock with lava, and (3) volcaniclastic rocks.

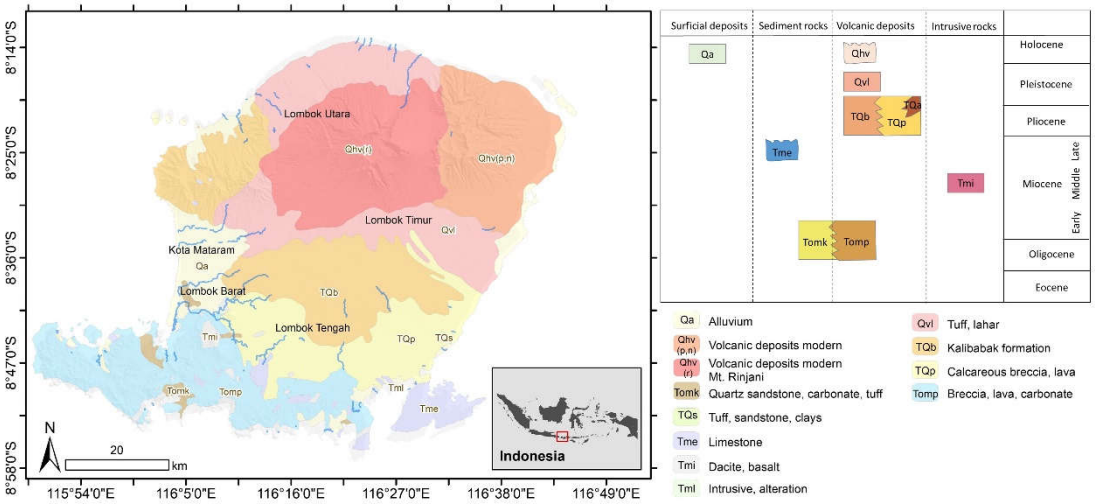

Figure 1.4. Geological map of Lombok (Mangga et al. 1994).

1.2.2. Volcanic Arc of Lombok

The emergence of volcanic arcs on Lombok is not only influenced by a single factor, subduction of the Indo-Australian plate over the Java trench (~350 km in a southerly direction from the island) but also the smaller subduction of the Flores oceanic crust on the northern part, which is located along the Flores thrust (~60 km) (Zubaidah et al., 2014). Therefore, the Sunda and Banda volcanic arcs are responsible for several major volcanic eruptions since the Holocene (Hall, 2009; 2012; De Maisonneuve and Bergal-Kuvikas, 2020). In this zone lie three volcanoes that have

experienced volcanic explosivity index (VEI) 7: Batur in Bali (34.6 ka), Samalas in Lombok (1257 CE), and Tambora in Sumbawa (1815 CE) (De Maisonneuve and Bergal-Kuvikas, 2020). In the Common Era, eleven volcanoes have shown activity, recorded either by good or rough volcanological data, as shown in Figure 1.5.

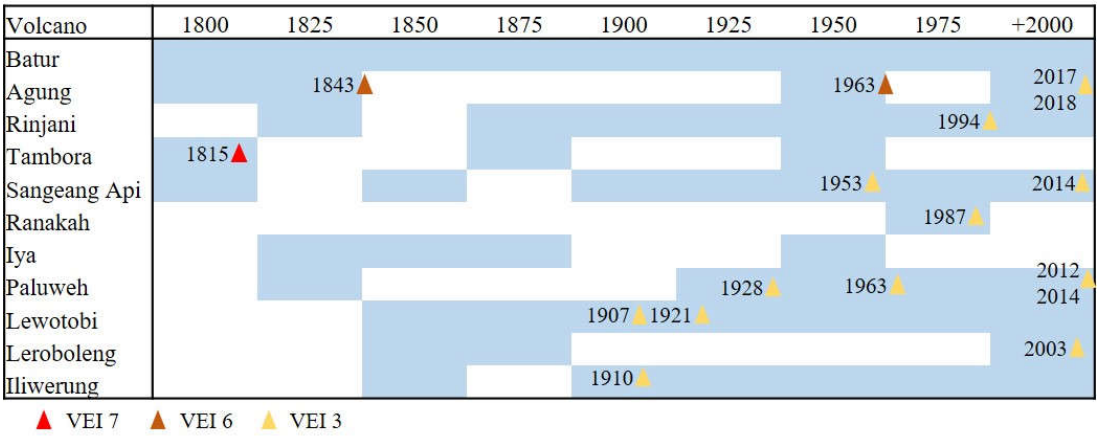

Figure 1.5. A chart of the 2000-year eruption history in the lesser Sunda arc (De Maisonneuve & Bergal-Kuvikas, 2020).

The origin of volcanism in Lombok has been proposed using magnetic and gravity field anomaly investigations (Zubaidah et al., 2014). It was revealed that the formation of volcanoes in this region was preceded by dacitic and basaltic intrusion (Tmi rock formation, see Figure 1.4). It was raised above the sea level for the first time during the Late Miocene. The intrusion processes then ceased, and the first volcano began to rise in the northern area, resulting in the sequence formation of tertiary lava (TQp) and the second tertiary lava formation (TQb). During the Pleistocene, the quaternary magmatic intrusion was initiated, resulting in the quaternary lava formation (Qvl) through an old crater followed by normal faults in this region. The recent magma intrusion from both subduction sides resulted in the second quaternary lava (Qvh) through the new magma vent of Samalas and Rinjani, while the old crater (Sembalun, G. Pusuk, G. Nangi) manifested in the geothermal area (Hadi et al., 2007).

A detailed model of volcanism processes in Lombok from pre-Holocene to the present day was proposed (Métrich et al., 2017; Rachmat et al., 2016). In the pre-Holocene, three magma chambers were supplying Samalas, Rinjani, and Propok (Figure 1.6). The evolution continued to the magma amalgamation process resulting in one large magma chamber that only supplied Samalas. This amalgamation process

took at least 2000 years. This magma chamber is the main reservoir that sustained the plinian eruption of Samalas in 1257 CE. The caldera of Rinjani (Segara Anak) was formed during this eruption (Lavigne et al., 2013). Formerly, two mountains existed in this area, but after the eruption, this location was often called the Rinjani complex, which includes a caldera, Segara Anak lake, Barujari volcano, and Rinjani peak. In the present day, the magma chamber is relatively small and deep. Within the caldera, the magma chamber only sustains the Barujari cone (±2376 m.a.s.l), while two others small cones are inactive; Anak Barujari (±2112 m.a.s.l) and Rombongan (±2110 m.a.s.l) (Rachmat et al., 2016). Several explosive activities in this volcano complex are reported, (1) at 11,900 BP dated from thick scoria deposits, (2) at 6000 BP, and (3) 2550 BP; both are dated from dacitic pumice fallout deposits (Nasution et al., 2004; Métrich et al., 2017).

1.3. Problems and Research Questions

The total ejected volume of the 1257 CE Samalas eruption is ~40 km^3 dense rock equivalent (DRE) (Lavigne et al., 2013; Vidal et al., 2015). This voluminous ejected material from the Samalas eruption in 1257 CE have been mapped, i.e., the massive pyroclastic influx in the northerly, westerly, and easterly directions (Lavigne et al., 2013; Vidal et al., 2015). However, in the southerly direction, the emplacement of PDCs was deflected by a topographic barrier (Vidal et al., 2015). This topographic barrier is a hilly area composed of hummocks, the typical landform formed by debris avalanche deposits (Hayakawa et al., 2018; Salinas & López-Blanco, 2010; Yoshida, 2014; Yoshida et al., 2012). This debris avalanche deposit (DAD) is identified on the Geological Map of Indonesia as the Kalibabak rock formation, which formed in the Pleistocene (Mangga et al., 1994).

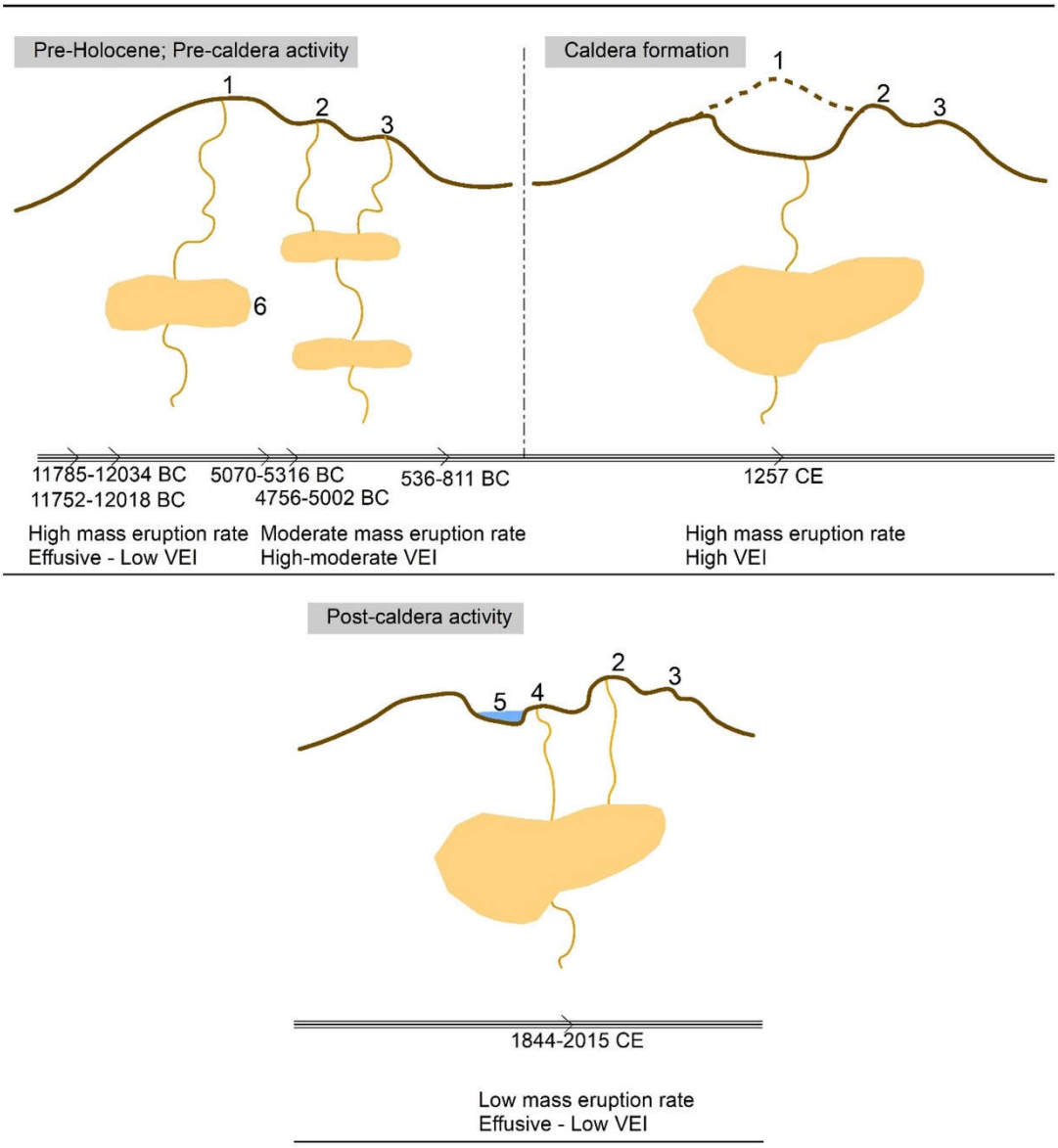

Figure 1.6. Schematic evolution of volcanic activity in Samalas-Rinjani complex (Métrich et al. 2017). Note: 1. Samalas; 2. Rinjani; 3. Propok; 4. somma-volcano; 5. caldera-lake; 6. magma chamber.

No further information describes this DAD, as well as the preceding and the following geomorphological processes; therefore, its formation remains a mystery. The process of DAD formation clearly influences landscape changes in the proximal, medial, and distal areas. Although a reconstruction of the pre-caldera edifice of Samalas has been conducted (Lavigne et al., 2013), the structure of the pre-caldera summit may not be fully intact as previously modeled due to the former scar of the avalanche's caldera. In Indonesia, the study of DAD is also limited, e.g., in Galunggung (Bronto, 1989;

MacLeod, 1989), Raung (Siebert, 1984; 2002; MacLeod, 1989), and Papandayan (MacLeod, 1989; Nursalim et al., 2016). The discovery of DAD in Lombok might be beneficial for updating the list of Indonesia's collapsing volcanoes and the world's gigantic DAD.

- The first set of research questions based on these issues is: what are the characteristics of DAD in Lombok? When did the volcanic debris avalanche in Lombok occur? What was the condition of the landscape before and after this avalanche?

The northern, western, and eastern parts of Lombok is heavily covered by the ejected material from the 1257 CE Samalas eruption. Only a limited area on the eastern part has been investigated: the land surface drastically aggraded by 5–30 meters, and the river valleys shifted after the eruption of Samalas in 1257 CE (Mutaqin et al., 2019). The northern and western parts may be experiencing the same processes. The investigation of landscape evolution in these areas is necessary, especially in the western part where Mataram, the capital city of the Nusa Tenggara Barat province is settled. The investigation results might have benefits for other fields of study, such as history and archaeology, i.e., by reconstructing the ancient landscape condition of Lombok before the thirteenth century and its dynamics in the subsequent centuries.

Preliminary insight into stratigraphic evolution in this area has been investigated using seismic measurement; Mataram was formed by a massive influx of alluvium deposits infilling the ancient basin and valleys (Harsuko et al., 2020). In Indonesia, limited studies have been conducted related to paleo-topographic reconstruction. However, various methods have been developed for topographic reconstruction, using geomorphological, geological, and geophysical approaches (Łajczak et al., 2020; Pröschel and Lehmkuhl, 2019). These different approaches, if performed together, might result in a development method for paleo-topographic reconstruction. In addition, this investigation might be helpful for revisiting the deposit's map of the 1257 CE Samalas eruption.

- The second set of research questions based on these issues is: to what extent did the Samalas eruption in 1257 CE cause landscape evolution in the Mataram area?

What were the paleo-topographic conditions like in Mataram prior to the Samalas eruption? How did the transformation process occur?

The name of Samalas volcano is mentioned in the indigenous written source from Lombok, i.e., the Babad Lombok: "Mount Rinjani avalanched and Mount Samalas collapsed, followed by large flows of debris..." (Suparman, 1994). Other indigenous written sources that describe the story of a volcanic eruption are Babad Suwung and Sembalun. However, only Babad Lombok had the official transliteration version from the Ministry of Education and Culture, Indonesia (Suparman, 1994). Along with Babad Lombok, Babad Suwung and Babad Sembalun depict volcanic eruption events in Lombok. However, only limited texts from these sources have been investigated (Lavigne et al., 2013; Mutaqin and Lavigne, 2019). Many others related to civilization's response to the eruption and its resilience strategies remain concealed. Despite the myriad of studies of volcanoes related to human history, issues on the inhabitant's response and resilience strategy remain a lack of attention (Martin, 2020).

There is no comprehensive description that chronologically explains the impact of the 1257 CE Samalas eruption on the population. Given that the 1257 CE eruption had a significant scale, lessons on how to face and survive a catastrophic event which is recorded in the written sources, are valuable information for the present generation as a reference for risk reduction strategy of a volcanic eruption. The illustration of the societal conditions of Lombok in those three written sources may also help trace the hitherto lost ancient civilization and rediscover the cultural landscape of Lombok before the thirteenth century.

- The third set of research questions based on these issues is: could the characteristics of ancient civilizations in Lombok be traced through written sources? What was their response in dealing with volcanic eruptions? How did they rebuild their civilization after being destroyed by volcanic eruptions?

1.4. Objectives and Thesis Outline

In the framework of the “cotutelle” PhD thesis (University of Paris 1 – Pantheon Sorbonne and Universitas Gadjah Mada), this study is founded by the Ministry of Education, Culture, and Technology Republic of Indonesia started in October 2019. This

thesis aims to demonstrate the usefulness geomorphological approach to investigate the landscape evolution due to volcano eruptions and evaluate the geographical context of historical written sources. Based on research problems and questions, this thesis has three principal objectives:

a) to reconstruct the Holocene sector collapse and a far-reaching debris avalanche deposit which transforming Samalas volcano's edifice and surrounding landscape.
b) to reconstruct the landscape evolution of the western part of Lombok following the 1257 CE eruption of Samalas
c) to analyze the societal impacts, emergency response, recovery, and resilience strategies of Lombok's inhabitant following the 1257 CE eruption of Samalas.

To elaborate on these objectives, this thesis is divided into seven chapters.

- Chapter 1: Introduction

This chapter provides a general introduction to the research, including the research context, presentation of the study area, problems and research questions, and objectives.

- Chapter 2: State of the Art

This chapter provides a review of the study on the impacts of volcanic eruption, paleo-topographic reconstruction, and the use of historical sources to analyze volcanic eruption and the following impacts. Some part of this chapter has been published in the Geosciences MDPI Journal (2021). This chapter also presents the conceptual framework of the study, specifically on each objective of the research.

- Chapter 3: General Methodology

This chapter displays the method used in this study, including the area of interest, data requirement, acquisition, and analysis. The detailed method for each objective is also presented in Chapters 4-6.

- Chapter 4: The Kalibabak Debris Avalanche at Samalas Volcano

This chapter presents the new discovery of debris avalanche deposit (DAD) in Lombok. This gigantic DAD has been successfully dated using radiocarbon dating. The dynamics of this debris avalanche is also evaluated using geomorphological approach: morphology, morphostructure, and morphochronology.

- Chapter 5: Evolution of the Mataram Plain Following the 1257 CE Samalas Eruption

This chapter presents the paleo-topographic and paleo-hydrographic modeling of the Mataram plain through various data to answer to second problem and research question. It also presents the depositional patterns of Mataram plain, which involve abrupt and progressive changes. This chapter contains a published article in the Journal of Earth Surface Processes and Landforms (2023).

- Chapter 6: The 1257 CE Cataclysmic Eruption of Samalas Volcano Revealed by Indigenous Written Sources

In this chapter, three old written sources from Lombok are evaluated to rediscover the history of Lombok before the thirteenth century, especially related to the volcano eruption of Samalas in 1257 CE. It also presents the chronology during the emergency and recovery period. The location of a lost ancient civilization is proposed by tracking its location using geographical features described in the sources. This chapter contains a published article in the Journal of Volcanology and Geothermal Research – Elsevier (2022).

- Chapter 7: Conclusions and Perspectives

This chapter presents the overall conclusion of the study. This chapter also provides an outlook for further development studies related to similar topics.

CHAPTER 2

Following the formulation of the thesis objectives, namely the use of a geomorphological approach to study the evolution of landscapes due to volcanic eruptions and the evaluation of the geographical context of written sources, several related issues are addressed in this chapter. It begins with a review of the literature on the impacts of volcanic eruptions, which vary according to the magnitude and type of eruption. There are several approaches to assessing the impact of volcanic eruptions, including topographic reconstruction. For social impacts, the utilization of written sources is crucial because such documents may contain the memories of past generations and eyewitnesses. This chapter brings the conceptual framework of the study, focusing on each research objective to determine the critical parameters to be investigated.

STATE OF THE ART

2.1. Literature Review

2.1.1. Impacts of Volcanic Eruptions

This section contains parts of an article published in Geosciences (MDPI) 2021.
https://doi.org/10.3390/geosciences11030109

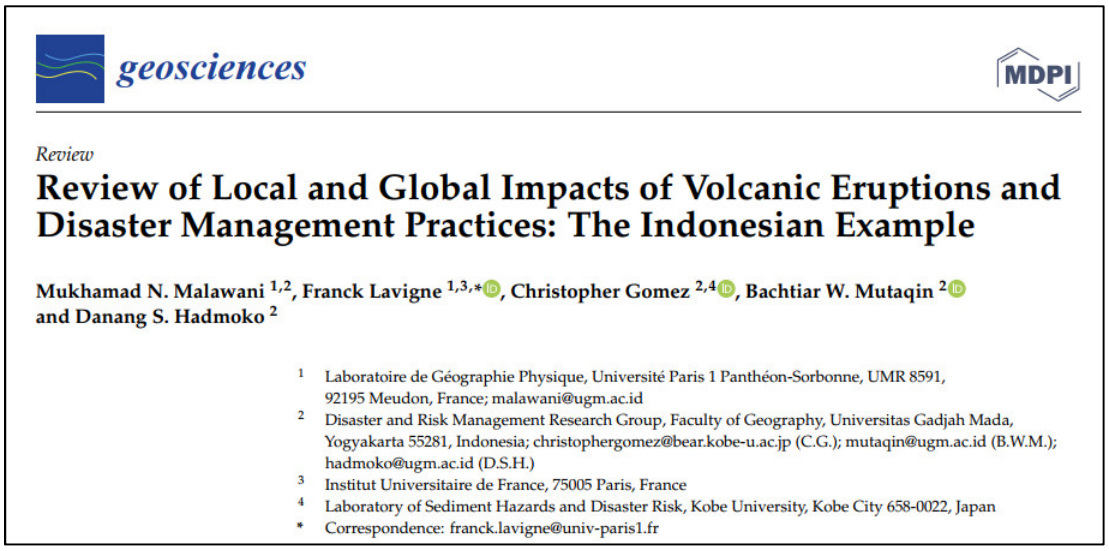

geosciences

MDPI

Review

Review of Local and Global Impacts of Volcanic Eruptions and Disaster Management Practices: The Indonesian Example

Mukhamad N. Malawani [1,2], Franck Lavigne [1,3,*], Christopher Gomez [2,4], Bachtiar W. Mutaqin [2] and Danang S. Hadmoko [2]

1 Laboratoire de Géographie Physique, Université Paris 1 Panthéon-Sorbonne, UMR 8591, 92195 Meudon, France; malawani@ugm.ac.id
2 Disaster and Risk Management Research Group, Faculty of Geography, Universitas Gadjah Mada, Yogyakarta 55281, Indonesia; christophergomez@bear.kobe-u.ac.jp (C.G.); mutaqin@ugm.ac.id (B.W.M.); hadmoko@ugm.ac.id (D.S.H.)
3 Institut Universitaire de France, 75005 Paris, France
4 Laboratory of Sediment Hazards and Disaster Risk, Kobe University, Kobe City 658-0022, Japan
* Correspondence: franck.lavigne@univ-paris1.fr

Volcanic eruptions are considered major (very large) when the Volcanic Explosivity Index (VEI) ≥ 5 (Hickson et al., 2013; Newhall and Self, 1982). The nature of the impacts of a VEI ≥ 5 eruption ranges from the destruction of a city, an entire region, climate disturbances as well as to air travel (Lavigne et al., 2013; Lechner et al., 2018; Newhall et al., 2018). Even an eruption with VEI < 5 may also have the potential to modify the environment and landscape particularly in proximal and medial facies, as well as surrounding human societies (Aydin et al., 2013). The variety of environmental destructions due to volcanic eruption differs from primary (e.g., summit collapse, vegetation burning, death), secondary (e.g., atmospheric cooling, global warming), and tertiary (e.g., flood, famine, disease) effects. It is mostly generated by gas emissions, ashes, lava flow, pyroclastic flow, lahar, debris flow, and landslide which results in local and global impacts (Aydin et al., 2013). The variety of impacts can be simplified at the local scale by their consequence in various geographical features. Geographical features are any features on the Earth's surface, whether natural or not, which can be characterized spatially and temporally (Campelo and Bennett 2013). It may be classified into four

categories: (i) the drainage system, (ii) the structure morphology, (iii) the water bodies, and (iv) the society and environment (Hickson et al., 2013; Waythomas 2015).

Impacts on drainage system

Volcanic eruptions can lead to geomorphological transformations in valleys, talweg, and the hydrographic network due to erosion and sedimentation processes. For example, at Merapi volcano, the sediment supply from pyroclastic density currents into the river network leads to riverbed aggradation and subsequently riverbed incision (Gob et al., 2016). The river valley morphology has changed from the old Merapi (before 4.8 ka BP) to the new Merapi (after 4.8 ka BP) edifice by detrital fan deposits, andesitic lava flows, tephra, lapilli, and ash layers (Selles et al., 2015). These materials buried the eastern drainage system of Merapi during a major flank collapse. During the 2006 CE eruption, Merapi's block-and-ash flow covered the interfluve region and the main valley on the southern flank as long as ~7 km (Gertisser et al., 2012). It indicates that the materials produced by volcanic eruptions are substantial in shaping morphology and channel stability. In the case of lahar/pyroclastic input, the most hazardous location along a drainage system is river confluence. For instance, the Mapanuepe and Marella rivers' confluence widened up to 1.3 km after lahar input from the 1991 CE Pinatubo eruption in Philippines (Umbal and Rodolfo, 1996). In the tropics, sediment-discharge in volcanic rivers increases during and after eruptions due to lahars, which can be either eruption-induced or rain-triggered during the rainy season (De Belizal et al., 2013; Künzler et al., 2012; Lavigne et al., 2000).

Channels that are buried by lahars is often creating difficulties for extracting the necessary water for everyday uses. For example, lahars on the southern flank of Merapi obstructed the irrigation channels for three years after the 2010 event, and this led to the worst harvest in the last decade (Sarrazin et al., 2019). Furthermore, when volcanic materials settle in the drainage system, they reduce the system capacity and can cause overbank floods during heavy rainfall (Todesco and Todini, 2004). The morphology of a river valley can transform dramatically due to lahars, predominantly in two ways: (1) burial of the main channel and (2) scouring of a new valley and, therefore, abandon of the former one (Ville et al., 2015). During the 2011 Merapi lahar events, a new 1.5 m-wide river channel formed as the lahar came through and eroded the main road of Sirahan village on the western flank (Hadmoko et al., 2018). The

example of a river valley on Merapi that has been buried by lahars and now abandoned is presented in Figure 2.1.

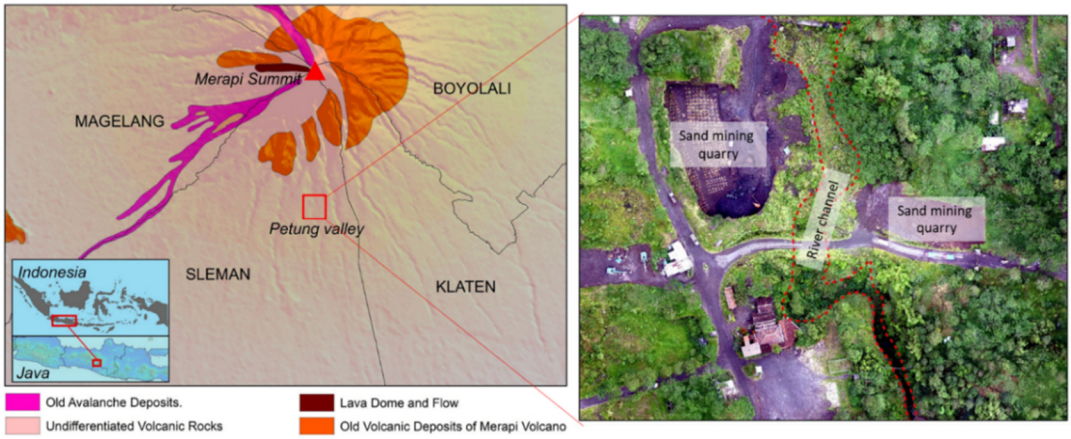

Figure 2.1. The abandoned channel of Petung River, on the southern flank of Merapi after lahar event in 2011. It is located in undifferentiated volcanic rock formation (left). An aerial image of Petung River segment was taken in 2018 during the rainy season (right) (drone image by Handayani, 2018).

Impacts on the volcanic structure

An eruption may alter the structure of a volcano and its evolution, depending on the type of eruption. On andesitic and rhyolitic volcanoes, structural changes during the growth of lava domes are frequently observed using geophysical monitoring systems, or other methods such as aerial photographs, which allow detecting even minor changes (Darmawan et al., 2018a). Hydrothermal alteration during the dome growth is often accompanied by structural weakening that potentially causes sector collapse (Darmawan et al., 2018b). Dome growth during a pre-eruptive event may also control a crater displacement, as identified in the 2007–2008 CE Kelud eruption in East Java, Indonesia (Jeffery et al., 2013). However, dome growth can be associated with the VEI, i.e., a faster dome growth most likely creates a high VEI (Ogburn et al., 2015).

Volcano edifice can drastically evolve in two ways, i.e., caldera-forming eruption and sector collapse. Several volcanoes in Indonesia formed a caldera after a major eruption. There are three infamous volcanoes that resulted in caldera during the historic time in Indonesia, i.e., Samalas in Lombok (1257 CE), Tambora in Sumbawa (1815 CE), and Krakatoa in the Sunda Strait (1883 CE) (Lavigne et al., 2013; Rachmat

et al., 2016; Zaennudin, 2010). Compared to the two others, caldera in Krakatoa is non-visible due to total collapse of the volcano in 1883 CE (Madden-Nadeau et al., 2021). Samalas caldera is the largest (~6 km-wide) (Figure 2.2A–C). The caldera-forming eruption of Samalas was also responsible for extreme morphological changes in its eastern part of the island. The 1257 CE eruption ejected at least 4.4×10^6 m^3 of pumice rich PDCs forming deposits with a thickness up to ~30 m, and it has significantly changed the valley pattern of eastern Lombok Island back in the year 1257 to the one existing today (Mutaqin et al., 2019).

Many factors can lead to sector collapse during the process of eruption. Most of them are destabilizing factors such as an earthquake (tectonic faulting), magma intrusion, hydrothermal activity, gravitational loading, and progressive shearing (Norini et al., 2020; Reid et al., 2010). Hummocky hills are typically formed by debris-avalanches, which induces morphological transformation through two ways: obstacle-free spreading and valley-filling distribution (Yoshida, 2014). The textural materials (wet and dry) of hummocky hills is valuable to characterize their triggering factor, such as in Colima volcano (Mexico): dry materials most probably result from volcano-tectonic deformation, whereas wet materials are likely due to phreatic activity (Roverato et al., 2011).

In Indonesia, three locations with extensive hummocky terrain resulting from debris avalanches can be observed from DEMs and aerial imagery. (1) In Tasikmalaya, West Java, the hummocky hills formed after an eruption of Galunggung volcano in 4200±150 BP that ejected 20 km^3 of materials, creating a horse-shoe caldera (Figure 2.2D). Debris avalanche at that time formed hummocky hills 6.5-23 km away from the summit (Bronto, 1989). (2) The hummocky hills located in Jember, East Java, resulted from Gunung Gadung, a composite volcano of Raung (Siebert, 2002). The sector collapse at Gunung Gadung also left a horse-shoe shape with 13 km long and 8.5 km wide at the branch (Figure 2.2E). Abundant hummocks can be found in the proximal-medial facies, and smaller hummocks with size <20m-height scattered in distal facies (Siebert, 2002). (3) Another hummocky hills system has been identified on Lombok Island, with total number of hummocks is >750.

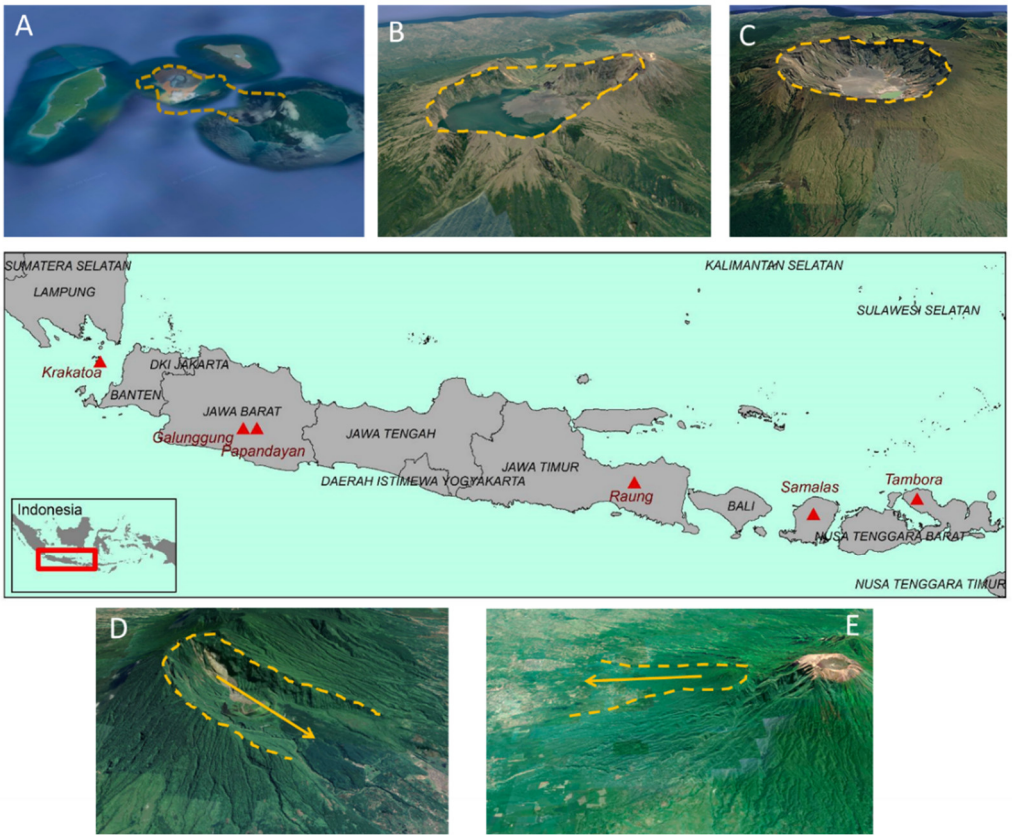

Figure 2.2. Massive caldera-forming eruptions during modern historic time in Indonesia: (A) Krakatoa, (B) Samalas, and (C) Tambora. The morphological remnant of horse-shoe edifice resulted from sector collapse of (D) Galunggung and (E) Gunung Gadung, Raung volcano, visible from Google Earth imagery.

Impacts on the water bodies

The impacts of volcanic eruptions on water bodies include impacts on lakes, sea or ocean, and manmade reservoirs. At some volcanoes, water bodies are distributed at the volcano's foot. They can also be the results of volcanic eruption and collapse, such as Mt. Bandai in Japan, where a group of lakes was formed by the sector collapse (Yamamoto et al., 1999). At the summit of the volcano, another type of water body is the crater lake and the caldera lake. In turn, the water-bodies can affect the eruptions, with notably the frequent breakout floods from crater lakes that can turn into lahars (Lee et al., 2018; Schaefer et al., 2018). In Indonesia, access to water is important as in Merdada caldera lake, Central Java, a massive water extraction for agricultural purposes (Sudarmadj et al., 2019). The modification of the chemistry of a crater and a caldera lake can have significant implications, notably in the pre and post-eruption

(Gunkel et al, 2008). Volcanic ash deposits in a lake system can increase water toxicity to living biota (D'Addabbo et al., 2015). Tephra and ashfall can contaminate the lacustrine ecosystem (Mayr et al., 2019), e.g. in Lake Van (Eastern Anatolia, Turkey) (Sumita and Schmincke, 2013). However, hazards and managements related to volcanic lake's water quality are poorly developed (Gunkel et al., 2008). For instance, water quality monitoring of volcanic lakes is useful for determining water's common uses (Sudarmadji et al., 2019).

One of the well-known impacts of volcanic eruptions on water bodies is tsunamis. Volcanic eruptions can trigger tsunami through several processes: underwater explosion, volcanic blast, pyroclastic flow, underwater caldera collapse, subaerial failure, and submarine failure (Paris et al., 2014). At least 24 known volcanic eruption-induced tsunamis in Indonesia are listed (Mutaqin et al., 2019). The latest one, which occurred in the Sunda Strait between Java and Sumatra Island in December 2018, was triggered by the eruption of Krakatoa volcano and its partial collapse, as shown from the Sentinel imagery (Figure 2.3). Prior to this event, Giachetti et al. (2012) modeled a flank collapse with a volume of 0.28 km^3 that would generate a tsunami with an initial wave height of 43 m and reach the Java coastline in 35-45 min. There are plenty of similar examples parts in other of the world, notably along the subduction-arcs archipelago, e.g., the 3500-year B.P. tsunami triggered by the eruption of Aniakchak volcano in Alaska (Waythomas and Neal, 1998) and the Late-Bronze age tsunami in Crete and Turkey triggered by the eruption of Santorini volcano in Greece (Novikova et al., 2011).

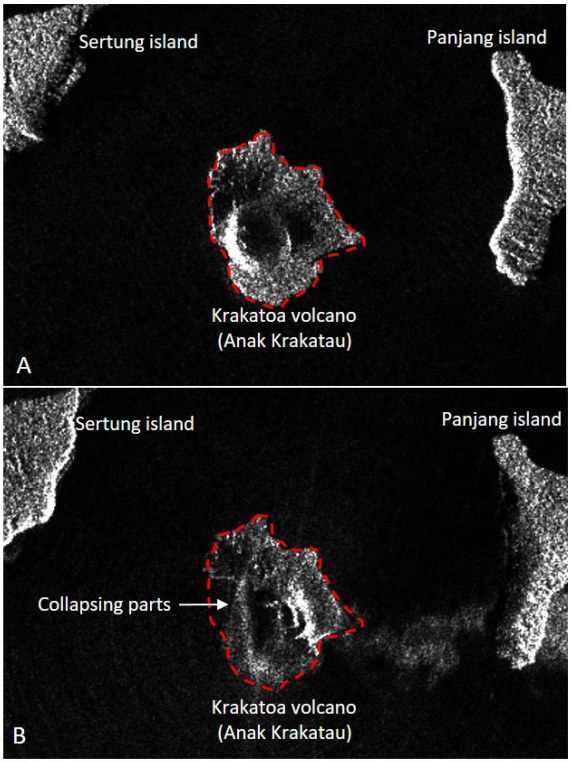

Figure 2.3. Comparison of the Sentinel images (https://apps.sentinel-hub.com/eo-browser/) pre (A) and post-eruption (B) of Krakatoa in December 2018. The red-dashed line marks the initial volcanic island, and the white arrow shows the area of collapse (European Commission, 2018).

Impacts on the society and environment

Major volcanic eruptions can also cause fatal incidents, as indicated by the number of victims. The seven eruptions with the most significant death tolls globally are over 5,000 fatalities (Brown et al., 2017), among of them, four events are located in Indonesia (Table 2.1). The largest number of victims ever recorded in modern history is 36,000 casualties during the 1883 Krakatoa eruption. However, the victims were mostly killed by the eruption-induced tsunami. The highest fatalities caused by a direct impact are recorded in the 1902 Pelée eruption that involved a PDC surge and killed 28,000 people. We assume that the 1257 CE Samalas eruption may also have large death tolls in Indonesia's modern-historical eruptions. Indeed, the Babad Lombok mentions that the city of Pamatan had an estimated population of more than 10,000 inhabitants when the eruption destroyed it.

Table 2.1. List of most enormous fatalities due to volcanic eruptions since 1500 (source: Brown et al., 2017).

Volcano (Year)	Country	Fatalities
Krakatoa (1883)	Indonesia	36,000
Mount Pelée (1902)	Martinique	28,000
Nevado del Ruiz (1985)	Colombia	24,000
Tambora (1815)	Indonesia	12,000
Unzen (1792)	Japan	10,139
Kelud (1586)	Indonesia	10,000
Kelud (1919)	Indonesia	5110

In the event of an eruption, people living on and near the volcano are likely to be directly impacted, which for the farming population means loss of livelihood and access to its means, e.g., in Merapi (Indonesia) and San Vicente (El Salvador) (Bowman and Henquinet, 2015; Warsini et al., 2014). In Indonesia, numerous ancient routes and cities are located on and near active volcanoes. For instance, the ancient Mataram Kingdom of Central Java had routes that climbed on Merapi and Merbabu volcanoes, with temples along the road and associated settlements, to avoid the swamp areas of the Borobudur basin (Gomez et al., 2010). Thus, despite being fertile, many cities and villages are located close to active volcanoes for economic and historical reasons. Similar cases are also figured in Lombok. Based on written sources (Babad Lombok), the colossal eruption of Samalas has buried Pamatan, the capital city of Lombok, which is located in the foot-slope of the volcano. In addition, this ancient city was occupied by thousand of inhabitants, predominantly working on agriculture and aquaculture activities. The written source also described how they responded and conducted an evacuation to avoid the hazards and finally built a new civilization that completely differed from the former. This example emphasizes that ancient civilization also faced livelihood shifting due to volcanic eruptions.

The fragmentation of the volcanic material into fine ash and lapilli creates soils that are rich yet light to work with, and the volcanoes of Indonesia all have vegetated slopes. This land-cover often gets disrupted by eruption processes and there is a balance of vegetation destruction and revegetation occurring on volcanoes (e.g., Tsuyuzaki, 2019). This changing balance is often used to determine the extent of the

volcanic deposits (Syifa et al., 2018). This results from the burying process and the burning process. It was shown at Mt. Shiveluch in Kamchatka and Sarychev Peak in the Kuril Islands (Russia), the pyroclastic surge and lava flows traveled through forest areas burned hectares of trees (Grishin, 2009, 2011). The prediction analysis shows that vegetation recovery requires several decades after the eruption event (Grishin, 2011). On volcanic islands, where most of the land-cover can be lost, the return of natural vegetation succession is controlled by seed dispersals and soil conditions, as it has been shown on the Krakatoa Volcano (Tagawa, 1992). Human intervention is also known to influence vegetation successions and alter the vegetation species that used to grow before an eruption. The vegetation on the flanks of Mt. St. Helens volcano started to increase in number in the first 14 years after the eruption, notably accelerated by management practices (Teltscher and Fassnacht, 2018).

2.1.2. Topographic Reconstruction

The topography or landscape reconstruction can be divided into two different paradigms, i.e. traditional and modern. The traditional topography reconstruction consists of grading and shaping the landscape using a two-dimensional hillslope model, which has an integrated process-response system. In the development of this study, the concern is geomorphic processes on drainage basin, in which digital elevation model (DEM) play as a main data. In general, the geomorphic processes consist of various analyses, i.e. (1) pre-disturbance landscape, (2) geomorphic agent/characteristics, and (3) topographic reconstruction/modelling of steady-state landscape (Toy and Chuse, 2005). Study of topographic reconstruction has several advantages for other studies. In recent decades, it has contribute to the development of archaeological study, which helps describe the paleo-surface conditions in which humans live and conduct their activities (Vermeer et al. 2014).

The terms paleo-surface and paleo-topography are often used to define the Earth's past topographic conditions. Paleo-topography is also called initial topography when it is related to erosion and sedimentation (Temme et al., 2011, 2017). Despite their usefulness for tracking back the landscape condition, the initial topography can also be used to investigate landscapes evolution that have changed slightly over time (van der Meij et al., 2017, 2020). The crucial data for paleo-topographic reconstruction

is paleosol (e.g. depth and age of paleosol) (Vogel and Märker, 2010; 2011; 2012). The difference between the current level of the soil surface and the paleosol surface is the baseline for determining the thickness of the buried material (Pröschel and Lehmkuhl, 2019; Vogel and Märker, 2010). In contrast, if the paleosol is absent, the known buried stratigraphic layer is a key for determining the paleo-surface. In a dramatic change of landscapes such as induced by volcanic eruption, mass movement or tectonic movement, the paleosol has often disappeared. It has become a common problem for paleo-topographic reconstruction (van der Meij et al., 2017).

The current methodological trend for paleo-topographic study is to use various approaches to obtain the depth of the paleosol. Data and computational analysis such as contour generation of paleo-topography is helped through geographic information system (GIS). The digital elevation model (DEM) of the present topography can be obtained by using high-resolution data such as LiDAR and aerial laser scanning (ALS) (Łajczak et al., 2020; Pierik, et al., 2016; Pierik et al., 2017). Real time kinematic (RTK) measurement is also useful for obtaining the present elevation data. The various methods for peleo-topographic modeling using GIS can be divided into two different types, i.e., bottom-up and top-down methods (Meulen et al., 2020) (Figure 2.4). The difference between these two methods is the approach to paleo-DEM generation. The bottom-up method uses depth to paleo-surface data, whereas the top-down method uses the rate of landscape change/evolution. The similarity between the methods is the requirement for paleo-elevation/surface data.

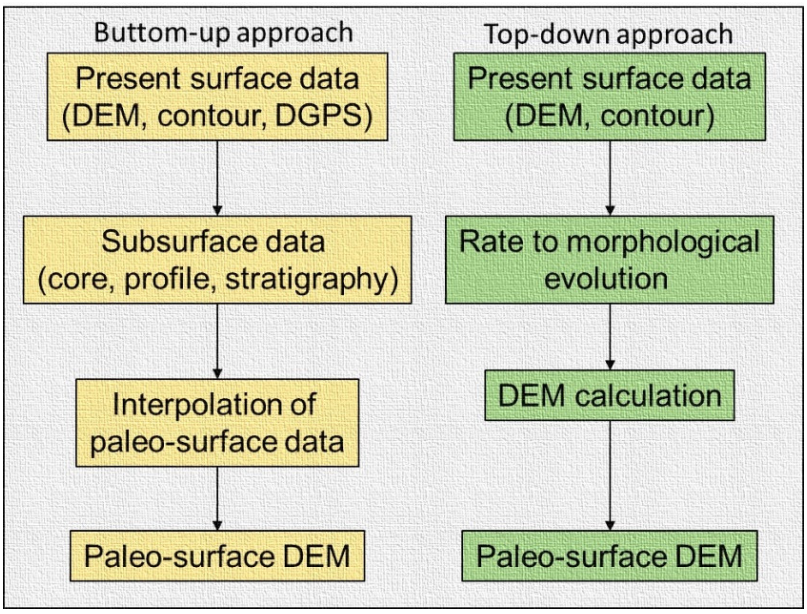

Figure 2.4. Bottom-up and top-down approach in paleto-pographic reconstruction (after Meulen et al., 2020).

One of the recommended methods to obtain paleo-elevation/surface data is using outcrop, borehole or core data. Alternatively, observation of stratigraphy layer data from water-wells is beneficial for supporting paleo-surface data (Mutaqin et al., 2019). Another method is using geophysical surveys, such as ground penetrating radar (GPR) and geoelectrics measurement (resistivity). Geophysics surveys ultimately allows detection of subsurface materials that are beneficial for interpreting paleo-surface (Argote-Espino et al., 2016). However, paleo-topographic reconstruction in built up areas is more challenging due to complex human activity affecting the stratigraphy or sediment layer. In this case, an ancient map is helpful for attributing past topography or paleo-surface data (Pröschel and Lehmkuhl, 2019).

2.1.3. Volcanic Eruptions in Historical Sources

The phenomenon of volcanic eruptions throughout human history is often documented in myth, folktales, legends, songs or verses that were handed down from generation to generation (Blong, 1982; Cashman and Cronin, 2008). This tradition then shifted into the manuscript era, when a story or idea was documented in the form of a book, script, or other writing compilation, which are usually called written records/sources. The story within the written source generally reflects the direct experience of the writer themself as eyewitness account or reports from other

eyewitnesses (Principe et al., 2004; Trigo et al., 2010; Ulusoy et al., 2019). Written sources are typically divided into two types: (i) primary sources providing direct experience or statements from an eyewitness, and (ii) secondary sources providing interpretation of the primary source (Garrison et al., 2018).

Several remarkable eruptions that are recorded in written sources have contributed significantly to the development of the study of volcano and human history. The oldest eruption that is described in detail in a written source is the eruption of Vesuvius in 79 CE (Retief and Cilliers, 2005; Sigurdsson et al., 1982). However, the oldest human record of volcanic eruption might be located in Turkey, i.e., a pictograph that describes the eruption of the Cakallar cone in the Bronze Age (Ulusoy et al., 2019). Eight centuries after the Vesuvius event, in 934 CE, with the Eldgja volcano eruption in Iceland, it was reported that the impacts reached several parts of the world. In China, this eruption, reported in several Chinese historical sources, e.g. Jiuwudaishi and Zizhitongjian, was responsible for the sudden drop in temperature that killed hundreds of people in the country (Fei and Zhou, 2006). This eruption was also responsible for the five days of solar dimming in North Africa, as reported in Rawḍ al-qirṭās (1843) (Brugnatelli and Tibaldi, 2020). Through these written sources, it is known that the eruption of Eldgja impacted globally and triggered societal disturbances in distant parts of the world.

In the medieval era, the eruption of Etna in Italy in 1643 was also documented in historical sources. A document reported by S. Randelli, which is relatively complete, describes the nature and duration of the eruption and the volcanic products. However, the reconstruction of the volcanological and achromagnetic data also presents excellent coherence with the description of S. Randelli (Branca and Vigliotti, 2015). In the eighteen-century, the eruption of an Icelandic volcano, the Laki volcano, had impacts reaching North Africa. As written by Al-Muṣ'abi, a huge fog and smoke covered southern Tunisia for about half a month and was followed by plague in February 1785 (Brugnatelli and Tibaldi, 2020). The next one is the report from Raffles that describes the effects of the Tambora volcano eruption over the Indonesian archipelagos (Brönnimann and Krämer, 2016; Oppenheimer, 2003). The eruption of Tambora in 1815 CE is documented in his book History of Java (1817) and his Memoirs (1830), which contain a detailed eyewitness description of the eruption processes and effects

(Oppenheimer, 2003). In the same century, on a volcanic island in Sunda Strait, Indonesia, the Krakatoa volcano erupted resulting in much violence. This event is reported by Verbeek (1884) in a very detailed manner (Figure 2.5). Verbeek's report is supposedly the most recent detailed eyewitness description of volcanic eruption, containing volcano forecasting, nature and timing of the eruption, impacts, deposit volume calculation, chemical components of ejected materials, and tsunami wave generation.

I have concluded from this that the most violent explosions took place at the following hours: August 27, 5h35m; 6h50m; 10h5m; and 10h.55m Batavia time. By far the most violent of these four was the explosion of 10h5m. Then also an air wave was propelled from Krakatoa which spread in a circular form round this point as pole along the surface of the earth, and travelled no less than three and a quarter times round the whole circumference of the earth. (Verbeek, 1884)

On Tuesday the 11th the reports were more frequent and violent through the whole day: one of the most powerful occurred in the afternoon about 2 o'clock, this was succeeded, for nearly an hour by a tremulous motion of the earth, distinctly indicated by the tremor of large window frames; another comparatively violent explosion occurred late in the afternoon, but the fall of dust was scarcely perceptible. The atmosphere appeared to be loaded with a thick vapour: the Sun was rarely visible, and only at short intervals appearing very obscurely behind a semitransparent substance. (Raffles, 1817 in Oppenheimer, 2003)

Figure 2.5. Example of Verbeek's and Rafles's description as the eyewitness (Oppenheimer, 2003; Verbeek, 1884). These descriptions categorizes as primary written source.

In the study of volcanoes, the combination between historical or written sources and volcanology provides a better illustration of past eruptions. It emphasizes several aspects: (i) physical study or volcanology can provide the nature and timing of volcanic events in the past; (ii) history-archeological study provides the characteristics of the population, migration, and abandoned sites or artifacts; and (iii) the societal response inferred from historical accounts reflects the scale of disruption in the past (Cashman and Giordano, 2008). Learning about the impacts on ancient human populations is a better way to illustrate how past eruption affects the human population and is beneficial in preparing for a future event (Cashman and Giordano, 2008; Martin, 2020; Pyle, 2017).

The issues that have remained discussed in detail among the various studies of volcanic eruptions from historical accounts or written sources are related to (1) the

population's response to the eruption; and (2) how the population conducted emergency response, recovery, and resilience strategy. Not all historical sources are well-documented and archaeological, or eyewitness data is not always available is the main challenge in addressing these issues. Analysis on these issues can provide insight into whether ancient populations implemented disaster management as it is known today. In addition, it can also be used as a lesson on how to survive a catastrophic event. A study by Martin (2020) discusses the short- and long-term responses of inhabitants during past volcanic eruptions. This research relied on a literature review, while a preliminary study on this topic was conducted by Riede (2019). However, these studies made a significant contribution to this topic, namely assessing the past vulnerability condition using the case of Pompeii inhabitants amid the Vesuvius eruptions in 79 CE. Past vulnerability can assess using several key variables, e.g., magnitude and duration of the eruption, recurrence, area coverage, population density, economy, food, mobility, and social network (Martin, 2020). Information on the past vulnerability is essential for identifying the response and resilience strategies conducted by the past civilization (Martin, 2020; Riede, 2019).

2.2. Research Framework

The impacts of volcano eruption might be predicted using the VEI scale. The higher on the VEI scale, the more likely it will cause more disruption, moving from a local to a global scale (Newhall and Self, 1982; Newhall et al., 2018). The local impacts of volcano eruptions are more complex than the global impacts because they deal with geomorphological aspects (Waythomas, 2015). On a global scale, even the global community can be impacted by a volcano from a distant part of the world, but the event frequency is low (Bertrand et al., 1999; Brown et al., 2017). It is related to climate disruption (Brönnimann and Krämer, 2016), air traffic (Gislason et al., 2011; Picquout et al., 2013), and coincident impacts such as famine and plague (Fei et al., 2007; Fell et al., 2020; Guillet et al., 2017). The local impacts on edifice morphology, drainage system, and water body are related to physical impacts that may lead to the landscape (topographic) evolution. The approach to landscape evolution modelling are vary. Simultaneously, the environment and societal impacts from local impacts, together with global impacts, influence the human response to eruption (Figure 2.6). For the ancient

eruptions, investigation of historical sources is necessary to discover the impact on human and their response.

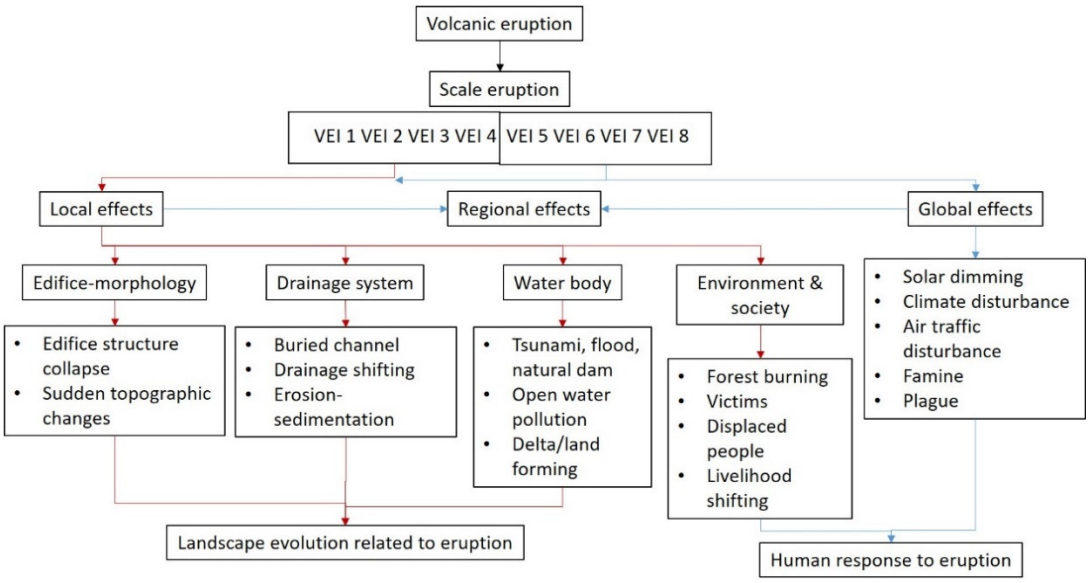

Figure 2.6. Research framework for the study of the impacts of volcanic eruptions on landscape evolution and society.

2.2.1. Far-reaching DAD in Lombok

Debris avalanches modify the volcano's shape, typically leaving a horseshoe shape in a volcanic edifice and sudden morphological changes in the medial and distal parts, i.e., massive aggradation of the terrain and the formation of hummocky hills. This process is one of the significant factors that can drastically change the landscape. In Indonesia, studies on DAD are limited. Several studies, such as in Raung volcano, have successfully identified geomorphic features of the DAD (Siebert, 1984). Litho-stratigraphy and age analysis have also been conducted at debris avalanche in the Galunggung volcano (Bronto, 1989). However, modeling of the debris avalanche emplacement processes was missing in Indonesia's DAD. It may be beneficial to modify the topographic model of Samalas and Rinjani volcanoes before the major eruption in 1257 CE. A simple mathematic for an emplacement process can be conducted using friction number (H/L; height/longitudinal distance) (Siebert 1984, 2002), whereas for 3-dimensional model need to conduct through geographic information system (GIS) analysis (Kelfoun and Druitt, 2005; Davies et al., 2010; Hayakawa et al., 2018; Minimo and Lagmay, 2016; Valverde et al., 2021).

Various metrics and morphological characteristics are widely applied for characterizing DAD, such as the number of hummock, travel distance, area, slope, height, direction, etc. (Delcamp et al., 2017; Salinas and López-Blanco, 2010; Yoshida, 2014; Yoshida et al., 2012). Since the stratigraphic description of the DAD was never performed in Lombok, this analysis is may be the first to be conducted (Figure 2.7). The stratigraphic analysis is also crucial in characterizing the DAD (Norini et al., 2020; Roverato et al., 2011; Valverde et al., 2021; Vezzoli et al., 2017). The age of rock formation in the DAD area is yet to be investigated, except indicated by the geologic map, i.e., Pleistocene (Mangga et al., 1994). This age needs to be evaluated and detailed, as it may be much younger. Another important parameter that requires to be revealed is the triggering factor of the debris avalanche, either related to the eruption or not. Catalogs of eruptions during the Holocene on Lombok have been compiled (Métrich et al., 2017; Nasution et al., 2004). It is useful as a reference for assessing the relationship between the age of the DAD and the age of the eruptions that have been occurred.

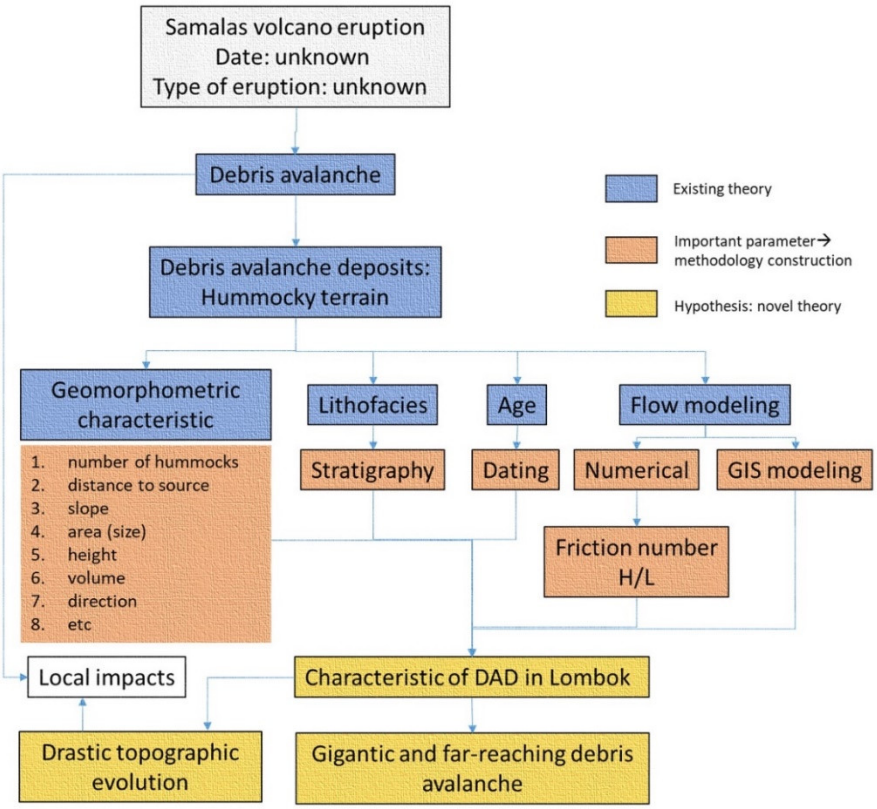

Figure 2.7. Conceptual framework of debris avalanche analysis in Lombok.

2.2.2. Landscape Evolution of the Mataram Plain

Research on large-scale landscape changes is rarely conducted in Indonesia because it is only conducted in a narrow area, such as changes in the river morphology and changes in the morphology of volcanic domes (Darmawan et al., 2018; Hadmoko et al., 2018). Observation on the landscape changes can be distinguished into two types, namely vertical and horizontal. Vertical observations require data in the form of stratigraphic charts (Luberti, 2018), while horizontal observations may require historical map, and series of satellite images (Bi et al., 2021). In Lombok, the eruption of Samalas in 1257 CE caused landscape changes throughout nearly the entire island (Lavigne et al., 2013). The massive discharge of pyroclastic flows causes the local impacts: produced many buried landscapes in Lombok with surface differences of up to 40 meters from the present surface (Mutaqin et al., 2019; Vidal et al., 2015). Litho-stratigraphic evidence for this deposition is provided through a stratigraphic models and isopach maps of the fallout deposits (Lavigne et al., 2013; Vidal et al., 2013). Only the eastern region has modeled its buried landscape (limited only for paleo-DEM and drainage shifting) (Mutaqin et al., 2019).

The buried landscape is also present in several areas, whether directly or indirectly related to volcanic eruptions. In Poland, Krakow city experienced topographic changes during the last millennium averagely increased 2-6 meters due to fluviatile and anthropogenic deposits (Łajczak et al., 2020). Anthropogenic deposits also buried the landscape before Roman civilization in Achen, Germany, for about 3 meters maximum (Pröschel and Lehmkuhl, 2019). Other modelings of paleotopography related to anthropogenic deposits were also conducted in Rome (Luberti, 2018) and Padua, Italy (Mozzi et al., 2017). These researches mainly involve two parameters, namely the current landscape and the ancient/buried landscape (Figure 2.8). Between these two parameters, Łajczak et al. (2020) introduced another essential parameter for describing topographic changes: the delta-high of topography. This parameter is beneficial for reconstructing the rate of sedimentation and volume estimation of deposits between two different times (ancient-present). Another famous city that has a buried topography is Pompeii, Italy, which was affected by pyroclastic

flows from the 79 CE eruption of Vesuvius (Vogel et al., 2011). This area has similar depositional processes and morphological characteristics to study area in Lombok.

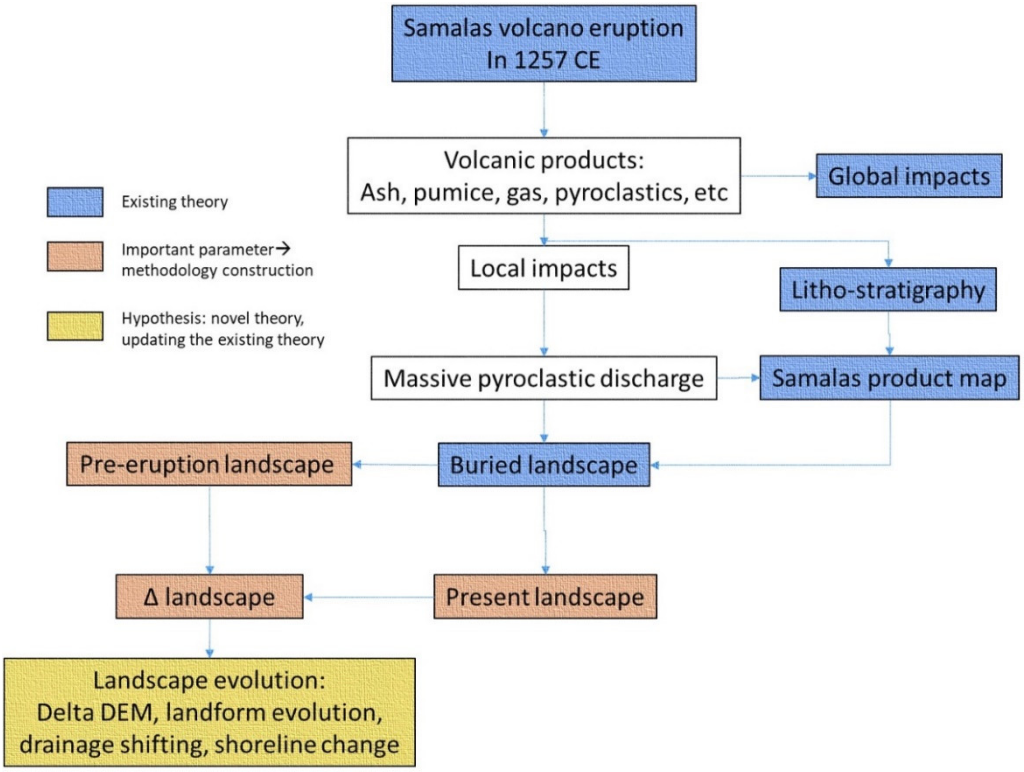

Figure 2.8. Conceptual framework of the landscape evolution analysis in Mataram, Lombok.

2.2.3. Social Impacts and Human Response to the1257 CE Eruption of Samalas

Another type of local impact due to volcanic eruptions is the impact on society and the environment. In the case of the Samalas eruption, the local impact related to societal and environmental conditions has not yet been completely identified. The social and environmental impacts of several historical eruptions in Indonesia are partially revealed by historical sources, such as the Tambora, Krakatoa, Merapi, and Kelud eruptions (Andreastuti, 2006; Brata et al., 2013; Cahyono, 2012; Oppenheimer, 2003). In other parts of the world, such as Europe, where the writing culture is strong, written sources are widely used to reveal this subject, e.g. in Etna, Eldgjá, and Pompeii (Branca and Vigliotti, 2015; Brugnatelli and Tibaldi, 2020; Sigurdsson et al., 1982). The vulnerability assessment of ancient civilizations can also be performed with the help of written sources (Martin, 2020). Those various studies concluded that the

condition of civilization development would determine the response constructed by the community (culture, knowledge, local wisdom, and experience) and in the emergency, recovery, and resilience phases (Figure 2.9). Using similar approach, the social and environmental impacts in Lombok will be revealed through the indigenous written sources from Lombok, e.g., Babad Lombok, Suwung, and Sembalun. The Lombok sources have a different value, i.e., present the geographical features such as toponym.

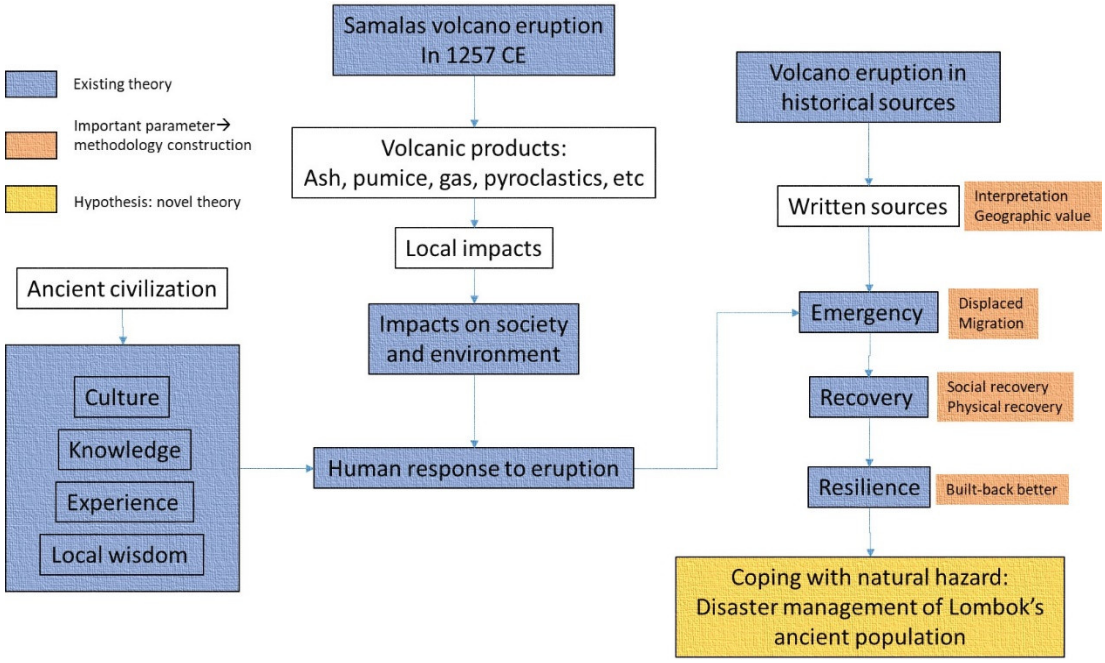

Figure 2.9. Conceptual framework on the analysis of human response to the 1257 CE eruption of Samalas volcano.

CHAPTER 3

The identified critical parameters for each objective in the previous chapter are handy in developing the data acquisition methods and data analyses. This chapter presents the general methodology and the areas of interest for each objective. Several ways to collect data are described, such as field surveys, archival data collection, field measurements, and geospatial data collection. The analysis of each dataset to achieve the objectives is also explained. However, the details of the different analysis methods are explained in Chapters 4-6 of this thesis in the form of scientific articles.

GENERAL METHODOLOGY

3.1. Area of interest

The area of interest in this study is divided into three areas according to the objectives (Figure 3.1). The first objective is focused on the area that is occupied by the debris avalanche deposits (Figure 3.1A). These deposits cover approximately ~500 km^2 in the middle part of Lombok island. This area is administratively included in the Central and East Lombok regency. The summit of Samalas volcano is also included to the area of interest for this objective, especially for modeling purpose of the paleo-topography and debris avalanche emplacement. The second objective is to focus on the area ranges from north to south between the Punikan-Tampole mountain range and Pengsong hill (Figure 3.1B). It is believed that this area is totally occupied by the PDC deposits of the 1257 CE Samalas eruption according to the previous suggestion by Lavigne et al. (2013) and Vidal et al. (2015). In order to investigate the third objective related to the inhabitant response following the eruption, the respective area is the entire island of Lombok (Figure 3.1C). The distribution of inhabitants' migration following the eruption of Samalas was scattered to the entire island of Lombok. Some of them might have migrated to Sumbawa Island.

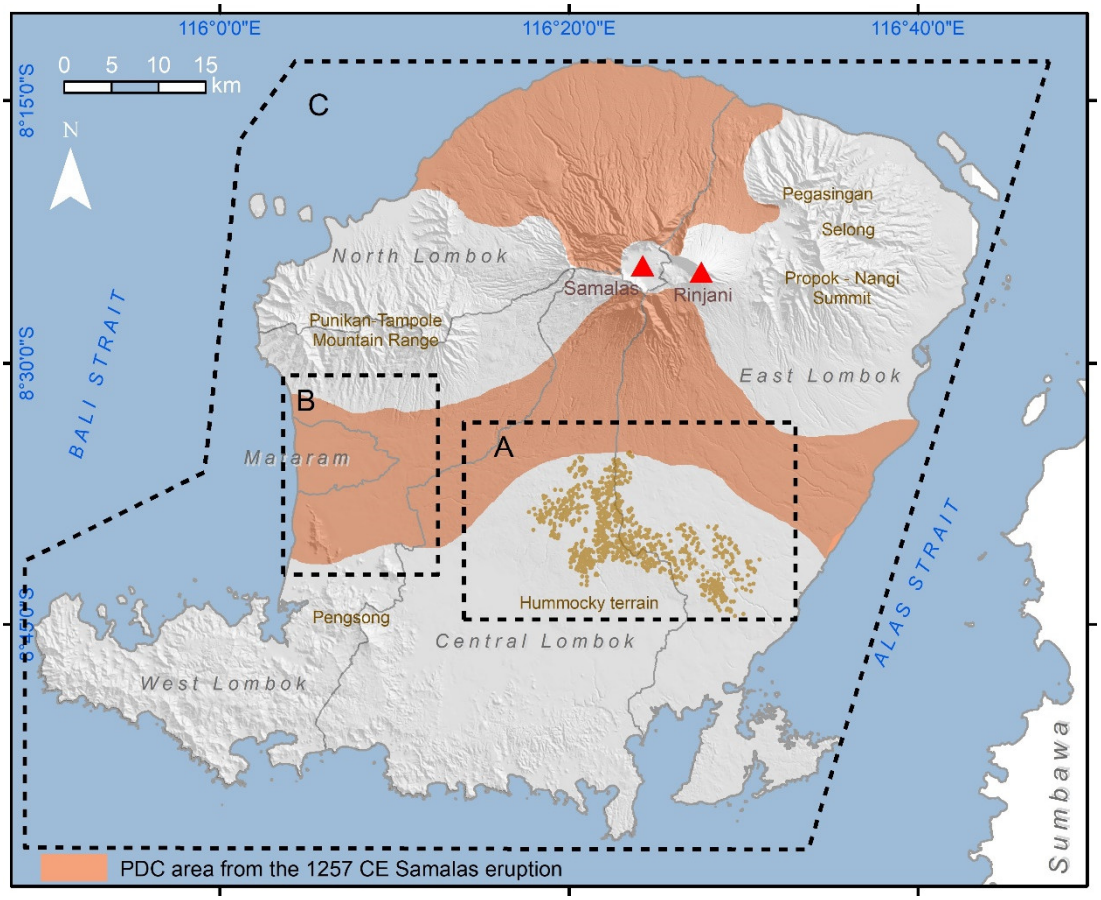

Figure 3.1. The division of the area of interest based on each research objective.

3.2. Data Requirement and Acquisition

A. Reconstruction of Debris Avalanche in Lombok

Analysis of debris avalanche in Lombok involves four datasets: morphology, structure, chronology, and paleo-topography (Table 3.1). Various data sources are needed: field surveys, geospatial data, and archival data. In this analysis, most morphological datasets are generated from geospatial data sources such as satellite imagery (Sentinel), DEMNAS (*DEM Nasional*), and RBI (*Rupa Bumi Indonesia*) map. Sentinel images were retrieved from https://apps.sentinel-hub.com/eo-browser/. Additional DEM, i.e., SRTM (*Shuttle Radar Topography Mission*), was retrieved from https://earthexplorer.usgs.gov/. These data sources are beneficial in delineating the hummock (Figure 3.2). With this delineation, the number, shape, and form of hummocks can be determined, as well as the area of the individual hummock.

Table 3.1. Datasets required for the reconstruction of debris avalanche in Lombok.

No	Dataset	Data type	Source
1	Morphology	Number of hummock	RBI, DEMNAS, satellite image
		Shape of hummock	RBI, DEMNAS, satellite image
		Form oh hummock	RBI, DEMNAS, satellite image
		Distance	RBI, DEMNAS
		Area of hummock	RBI, DEMNAS
		Slope	RBI, DEMNAS
		Flow accumulation	RBI, DEMNAS
		Topographic aspect	RBI, DEMNAS
		Density	RBI, DEMNAS
2	Structure of DAD	Stratigraphic profile	Field survey, archival data
		Resistivity profile	Field survey
3	Paleo-topography	Pre-collapse summit topography	DEMNAS, SRTM
		Present topography	DEMNAS, SRTM
4	Chronology	Radiocarbon age	Field surveys

The morphological dataset also covers the characteristic of the whole DAD, such as area, slope, flow accumulation, aspect, and hummock density. Field surveys were conducted throughout DAD to collect several data such as outcrop, samples for dating, and resistivity measurements (Figure 3.3). These data type is beneficial for analyzing the structure of DAD. Samples for dating analysis were collected in the middle and front areas of DAD, with a total of 10 samples. Archival data on stratigraphy were collected from the Department of Energy and Mineral Resources, Nusa Tenggara Barat province.

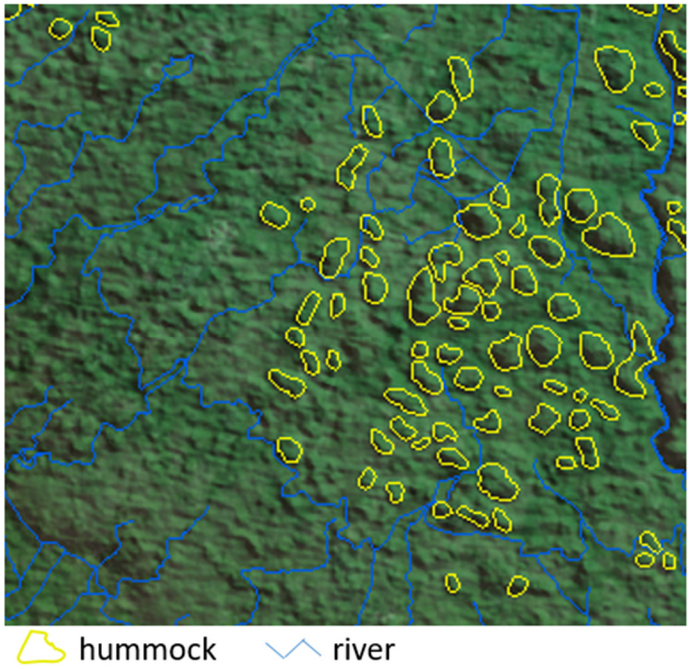

Figure 3.2. Example of hummock delineation.

Figure 3.3. Resistivity measurements in the DAD area.

B. Landscape evolution in the Mataram plain

The paleo-topographic reconstruction in the Mataram plain requires three datasets, namely topography, lithostratigraphy, and resistivity (Table 3.2). The topographic dataset is related to the current topographic condition derived from recent data such as topographic maps, digital elevation model (DEM), and field measurements. The topographic map used in this study is from Peta Rupa Bumi Indonesia (RBI) with a spatial resolution of 1:25,000. Therefore, with this resolution, the contour map is at 12.5

m interval. Using the same data source, rivers and shoreline can be obtained. A more detailed topographic dataset can be obtained from DEMNAS (DEM nasional) with an average resolution of ~8 m. The RBI and DEMNAS data are accessible at https://tanahair.indonesia.go.id/portal-web/. In order to obtain detailed elevation data in the coastal area, Real-Time Kinematik measurements were conducted. A total of 79 locations were measured using this method to obtain elevation points.

Combined methods were applied to obtain stratigraphic dataset. It consist of two methods, field observation and archival data collection. Field observations were conducted in the Mataram area and surroundings, particularly in searching the outcrop. However, due to densely populated areas, outcrops are limited, mainly found in riverbanks and exposed land for quarrying and agriculture purposes. To assist these acquisition methods, water-well observation is helpful in collecting data of the subsurface condition (Figure 3.4). Drillings were also conducted in several sites, which also collected sampling data for radiocarbon dating.

Table 3.2. Datasets required for reconstruction of landscape evolution in the Mataram plain.

No	Dataset	Data type	Source
1	Topography	Elevation	RBI map, RTK measurement, DEMNAS
		Contour	RBI map
		Rivers	RBI map
		Shoreline	RBI map
2	Stratigraphy	Stratigraphy	Outcrop, drilling, water wells observation, archival stratigraphic data
3	Resistivity	Inverted resistivity profile	Field measurement

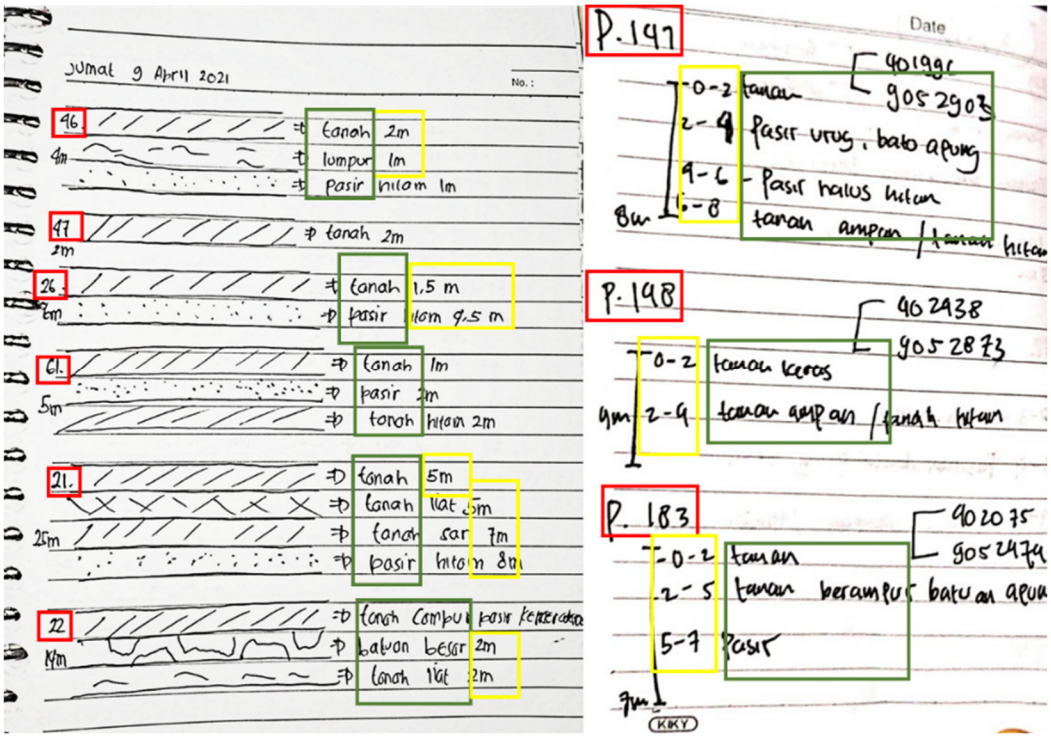

Figure 3.4. Examples of data from the water-well observation. Red box: sample name; green box: material type; yellow box: depth.

The last dataset is resistivity which was collected by field measurements. The measurement campaigns were conducted in 16 lines toward N-S and W-E, i.e., transverse and parallel to the main axes of fluvial and PDC flows. Universitas Mataram and Research Center for Geological Disaster, National Research and Innovation Agency (BRIN) were involved during these measurement campaigns. Measurements were conducted using Superstring R8/IP equipment with 56 Swift electrodes with various spacing: 4, 5, and 10 m. These spacings allowed us to observe subsurface conditions up to 56 - 142 m depth

B. Social impact of the 1257 CE Samalas eruption

Several historical sources were collected to analyze the social impact and human response following the 1257 CE eruption of Samalas (Table 3.3). Three written sources collected from Lombok are Babad Lombok, Babad Sembalun, and Babad Suwung. In collecting the historical dataset, Babad Lombok was obtained from the Museum of Nusa Tenggara Barat (Figure 3.5). The online version can also be found at this link: https://repositori.kemdikbud.go.id/1487/. A copy of Babad Suwung was also obtained from this museum. A translated version of Babad Lombok has been officially published (Suparman, 1994), unfortunately not for Babad Suwung. Similarly, Babad Sembalun has

yet to have an official printed translation. Therefore, copies of the translated version made by the museum and the caretaker in Sembalun were provided as a source of reference for interpreting the *babad*. The geographic feature dataset, i.e., the toponym was collected from RBI map and field surveys. The toponym data is very useful for the geographical reconstruction of the story from the babad. Field surveys were conducted because not all toponyms mentioned in the *babad* are included in the present topographic or administrative maps (RBI).

Table 3.3. Datasets required for analysis of impacts of the 1257 CE Samalas eruption.

No	Dataset	Data type	Source
1	Historical sources	Account of Babad Lombok	Museum of Nusa Tenggara barat (NTB) and online repository
		Account of Babad Sembalun	Customary village of Sembalun
		Account of Babad Suwung	Museum of Nusa Tenggara Barat (NTB)
2	Geographic feature	Toponym	RBI map, field survey

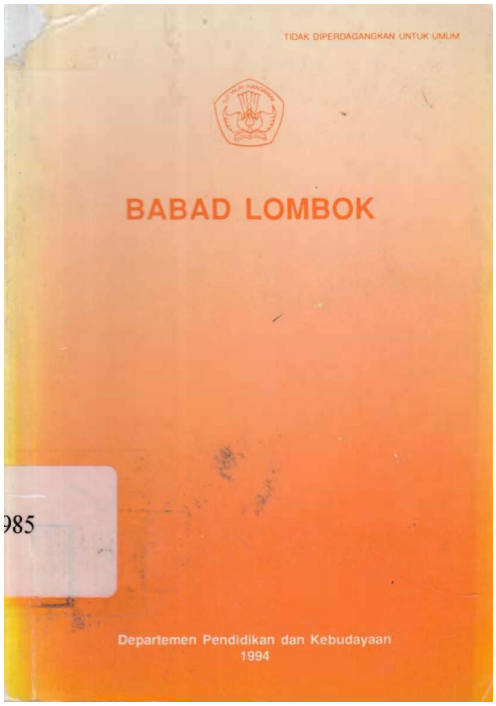

Figure 3.5. Cover book of Babad Lombok transliterated version by Lalu Gde Suparman (1994).

3.3. Data Analysis

A. Analysis of debris avalanche in Lombok

Analysis of morphometry of the hummocky DAD is based on several previous researches, e.g., Salinas and López-Blanco 2010; Yoshida 2014; Yoshida et al. 2012. The structure analysis requires essential data in the form of stratigraphy. Some stratigraphic data in the hummock areas are interpolated transversely and longitudinally along the direction of the hummock to visualize the general bedding of DAD. This analysis will provide an overview of the DAD depositional pattern from the "tail" to the "front" of the DAD. An interpretive analysis using geoelectrical data (resistivity) is also very important to further describe the structure formation of DAD. Stratigraphic descriptions were also performed in the field to distinguish different facies of DAD. The classification of DAD facies is based on Bernard et al. (2019) which consists of boulder size (grain/clast, boulder, megablock, toreva, matrix).

Several researchers use radiocarbon (C14) for dating to interpret the ages of DAD. In this study, the age of DAD will be revealed using this method. The targeted sample is a paleosol or sediment below the DAD deposit. The samples were sent to Poznan

Radiocarbon Laboratory (Poland) and Beta Analytic Inc. (USA). However, in the case of Lombok, paleosol may be absent because it was eroded during the process of travel and deposition. The exposed paleosol may also have been mixed with the older deposits at the foot of the DAD. Therefore, dating on DAD is a challenging task. To address this issue, dating is performed on the alluvial deposits or presumed paleosol below DAD deposits and the lowest soil horizon above DAD's boulder. Finally, age estimation of the DAD is provided within the range of the two dating ages.

Modeling of debris avalanche flow is challenging, especially if the volcano body has been collapsed and no horseshoe or landslide scars are visible, such as in Samalas volcano. However, a modified Samalas pre-caldera summit from Lavigne et al. (2013) using ShapeVolc (Lahitte et al., 2012; Dibacto et al., 2020) can be used as a steady-state of the volcanic body before sector collapse occurs. The volume and direction of hummock parameters become essential keys to reconstructing the estimated shape of the volcanic body after the avalanche process. Minimo and Langmay (2016) and Valverde et al. (2021) used GIS (geographic information system) approach to model the debris avalanche flow and dynamic, one of which is such as using VolcFlow (Kelfoun & Druitt, 2005). Running the model using VolcFlow is relatively convenient if the landslide scar is visible on the volcanic body. However, in the case of Lombok, the scarp was not visible, so the model using VolcFlow had to be tested for trial and error. Alternatively, the reconstruction can be done using a 2D model employing contour line projection (Hayakawa et al., 2018).

B. Analysis of landscape evolution in the Mataram Plain

The landscape evolution analysis through paleo-topographic reconstruction in Lombok was performed using the top-down method Meulen et al. (2020). This method requires the two main datasets, namely topography and stratigraphy. These two datasets are important to calculate the paleo-surface position or the delta-h (Δh). These data are measured on each stratigraphic point. The point of Δh then interpolated to generate the delta-DEM (DDEM). The interpolation method was performed using kriging. Several researchers highly recommend this interpolation method to interpolate the paleo-topographic modeling, for example, Mutaqin et al. (2019), Pröschel and Lehmkuhl (2019), van der Meij et al. (2017), Vermeer et al., (2014), and Vogel and Märker (2010). The paleo-topographic model is obtained by performing DEM subtraction (Schmidt,

2018), i.e., the current DEM (CDEM) is subtracted by the DDEM to produce the paleo-DEM (PDEM). The PDEM result is then validated using root-mean square error (RMSE).

After validating the PDEM, the next step is to construct the paleo-river using the flow accumulation model in ArcMap. The results of this operation were then validated by comparing paleo-rivers with the current river line. The PDEM is also beneficial for the paleo-shoreline modelling. paleo-shoreline was determined by reclassifying the PDEM: the value < 0 meters is classified as marine area. Radiocarbon dating on coral sediment is also used as a reference for chronological sequence of sedimentation process in Mataram Plain.

C. Analysis of the social impacts and inhabitant's response following the 1257 CE Samalas eruption

The principal outcome of the three *babad* from Lombok analyses is determining the inhabitant's response to the Samalas eruption in 1257 CE. Three *babad* are self-contained of the story before the eruption, during the eruption, and after the eruption. Therefore, the stories about the societal impacts of the Samalas eruption can be investigated further. The analysis is conducted by tabulating the various verses related to the Samalas eruption into three phases: before, during, and after the eruption. The tabulation of the transliterated version of the *babad* is then interpreted before being cross-checked and discussed with a *babad* expert and local linguist. The geographical approach is used to assist in the interpretation of the *babad* manuscripts, such as the spatial aspect of the toponym and the environmental aspect of the eruption impact. Various researchers have practiced these analyses in addressing historical/written sources containing the description of volcano eruptions, e.g., Branca et al., 2015; Brugnatelli & Tibaldi, 2020; Jenkins et al., 2020: Mutaqin and Lavigne, 2019.

Verification from chronicle experts and linguists is beneficial to ensure that translations are correctly spelled and avoid misinterpretation. They also helped find the meaning of toponyms, analyze the possibility of a transforming name, and its location on the current map. Toponymic mapping can describe the distribution of population migration. Thus, it can trace the primary source of migration movement amidst the cataclysmic eruption of Samalas. The migration path is then beneficial for tracing the lost speculative city, i.e., Pamatan city. It also helps to figure out the ancient landscape of

Lombok. The regional stratigraphic frameworks from Lavigne et al. (2013) and Vidal et al. (2015) are used to confirm the reliability of the ancient landscape, migration path, and ancient village mapping.

3.4. Conclusion

This chapter presents the various types of data requirements, data sources, and the data collection and analysis method. It can be summarized that three types of data are essential in this study, namely geospatial data (e.g., DEM, imagery, maps), field data (e.g., outcrop, resistivity measurements), and archived data (e.g., stratigraphy, written sources). The geomorphological perspective serves as a critical element in data analysis by investigating morphology, structure, arrangement, and chronology. The combination of geographical perspectives (e.g., space, time, environments) and historical perspectives is also an important element in data analysis for this study. The methodology applied in this study has been scientifically tested and used in previous studies. It has also been improved in accordance with the conditions of data availability, the characteristics of the study area, and the objectives of the analysis. The details of each methodology are described in the result chapters (Chapter 4, 5, and 6) in the form of scientific articles.

CHAPTER 4

The studies of debris avalanches in Indonesia are limited. Although 70 possible debris avalanches were identified, only a few have been extensively studied. This chapter discusses an old debris avalanche from Samalas volcano in Lombok, which has never been studied before. This topic is essential to conduct because the DAD in Lombok is likely among the largest in Indonesia. The sector collapse and the resulting deposit contributed significantly to the Holocene landscape evolution of Lombok Island and played a key role in the distribution of the PDCs during the 1257 CE eruption of Samalas volcano.

THE KALIBABAK DEBRIS AVALANCHE AT SAMALAS VOLCANO

Abstract

The Kalibabak debris avalanche deposit (DAD) that mantles the southern flank of Lombok Island (Indonesia) had not been investigated comprehensively as yet. This contribution bridges this research gap. The method is based on a combination of morphological and internal architecture analysis and radiogenic dating, paleotopographic modeling, and numerical simulation of the DAD. A set of geospatial data supports this method, topographical and geological maps, Digital Elevation Models (DEMs), satellite imagery – in combination with stratigraphic data constructed from field surveys, archived data, and electric resistivity data. Results show that the DAD from Samalas volcano covers an area of 535 km^2, with a deposit width of 41 km and a runout distance up to 39 km from the source. The average deposit thickness is 28 m, reaching a measured local maximum of 58 m. The calculated volume is ~15 km^3. Andesitic breccia boulders and a sandy matrix dominate the deposit. Using ShapeVolc, we reconstruct the pre-DAD paleotopography and used the reconstructed DEM to model the debris avalanche (VolcFlow program). The model provides an estimate of the flow characteristics, but the extent of the modelled deposit does not match the present-day deposit for several reasons: the lack of information on the previous caldera that collapsed and limited understanding of how DADs translate across the landscape. The origin of the DAD was confirmed from 10 radiocarbon dating samples, which indicate that it dates back to 8 ~ 4 k.a. (i.e., 7,000-2,600 BCE). The dating strongly suggests that the DAD was potentially triggered by a subplinian eruption previously dated between 7 and 2.5 ka (i.e., 5,000-500 BCE), which produced the significant pumice fall (Propok pumice) deposits. The gigantic DAD in Lombok therefore occurred between 5,000 and 2,600 BCE.

Keywords: debris avalanche; paleotopography, landscape evolution; Samalas volcano

4.1. Introduction

Volcanic sector collapse and the associated debris avalanches transform the whole volcanic structures and the surrounding, generating typical hummocky structures (Hunt et al., 2018; Siebert, 1984). Examples of significant volcanic sector collapses due to a lateral eruption or lateral blast include the eruption of Bezymianny (Russia) in 1956 (Siebert et al., 1987; Belousov et al., 2007), Mount St. Helens (USA) in 1980 (Glicken, 1996; Voight et al., 1985), and Soufrière Hills (Montserrat) in 1997 (Belousov et al., 2007). Furthermore, debris avalanches can create cascading hazards, particularly when entering a lake or the sea (Camus et al., 1992; Capra et al., 2002), such as the tsunami generated on 22 December 2018 following the Krakatoa sector collapse (Grilli et al., 2019). The global inventory of debris avalanches has registered 1001 events from 594 volcanoes in 52 countries (Dufresne et al., 2021). Among the archipelago countries, Indonesia has over 130 volcanoes. However, although 70 cases of debris avalanches have been inventoried in this country (MacLeod, 1989; Dufresne et al., 2021), only a few studies have attempted to provide the detailed characteristics of their deposits. Some historical debris avalanche events left massive deposits covering wide areas at the footslope of the volcano, such as Gede (MacLeod, 1989), Galunggung (Bronto 1989), Raung (Siebert, 2002; Moktikanana et al. 2021), Merapi (Bronto et al., 2014), and Papandayan in 1772 CE (Pratomo, 2006; Siebert and Roverato, 2021). This last event is believed to have caused 2,957 fatalities (Dufresne et al., 2021).

Dome intrusions, phreatic explosions, and slumping caldera walls are the main trigger of debris avalanche, and more rarely it can also be set off by earthquakes, heavy rain, or snowmelt (Siebert, 1984; Voight et al., 1983). The speed of debris avalanche can reach ~50 to-150 m/s, and the distance covered be tens of kilometers from the source of the sector collapse (Lomoschitz et al. 2008; Ui et al., 1986; van Wyk de Vries and Davies 2015). It results in significant modification of the volcanic landscape and surroundings (Cortés et al. 2010). On the volcano, the sector collapse generally leaves a horseshoe-shaped scar, which can lead to the total collapse of the volcano, or be of smaller amplitude and can even disappear with the growth of a new cone (Bronto et al., 2014). In the surrounding areas, the transported material usually creates a hummocky terrain in the medial to distal area (Siebert, 1984; Lomoschitz et al. 2008; Vezzoli et al. 2017). Hummocks have a distinctive hilly morphology that is easily differentiated from

the surrounding land, thus becoming of the signature of a debris avalanche deposit (DAD) (Hayakawa et al., 2018; Ui 1989; Paguican et al., 2014).

The spatial distribution of DADs and the formation of hummocks are influenced by the material composition (Salinas and López-Blanco 2010; Bernard et al., 2009). It is mainly breccia and unconsolidated materials of various fragment sizes, such as sand, gravel, pebbles, and large boulders (Roverato et al., 2011). Depending on its lithofacies, a DAD can be divided into three types: syn-eruptive DADs, hybrid DADs (gravitational flows, coarsely stratified, poorly sorted); and lahar-transform DADs (rapid flows and hyperconcentrated flows) (Bernard et al., 2019). The classical parameter H/L can be used to illustrate debris avalanche mobility, where H value represents the maximum elevation source or drop height of the displaced mass, and L is the run-out distance (Ui et al., 1986; Siebert et al., 1995). The H/L ratio will generally decrease when the volume of deposits is large (Ui et al., 1986). The shape of the hummocks can also be used to infer the direction of the flow, especially the elongated hummocks that are parallel to the direction of flow (Dufresne and Davies, 2009). A group of aligned hummocks that coincide with the flow direction is called a hummock train (Shea et al., 2008).

In East-Indonesia, a large-scale DAD covers a large portion (>500 km^2) of Lombok Island. Despite of its extent, only limited research exists, and preliminary investigation has not provided a detailed analysis of the morphology, lithology, age, nor the emplacement mechanisms (Malawani et al., 2020). It has also been shown that it controlled the 1257CE pyroclastic density current (PDC), playing an essential role in the geomorphologic evolution of the Island (Vidal et al. 2015; Mutaqin et al. 2019). The most intriguing feature of this undated debris avalanche is the lack of a typical horseshoe-shaped scar, as it has been completely erased by the 1257 CE caldera-forming eruption of Samalas volcano. In this present study, we aims to reconstruct the source of the debris avalanche, the pre-event topography as well as the flowing mechanism. These objectives will be achieved by defining (1) the morphology of the DAD, (2) the internal structure and stratigraphy of the DAD, (3) the modeling of the pre-DAD topography, (4) mass flow modeling, and (5) dating of the event.

4.2. Geological Setting

The Samalas volcano is part of the Rinjani Volcanic Complex, located on Lombok Island (Figure 4.1). Samalas volcano erupted in 1257 CE, leaving a ~6 km wide caldera (Lavigne et al., 2013; Vidal et al., 2015). This caldera is filled by the Segara Anak lake and a rising volcano called the Barujari, which was formed from lava ejected from a new vent in the eastern part of the lake (Rachmat et al. 2016). Six main lava flows were recorded following several effusive eruptions of Barujari in 1944, 1966, 1994, 2004, 2009, and 2015 (Abdul-Jabbar et al., 2019; Solikhin et al., 2010). The Geological Map of Indonesia (1:100,000) displays a large volcaniclastic deposit called Kalibabak Formation, which is characterized by volcanic breccia rocks (Mangga et al., 1994) (Figure 4.1) in the southern part of this volcanic complex. It has very poor sorting, closed fabric, and angular shaped rock fragments (Maryanto, 2009). This formation is predominantly composed of andesitic materials, such as porphyry andesite, basaltic andesite, and basalt (Maryanto et al., 2009).

The observed outcrops along the river banks and on the road-side show that the Kalibabak Formation is composed of heterogenic lithic fragments, dominated by pebbles (5-50 cm) and boulders (up to 2.5 m). Data gathered by Maryanto (2009) on the grain size of 34 samples of breccia matrices in the Kalibabak Formation show that the deposit is poorly sorted with a matrix of sandy gravel (71%). The content of clay material is very low (<5%), suggesting that the water content was limited during the depositional process (Maryanto, 2009). Resistivity investigations of the Kalibabak Formation revealed that it is up to 21 meters thick, and with no significant water content (Sukandi, 2017).

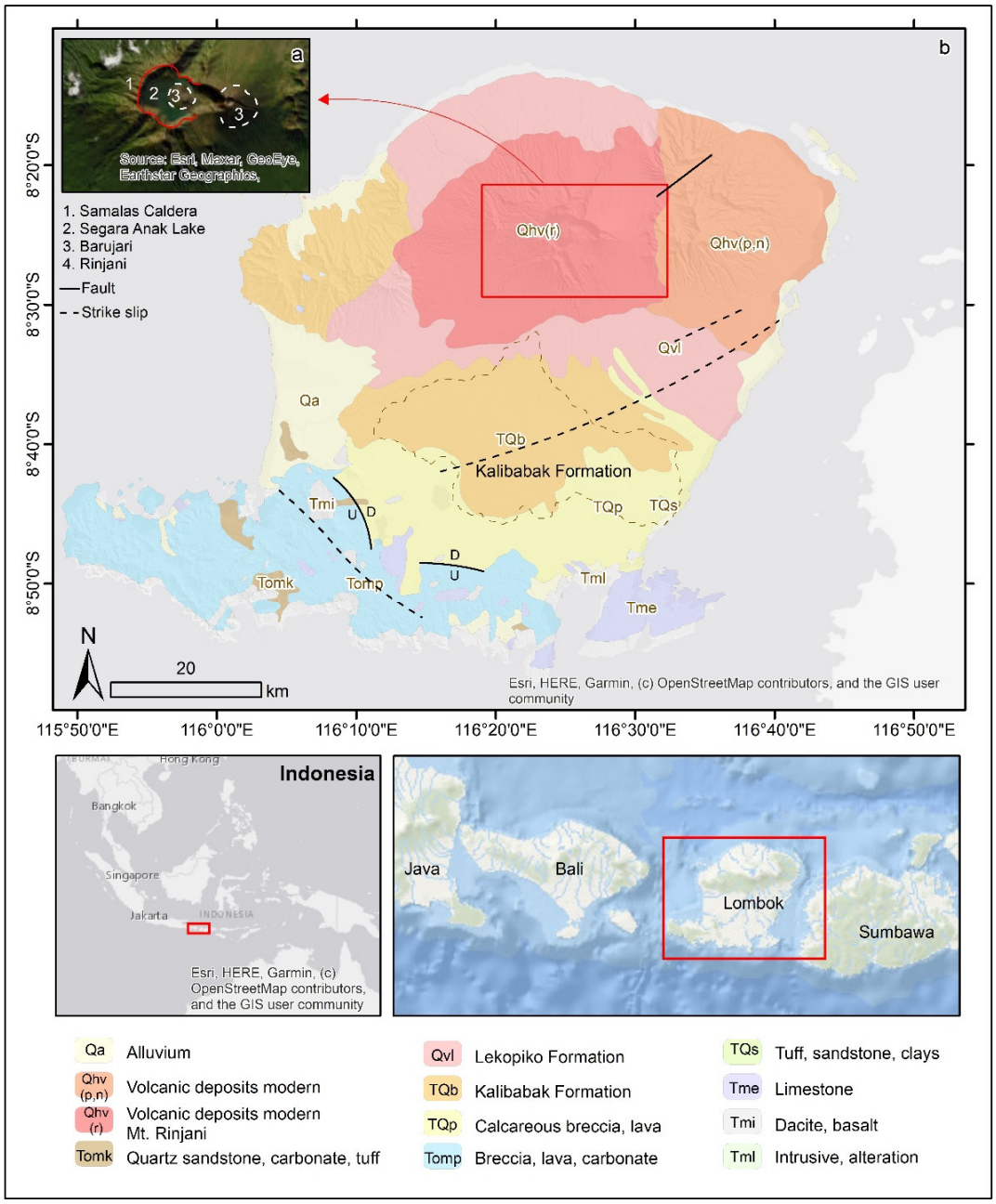

Figure 4.1. Geological Map of Lombok. This map shows that Lombok is composed of volcanic complexes in the north, sedimentary materials in the middle, and uplifted tertiary mountain ranges in the south. The boundary of DAD is indicated by brown-dashed line.

The shape of the Kalibabak formation is wider in the middle and lobate at the distal area. The boundary between the edge and surrounding areas is distinct. To the North of the Kalibabak, the younger Lekopiko formation (Fig. 4.1) is made of a mixture of pyroclastic materials from lahars and pumiceous tuffs (Mangga et al., 1994). The Lekopiko Formation was formed by the syn- and post-eruptive materials of the 1257 CE

eruption of Samalas, and its limit on the geological map corresponds to the limit of the Samalas deposit map provided by Lavigne et al. (2013) and Vidal et al. (2015). Both formations have been attributed to the Samalas volcano. The characteristics of Kalibabak Formation, both the surface and subsurface structure strongly suggest that this formation is a DAD. Since it is identified as Kalibabak Formation on the Geological Map, we called this massive DAD originating from Samalas volcano as Kalibabak DAD.

4.3. Methodology

4.3.1. Morphological Analysis

The morphological analysis of the whole DAD and single hummock was performed. First, we acquired a set of satellite imagery and the digital elevation model (DEM). Two imageries from Sentinel-2 (https://apps.sentinel-hub.com/eo-browser/) and World Imagery from ESRI in ArcMap have been used. The DEMs data used in this research is the DEMNAS (DEM *Nasional*) from the Geospatial Information Agency of Indonesia (https://tanahair.indonesia.go.id/demnas/#/) and SRTM (*Shuttle Radar Topography Mission*) derived from https://earthexplorer.usgs.gov. DEMNAS has been developed from several data sources: IFSAR (5 m resolution), TERRASAR-X (5 m resampling resolution), and ALOS PALSAR (11.25 m resolution) using the EGM2008 vertical datum. The spatial resolution of DEMNAS is 0.27 arc-seconds (~8 m). Completing this dataset the (12.5 m line-intervals) topographic map of Indonesia (*Rupa Bumi Indonesia*) has also been used.

The hummocks were mapped to calculate their spatial distribution, and then classify those according to the morphological parameters. These parameters are the 2D hummock's shape (Bernard et al., 2021), the 3D hummock's form (Bernard et al., 2021), the distance of each hummock to the present caldera (Hayakawa et al., 2018; Siebert, 1984), and the ratio area/size of each hummock (Yoshida, 2014). A plot of the relationship between the hummocks' size and distance from the source was also constructed to analyse the spatial distribution of the morphology as hummocks have been shown to decrease in size with the distance from source (Yoshida, 2013).

After completing the identification of individual hummocks, the next step was to delineate the DAD boundary (Figure 4.2) using the outermost hummocks, and considering the outer limit of the Kalibabak Formation as the maximum extent of the DAD. The differentiation between the different units also relied on the profile line, slope, aspect, and drainage accumulation, as they are commonly used to characterize the morphology of landforms (Garajeh, et al., 2022). Within the DAD area, spatial differentiation based on the density of hummocks has been calculated within the DAD boundary, to identify the clustering of hummocks (hummock train) that are parallel to the flow direction (Shea et al., 2008; Procter et al., 2021). The deposit domains (toreva, hummock, and piedmont domains) (Andrade and van Wyk de Vries, 2010; Norini et al., 2020; Paguican et al., 2014) were also mapped based on the morphological characteristics.

4.3.2. Subsurface Analysis

A. Stratigraphic Survey

Stratigraphic data at 26 locations was collected from field surveys in the exposed areas of opencuts (from mining activity and road construction) and riverbanks (Figure 4.2). Such visual observations have proven precious allies in identification DAD facies (Valverde et al., 2021). To complete the outcrops, a data from 10 sediment cores provided by the Energy and Mineral Resources Agency (ESDM) of West Nusa Tenggara Province were collected, as well as from previous publications (Maryanto, 2009; Maryanto et al., 2009). The stratigraphic data were used to measure the thickness of the DAD. The thickness of the DAD is crucial for calculating the volume and reconstructing the topography of the former Samalas's edifice.

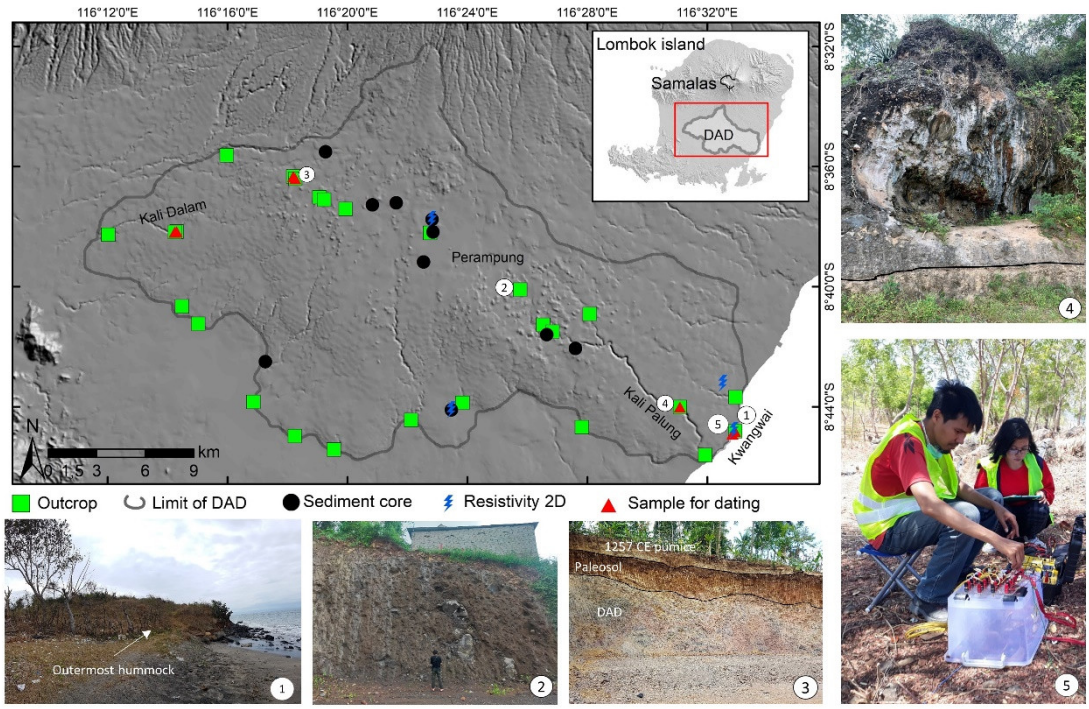

Figure 4.2. Map of sampling sites: outcrop, core, resistivity, and dating. Photos of field survey: the outermost hummock (1), opencut hummocks (2 and 3), escarpment in the river valley (4), and resistivity measurement (5).

B. Resistivity Measurement

The resistivity measurements campaign was conducted together with the LIPI (now BRIN, *Indonesian Research Agency*) and UNRAM (*Universitas Mataram*). Measurements using Dipole-Dipole configuration were conducted with a span of ~1000 m in total at Surabaya-Lepak, East Lombok (Figure 4.2). The locations were chosen to investigate the subsurface conditions on the distal part of DAD and to verify the limit of the DAD. The measurements were conducted using the SuperSting R8/IP with 56 swift electrodes. This configuration employed 10 m electrode spacing allowing us to observe the subsurface condition up to ~142 m deep. The data was then inversed into a 2D resistivity profile.

Additional resistivity measurements using a Wenner configuration were conducted on eight lines (150-300 m), with three in Jenggik (the upper area of the DAD), three in Kwang Wai (in the hummock hills), and two in Janapria (the distal area) (Appendix A; Table A1). All resistivity results were interpreted to delineate the limit of DAD layer based on a resistivity value matching with the stratigraphic layers

from two referenced cores in Jenggik and Janapria, and in comparison with previous measurements (Wiranata et al., 2018).

4.3.3. Paleo-topographic Modeling

In order to reconstruct the morphology of Samalas volcano before the debris avalanche, the pre-collapse topography was modeled using the ShapeVolc model (Lahitte et al., 2012; Dibacto et al., 2020). For this reconstruction, we have initially identified and separated the volcanic sectors of Samalas volcano that were part of the Old Samalas (< 1257 CE) from those of the Young Samalas (Figure 4.3a). From this division, the ridges of the Old Samalas were used as the constraining points (CPs) to model the pre-collapse edifice (Figure 3b), as they are relatively stable compared to the other features more subject to erosion and deposition (Dibacto et al., 2020). The low-land CPs were generated by subtracting the deposit thickness (field data) from the present topography of the DAD, based on the stratigraphic analysis (Figure 4.3b).

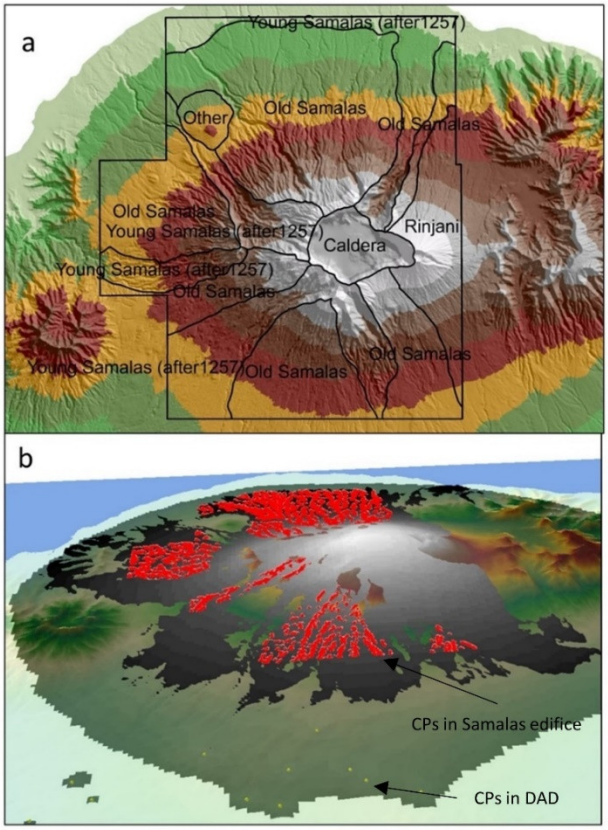

Figure 4.3. Topography differentiation of the Samalas edifice between Old and Young Samalas (a) to generate constraining points (CPs) for reconstructing the pre-

collapse topography (b). Red points are CPs in the Samalas edifice, and yellow are CPs in the DAD.

4.3.4. Metrics Calculation

The metrics of the DAD (Table 4.1 and Fig. 4.4) have been calculated from the 11 parameters summarized by Bernard et al. (2021), using a combination of the topographic data and the pre-DAD topography (Fig. 4.4). Although most of the parameters can be calculated directly from the topographic map, the volume of the DAD may have a considerable error (Bernard et al., 2021). To palliate this issue, we have applied two methods to calculate the volume: first, using the calculation formula shown in Table 1, and second, subtracting the present DEM from the pre-avalanche DEM (PDEM). This PDEM is the topography before the DAD, which was created by kriging interpolation of the pre-DAD points (PSs). The difference between the present altitude and the thickness of the DAD defines the PS. In the case of the DAD in Lombok, although the pre-avalanche topography is a reconstruction result and the DAD thickness data is also limited, the average volume from these two measurements may be the best estimation we can obtain.

Table 4.1. Description and calculation formula of debris avalanche metrics (Bernard et al., 2021).

No	Parameter / Acronym	Description
1	Deposit length / L_D	Distance from the front to the tail
2	Deposit width / W_D	Maximum distance between the margins
3	Deposit area / A_D	Surface area in plain view
4	Deposit height / H_D	Altitude difference between the tail and the front
5	Deposit declivity / α_D	Average slope ($\alpha_D = H_D / L_D$)
6	Deposit thickness / T_D	Average thickness
7	Deposit volume / V_D	Volume calculation ($V_D = A_D / T_D$)
8	Deposit aspect ratio / AR_D	Ratio between the average thickness and the radius of circle area ($AR_D = T_D / \sqrt{A_D/\pi}$)
9	Runout distance / L	Distance from the head (scar) to the front
10	Drop height / H	Altitude difference between the maximum pre-landslide topography and the front

11	Friction coefficient / H/L	Ratio between the drop height and runout distance

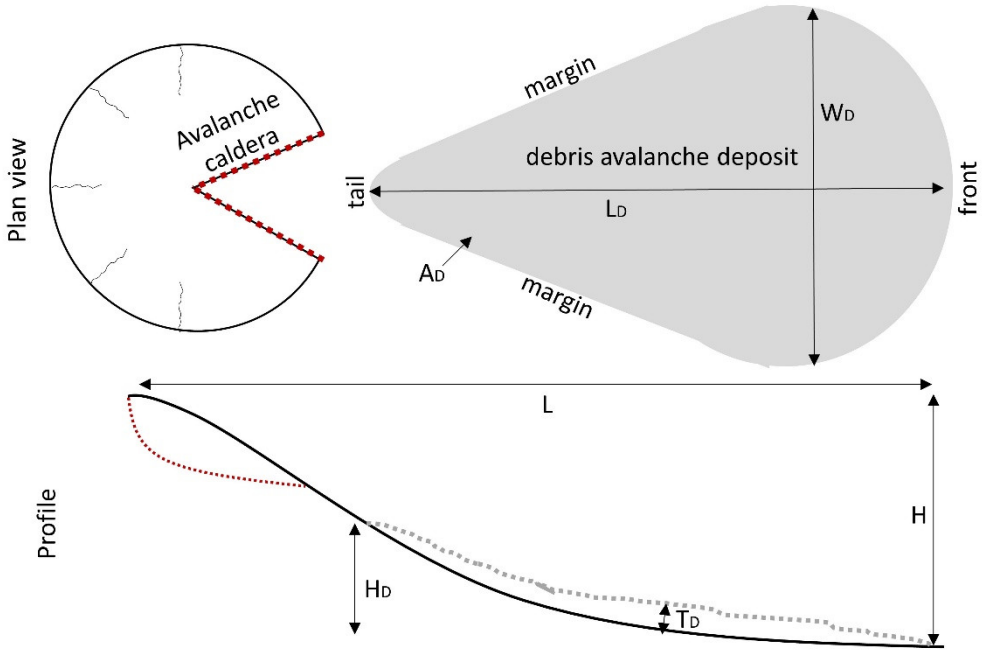

Figure 4.4. Sketch and cross-section of debris avalanche metrics.

4.3.5. Debris Avalanche Modeling

To explore the shape, the location and the orientation of the caldera avalanche, we have used VolcFlow (Kelfoun 2011) and we have tried to reproduce the observed debris avalanche deposit. The VolcFlow numerical code has been designed to simulate volcanic flows and especially debris avalanches on land or underwater (Kelfoun and Druitt, 2005; Kelfoun et al., 2010; Paris et al., 2017). VolcFlow needs the surface of the topography before the collapse, the topography of the sliding surface as well as the rheological parameters of the avalanche. The VolcFlow simulations used the paleotopography reconstructed using ShapeVolc, where the Samalas summit was fully restored and the DAD deposit at the lower part was removed. Several shapes and orientations of the sliding surface were explored using a spoon-like morphology defined by:

$$z_s = e^{-a \times r} + b\theta^2 + z_{\min} \quad \text{..... (Eq. 1)}$$

In the Eq. 1, r is the radial distance and θ the tangential distance. The parameters a, b and z_{min} define the depth and the width of the caldera avalanche and its elevation. We varied them while imposing a destabilised volume compatible with the field observations (~15 km^3). We also varied the orientation of the radial distance from N180 to N210. Based on previous studies (e.g., Kelfoun and Druitt, 2005; Kelfoun et al., 2010; Paris et al., 2017), we have used a rheology made by a yield strength T and a turbulent stress $\xi\rho u^2$ where ρ is the avalanche density and u its velocity (Kelfoun, 2011). For debris avalanche previously studied, the value of T is about 50 kPa and the value of ξ (Voellmy coefficient) lower than 0.01. The VolcFlow simulation utilized the modeling results of paleotopography performed using ShapeVolc, where the Samalas summit was fully restored, and the DAD deposit at the lower part was removed.

4.3.6. Radiocarbon Dating

Paleosols and detritus sediments above and below the DAD unit were sampled for dating the debris avalanche (Figure 4.2). We collected samples (1) below the DAD to estimate the maximum age, and (2) samples above the DAD limit to estimate the minimum age. This bracketing method of DAD is based on the method applied at the Antuco volcano (Chile) (Romero et al., 2022), because dating of past debris avalanche events is particularly challenging when no charcoals are found (Grosse et al., 2022), as it was the case in this research.

Dating was performed on ten samples from four different sites, consisting of four paleosols above the DAD, four paleosols below the DAD, and two detritus sediments below the DAD. The paleosols above the DAD layer are buried by the syn-eruptive deposits of the 1257 CE Samalas eruption and have formed relatively thick soil (~1 m). Two paleosols below DAD at a distance of ~300 m one from another were collected from Kali Dalam river valley (Figure 4.2). Paleosol samples from Kwang Wai beach were collected on the marine notches (hummock cliff). The outermost hummock in Kwang Wai beach was chosen as the sampling site because this location is predicted to have minimum paleosol erosion. Two detritus sediments were collected from Kali Palung river valley and exposed beach-floor at Kwang Wai beach (Figure 4.2). The results of laboratory analysis are given as age BP (Before

Present-before 1950 CE). These ages were then calibrated using Calib 8.2 (http://calib.org/calib/) employing the SHCal20 curve (Hogg et al. 2020). The calibrated ages were then correlated to the previous dating of Rinjani Volcanic Complex eruption chronology since the Holocene (Nasution et al., 2010; Métrich et al., 2017).

4.4. Results

4.4.1. Morphological Characteristics

The 2D shape of hummocks is defined by the circular form of individual hummock delineations: elongated, rectangular, polygonal, and rounded hummocks. A total of 1704 hummocks have been identified. Rounded hummocks dominate the study area, with 771. Elongated hummocks that indicate the mass flow direction comprise 16% of the total (265 hummocks). The 3D form of hummock in conical and ridge has an almost similar distribution, comprising 41% and 43% of the total, whereas the pyramidal hummock is only 3% (44 hummocks). The mapping results show that the hummock shape is not related to the sliding distance. All hummock shapes are well distributed across the DAD body. However, rounded hummocks have the farthest coverage compared to the other shapes. Similarly, all hummock forms are well distributed in the DAD body, except for the pyramidal form, which is only present in the middle area.

The farthest hummock is 39.5 km from the present caldera, whereas the nearest is 18.6 km. The majority of hummocks are distributed around 30-31 km from the present caldera rim (Figure 4.6a). The outermost hummock was identified in the Kwang Wai beach, which formed a ~3 m high cliff. In this location nearly half of the hummock hill has been eroded by the sea waves. At distances below 23 km, the number of hummocks is relatively low, whereas further than 23 km from the caldera rim, the distribution gradually increases to a maximum distribution at 31 km. After reaching this distance, the hummocks' density rapidly decreases (Figure 4.5c, 4.5d). Large hummocks with an area >8 ha is distributed across a distance of 22-23 km, whereas the average size of hummocks (2 ha) is distributed along the entire DAD body (Figure 4.6d). Based on its distribution, the hummocks of the Kalibabak DAD are not following the general distributive pattern of hummock, i.e., hummocks

decrease in size with increasing distance from the source. The hummocks with above-average size were found at a maximum distance of 30 km. The linear correlation also suggests that the relationship between area and distance is very low, with R-squared value of 0.02.

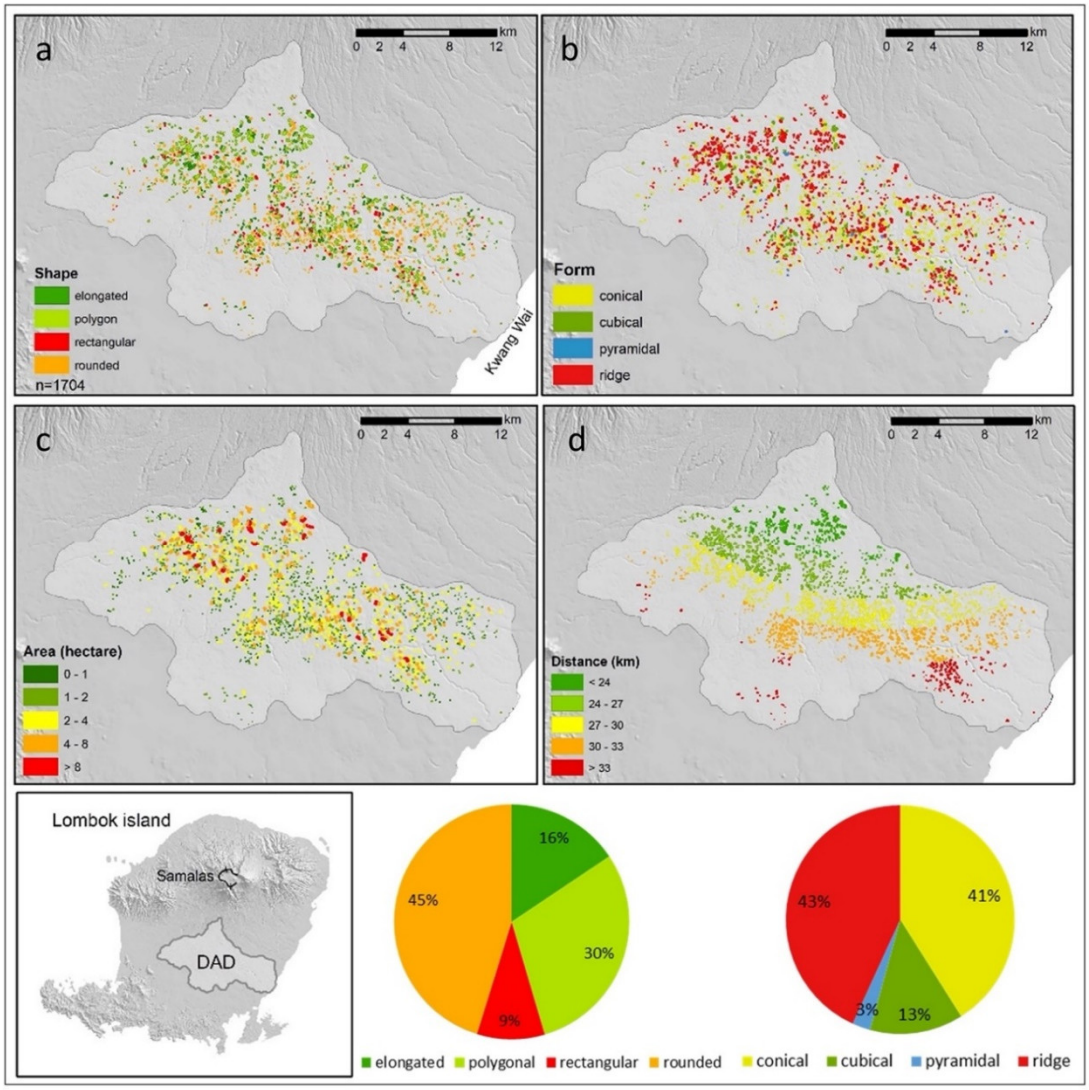

Figure 4.5. Map of morphological characteristics of individual hummocks: shape (a), form (b), area (c), distance (d). Pie charts indicate the percentage of hummock shape (left) and hummock form (right).

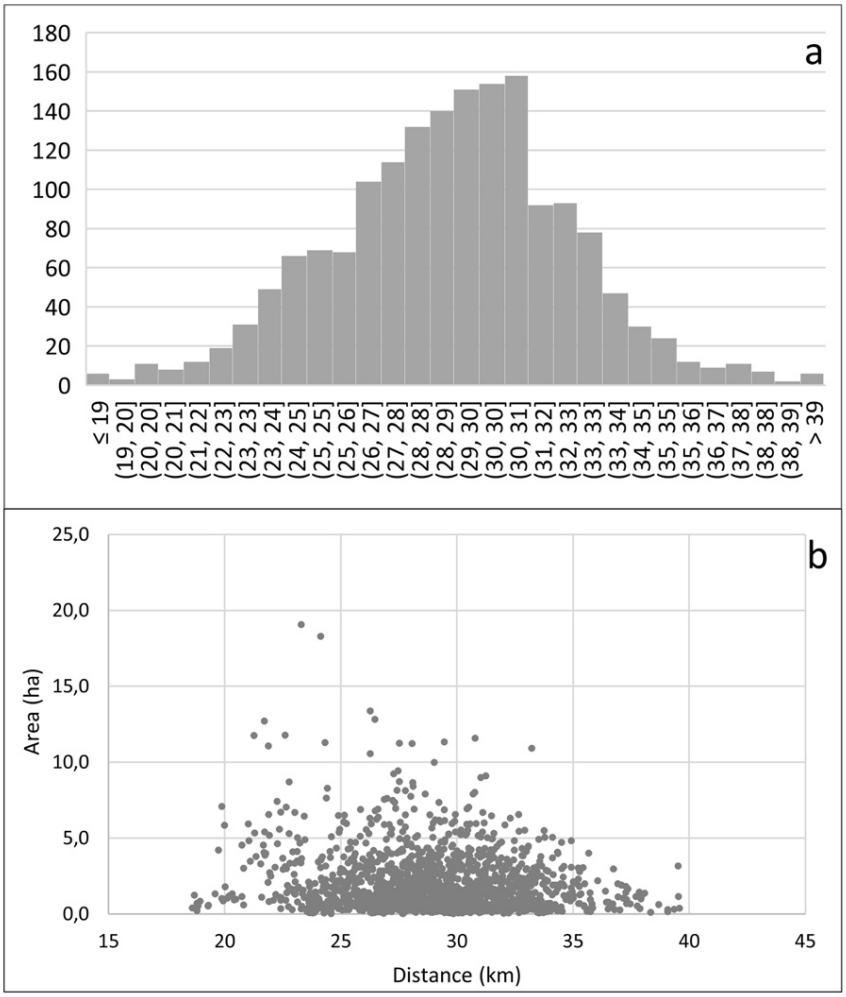

Figure 4.6. Histogram of hummocks distribution (a) and chart of area vs. distance from the source (b).

Relatively flat slopes dominate the entire DAD, indicating the intra-hummock area. Steep slopes are distributed in river valleys, such as Kali Dalam in the west and Kali Palung in the east (Figure 4.7a). The slope information indicates that the river valleys have the steepest slope, showing subsequent intense erosion in these areas. Flow accumulation analysis helps detect this post-collapse deposition process. The analysis of flow accumulation analysis in the DAD shows that the drainage system is centered on three river valleys, namely Kali Dalam in the west, Kali Dodokan in the middle, and Kali Palung in the east (Figure 4.7b). Three dominant aspects (azimuth of terrain surface) are also present in the study area: southeast, south, and southwest. (Figure 7c). This aspect domination may provide an additional information for interpreting the flow behavior of the DAD. The mass flow

is mainly oriented southwards, and as the paleo-slope gradually turns gentler, it then spreads towards the southeast and southwest. This suggestion is also supported by the characteristic of hummock density that clustered in the middle-south area (Figure 4.7d). This area is suggested as the centroid of DAD, where the distribution of hummocks is the densest (18/km^2, with an average of 3/km^2)

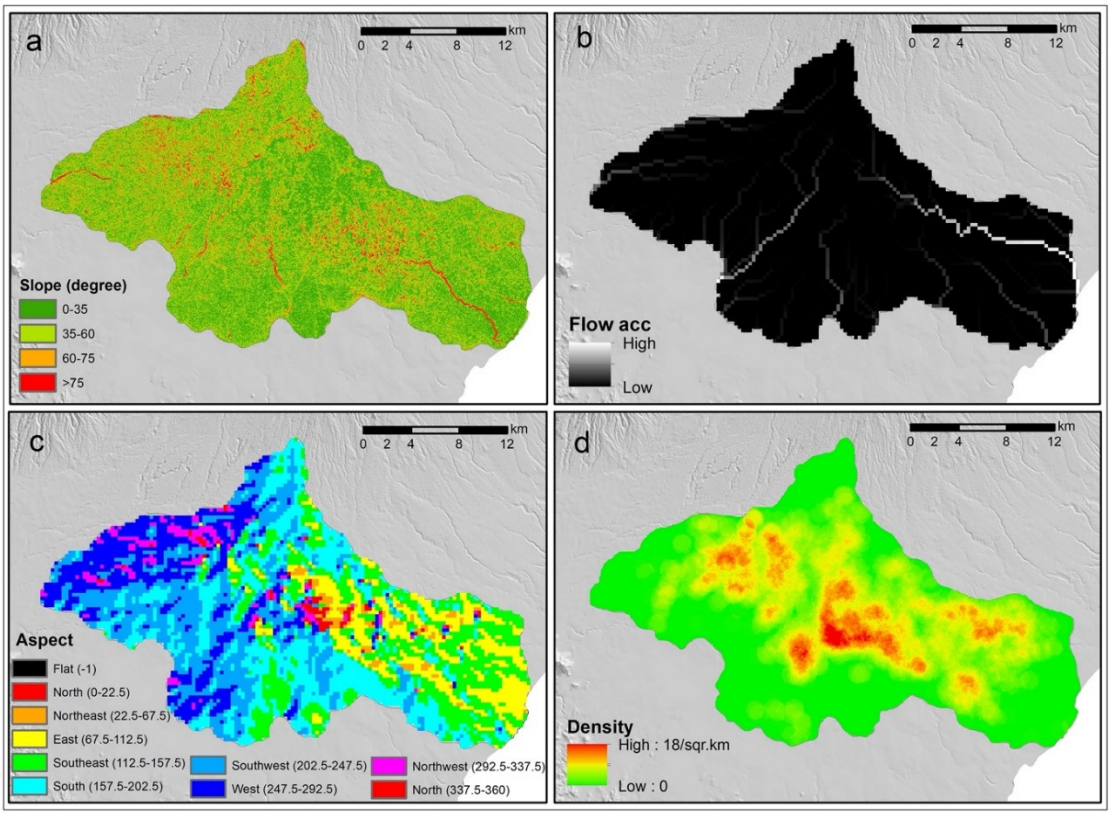

Figure 4.7. Map of morphological characteristics of DAD: slope (a), flow accumulation (b), aspect (c), hummock density (d).

Three main domains of the DAD can be distinguished between toreva, hummock, and piedmont (Figure 4.8a). Toreva occupies a small part of the upper area of the DAD with ~3 km along a linear transect (Fig. 4.8b). The hummock domain is the largest unit in the DAD of Samalas with ~18 km span. The piedmont domain is smaller, covering ~5 km long in the distal part of DAD. Two colluvial fans have been identified in the southern area, characterized by redelivery of debris avalanche deposits, involving mass wasting and fluvial transport. Other profile lines in the W-E (line CD) and the N-S (line EF) directions show the configuration of the densest area of the hummock. (Figure 4.8cd). In these two topographic profiles, “h” marks the peak of each hummock. On the profile CD (Figure 4.8c), nine hummocks

have been identified, with an average distance of 350 m between each. A wider space separates the hummocks on profile EF (Figure 4.8d), with an average of 450 m between identified hummocks. Across these two profiles, most hummocks are 7 m high and can reach a maximum of 20 m.

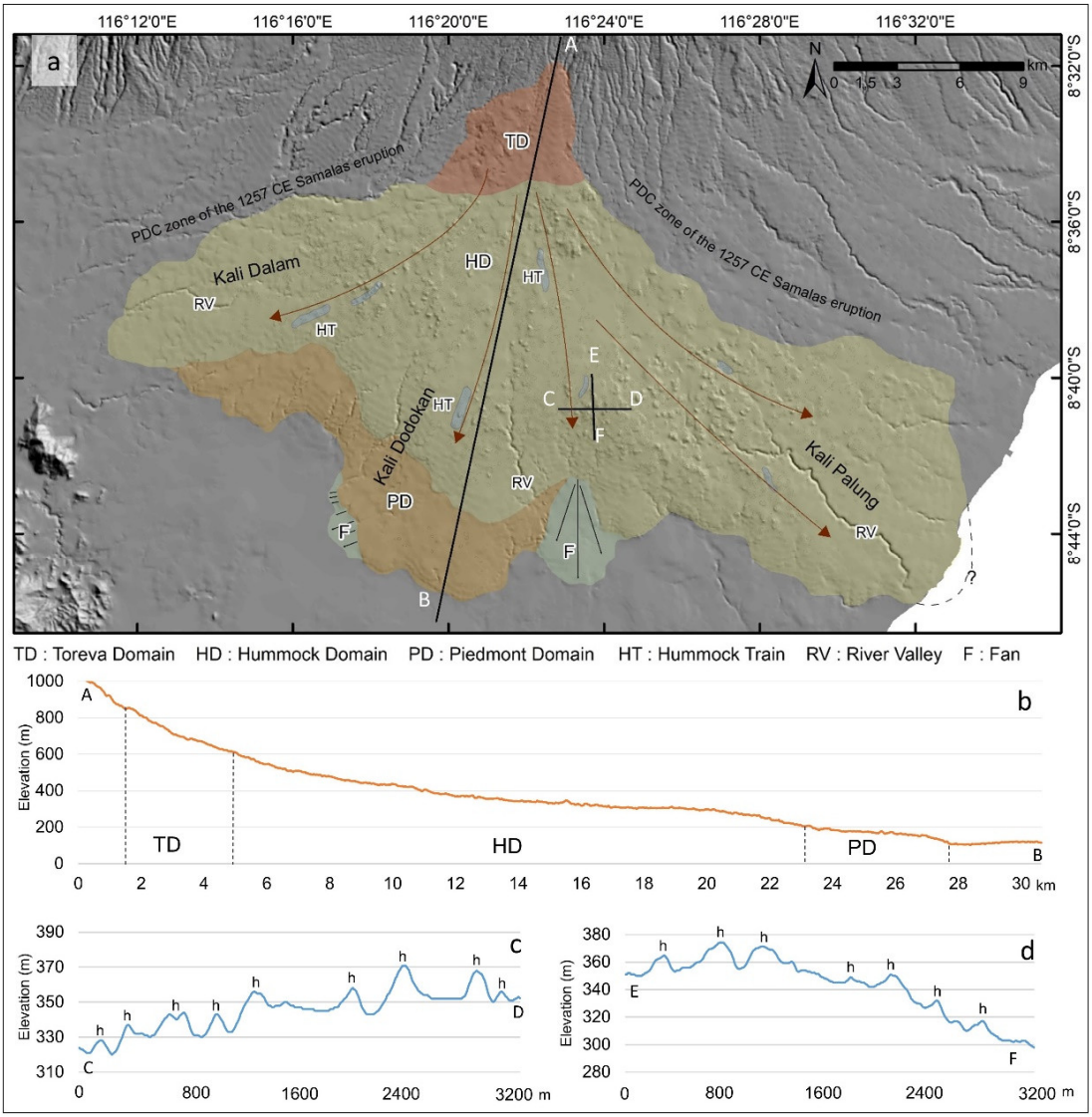

Figure 4.8. Map of the DAD extent in Lombok, (a) showing the delineation of DAD domain and the suggested mass flow directions. (b) The profile line AB displays the topography from upper to lower area of DAD along N-S axis. A sudden break of slope indicate the boundary of DAD area. Profile lines CD (c) and EF (d) in the densest area of hummock indicate the configuration of peak, valley, and flat areas of hummocks.

Hummock trains (HTs) are distributed in the middle and lower parts of the hummock domain. The HTs in Kalibabak DAD generally indicate three directions: the west part indicates a southwest direction, the middle part indicates a southward direction, and the east part indicates a southeast direction. The extension of the HTs (dark-brown arrows in Figure 4.8a) can be used to portray the possible direction of the avalanche flow. Other morphological characteristics, such as aspect and hummock density, have also supported this suggested flow direction.

4.4.2. Structure of DAD

Two types of deposits have been found along the river channels: (a) large boulder blocks and (b) clast-matrix mixtures. In the middle stream of Kali Palung river (26 km from the caldera rim, Figure 4.9a), large boulder blocks are scattered along the river channel. These large boulder blocks, which are visible during low water-stage are derived from erosional processes along the valley of Kali Palung. In the distal area of the DAD, 35 km from the caldera rim, rivers are dominated by clasts of smaller size mixed with a sandy matrix (e.g., in the Perampung river). Over this DAD deposit, fluvial material composed of sandy silt cover this DAD layer (Figure 4.9b). In another part of the Kali Palung valley, at 35 km from the caldera, blocks and clasts dominate the DAD, which is up to 10 m thick (Figure 4.9c). The DAD at this location is directly in contact with an older weathered layer, identified as a calcareous breccia formation named the Kali Palung (Mangga et al., 1994).

Twenty-nine kilometers to the south of the caldera rim, nearly homogeneous DAD structures can be observed, with sheeted lava (Figure 4.9d) including jigsaw cracks (Figure 4.9e). Another hummock located at 28 km south of the caldera rim, contains more than 75% sand matrix. Many clasts are also visible, along with meter-sizes clasts (Figure 4.9f). In this sector of the volcanic flank no pyroclastic material could be observed, while in the southwest sector, at 23 km distance from the caldera rim, a mantle of pumice-fall from the 1257 CE Samalas eruption can be observed. In locations where the pumice layers were found, a relatively thick (~1.5 m) paleosol developed in between the Samalas 1257 CE eruption and the DAD, showing that the two events were not concomitant (Figure 4.9g).

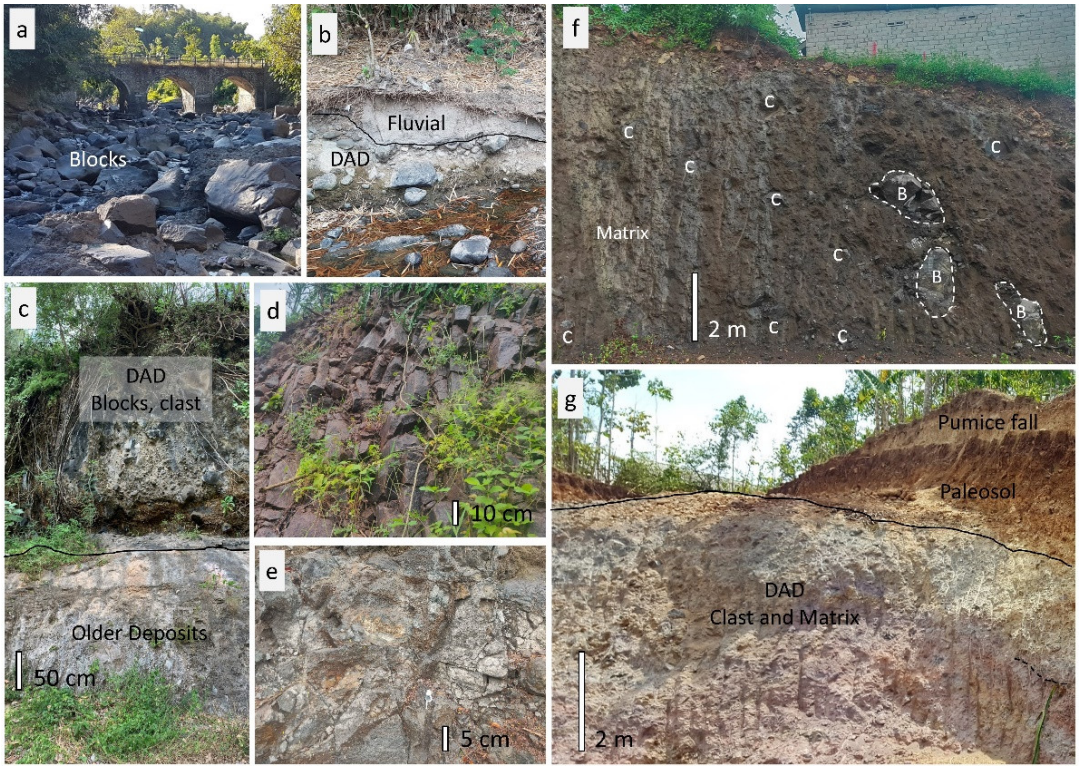

Figure 4.9. Structure of the DA in various locations. (a) Scattered boulders along the river channel in the middle stream of Kali Palung. (b) The DAD in Perampung river banks is covered by fluvial deposits. (c) Another place in the Kali Palung valley, block and clast are dominated the escarpment. Sheeted lava (d) is observed in the opencut hummock with some jigsaw cracks (e). (f) An opencut hummock composes of blocks (B), clasts (C), and matrices. (g) A complex outcrop in the western part of the study area records the pumice fall from the 1257 CE eruption, paleosol, and DAD facies (clast and matrix).

Completing the outcrop observations, a total of 10 cores were collected from ESDM (Figure 4.10). Based on these data, the lithological type of the DAD could be confirmed to be a mixture of breccia, lava, boulders, and consolidated tuff-gravelly sand, overlain by recent soil of varying thicknesses. The formations underneath the debris avalanche deposition have similar characteristics in most cores. It is characterized by weathered tuff-lapilli, calcareous breccia, and gravelly sand with boulder, and can be linked to the Kali Palung rock formation (Geological Map; Mangga et al., 1994). The minimum thickness (12 m) of the DAD is located at the Janapria core (Figure 4.10a), whereas the maximum thickness (58 m) is found from the Peresak Daye core (Figure 4.10b), and from the Suwangi core (55m). Correlation between cores in the NS direction (Jenggik-Janapria) shows that the DAD thickness

significantly decreases according to the flow direction (Figure 4.10a), whereas in the WE direction (Sapit-Tanak Kaken), the DAD's thickness increases in the center and decreases near the margins (Figure 4.10b).

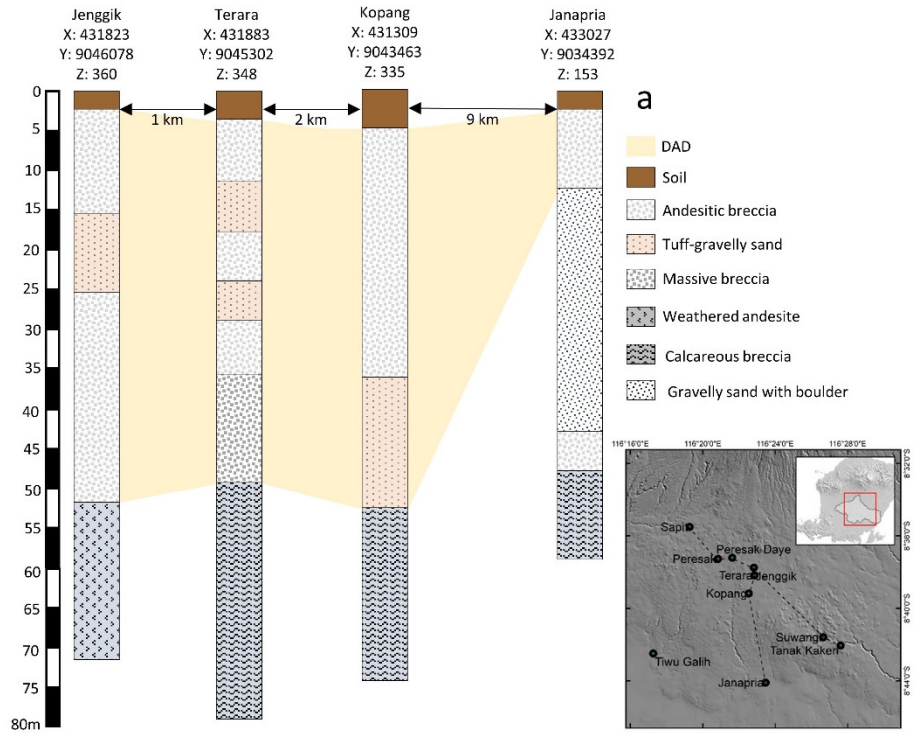

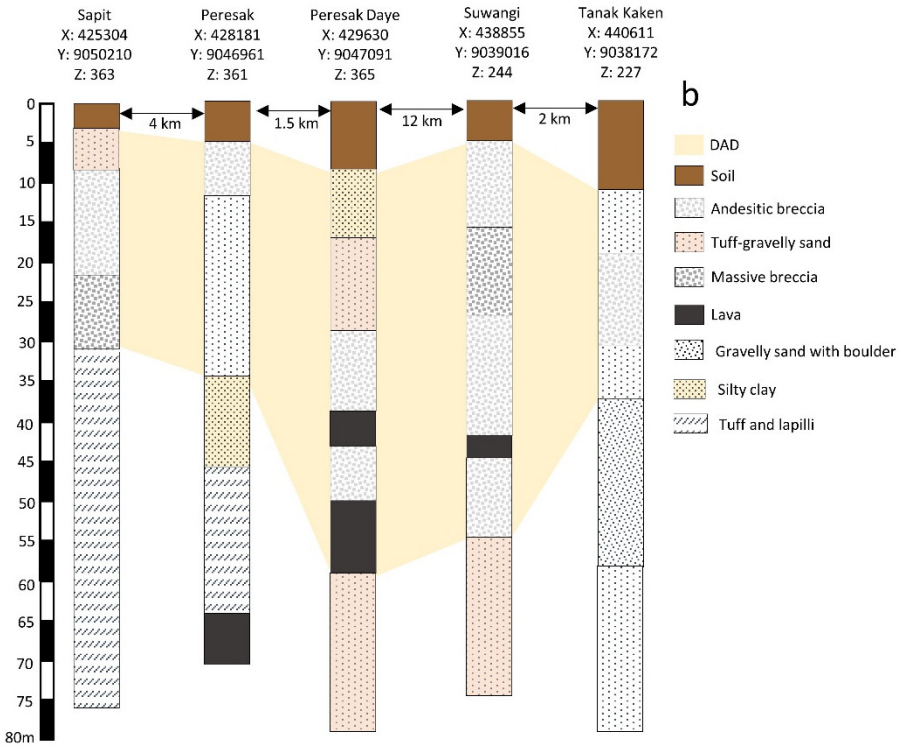

Figure 4.10. Lithological information of cores in the DAD. Correlations between deposits associated with the DAD demonstrate the variety of thicknesses.

As outcrops and core data are punctual in space, 2D electric resistivity transects were acquired in Lepak, East Lombok, and have a length of 550 m each, providing a spatial window on the deposit (Figure 4.11). The DAD in Lombok is characterized by resistivity values in the range of 30-300 ohm-m. Two measured lines AB and CD show that the DAD layer has contrasting boundaries with the basal material, which has a lower resistivity value (a small value indicates a high-water content or highly saturated layer). The boundary between the DAD and the older material along the line AB forms a continuous boundary (black line) at a depth of 20-30 m. The upper layer of the line AB displays two layers of low-resistivity that can be interpreted as a fluvial deposit covering the DAD layer. A chopped hummock due to anthropogenic activity is also identified at a distance of 250-370 m from point A (Figure 4.11). On the line CD, the limit of the DAD is more irregular in depth, indicating either that (1) the paleo-topography is irregular, or that (2) the DAD has eroded the paleo-topography. The paleo-topography of this location may be composed of weak materials that are not resistant to erosion. Similar to the line AB, small fluvial infills are also found on the line CD. With these results, resistivity analysis demonstrates that the geophysical survey helps characterize DAD's depositional pattern and portrays the form of paleo-topography. Other resistivity measurements in various locations of the DAD is presented in the Appendix A (Table A1).

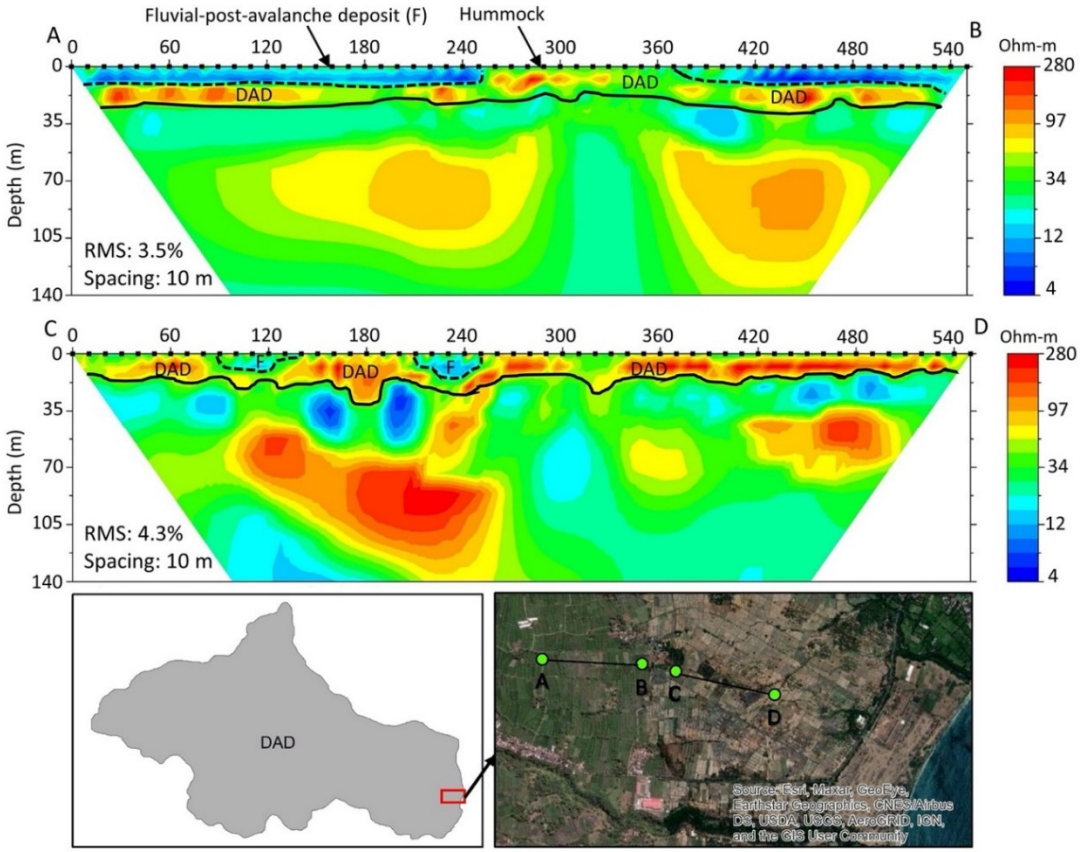

Figure 4.11. Interpretation of the resistivity profiles in the eastern part of DAD.

4.4.3. Paleo-topography

Field observations combined with DEM data was used to simulate and reconstruct the pre-collapse Samalas volcano (Figure 4.12a). Based on our morphological reconstruction, the pre-avalanche summit was located at ~3.6 km from the current summit of Rinjani and adjacent to the current Barujari vent (~500 m). The reconstructed summit has average slope of 35%. In comparison to the Rinjani, the Samalas has a larger circular body (Figure4.12a). Best estimation using ShapeVolc indicate that former Samalas (pre-avalanche) has a maximum height of 4207 m, higher ~480 m than the current Rinjani. The topographic profile A-B (Fig. 4.12b) of the DAD demonstrates that the stratocone of the former Samalas was ~1,500 m higher than the caldera rim (Figure 4.12b). The pre-avalanche and the present topographic profiles intersect at ~8 km from the simulated former summit. According to the topographic simulation (Figure 4.12b), the possible length of the caldera that released the debris-avalanche was of 7-8 km horizontally and with a maximum depth of ~1.5 km.

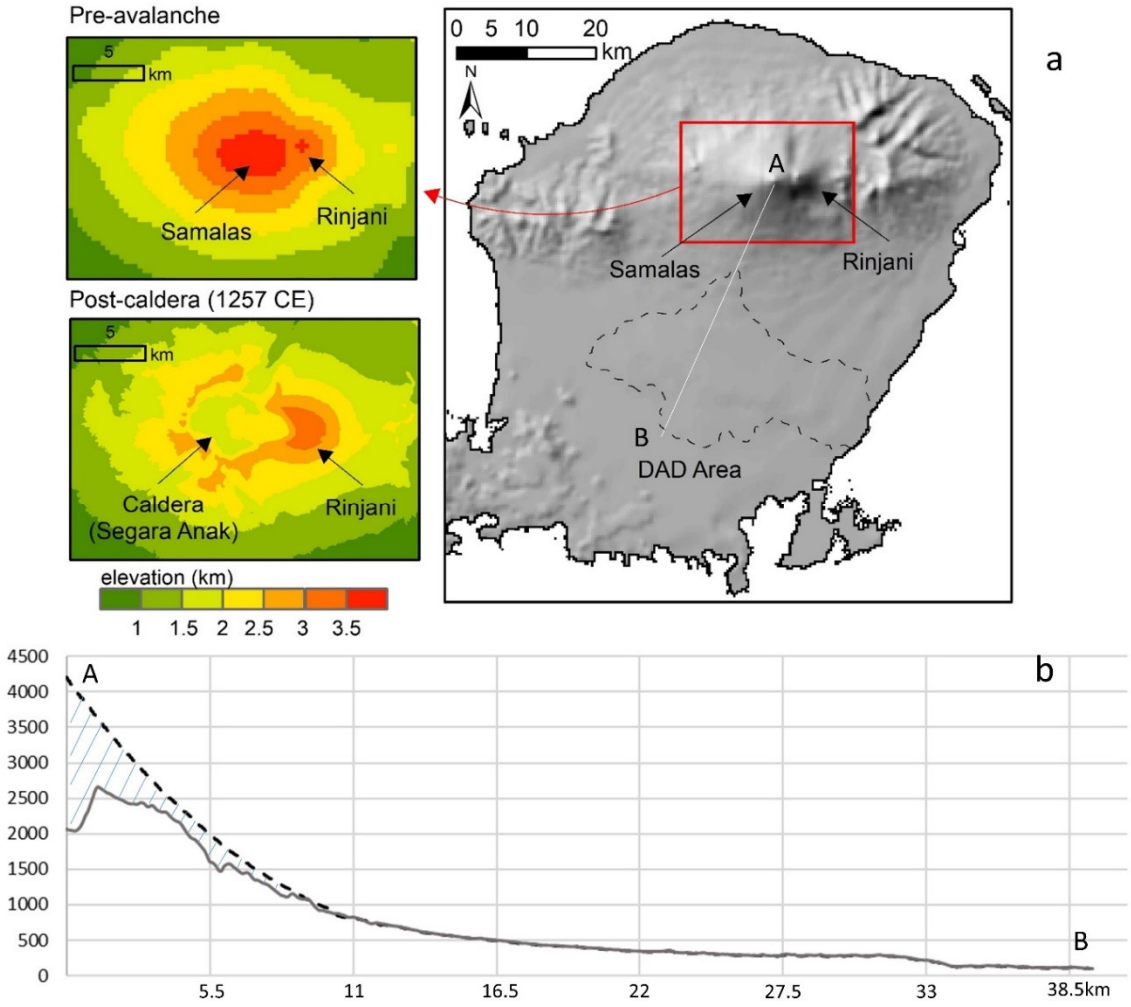

Figure 4.12. (a) Comparison of the paleo- and present-day DEMs of the Samalas summit. (b) Profile line from the summit to the distal area shows the topographic differences between the paleo- and present-topography.

4.4.4. Metrics of the DAD

Based on the calculated metrics (Table 4.2), the length (L_D) of the DAD is smaller than its width (W_D), displaying a stretching-fan shape. The thickness of the DAD was then calculated to be approximately 28.5 m on average. According to the classic geometrical formula (Table 4.2), the volume of the DAD can be estimated to be 15.3 km^3, which compares well with the DEM subtraction method, which yields 14.9 km^3, or 15.1 km^3 if we average both results. The measurements also show that the tail of the flow is at 685 m.a.s.l. while the front travelled to a final altitude of 114 m.a.s.l. This gives an H_D value of 581 m. By comparing H_D and L_D values, we get an average slope of 2%. Although the overall slope has been mapped (Figure 4.7), this

metric is important for characterizing DAD in Lombok that can be used for comparison with other DADs. The length (L) of the debris avalanche from the source to the front is 39.3 km, with a maximum drop height of 4 km. Comparison of these two metrics results in the H/L value of debris avalanche in Lombok being 0.1.

Table 4.2. Metrics of the debris avalanche in Samalas volcano, Lombok.

No	Parameter	Value	No	Parameter	Value
1	L_D	25 km	7	V_D	15.1 km^3
2	W_D	41 km	8	AR_D	2.1
3	A_D	535.7 km^2	9	L	39 km
4	H_D	581 m	10	H	4.1 km
5	α_D	2%	11	H/L	0.10
6	T_D	28.5 m			

4.4.5. Modeling of the Debris Avalanche Flow

The debris avalanche was further simulated using VolcFlow. In this simulation, we conducted four simulations to evaluate the debris avalanche propagation from Samalas volcano (Appendix A; Table A2). The first simulation employed a volume of ~15 km^3 and considerable yield strength (50 kPa) to determine the avalanche propagation and area of coverage for a dense material. Results show that the simulated deposition poorly match the actual deposit (Figure 4.13a). However, the maximum deposit depth of this simulation (60 m) is nearly similar to the maximum measured depth from the outcrop (58 m).

The second simulation was conducted with the same volume with moderate yield strength (20 kPa). The result of this simulation has further and broader coverage but has yet to cover the most distal part of the original deposit (Figure 4.13b). The third simulation used a lower value of yield strength (7 kPa). This indicates a less compacted material compared to the previous simulations. The result of the third simulation is most similar to the original DAD in shape and coverage (Figure 4.13.c). In the south distal part, the limit of the front is relatively similar, as well as in the southeastern part, the avalanche has reached the shoreline.

The last simulation used a standard yield strength that is generally applied for simulating DAD propagation, which is 50 kPa, similar to the first simulation. However, this simulation used a double volume of the calculated volume (i.e., ~30 km^3). The result shows that the final propagation of DAD reaches the outer boundary of the original DAD, although the final form is not identical. The resulting maximum deposit thickness also reached twice the measured maximum DAD depth. Based on this fourth simulation, it can be assumed that the Kalibabak DAD may be characterized by lower yield strength. The simulation might be more accurate if the scar of the caldera avalanche is visible since the volume between the caldera avalanche and the deposit can be compared, as well as the starting point of the emplaced material can be determined.

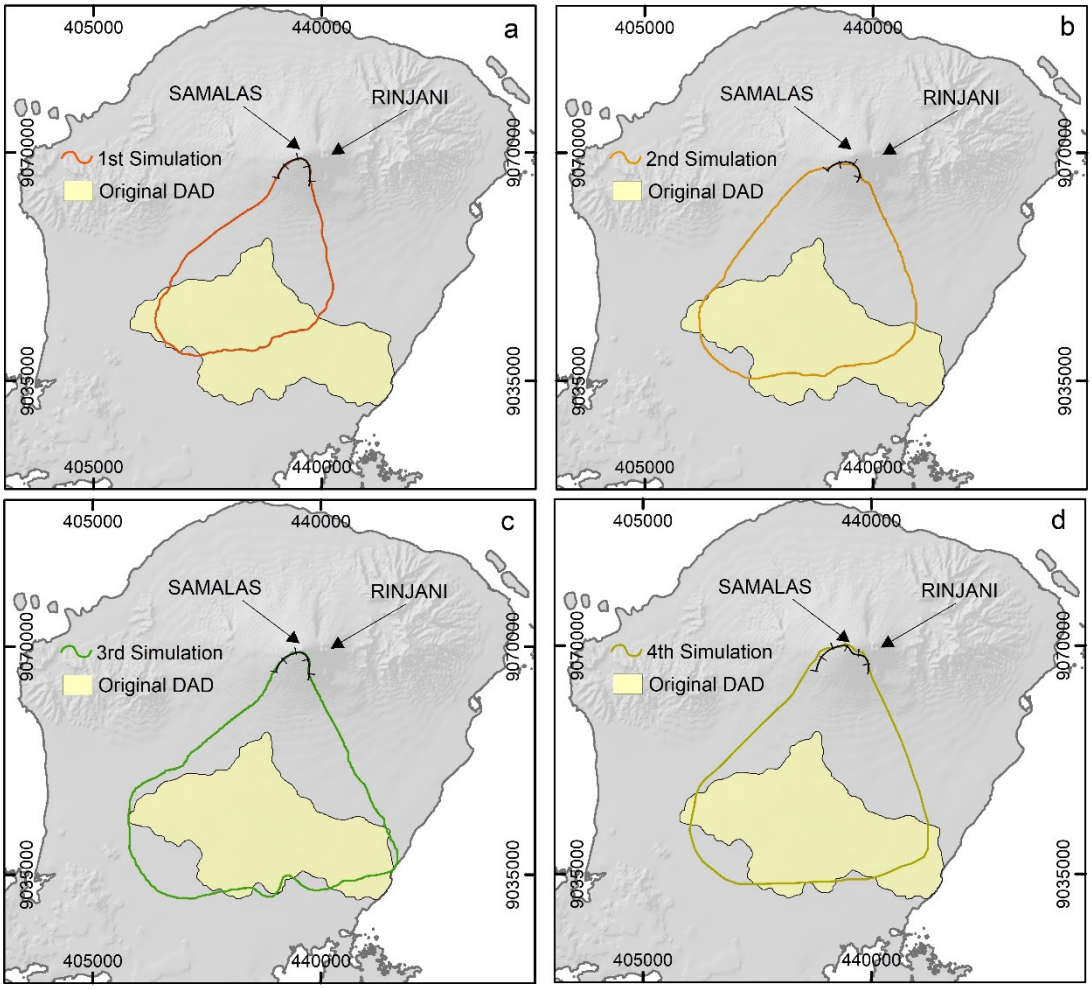

Figure 4.13. Comparison of the simulated and original DADs; ~15 km^3 and 50 kpa (a); ~15 km^3 and 20 kPa (b); ~15 km^3 and 7 kPa (c); ~30 km^3 and 50 kPa (d).

4.4.6. Age of Debris Avalanche

The results of radioactive dating of the soil sandwiched between the DAD and the 1257 eruptive material display ages ranging from 2,600 BCE to 1,300 BCE, with one younger date of 470 CE (Table 4.3). This supports the thesis that the DAD was not emplaced by the 1257 eruption, but is much older than the eruption. The maximum age constraint of the DAD in Lombok is determined based on the dated material below the DAD. The results are more diversified, with a range of ~10,000 years. The oldest calibrated age obtained from a paleosol in the Kali Dalam Valley is 17,900 BCE. Nearby, in the same valley, another paleosol sample yielded a calibrated age of 16,000 BCE. A sample from Kali Palung, which has a similar stratigraphic sequence to Kali Dalam, but is located in the distal part of the DAD, yielded a calibrated age of 11,400 BCE. At Kwang Wai beach, in the edge of the DAD, two materials below the coastal hummock yielded calibrated age of 7,000-7,600 BCE. At this site, the exposed seafloor (KW2) is dated at 10,100 BCE. Located closer to the caldera rim (27 km), the paleosol covered by the DAD at Kali Dalam may have undergone significant erosion during flow; therefore, the sampled paleosol is likely much older than the avalanche. In contrast, the exposed materials beneath the DAD at Kali Palung and Kwang Wai beach, which is located 34 km and 39 km from the caldera rim respectively, are much younger because erosion may have decreased. Based on our dating, the age of the Kalibabak DAD would be between 7,000 and 2,600 BCE.

Table 4.3. Radiocarbon ages of the paleosols and sediments related to the Kalibabak DAD.

No	Site	Type	Age BP	Calibrated age (BCE)	Median probability (BCE)
1	Selebung (DAD 1)	Paleosol above DAD	3,080±30	1,412-1,199	1,300
2	Selebung (DAD 2)	Paleosol above DAD	4,100±50	2,706-2,468	2,616
3	Selebung (DAD 3)	Paleosol above DAD	3,120±50	1,451-1,200	1,336
4	Selebung (DAD 4)	Paleosol above DAD	1,635±30	410-542 (CE)	470 (CE)
5	Kali Dalam 1	Paleosol	14,490±60	16,362-	16,264

No	Site	Type	Age BP	Calibrated age (BCE)	Median probability (BCE)
	(KD1)	below DAD		16,005	
6	Kali Dalam 2 (KD2)	Paleosol below DAD	16,490±50	18,090-17,655	17,903
7	Kali Palung (KP)	Detritus sediment	11,580±230	11,919-11,108	11,480
8	Kwang wai 1 (KW1)	Paleosol below DAD	8,620±330	8,467-6,772	7,675
9	Kwang wai 2 (KW2)	Compacted detrital sediment	10,380±300	10,830-9,253	10,133
10	Kwang wai 3 (KW3)	Paleosol below DAD	8070±500	8,242-5,983	7,009

4.5. Discussion

4.5.1. Gigantic debris avalanche in Indonesia

A previous study reported that there have been 70 volcanic sector collapses that produced DADs in Indonesia (MacLeod, 1989). Since this data was developed by the interpretation of aerial imagery, 54 were considered probable events, while the remaining 16 were possible events. These numbers are used to rank Indonesia in the global inventory of volcanic debris avalanches (Dufresne et al., 2021). However, only 11 DADs from this list have been subjected to morphometric measurements, and only four were successfully dated (Siebert et al., 1987). Our work provides a new case study to add the current database. In Indonesia, most DAD volumes vary from 1 to 5 km^3, with an area of 50-250 km^2 (MacLeod, 1989). The known broadest DAD in Indonesia is located at the foot of Raung volcano, with a travel distance up to ~80 km, and an area of ~650 km^2 (MacLeod, 1989, Siebert, 1984). Based on the inventoried data, the Kalibabak DAD ranks third in Indonesia based on its volume, below the DAD from Raung and Galunggung (Siebert, 2002).

To determine its position in the global context, the metric of DAD in Lombok needs to be compared with other DADs worldwide. In the East Asian region, Japan is among the countries with the largest number of DADs (Ui et al., 1986; Siebert, 1987). From all the debris avalanches that have occurred in Japan, no significant DAD has a volume of >10 km^3, and the farthest travel distance (L)

reaches 32 km. As well as compared to the Philippines, New Zealand, Melanesia, and Kuriles-Kamachatka regions, the Kalibabak DAD in Lombok is significantly bigger than all DADs in those regions. Several Holocene DADs worldwide are comparable in volume to the one produced by Samalas, e.g., Meru, Tanzania (10-20 km^3), Feugo, Guatemala (15 km^3), and Antuco, Chile (15 km^3) (Siebert, 2002). Based on this inventory (Siebert, 2002), the Kalibabak DAD from Samalas volcano ranks eighth among the largest (>5 km^3) Holocene DADs worldwide.

4.5.2. Triggering mechanism

Identification of the triggering factors that cause a volcanic collapse is challenging, especially when it occurred in the past and no direct observations are available (Özdemir et al., 2016; Valverde et al., 2021). Several factors can trigger a collapse of a volcano, such as earthquake or fault activity, volcanic eruption, or dyke intrusion (Belousov et al., 2007; Tibaldi, 2001). It can be triggered by single or multiple factors. There are no fault lines beneath the Rinjani volcanic complex that are likely to cause significant earthquakes (Figure 4.1b). The major earthquake source zones are located in the north (Flores Thrust) and south of Lombok (Indo-Australian subduction) (Harsuko et al., 2020). A series of recent earthquakes in the northern region of Lombok island in 2018 (6.9 Mw) caused significant damages and landslides in Lombok. Identification using satellite images provided data of 9,319 minor landslides with a total area of 10.39 km^2, predominantly located in the mountainous areas (Ferrario, 2021). Although the epicenter is located on the northern slope of the Samalas-Rinjani complex and has affected ground deformation, the volcanic activity in Samalas-Rinjani remains normal without significant escalation (Wibowo et al., 2021). Earthquakes and fault activity may be possible triggering factors in other locations, but not for a large volcanic avalanche in Lombok.

The regional stratigraphic frameworks that have been established (Nasution et al., 2004; Vidal et al. 2015; Métrich et al., 2017) can be used as benchmarks for establishing the relationship between eruptions and the Kalibabak DAD (Figure 4.14). Correlation between the age of DAD and stratigraphic framework was also demonstrated in Shiveluch volcano (Russia) to determine the association between debris avalanches and eruptive events (Ponomareva et al., 1998; Belousov et al.,

1999). Holocene activity in the Rinjani-Samalas complex was dominated by basaltic explosive activity that produced scoria fall and PDC deposits between 11,000 and 5,300 BCE. Large explosive eruptions were absent during this period. The subsequent period (~5,300-800 BCE) was characterized by effusive and explosive volcanic events. For example, the Rinjani volcano expelled the Lembar trachy-dacite lava flow. Scoria fall, which is a typical product of explosive basaltic eruption, were also identified on the northern slope of Samalas. The radiocarbon dating of two charcoals in this deposit yielded 4,700-5,000 BCE (Métrich et al., 2017). Lastly, a younger pumice deposit overlying the scoria fall deposit, i.e., the Propok pumice, was ejected eastward during the subplinian eruption of Samalas, with an estimated volume of 0.1 km^3 (dense rock equivalent-DRE) (Nasution et al., 2004). Based on the proposed age of the DAD (7,000 – 2,600 BCE) obtained from radiocarbon dating (Table 4.3), we argue that the debris avalanche event was likely triggered by this eruption, between 5000 BCE (i.e., after the scoria fall) and 2,600 BCE (i.e., the youngest date of the material beneath the Kalibabak DAD).

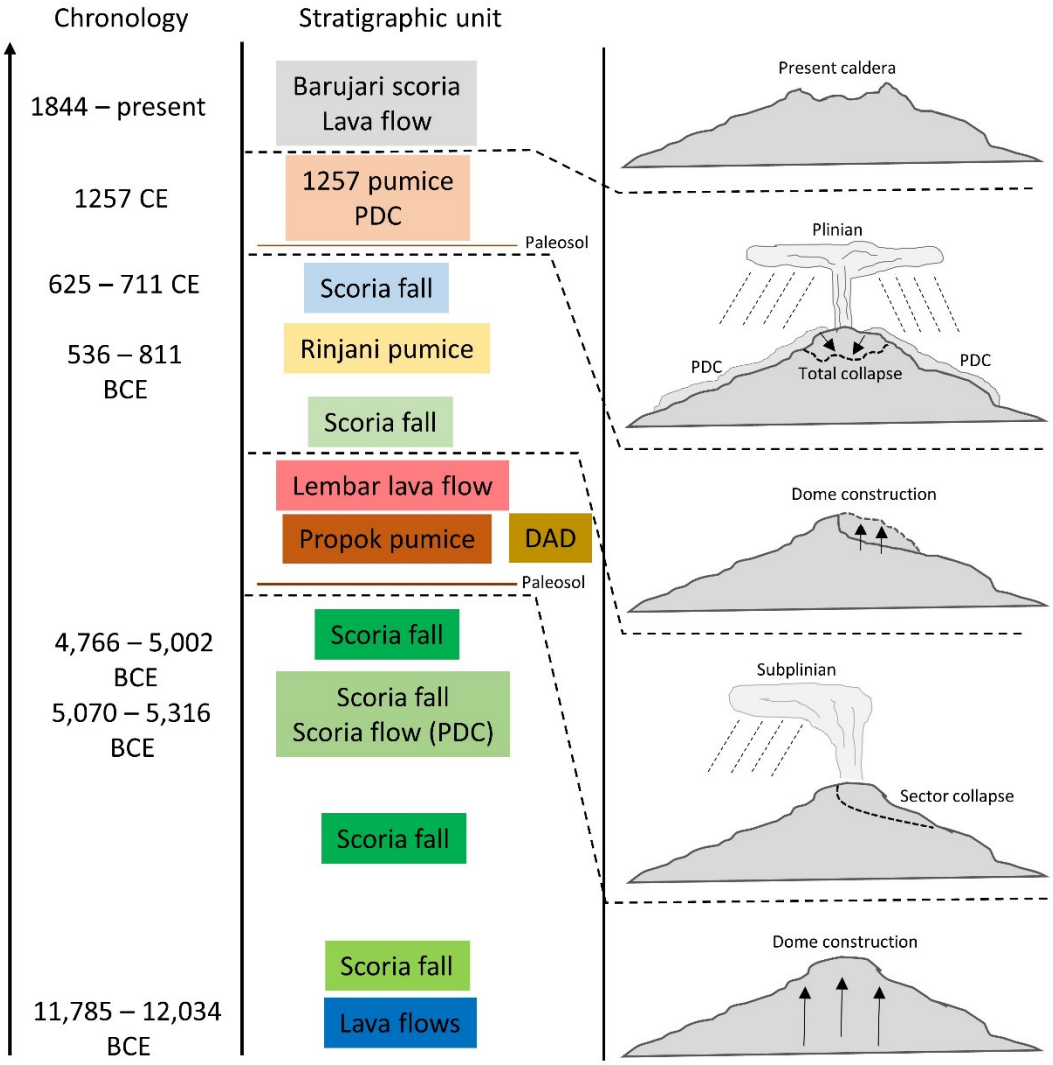

Figure 4.14. Stratigraphic framework and chronology of the landscape dynamics in Samalas volcano.

4.5.3. Emplacement Dynamics

The long runout distance of Kalibabak debris avalanche deposit is not subjected due to the massive presence of water or a lahar-transform mechanism The unusual runout distance of 39 km, with a H/L ratio of 0.1, is predominantly caused by the intense rock fragmentation in the deposit (Figure 4.15). This process is a significant factor in the peculiar and long runout mass distribution. Rock fragmentation produces high-velocity fragments moving in all directions, resulting in isotropic dispersive stress within the translating rock mass, as indicated by the jigsaw crack in the deposit (Davies et al., 1999). A longitudinal dispersive force consequently acts in the direction of reducing the mass depth. It tends to cause the

rear part of the avalanche to decelerate and halt while the front part tends to accelerate.

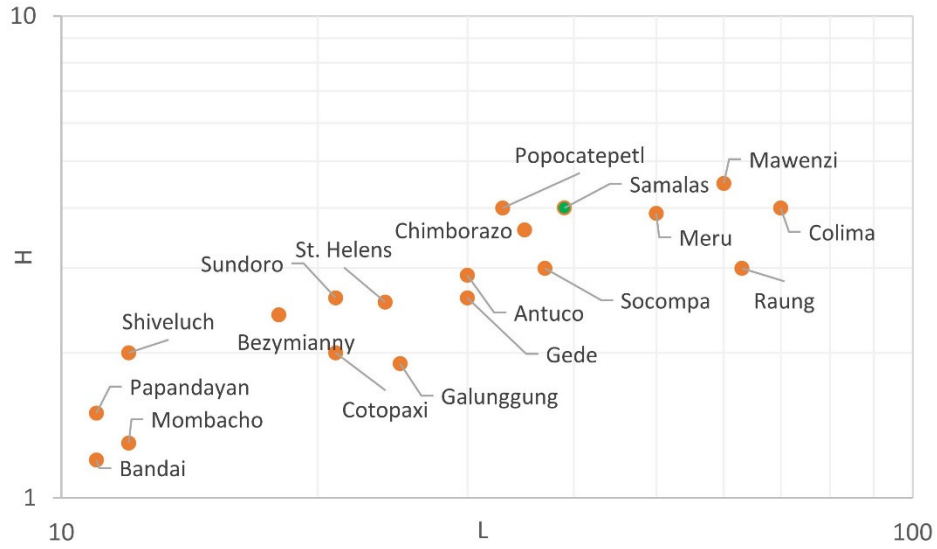

Figure 4.15. Comparison of friction coefficient (H/L) for various debris avalanches worldwide (data from Siebert et al., 1987).

The comparison of the four simulations with the original boundary of the DAD suggests that the Kalibabak debris avalanche is complex to simulate. However, the VolcFlow models assisted us in better understanding the dynamics of DAD emplacement in Lombok. The third simulation may be the best approximation (Figure 4.13c). However, field conditions indicate that the structure of the DAD is not composed of fluid materials such as lahars or highly saturated materials. Therefore, we suspect that two sequences occurred during emplacement (Figure 4.16); zone I is freely spreading material emplacement type, while zone II is a canalized or valley-filling (Yoshida, 2014). The simulation also demonstrates that the area of original deposit may be bigger that the actual delineated boundary. The intersection area between the simulated DADs and the original DAD could be suggested as part of Kalibabak DAD. This area is occupied by material that remained near the source, which may be in the form of toreva or slumped blocks. However, due to the enormous PDCs in 1257 CE and subsequent lahars, this area was buried and is not visible as a DAD area. The predicted avalanche caldera at Samalas volcano has a maximum length of 7 km and a width of 5 km. Based on its volume

(~15 km^3), the average depth of the avalanche caldera would be ~430 m. The former scar of this caldera is not recognizable in the present topography. In the post-avalanche period, the scar was probably fully or partially covered by a new dome structure, which subsequently comprised the ~40 km^3 volcano edifice that collapsed during the 1257 CE eruption (Lavigne et al., 2013).

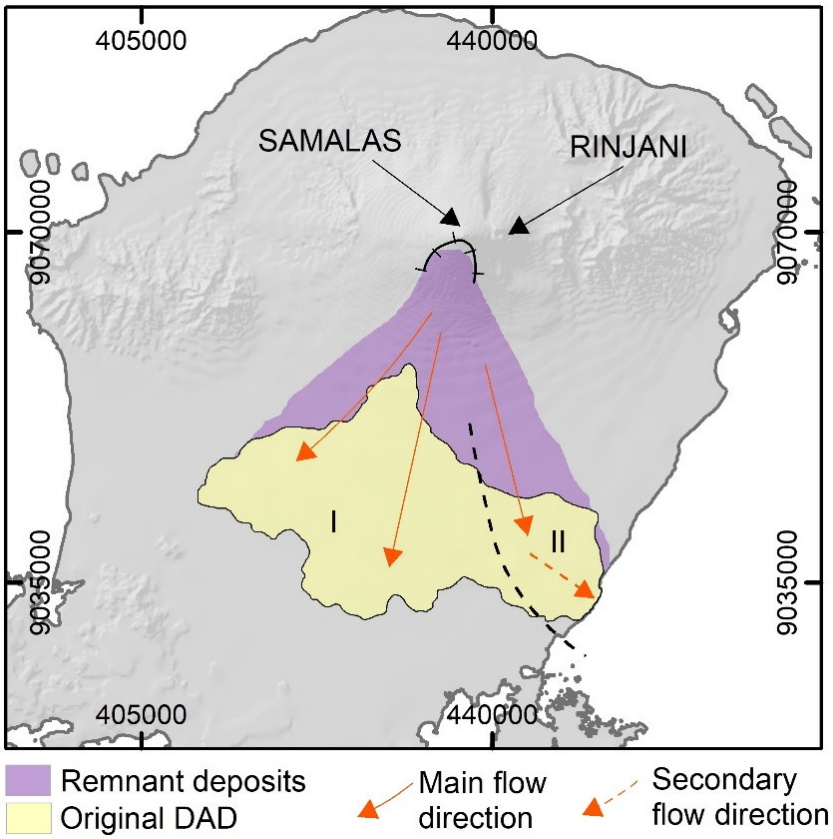

Figure 4.16. Emplacement dynamic of the Kalibabak debris avalanche from Samalas volcano

Although all VolcFlow simulations failed to enclose the original deposit, several factors may explain these discrepancies. The primary factor is attributed to the volume of removed material being larger than the calculated volume. The lack of stratigraphic data in the DAD region increases the uncertainty in calculating the volume (Bernard et al., 2021). The original volume of emplaced materials may exceed 20 km^3.

The second factor relates to the triggering mechanism. The occurrence of a directed blast may have influenced the widespread avalanche propagation. We argue

that the vast runout Kalibabak DAD was possibly due to a Bezymianny-type eruption (Siebert et al., 1987) and likely accompanied by a lateral blast such as at Mount St. Helens in 1980 (Belousov et al., 2007; Glicken, 1996; Siebert et al., 1987). However, it is still being determined that a blast could have triggered the avalanche at Samalas volcano since no blast deposits have been found yet. Information on the Propok pumice and associated eruption that likely triggered the Kalibabak DAD remain limited (Nasution et al., 2004; Metrich et al., 2017). Therefore, even if this eruption has been considered subplinian until today, it is not impossible that it was a plinian eruption.

The last factor is related to the paleo-topography of the south-eastern part of Lombok, which differs from the reconstructed DEM. The pre-collapse topography of this region may be more complex, with various valley forms. A canalized or valley-filling flow mechanism (Yoshida, 2014) is proposed to involve the far-reaching deposition in the southeastern part of the island. The morphological characteristics of DAD (Figure 4.8a) and VolcFlow simulation results (Figure 4.13) have supported this hypothesis. The ancient valley of Kali Palung may have helped the DAD flow to be extended and canalized, resulting in a further runout towards this direction. An example of valley-filling DAD in Indonesia with a significant runout distance is the DAD from Raung volcano, which propagated through a broad valley between Iyang-Argapura Volcanic Complex and Meru Betiri Mountain (~10 km) (Moktikanana et al., 2021). Another example of canalized DAD is from Antocu volcano (Chile), which traveled through a relatively narrow (~6 km) river valley (Laja river) (Romero et al., 2022).

4.5.4. Landscape evolution

Volcanic activity has occurred in Lombok since the Pliocene (Zubaidah, 2010). However, the stratigraphic framework in this region provides chronology since the Holocene (Nasution et al., 2004; Métrich et al., 2017). It was initiated by the stratocone building stage since 11 ka with predominantly effusive eruptions (Figure 4.14). This process continues until it enters the second stage, which has evolved into explosive eruptions. The climax occurred when a subplinian (possibly as plinian) eruption that likely led to a debris avalanche that mantled the southern

flank and distal area of the volcano. It buried an area of 500-700 km^2 with a maximum runout distance of deposition up to ~39 km. The H/L ratio of Kalibabak DAD at 0.1 and is clustered in the volcanic landslide group, close to Chimborazao and Meru (Figure 4.15). The avalanche from Samalas also travelled at high speed. Although the modelling from VolcFlow produced an estimated velocity, the model failed to enclose the present deposit. Therefore, the runout velocity has been recalculated using the friction loss and potential energy of avalanche run-up formula from Naranjo and Francis (1987) (Appendix A; Table A3). The calculation suggests the velocity is ~65 m/s or requires about 10 minutes from start to end. With this high velocity, it is expected that significant erosion has occurred during the downstream travel. The triggering mechanism and its velocity also illustrate how large boulders can be dispersed over long distances.

After the complete deposition of the DAD, it is entered the post-avalanche stage, where erosion and resedimentation processes were initiated. Probably only a few lahars were generated during this stage due to the absence of abundant pyroclastic material. A fluvial modifying stage may have created new river channels (Manville et al., 2009), and slow mass-wasting likely occurred on the front lobes. The river channel stabilization continued to develop (Gran et al., 2011), and the volcano entered the new stratocone building stage after the sector collapse.

A plinian eruption attributed to Rinjani by Nasution et al. (2004) occurred between 800-500 BCE, which produced significant pumice dispersal (Rinjani Pumice). Following this eruption, magma amalgamation occurred beneath the Samalas-Rinjani complex for ~2 ky (Métrich et al., 2017). The large magma reservoir then sustained the plinian eruption of 1257 CE through the Samalas vent resulting in the large caldera (~6 km) and voluminous PDC deposit (Lavigne et al., 2013). The PDCs mantled the wide area of Lombok in the SW, NW, N, NE, and SE directions (Vidal et al., 2015; Mutaqin et al., 2019). Similar to DAD, PDC also aggraded the topography up to ~50 m. The dynamics of formation-destruction of the volcanic edifice in Samalas volcano may be similar to Usu volcano, Japan, which was destroyed by sector collapse and followed by plinian eruption after a thousand-year gap (Goto et al., 2019). This series of volcanic activities demonstrates the dynamics of landscape following explosive eruptions, starting from landscape

forming, mantling, and modifying (Manville et al., 2009). Lombok is an example of a region that significantly experienced abrupt landscape evolution due to volcanic eruptions, particularly caused by sector collapse leading to a gigantic DAD and caldera-forming eruption leading to voluminous PDC.

4.6. Conclusion

The present analysis of the Holocene Kalibabak debris avalanche of Samalas volcano in Lombok shows that the DAD is one of the largest in the Asian region with a measured area of 535 km^2 and a volume of ~15 km^3. This fan-shaped DAD widened in the center (41 km) and had a runout distance up to 39 km from the source. This sector-collapse of the Samalas volcano occurred between 5,000 and 2,600 BCE. The DAD provides an example of the complexity in reconstructing past debris avalanche when the source-caldera has been completely erased (in the present case due to the 1257 CE caldera-forming eruption). It is also challenging to determine the possible triggering factor of the debris avalanche because various juvenile and pyroclastic deposits above, below, or incorporated within the DAD were absent from the outcrops. A possible correlation may be proposed with the stratigraphic record of the Samalas-Rinjani Volcanic Complex, and a subplinian eruption of the Samalas volcano may have been responsible for triggering the massive debris avalanche in Lombok.

CHAPTER 5

Now it is recognized that Lombok experienced significant landscape transformation due to a large sector collapse during the Holocene. This rupture produced a widespread debris avalanche deposits in the central region of Lombok Island. It is well recognized that the flows of PDC from 1257 CE were highly influenced by the hummocky topography created by the Holocene DAD. The deflected PDCs have buried large areas in the southwest flank of the volcano with a maximum depth of ~50m. The landscape evolution on this region, i.e., the Mataram Plain, has never been investigated. This chapter demonstrates that the Mataram plain experienced abrupt landscape change due to PDC deposition and progressive landscape change due to lahars and fluvial resedimentation.

EVOLUTION OF THE MATARAM PLAIN FOLLOWING THE 1257 CE SAMALAS ERUPTION

Abstract

The 1257 CE eruption of Samalas volcano, Indonesia, buried the entire island of Lombok beneath various thicknesses of pyroclastic material during this Volcanic Explosivity Index (VEI) 7 event. This study aims to reconstruct the paleo-topography of western Lombok before the Samalas eruption in 1257 CE and analyze the sedimentation processes that led to its landscape evolution over the last 700 years. Stratigraphic data were collected from various surveys, such as outcrops, coring, drilling, hand auger, and wells observation. Electrical resistivity tomography (ERT) measurements were performed to complement the stratigraphic data. A combination of stratigraphy, ERT, and topographic data from various sources (topographic map, DEM Nasional (DEMNAS), and Real Time Kinematic (RTK) measurement) is employed to determine the depth of the paleo-surface. Topographic modeling was performed by subtracting the delta-DEM (DDEM) from the current-DEM (CDEM). The result of this operation is a paleo-DEM, which is used to reconstruct the paleo-hydrographic features such as shoreline positions and river channels. Modeling results demonstrate that the relief has not been significantly modified, except in lowland areas, which is the sediment accumulation zone. River channels have experienced minor changes, except for the location of the river mouth and the degree of meandering. Significant changes occurred at the shoreline which has prograded by c. 1.6 km during the last 700 years. A schematic model is built to illustrate the evolution processes of the study area, consisting of the pre-eruption condition, the immediate post-eruption condition, and development of the current condition. This model further develops the previously proposed model with a higher resolution and simultaneously revises the estimated boundary of the pyroclastic density current (PDC) deposit from previous work.

Keywords: geomorphological impacts; landscape evolution; paleo-topography; volcanic eruption; Samalas volcano

This chapter corresponds to an article published in the Journal of Earth Surface Processes and Landforms. https://doi.org/10.1002/esp.5592

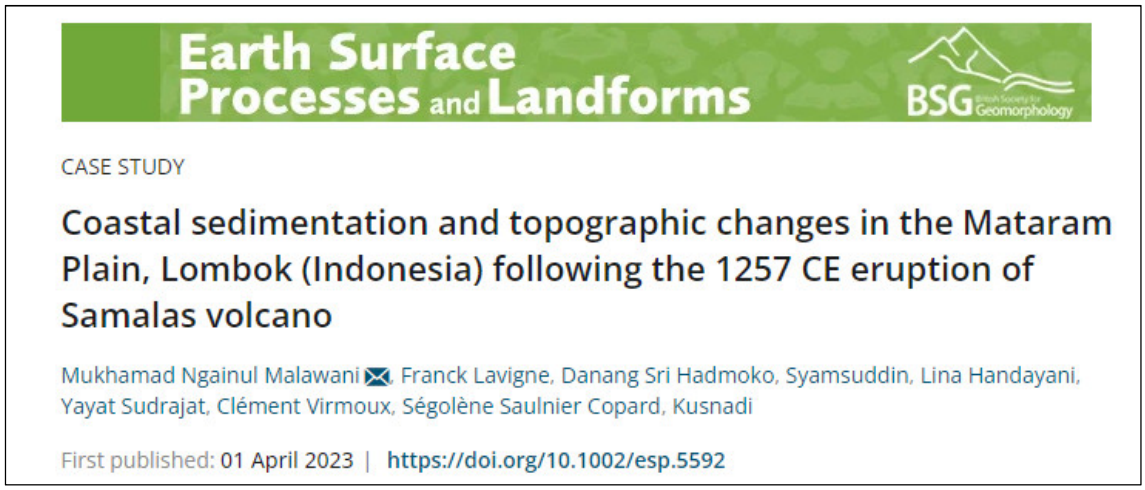

Earth Surface Processes and Landforms

BSG British Society for Geomorphology

CASE STUDY

Coastal sedimentation and topographic changes in the Mataram Plain, Lombok (Indonesia) following the 1257 CE eruption of Samalas volcano

Mukhamad Ngainul Malawani, Franck Lavigne, Danang Sri Hadmoko, Syamsuddin, Lina Handayani, Yayat Sudrajat, Clément Virmoux, Ségolène Saulnier Copard, Kusnadi

First published: 01 April 2023 | https://doi.org/10.1002/esp.5592

5.1. Introduction

Volcanic eruptions may have significant impacts on the landscape, either by forming or modifying the landscape (Newhall et al., 2018; Manville et al., 2009). The primary process in the eruption activity is typically a landscape-forming process, such as creating a cone, dome, or shield (de Silva and Lindsay, 2015). However, this process may ultimately cause landscape modification, both in the volcanic edifice itself and distal areas (de Silva and Lindsay, 2015; Newhall et al., 2018). In the case of a large eruption, a volcano edifice may be destroyed, resulting in a caldera (de Silva and Lindsay, 2015; Waythomas, 2015). The transport of abundant erupted materials can also cause significant erosion and sedimentation across the basin (Hadmoko et al., 2018; Thouret et al., 2014). These processes can occur during or long after the eruption which involved fluvial processes (Gob et al., 2016; Gomez et al., 2018; Segschneider et al., 2002), and if extended to the coastal zone, marine processes may also be involved (Hart et al., 2004). As a result, the dynamics of the sedimentary basin are strongly influenced by eruption activity (Németh and Palmer, 2019).

The sedimentary record in a basin provides a regional stratigraphic framework, which is crucial for mapping the evolution of the volcano-related landscape (Martí et al., 2018). Three phases distinguish the lithostratigraphic units of eruptive products, i.e., syn-, post-, and inter-eruptive phases (Németh and Palmer, 2019). In the case of large-scale eruptions, pre-eruptive topography can be buried by very thick deposits due to sudden pyroclastic inputs, e.g., from pyroclastic density currents (PDCs) during the syn-eruptive phase (Petterson et al., 2003; Pardo et al., 2019). Lahars in the post-eruptive phase can also cause significant land aggradation (Thouret and Lavigne, 2000; de Bélizal et al., 2013). Therefore, the resulting topography can completely differ from the pre-eruptive topography (paleo-topography).

Various approaches can be used to reconstruct the topographic transformation caused by transport-deposition-reworking of eruptive products. These include interpolation of lithostratigraphic datasets, such as outcrops, boreholes, and archaeological excavations (Lajczak et al., 2020; Pröschel and Lehmkuhl, 2019; Vogel and Märker, 2010). The combination of geophysical data and high-resolution Digital Elevation Models (DEM) is beneficial and may be the most efficient ways of working on

the evolution of topography (Gomez et al., 2021; Kirchner et al., 2018; Meulen et al., 2020; Mozzi et al., 2017; Schmidt et al., 2018; Vogel and Märker, 2010). The difference between the current ground surface level and the paleosol surface (paleo-surface) provides the baseline for determining the rate of topographic change (Lajczak et al., 2020; Luberti, 2018; Meulen et al., 2020). Paleosols are important marker for reconstructing paleo-topography (Lajczak et al., 2020; Vogel and Märker, 2010). However, paleosol erosion can pose a problem for paleo-topographic reconstruction due to the removal of a primary marker for determining paleo-surface. Alternatively, the paleo-surface can also be reconstructed using the thickness of constraining stratigraphic markers, which have been recognized within the regional stratigraphic framework (Vogel and Märker, 2010; Martí et al., 2018).

In Lombok, the Samalas eruption of 1257 CE produced voluminous deposits that covered almost the entire island due to thick pumice fallout and PDCs, resulting in post-eruptive lahars (Lavigne et al., 2013; Vidal et al., 2015). Pyroclastic density currents are fast-moving mixtures of hot volcanic particles and gases (Druitt, 1998), whereas lahars are mixed flows of rock debris and water (Mothes and Vallance, 2015). These deposits in Lombok have specific textural features which make them easy to identify and to distinguish from older deposits. White coarse-grained pumice fallout layers mark the start of the volcanic deposition, separating pre-1257 CE from the most recent material (Hiden et al., 2017; Lavigne et al., 2013; Mutaqin et al., 2019; Vidal et al., 2015).

The eruption of Samalas in 1257 CE ejected an estimated volume of ~40 km^3 dense rock equivalent (Lavigne et al., 2013; Vidal et al., 2015). The detailed stratigraphy of this eruption deposits has been reconstructed (Vidal et al., 2015). The eruption consisted of four phases. The initial Plinian phase (P1) was characterized by poorly-sorted and coarse-grained pumice fallout deposits(Vidal et al., 2015). A Plinian eruption produces high-viscosity lava and explosive ejections with medium-to-high levels of plume (Hickson et al., 2013). Another pumice deposit from the second phase (P2) overlies the first deposit, indicating no erosion between the two phases. In addition to fine-grained pumice, in this phase, the Samalas volcano also ejected accretionary lapilli, ashfall, and dilute PDCs, indicating phreatomagmatic processes. Phreatomagmatic describes the style of volcanic eruptions and the deposit types, when an explosive eruption is generated by the interaction between magma and groundwater (Németh and Kósik, 2020; Hickson et

al., 2013). The third phase (P3), which is also classified as Plinian, resulted in widespread pumice fallout which covered Lombok and some localities in the neighboring islands of Bali and Sumbawa. The final phase (P4) is characterized by voluminous PDC deposits with a maximum thickness of ~50 m (Lavigne et al., 2013; Mutaqin et al., 2019; Vidal et al., 2015). These PDCs have mantled a wide area, mainly towards the North, Southwest and Southeast from the Samalas caldera (Segara Anak caldera). In addition to the caldera-forming process, P4 also caused the partial summit collapse of Rinjani volcano (Lavigne et al., 2013) and co-PDC ashfall, which was found as far as ~500 km away in central Java (Vidal et al, 2015).

The 1257 CE Samalas syn-eruptive deposits display almost identical sedimentation processes to the 79 CE Vesuvius eruption in Italy (consisting of four phases; deposit types: pumice fallout, lapilli, and PDC) (Vogel and Märker, 2010; Vogel et al., 2011; Vogel and Märker, 2013). With an estimated duration of eruption of a minimum 12-15 hours (Vidal et al., 2015), the 1257 CE Samalas deposits can be considered as an isochronous layer. Therefore, the 13th century paleo-surface is preserved beneath the Samalas deposits and is accessible for stratigraphic investigations. In some parts, post-eruptive lahars and erosion could likely have removed the paleosol layer of the 13th century. However, similar to the deposits of Vesuvius eruption in 79 CE that buried the Sarno River plain, the recognized stratigraphic framework and deposit marker could be an advantage in estimating the thickness of the eruptive products and therefore the paleo-surface. Contact between syn-eruptive deposits of the 1257 CE Samalas eruption with the paleosol or other older deposits may constitute an unconformity bounded unit that delimited the paleo-surface (Lucchi, 2019; Paolillo et al., 2016).

Recently, the paleo-topography of the eastern part of Lombok has been modeled (Mutaqin et al., 2019). However, topographic transformations in the remaining parts of the island have never been investigated. This study aims to reconstruct the sedimentation processes following the eruption of Samalas in 1257 CE in Mataram and the surrounding area (SW direction from the present caldera). Focusing on the western part of Lombok, the present study provides a reconstruction of the paleo-topography and paleo-hydrography of this location, as well as the sedimentation patterns following the 1257 CE Samalas eruption which may help to describe the landscape evolution. In addition, the information about paleo-topographic conditions might be helpful as basic information for

further investigations related to the pre-eruptive civilization in Lombok. Currently, the western part of Lombok is the seat of the capital of the West Nusa Tenggara Province. Therefore, the chronology of the landscape evolution and the accompanying geomorphological processes of this area is of great interest.

5.2. The Mataram Plain

The Mataram Plain is located in the western part of Lombok, between hilly and mountainous areas (Figure 5.1A), the Pusuk-Tampole mountain range in the north and Pengsong Hill in the south. The Mataram Plain is dominated by flat morphology which is mainly occupied by PDC and lahar deposits according to the previous studies (Lavigne et al., 2013; Vidal et al., 2015). The morphology of this area causes many streams to converge towards the SW direction from the present caldera, which explains why the PDCs and post-eruptive lahar from the 1257 CE Samalas eruption also accumulated in this area. Hummocky terrain in Central Lombok also acted as a topographic barrier (Figure 5.1A), deflecting PDCs to the SW (Malawani et al., 2020; Vidal et al., 2015). Previous investigation in the Mataram area has shown that pyroclastic deposits filled various ancient basins with different thicknesses, inferred from seismic measurements (Sarjan et al., 2021). The profile line from the caldera rim of the Samalas volcano to the shoreline of Mataram undergoes gradual changes that characterize the morphology of a stratovolcano (Figure 5.1A).

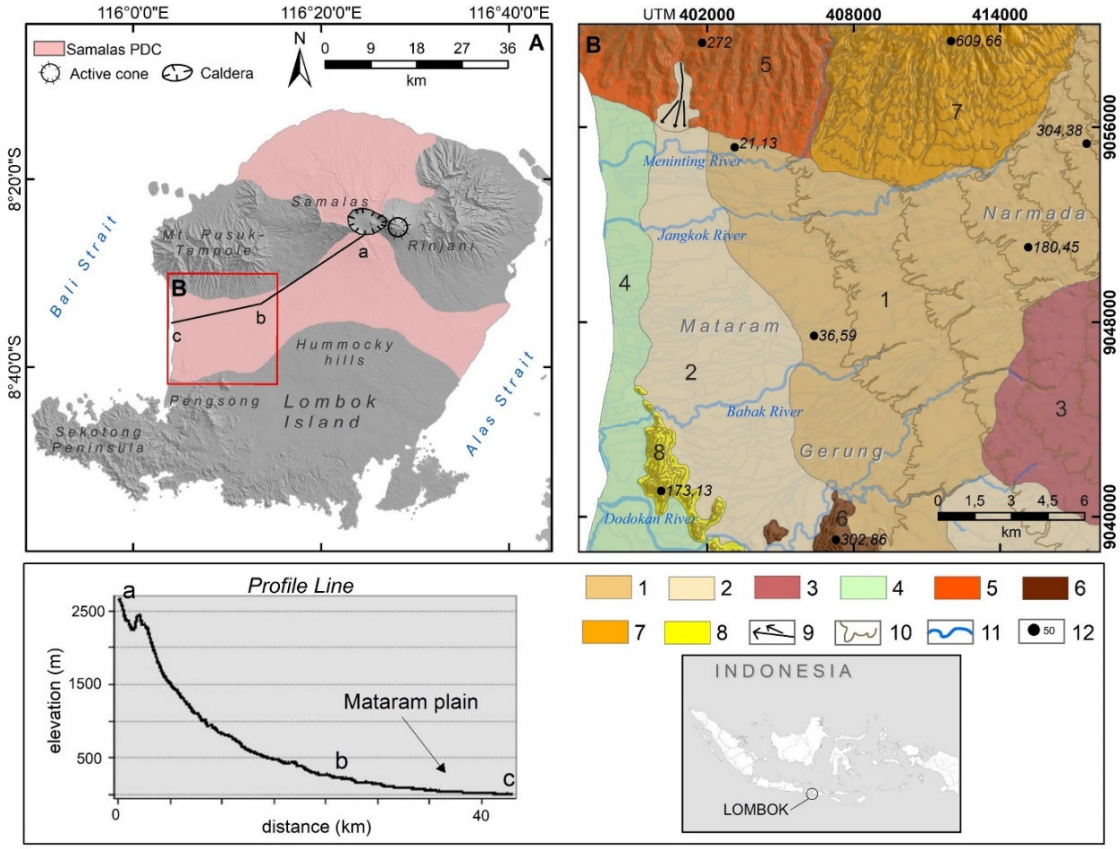

Figure 5.1. Maps of study area: (A) map of PDC deposits from the 1257 CE Samalas eruption (Vidal et al., 2015) and (B) Geomorphological map of the Mataram Plain and surrounds, constructed from field survey, topographic map (RBI map) and Geological map (Mangga et al., 1994). Geomorphological unit: 1: volcanic foot slope; 2: alluvial plain; 3: debris avalanche deposit; 4: fluvio-marine plain; 5: highly eroded old volcanic complex; 6: intrusive hill; 7: moderately eroded old volcanic complex; 8: residual hill; 9: alluvial fan; 10: contour line (50 m); 11: main river channel; 12: elevation point. Delineation of geomorphological units based on Geological Map, *Rupa Bumi Indonesia* (RBI) map, and DEMNAS.

The Mataram Plain is drained by three main river channels, i.e., the Meninting, Jangkok, and Babak Rivers. According to the Geological Map of Indonesia (Mangga et al., 1994), the surface material of the Mataram Plain is composed of Holocene alluvium, with fluvio-marine depositional landforms along the coastal area (Figure 5.1B). The northern mountain range of Pusuk and Tampole consists of two old volcanic landforms which formed during the Pleistocene. The Pusuk-Tampole mountain range is highly eroded and characterized by V-shaped river valleys. Many small alluvial fans result from extensive erosion and the sudden break of slope from steep to flat. The only sizeable alluvial fan is on the west side, near the Meninting River. In the southern part of the

Mataram Plain, there are residual hills several hundred meters high due to Tertiary uplift processes, and dacitic intrusions. The resulting hills have steeper slopes than the residual hills. The residual hills have undergone significant erosion of natural and anthropogenic (mining) origin - and mass wasting, giving them an irregular shape. Therefore, these hilly areas are excluded from the computational model of paleo-topographic reconstruction or non-area of interest (non-AOI).

5.3. Methodology

5.3.1. Data acquisition

A. Stratigraphic data collection

The stratigraphic dataset was obtained through field surveys and archival data collection (Figure 5.2). Since the study area is flat and densely populated (7,048 people/sq.km) (Statistics, 2022), such as in Mataram city, direct observation of outcrops is limited due to the scarcity of open-cut land, even on the riverbank due to artificial embankment. Outcrops were mainly found in areas exavated for agricultural or quarrying purposes. A stratigraphic dataset was also obtained by manual drilling using a soil auger, but this method appeared to be ineffective due to the large amount of sandy material. However, the lack of previous geological exploration in the Mataram area is also an obstacle to acquiring extensive stratigraphic data in Lombok. Five archived stratigraphic logs of sediment cores were obtained from the Faculty of Engineering, the University of Mataram (UNRAM), and the Department of Energy and Mineral Resources (ESDM) of the Nusa Tenggara Barat province.

Due to an urban environment that makes it difficult to access outcrop, and the limited availability of archived stratigraphic data, we required the use of existing water-wells to observe subsurface. When the subsurface layers in the water-wells were not visible, we conducted interviews and worked with professional and non-professional well-diggers to gather such data. Generally, the professionals have noted the locations of the wells they have made and the materials they have extracted. The extracted information from interviews provide data on the sediment type in each half-to meter-depth (Figure 3.4; Chapter 3). This survey was carried out by dividing the research area into a 350 x 350 m grid. Each grid is represented by a minimum of one water-wells data. However, occasionally, no sample points can be found in a grid

because there are no water-wells. This acquisition method is effective since the purpose is only to discover the limit of pumiceous materials, not to collect a detailed stratigraphy data. To calculate the accuracy level of water-wells data, we conducted matching tests of pumice layer boundary with referenced stratigraphy, such as coring, drilling, and outcrop. This test was applied in a flat area, on a grid size of 350 x 350 m according to the sampling grid of water-wells. The difference of depth between the pumice layer boundary on the water-wells and the referenced stratigraphy is defined as the error. Distance between two tested points is also measured to indicate the variation of a stratigraphic layer over a certain distance.

In the presentation of stratigraphic data, specifically for outcrops that record syn-eruption deposits of the 1257 CE Samalas eruption, the nomenclature or stratigraphic division is based on Vidal et al. (2015). In the case of stratigraphic data derived from other methods, the stratigraphic division is based on lithological characteristics. The main objective of this stratigraphic division is to determine the boundary of the pumiceous layers from the 1257 CE eruption of Samalas volcano.

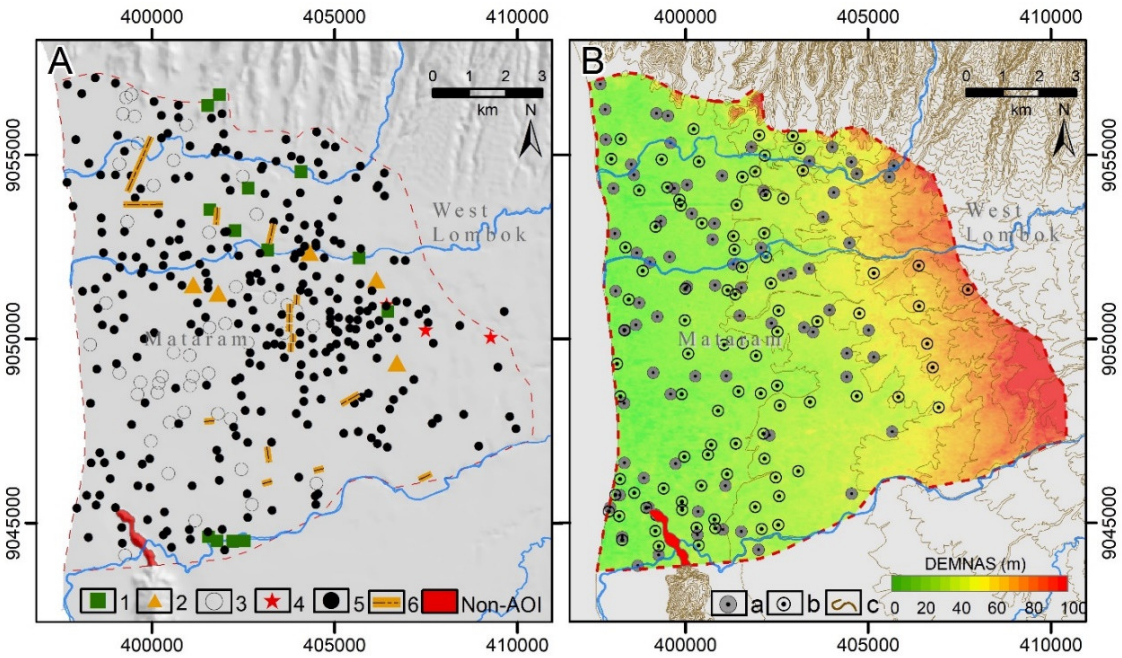

Figure 5.2. Various data compiled in this study. Stratigraphic points (Figure A) consist of 1: outcrop; 2: coring; 3: drilling; 4: hand auger; 5: water-wells data. Geophysics data (Figure A: 6) consist of 10 electrical resistivity tomography (ERT) measurement lines in the N-S and 6 lines in the W-E measurement direction. Topographic data (Figure B) consist of elevation point from real-time kinematic (RTK) measurement (a), RBI (*Rupa*

Bumi Indonesia) elevation point (b), RBI contour map (c), and DEMNAS (DEM Nasional, at ~8 resolution).

B. Geophysics data collection

Geoelectrical measurement or electrical resistivity tomography (ERT) was performed to investigate subsurface layers in the study area. A total of 16 sites were measured, ten oriented N-S (i.e., transverse to the main PDC flow direction and axes of fluvial remobilisation), and six oriented W-E (i.e., parallel to flow). The measurement campaigns were conducted in 2016 and 2017 in collaboration with the Indonesian Institute of Science (LIPI, now known as BRIN) and the University of Mataram, using Superstring R8/IP equipment with 56 Swift electrodes in a two-pole multi-electrode; dipole-dipole configuration. We used several electrode spacings: 4, 5, and 10 meters based on the measurement distance range, resulting in different measured depths. With these electrode spacings, we were able to observe subsurface conditions up to depth of 56 - 142 meters.

C. Topographic data collection

The dataset of the present topography (Figure 5.2B) was compiled from several sources: contour map with an interval of 12.5 m (map of *Rupa Bumi Indonesia* (RBI), 1:25,000), DEMNAS (DEM Nasional, resolution at ~8 m), and Global Navigation Satellite System (GNSS) measurements using real time kinematic (RTK) method. The RBI database and DEMNAS are accessible at https://tanahair.indonesia.go.id/. The RBI contour map are produced using photogrammetric method from aerial photos and ground control points. The DEMNAS is created by the Geospatial Agency of Indonesia, combining IFSAR (5 m), TERRASAR-X (5 m), and ALOS PALSAR (11.25 m) data. The RTK survey was performed to obtain more accurate elevation on each of 76 stratigraphic points, especially in the coastal area. At the same time, additional elevation points were also obtained from the RBI map. We also extracted river and shoreline data using the RBI map.

4.3.2. Data Processing

A. Present Elevation

A DEM of the study area was constructed by combining the RBI contour map, elevation point from RTK measurements, and DEMNAS extraction (Figure 5.2B). Compared to other DEM data sources, the constructed DEM from this combination is the most reliable current-DEM (CDEM) in the study area. Other DEM data sources such as SRTM (30 m) and ASTER (30 m) have lower resolution than RBI. Despite having better resolution (~8 m), in urbanized area such as Mataram city or in dense vegetation DEMNAS does not display a terrain model but a surface model. Therefore, we only extracted elevation points from DEMNAS and RBI data to assist the elevation points from RTK measurement, especially in the coastal area. Data integration began by interpolating elevation points using kriging through the Geostatistical Wizard in ArcMap. Only elevation points between contour 0 and 12.5 meters were interpolated and converted into a DEM. At this altitude range, the RBI contour is insensitive to the minor topographic variations, especially in the coastal area. Accordingly, the contours of the RBI are converted to a DEM using the Topo to Raster function in ArcMap. The results of the two DEMs were then combined to generate the CDEM of the study area with a resolution of 12.5 m.

B. Resistivity interpretation

In this study, measured resistivity data from field campaigns were treated using AGI (Advanced Geosciences Inc.) Earth Imager software for inverse resistivity modeling to obtain 2D profiles. In the inversion process, the iteration runs several times to produce a better model with low root-mean-square (RMS) error. The average error obtained in this inversion is 5.5%. The inverted resistivity models were then classified based on similar investigations in Lombok, especially related to pumice from the Samalas 1257 CE eruption (Hiden et al., 2017; Nugraha et al., 2022; Mutaqin et al., 2019). Drilling data also helped to interpret resistivity values for various sediment types, especially for distinguishing between sediment layers with pumiceous material and older sediment layers. For this study, the sediment layers containing dry pumiceous materials had a resistivity value $\geq$300 Ωm, whereas on the shallow water table the pumiceous layer had a resistivity value ranging from 30-300 Ωm. This

interpretation aims to distinguish between a layer containing pumiceous material and without pumice. The boundary line between these layers gives an impression of the paleo-surface condition before the 1257 CE Samalas eruption.

C. Depth to paleo-surface

The depth to paleo-surface represents the thickness of the Samalas deposit since the 1257 CE eruption. It is constrained by a paleosol layer or by the absence of the early Plinian pumice fallout deposits associated with phase P1-3 of the Samalas eruption. Figure 5.3 illustrates how to determine the depth to paleo-surface (Δh). The Δh was measured at each stratigraphic point. The difference between the present elevation and Δh gives a display of the past topographic surface (b) before the Samalas event (Figure 5.3A). This calculation (b=a-Δh) displays the paleo-topography as a 1D representation. For a 3D reconstruction, it is needed to do a further interpolation analysis using the Geostatistical Wizard in ArcMap. The input data is points of Δh. These data in the study area have a normal distribution, indicating that the kriging technique is the appropriate interpolation method (Mutaqin et al., 2019; Vermeer et al., 2014). In this process, kriging was performed by the smoothing method involving 58 neighbor points at each iteration, resulting in an elevation model of Δh or delta-DEM (DDEM).

The results of the kriging interpolation have a root-mean squared standardized error of 1.01 based on the calculation in Geostatistical Wizard, which is shown in Figure 5.3B. The area located farther from the stratigraphic point has a higher standard error up to 2.6. This value is close to the standard error of 2.8 for similar modeling conducted in East Lombok (Mutaqin et al., 2019). The central and the northern part of the study area have lower error values. In contrast, the peripheral area of the study area has more significant errors because it has no reference point outside the study area. This error value is also determined as an uncertainty value in calculating the volume of deposits that buried the paleo-topography. The volume of calculation is divided into two categories: sudden buried volume and progressive buried volume, employing the DDEM data through surface volume calculation in ArcMap.

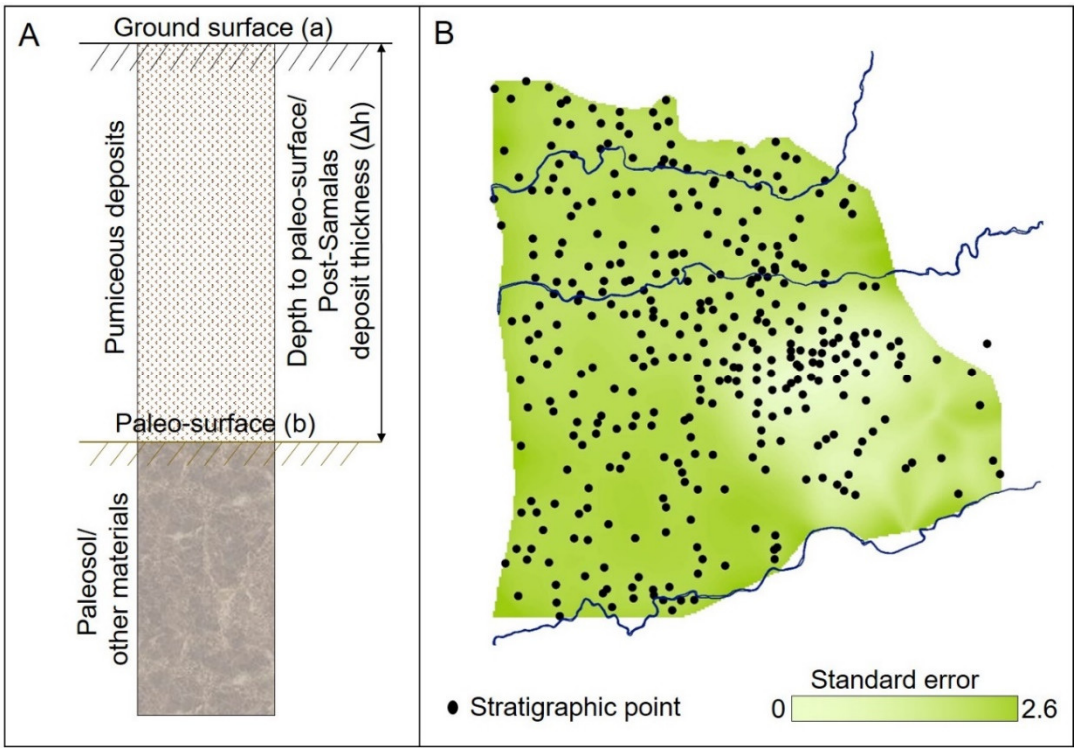

Figure 5.3. Illustration of the depth to paleo-surface measurement in each stratigraphic point (A) and standard error of DDEM modeling (B).

D. Topographic and Hydrographic Modeling

The method selected to build the paleo-topography is DEM deconstruction (Schmidt et al., 2018) through the raster calculator function in ArcMap. This method is also referred to as a top-down method (Meulen et al., 2020). Due to data availability, it is more reliable to use the deconstruction method instead of an inductive method (interpolation of paleo-surface points). Two DEMs were utilized for this operation which were inserted into the raster calculator toolbox in ArcMap, with the CDEM as the initial condition and the DDEM as the subtraction. The result of this operation is a paleo-DEM (PDEM) of the 13th century before the 1257 CE Samalas eruption. The paleo-topographic model was also reconstructed in 2D view using stratigraphic columns. This 2D view was also generated from the ERT measurement results: separating sediment layers with and without pumiceous material. Comparison of present and paleo-topographic profiles were also generated in E-W and N-S directions. This profiling method is also beneficial for describing shoreline and river valley displacement.

The hydrographic modeling consists of two objectives: paleo-river and paleo-shoreline models. The paleo-river reconstruction used the hydrologic model in ArcMap. The surface raster data used for this model is PDEM. The modeling workflow begins with the construction of a flow direction grid and then a flow accumulation grid. Using the contour map from the PDEM, the paleo-river channel was then refined by its correlation to the current stream conditions; meander and valley form. The meandering level was quantified by calculating the sinuosity ratio (SR); ratio of channel length to downvalley distance (Leopold et al., 1995). Another hydrographic reconstruction in this study was to distinguish land and sea boundaries before the 1257 CE Samalas eruption, i.e., the paleo-shoreline. The paleo-shoreline was identified by reclassifying the PDEM; <0 m refers to sea, whereas >0 m refers to land. The elevation boundary was then delineated to create a paleo-shoreline of the Mataram Plain. Radiocarbon dating was applied to a coral sample from sediment drilling to support the suggestion of paleo-shoreline and paleo-topographic evolution. The coral sample was sent to the National Nuclear Energy Agency of Indonesia (BATAN) for radiocarbon dating analysis and calibrated using Calib 8.2 (Stuiver et al., 2022) through the Marine20 database (Heaton et al., 2020).

5.4. Results

5.4.1. Stratigraphy and Depositional Processes of the Mataram Plain

The stratigraphic model of the Mataram Plain has not been investigated in detail before. In this study, we analyze the stratigraphic characteristics of the Mataram Plain to understand the depositional patterns during and after the Salamas eruption in 1257 CE. Based on the data collected for this study, stratigraphy in the Mataram Plain can be divided into four main layers: pre-eruption and paleosol, eruption deposit, post-eruption deposit, and recent soil. The first type of deposits in the study area are the pre-eruptive deposits which may consist of sandy material, bedrock, coral sediment, or paleosol. These deposits are located at the base of our stratigraphic column. Paleosol may not always be the basement of the Samalas deposits (syn- or post-eruptive). Other deposits such as bedrock or coral may help constrain the pre-eruption paleoenvironmental conditions. The next type of deposit is the initial deposit of the Samalas eruption, which is the deposit from the syn-eruptive processes from the first

(P1) to the fourth (P4) phase of the eruption. In some locations, this deposit is well preserved under the younger deposit: post-eruption sediments and recent soil. The third type of deposit is the post-Samalas deposits. These layers were deposited by reworked material after the 1257 CE eruption until recently. These deposits are the most frequent type in the study area and are usually thicker than other deposits (>3 m). In the Mataram Plain, this deposit is dominated by sandy materials mixed with pumice fragments. The sandy material ranges from fine to coarse and is mixed with gravel in several locations. The mixed pumice fragments indicate that this deposit results from the reworking of syn-eruptive deposits from P1 to P4. The upper sediment layer in the study area is a recent soil, which has varying thicknesses (0.5-2 m) with an average of one meter and a maximum of two meters. In this layer, anthropogenic infills are common, especially in the urban area of Mataram.

A stratigraphic column that records a nearly complete process of syn-eruptive deposition is situated at the Monjok outcrop (OC7) (UTM50S 403167x 9052419y), the riverbank of Jangkok River (Figure 5.4). At this location, the lower layer is a pumice fall from the first phase (P1). The base of this pumice layer is not visible in the outcrop due to its contact with the river. Above this layer, a weak (turbulent or dilute) PDC deposit is covered by thin pumice fall from the second phase (P2). Another pumice fallout from the third phase (P3) is lying on top of the P2 pumice fallout. The PDC of the fourth phase reached this location with a thickness of up to one meter. The upper part of this layer is slightly compacted and may have been eroded, and was then covered by gravelly sand deposits without any soil formation. This laharic type of sand-gravelly layer is relatively thick, reaching two meters. Another location near Jangkok River, the Sandubaya outcrop (OC9) (UTM50S 405669x 9052196y) was discovered on a small tributary riverbank. This outcrop recorded incomplete deposits from the Samalas eruption. PDC from the P4 in this location might have been eroded the P3 pumice fallout layer, indicated by a sub-horizontally bedded boundary between these layers. Other initial Samalas deposits are found on the riverbank of Babak River (OC13) (UTM50S 401782x 9044509y). Three types of syn-eruptive deposits were recorded in this location, i.e., ash, pumice fallout (P3), and PDC. The horizontally laminated sand in this outcrop may result from flooding of the Babak River. At the boundary between the Mataram Plain and the Pusuk-Tampole mountains, the pumice

fall deposits are well preserved in the stratigraphic layer (OC3) (UTM50S 401848x 9056638y). This layer is in contact with a paleosol from the andesitic-breccia parent material. It has a brown color and contains heavy-clay material.

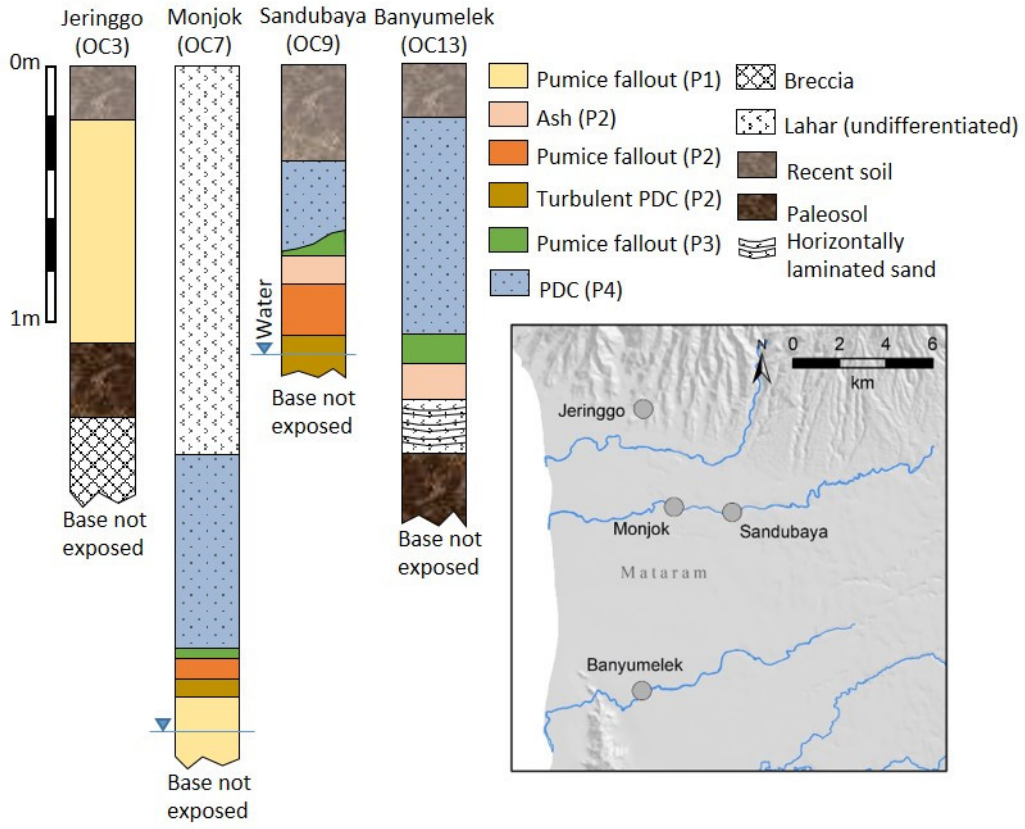

Figure 5.4. Stratigraphic columns of the Mataram Plain from field survey (outcrop data) that record syn-eruptive deposits (P1-P4) of the 1257 CE Samalas eruption. The nomenclature of these outcrops is based on the stratigraphic division of the previous investigation (Vidal et al., 2015).

The stratigraphic columns from coring, drilling, and water-wells survey also clearly illustrate the depositional processes in the study area. These data were classified according to lithological characteristics since most data had no records of syn-eruptive deposits, and data acquisition methods were not sufficiently robust to discern syn-eruptive deposits. Stratigraphic columns in the E-W direction (Figure 5.5) show that syn-eruptive deposits closer to the coastal zone have been completely reworked and transported into post-eruption deposits. In the central part of the study area, the coring data at the Islamic Center (UTM50S 401129x 9051474y) and Santika Hotel (UTM50S 401810x 9051248y) shows that the reworked material (post-Samalas)

is thicker than in other areas, reaching a thickness of nearly 10 m. Pumiceous deposits from syn- or post-eruptive are not present in Jangkok core (UTM50S 404315x 9052360y), except for a thick clay deposit which may correspond to reworked material from ash fall and dilute PDC (P2). It shows that the voluminous PDC of the fourth phase did not reach the study area except through the Babak and Jangkok River valleys. In the Babak valley, PDC reached the study area (~2 m thick) due to their deflection by hummocky terrain next to the Babak valley. As a result, the PDC follows the pattern of the Babak River valley. Similar to the Jangkok valley, an extension of the Sedau valley, the PDC that reaches this location is the remnant of the PDC surge that follows the valley pattern.

The water-well data is closely correlated with other stratigraphic data, making their availability helpful in optimizing the interpolation and extrapolation process. Our correlation test of this data type shows that water-well data has an average error of 0.7 m. From four sampling grids, the largest error is 1 meter, measured at a distance of 300 m from the water-well point to a referenced stratigraphy. The smallest error is 0.6 m at a distance of 51 m. This correlation test provides the distance of the tested points because stratigraphy can vary significantly even at close distances.

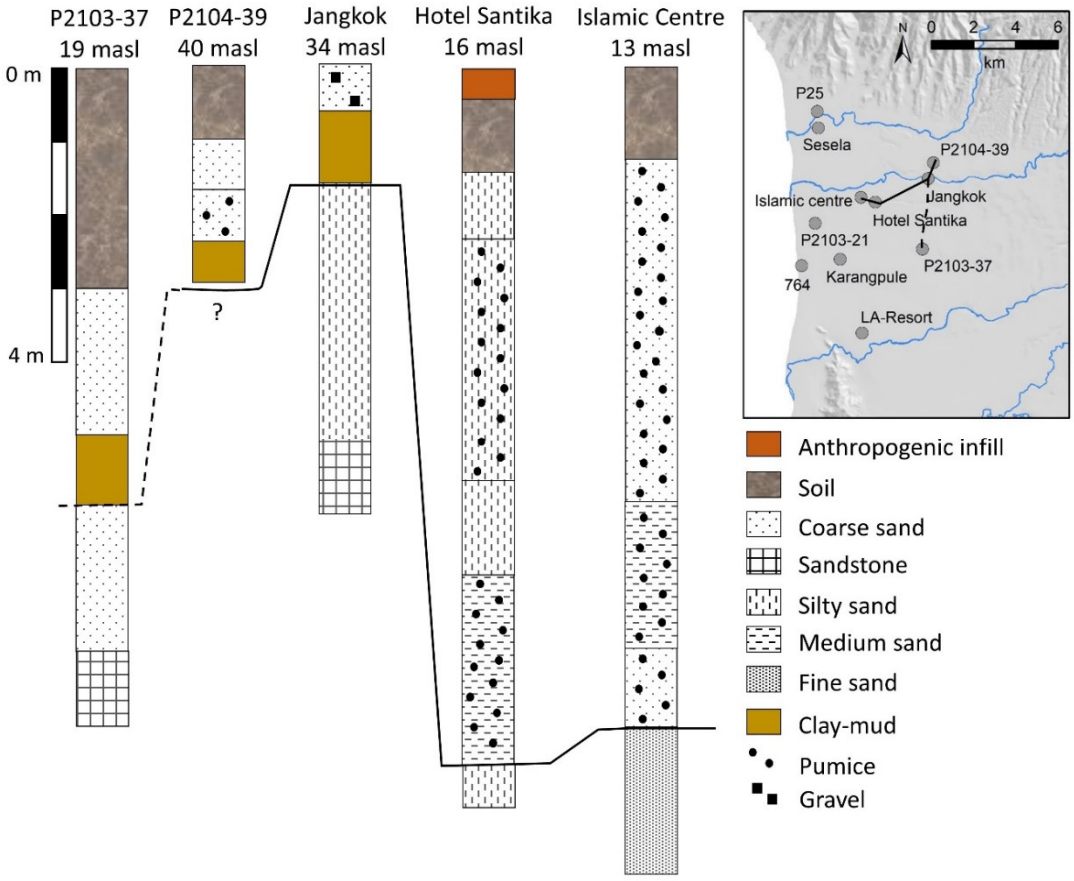

Figure 5.5. Stratigraphy columns and paleo-topographic boundary (black line) of the Mataram Plain in the E-W direction.

In the northern part of study area, some water-wells stratigraphy contain a "lumpur hitam" or "black clay-mud" layer as identified by the respondents (e.g., P2103-39). This deposit may correspond to the TPDC deposit of the second phase of the eruption (Appendix B). However, its occurrence is limited, and most are located adjacent to the stream courses, especially the Jangkok and Babak River. This indicates that these two rivers have had a vital role in the deposition of syn- and post-eruptive deposits. In the mouth of these two rivers, the present of similar sediment may indicate that formerly swampy area. Water-well data also records older materials such as bedrock and coral. In the local language, the widespread sandstone-breccia layer is called "ampan". Most water-wells in Mataram typically end in this layer (e.g., P2103-37). This bedrock is the extension of the sedimentary rock formation from the older deposit of Samalas-Rinjani volcanoes, i.e. the Lekopiko Formation (Mangga et al., 1994).

Water-wells in the southwestern part of the study area also contain a coral layer (e.g., 764) in the stratigraphic sequences, corresponding to the coral layer from drilling data acquisition (e.g., Karangpule and Sesela). These two drilling sites (Karangpule and Sesela) are located in the coastal area of Mataram (Figure 5.6). In the Sesela drilling site, corals are present at 11 m depth, and is mixed with reworked pumiceous fragments. The coral fragments in Karangpule drilling site were discovered at 8-12 m depth. The fresh coral at a depth of 11 m from this stratigraphic column was dated at 1646-1832 cal.CE (sigma 1). The coral fragments are fresh and possibly living coral in the shallow marine environment before being buried by the post-Samalas deposits. The pumiceous materials that buried the corals are mixed with sand, thus, indicating post-Samalas deposits or reworked materials. It is also demonstrated that in the coastal zone, the post-Samalas deposits are directly in contact with older material without any syn-eruption deposits. Syn-eruptive pumice might have also reached the sea but cannot bury corals with a relative-thick layer because it might be removed by sea currents and float instead of sinking and covering the corals. Given that corals persisted until ~1600 CE, this suggests that the sedimentation on the marine zone by the reworked syn-eruptive deposits has yet to be initiated immediately after the eruption. This zone was then progressively buried by the reworked materials or the post-eruptive deposits for at least three centuries after the eruption.

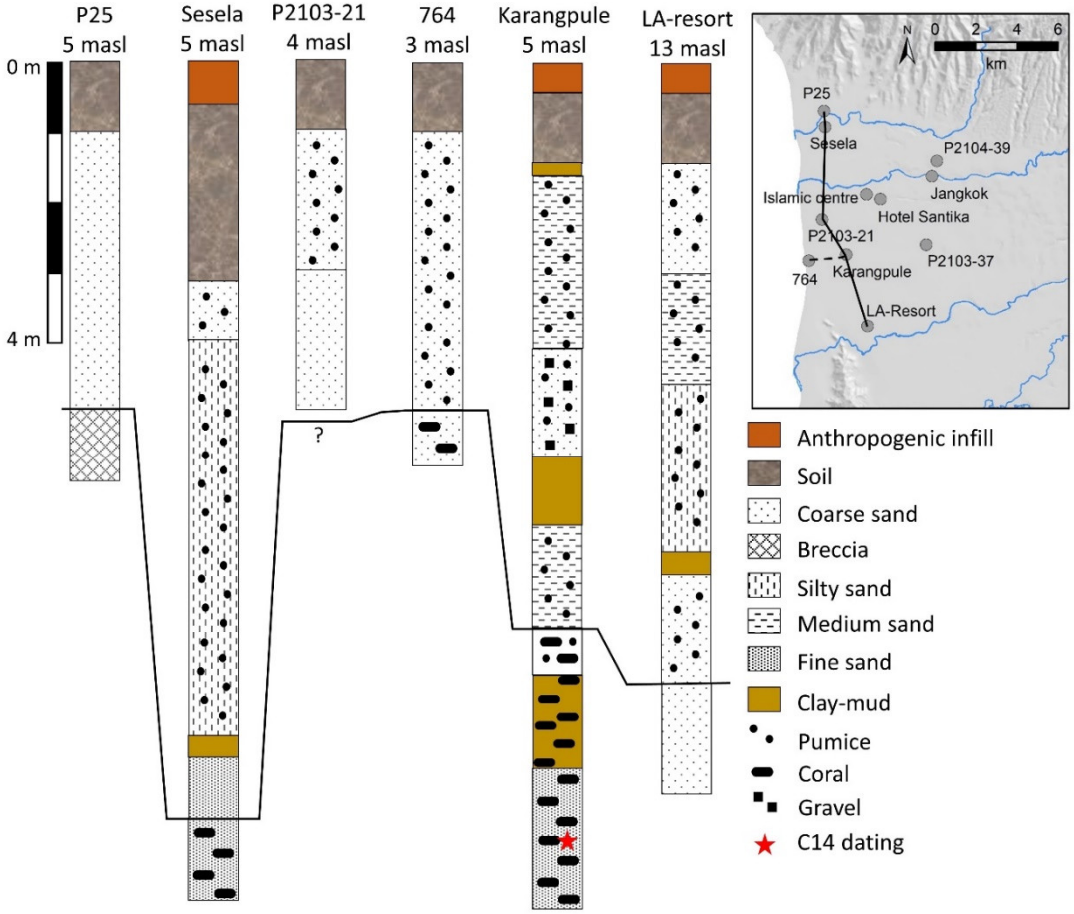

Figure 5.6. Stratigraphy columns and paleo-topographic boundary (black line) of the Mataram Plain in the N-S direction.

5.4.2. ERT cross-section

The subsurface condition of the study area can be divided into two layers based on the inverted resistivity cross-section results; sandy-pumiceous (dry: >300 Ωm/wet: 30-300 Ωm) and other finer materials such as clay and mud (<30 Ωm). This division is helpful in interpreting the limit of pumiceous layer as the boundary of the paleo-surface prior to the 1257 CE Samalas eruption.

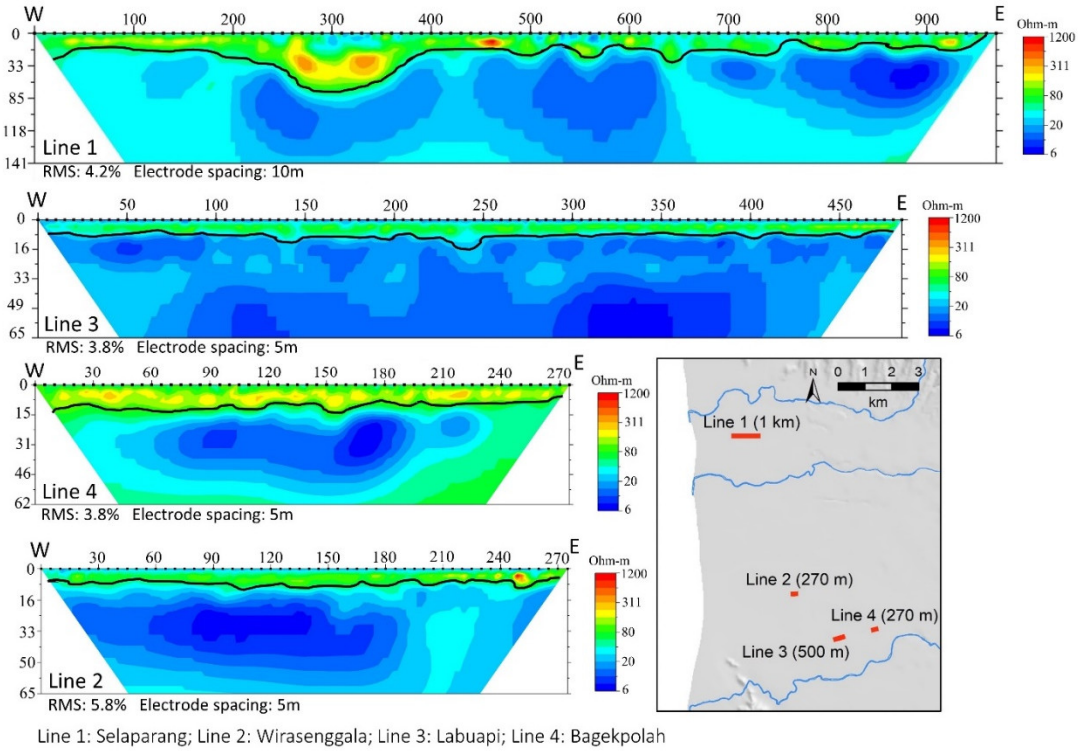

Figure 5.7. Inverted resistivity cross-sections of the Mataram Plain on the W-E direction. Blackline represents the limit of the pumiceous layer and the possible boundary of paleo-surface.

In the W-E direction, we present four inverted resistivity cross-sections in Figure 5.7. The remaining inverted resistivity data is presented in the appendix (Appendix B). The data is at good quality with low RMS errors in this measurement direction: the most significant error obtained is 5.8%, whereas the smallest is 3.8%. The Selaparang (Line 1) cross-section is one kilometer long. The highest resistivity in this line is 1200 Ωm. The pumiceous layer in line is identified by the resistivity value ranging from 30-1200 Ωm, distributed along the surface. The maximum depth of the pumiceous layer in this line is ~50 m from the present ground surface, located 230-380 m from W, which is formed in a small basin. Lines 2 and 3 have similar resistivity characteristics, where the pumiceous material is interpreted to have resistivity values ranging from 30-278 Ωm at shallow depths (8-14 m depth). On Line 4, the pumiceous layer has a distinctive value over other lines. On this line, the pumiceous layer has a value >100 Ωm because gravelly material is dominant on the surface, which is mixed with pumice. Lahar transport by the Babak River strongly influenced the depositional process at this location.

In the N-S direction, the average error of the four inverted resistivity lines is 6.6% (Figure 5.8). The sandy-pumiceous materials on Lines 5, 6, and 7 have a similar resistivity value (>300 Ωm). On Line 5, the maximum depth of the pumiceous layer is 12 m, whereas on Lines 6 and 7, the maximum depth is 14 m. In contrast to other lines, Line 8 has a resistivity value of the suspected pumiceous material ranging from 30 to 1200 Ωm. The resistivity value of the sandy-pumiceous layer on this line is relatively low compared to the other lines oriented N-S. Similar to W-E measurement lines, we suggest that this layer contains sandy-pumiceous materials with a high water content. Water-well data indicate that this area has a shallow ground water table. Another reason is due to measurement lines located in rice fields with an active irrigation system throughout the year. On Line 7, we conducted drilling up to 21 m. In the upper layer of the drilling data (0-2 m), sandy material with clay dominates. Below this layer, sandy material with pumice is present (2-6 m). The pumice fragments increased at the 6-8 meter depth. The mixing of pumiceous and sandy materials continues up to 12 m depth. Until 21 m depth, pumice is absent, only dark-colored clay mixed with sand is present. Observed water-wells in this location and the surrounding area also show similar sediment type.

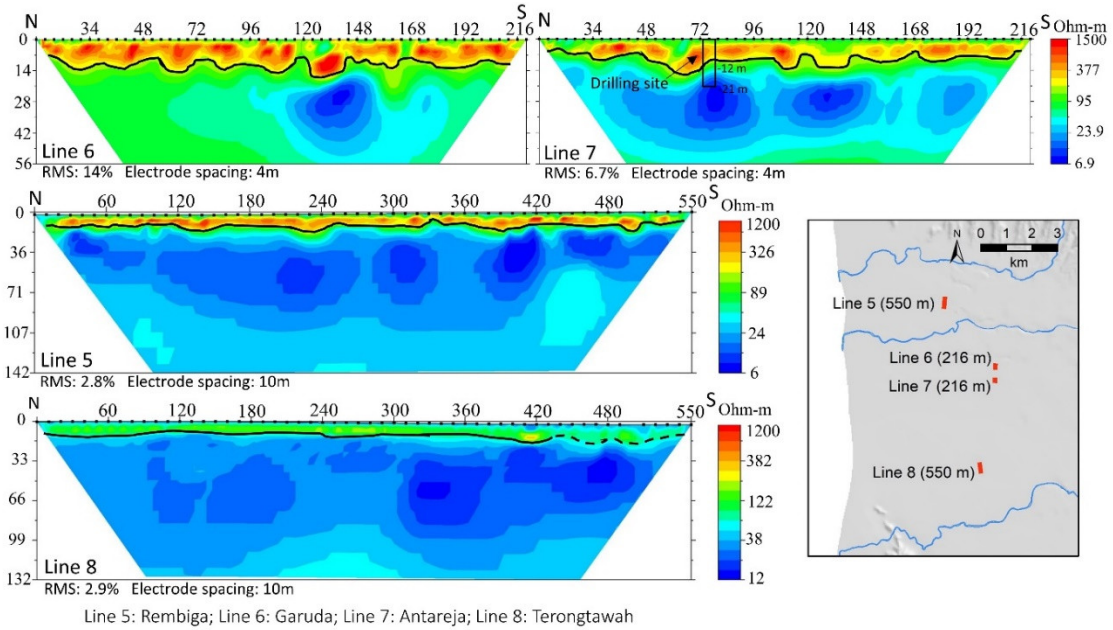

Figure 5.8. Inverted resistivity cross-section of the Mataram Plain on the N-S direction. Blackline represents the limit of the pumiceous layer and the possible boundary of paleo-surface.

On all resistivity profiles the pumiceous layer is laterally continuous near the surface, with a distinctive boundary with underlying material occurring at variable depths, reaching a maximum of 50 m on Line 1. Discontinuity is only present on Line 8 (430-550 m), where the suspected pumiceous layer on the surface is disturbed by human-induced processes such as quarrying and dumping of soil layers for agricultural purposes. If the maximum depth limit of the pumiceous materials on Line 1 (50 m) is compared with the present ground elevation (8 m), the small basin formed is indicated as a nearshore basin. This implies that before the 1257 CE Samalas eruption, there was a marine environment at this site. Based on these measurements, the ERT has a significant ability to investigate the position of the paleo-surface which also indicates topographic evolution in 2D data.

5.4.3. Paleo-topographic reconstruction

Paleo-topographic reconstruction of the study area was successfully conducted by DEM subtraction involving CDEM and DDEM, resulting in a PDEM with the same resolution (Figure 5.9AB). The entire study area has aggraded from the pre-eruption state to the current condition. However, the aggradation processes might also have occurred in the older volcanic complex area in the north study area due to the deposition of pumice fallout. Sediment accumulation tends to be concentrated in low-lying areas (<15 masl), which are also subject to significant topographic changes. The average thickness of the sediments burying the study area after the Samalas eruption is 4.6 m, whereas the thickest post-eruptive deposit measured in the stratigraphic data is 14 m. However, some locations were also directly affected by syn-eruptive deposits such as pumice fallout and PDC, although it was only maximum of ~3 m thick.

Comparison of 10 km long topographic cross-sections (line ab) shows a relatively similar relief (Figure 5.10A). A change in the shoreline is detected on this profile line, which progressed ~1 km from its previous location. The thickest post-Samalas lahar and fluviatile deposits occur c. 2.3 km upstream from the present shoreline, which lies at point 1 in the profile line. Approximately 5 km downstream of the profile line, the primary Samalas PDC deposits appear to terminate (point 2), although downstream aggradation of post-eruption volcaniclastics has obscured this paleo-topographic break in slope. This suggests that the topographic break in slope is

between the primary PDC deposits and the resedimented material, and is not represented at the modern surface. In the remaining 5 km, the topographic changes are varied, indicating that the sedimentation processes were complex. In this section, lahars and fluvial processes were the primary causes of topographic change. The source of the depositional material is the erosion of PDC deposits, which was then distributed by the main river channel and its tributaries that flow through the Mataram Plain.

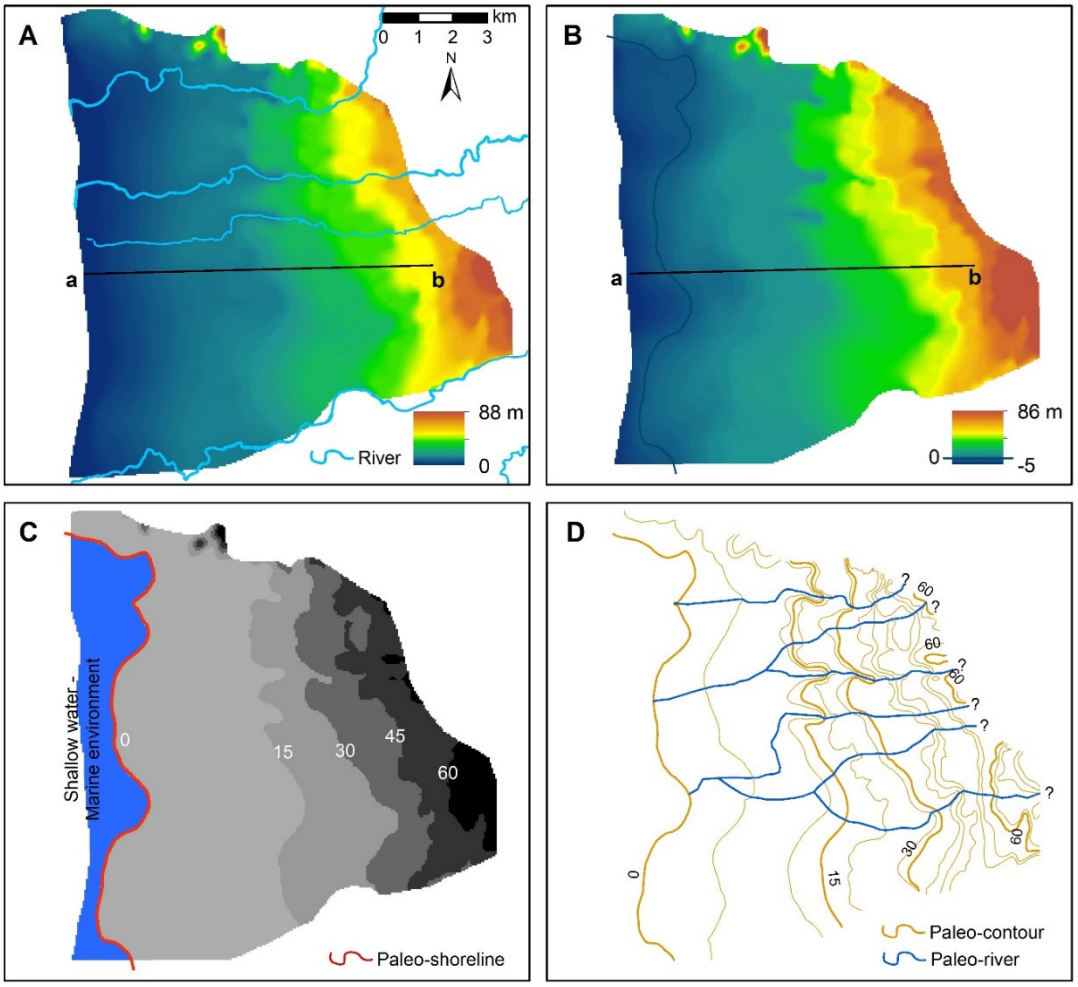

Figure 5.9. Comparison of the CDEM (A) and PDEM (B) of the study area. The PDEM is useful for delineating the paleo-shoreline (C) and reconstructing pre-eruption river courses through flow accumulation modeling (D).

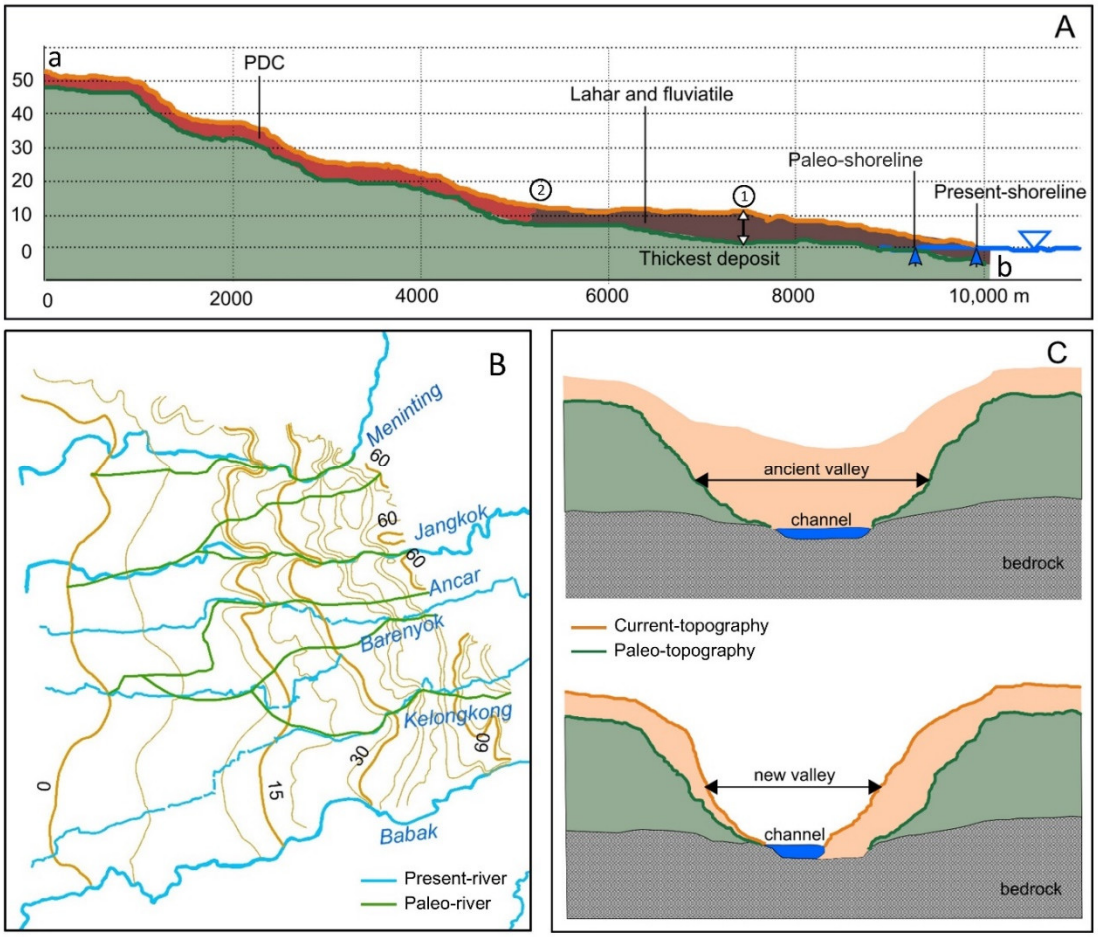

Figure 5.10. Topographic cross-section of the line ab (Figure 5.9) shows the comparison between current- and paleo-topography, and Samalas-related deposit thicknesses (A). Map of the paleo-river in the study area (B), and the illustration of river valley development (C).

The paleo-shoreline of the study area was successfully identified using the PDEM. The PDEM shows a similar relief pattern to the CDEM except in the coastal area, which is changed from a shallow-marine environment to a fluvio-marine depositional landform. Shoreline configuration in the past was not typically a straight shoreline but consisted of minor bays and headlands (Figure 5.9C). However, coral in the shallow-marine environment along the offshore area has been destroyed by sedimentation and human activities. Fluvial processes such as erosion, transport, and sedimentation are the main processes in distributing sediment from Samalas volcano, especially from the two rivers originating from Samalas volcano, namely the Jangkok and Babak Rivers. Three small watersheds formed on the SW foot slopes of Samalas (Ancar, Barenyok, and Kelongkong) also contributed to the redistribution of post-

eruption deposits. These three watersheds have similar sizes and shapes. The redistribution process was also sustained by the Meninting River originating from the older volcanic complex of Pusuk-Tampole.

Comparison between paleo- and present-rivers can detect hydrographic shifts in the study area (Figure 5.10B). The Meninting River in the north has experienced a sizeable change in its river pattern. Previously, this river had a straight channel (sinuosity ratio (SR): 1.01). After the Samalas eruption, the degree of meandering of this river increased (SR: 1.5), and the river mouth shifted southward. The paleo- and present-river valley form of Meninting is relatively similar at a paleo-elevation >15 m. The position of the river channel is relatively constant, except for the meander pattern, which shows a significant displacement, especially in the lowland area. A small delta was formed in the mouth of this river. This delta expanded and turned into a wider fluvio-marine depositional landform causing the land to move forward. Currently, no delta is formed at the Meninting River estuary but a spit.

In the low-lying area, significant changes also occurred in the Jangkok River. Previously, this river had an SR of 1.01, but now it has changed to 1.2. The mouth of this river has shifted northward while its tributary has now disappeared. The next river networks are Ancar, Barenyok, and Kelongkong. These river channels have experienced sizable shifts and developed their own river mouths. The upper Ancar River has significantly displaced and nearly merged with the paleo-channel of Barenyok River. During the evolution of the Barenyok River, whose upstream segment has experienced significant changes, has become the shortest river and the smallest watershed in the Mataram Plain. Kelongkong has also experienced drastic changes in its river mouth compared to other rivers. This river switched the position of its mouth up to 4 km to the south, towards Pengsong Hill. Based on paleo-river modeling, the upper courses of rivers in the study area have largely reoccupied their original channel (pre-eruption condition). Unlike the downstream area, the river channels were relatively unconfined and free to avulse and wander.

A distinctive alignment of right-angled kinks in the paleo-river courses of the Meninting, Ancar and Jangkok Rivers suggests there was a fault in the Mataran Plain. This fault may contributed to the merging of the Ancar, Barenyok and Kelongkong

Rivers. Currently, no faults are mapped in the geological map of the study area. However, the location of right-angled alignment is nearly aligned with the maximum observable PDC deposits. It may also represent the starting boundary for the resedimentation of reworked materials and post-eruptive deposits (Figure 5.10A; point 2).

The Babak River is omitted from hydrographic analysis due to its location, which is adjacent to the boundary of the study area. Hence, it will generate a significant bias when conducting flow-accumulation modeling. Based on its morphometric characteristics, this river may not have dramatic channel shifting similar to the upper Meninting River; it displays minor changes in the degree of meandering. This is because the hummocky terrain limits this river, and in the lower area, it flows through residual hills; therefore, its position is relatively stable. Changes occurred only at the Babak River mouth, a southward shift, indicated by a long spit (~1 km) which is considered the longest spit in western Lombok.

5.5. Discussion

Reconstruction of paleo-topography in this study is performed using DEM subtraction method. This method is similar to the top-down (Meulen et al., 2020) or retrogressive method (Werbrouck et al., 2011). This method was selected because it provides higher reliability for reconstructing the PDEM of the study area than the interpolation method on paleo-surface points or the bottom-up approach. The bottom-up approach (Meulen et al., 2020) requires a large quantity of elevation point data to reconstruct a PDEM with an accurate relief. However, access to large-scale data in the study area is limited. For example, to generate a PDEM, 20,000 elevation points are required to be extracted from the ancient map (Ullmann et al., 2019). However, no ancient map represents the relief configuration before the 13th century of the study area. The lack of legacy data from previous works in the study area is also one of the limitations to the availability of stratigraphic data. Legacy data may include previous surveys or researches, soil databases, and geologic coring (Vermeer et al., 2014). The use of legacy data is helpful in PDEM reconstruction: such as in Sandy Flanders, Belgium, up to 80% of legacy data from the total sample points was obtained to reconstruct its paleo-topography (Vermeer et al., 2014).

In the PDEM reconstruction of the study area, various sources of subsurface data have been collected. However, the stratigraphic data acquisition in built-up areas such as in Mataram city is more challenging due to complex human activity (Pröschel and Lehmkuhl, 2019). In this study, we utilized existing water-wells for stratigraphic observations, with the help of the owner and well-driller. However, all the information obtained from informants must be verified and cross-checked with other stratigraphic data in the neighboring area, such as from cores or outcrops, before entering the modeling process. We recommend this acquisition method as an alternative method to obtain data on the subsurface sediment layer if data accessibility through other methods (outcrop, coring, drilling, and legacy data) is limited. Although paleo-topography can still be reconstructed using minimal stratigraphic data and geomorphic markers (Elez et al., 2016), the water-well inventory data give the advantage of helping optimize 3D interpolation, especially in terrains where the paleo-topography is changing rapidly. This method is less accurate than other stratigraphic acquisition methods in the study area. However, instead of only producing a topographic section (2D profile) of the paleo-topography, as is the case for stratigraphic extrapolation (Amorosi et al., 2012), ERT or ground penetrating radar (GPR) cross-section (Abrams and Sigurdsson, 2007; Gomez et al., 2021; Silva et al., 2013), or isotope application (Tang et al., 2017), water-well inventory data were helpful in producing high-resolution 3D model.

Based on our analysis, we also recommend the ERT measurement method to illustrate the paleo-topography in 2D, especially when it has a contrasting layer such as in study area due to significant amounts of pumice material. If the sediment is relatively similar or without a known chronostratigraphic marker, this method becomes less effective to illustrate the paleo-topography. Correlation to the stratigraphic column is also necessary to help interpret the paleo-topographic boundary. However, ERT measurements are unable to distinguish between syn- and post-eruptive deposits.

We have successfully reconstructed the paleo-topography (2D and 3D) of the Mataram Plain prior to the Samalas 1257 CE eruption and the following aggradation to current conditions. The depositional process of syn-eruptive deposits in the study area is similar to the 79 CE Vesuvius eruption (Vogel and Märker, 2010; Vogel et al., 2011), whereas the depositional of post-eruptive deposits is similar to the 1991 Pinatubo eruption (Pierson et al., 1992). It can be divided into two, i.e., sudden deposition due to PDC

deposition and gradual deposition due to fluvial or laharic processes. The chronology of this second type of depositional process is complex to simulate because the local climate has strongly influenced the deposition since the eruption of Samalas in 1257 CE. In lahar and fluvial deposition modeling, climatic factors are also an important aspect to consider (Gomez et al., 2018; Lavigne et al., 2000; Gob et al., 2016). For instance, the paleoclimate evolution of Lombok remains unknown.

Our reconstruction revealed that the current shoreline of the study area lies ~1.6 km (average) westward from the paleo-shoreline prior to the eruption of Samalas in 1257 CE. Previous topographic modeling in east Lombok is unable to demonstrate the paleo-shoreline prior to the Samalas eruption (Mutaqin et al., 2019). In general, the average shoreline change due to sedimentation is 2.3 m/year. However, this change was not constant, but it possibly experienced an accelerated sediment-delivery rate due to heavy rainfall in any given year (Pierson et al., 1992). The remobilisation rate of reworked materials may follow an exponential decay curve of sediment transport whose maximum delivery occurred within 10-100 years after the eruption. However, in the case of heavily impacted basin such as in the study area, the exponential decay curve is insufficient to describe the long-term sediment transport (Gran et al., 2011).

The transported and deposited material in the study area clearly originated from the 1257 CE eruption. Samalas no longer produces significant pyroclastic products, except for deposits in the caldera due to the activity of Barujari Somma-volcano, e.g., the latest eruption in 2009 and 2015 (De Maisonneuve and Bergal-Kuvikas, 2020; Rachmat et al., 2016; Solikhin et al., 2010; Wiguna et al., 2016). In addition, although Rinjani is actively erupting, lahar deposition tends to move eastward because currently there is no drainage system from the Rinjani volcano flowing SW to the study area (Hadisantono et al., 2008).

Stratigraphic evidence shows that the PDC of Samalas 1257 CE did not reach the paleo-shoreline. This finding revises the estimated PDC emplacement boundary from previous works (Lavigne et al., 2013; Vidal et al., 2015) (Figure 5.11A). There is no evidence that the PDC reached the shoreline of Mataram (Figure 5.11B) because no PDC cliff-beach was formed, such as in the N, NE, NW, and SE directions of the caldera (Hadmoko et al., 2021; Mutaqin et al., 2019). In these areas, even after more than 700

years, the syn-eruptive PDC deposits remain observable in the beach areas (Figure 5.11C). Otherwise, beach topography in the study area (SW direction from the caldera) is flat with a sand-textured grain without any traces of syn-eruptive PDC deposits. The furthest observable PDC in the SW direction is in the Babak River valley, which is located at 2.3 km from the paleo-shoreline and 3.8 km from the current shoreline. The PDCs might be entering the ~2 km flat plain behind the paleo-shoreline with a thin deposit thickness (<1 m). The fluvial and lahar events subsequently removed it and created a laharic pumiceous flat plain, leaving no trace of PDCs.

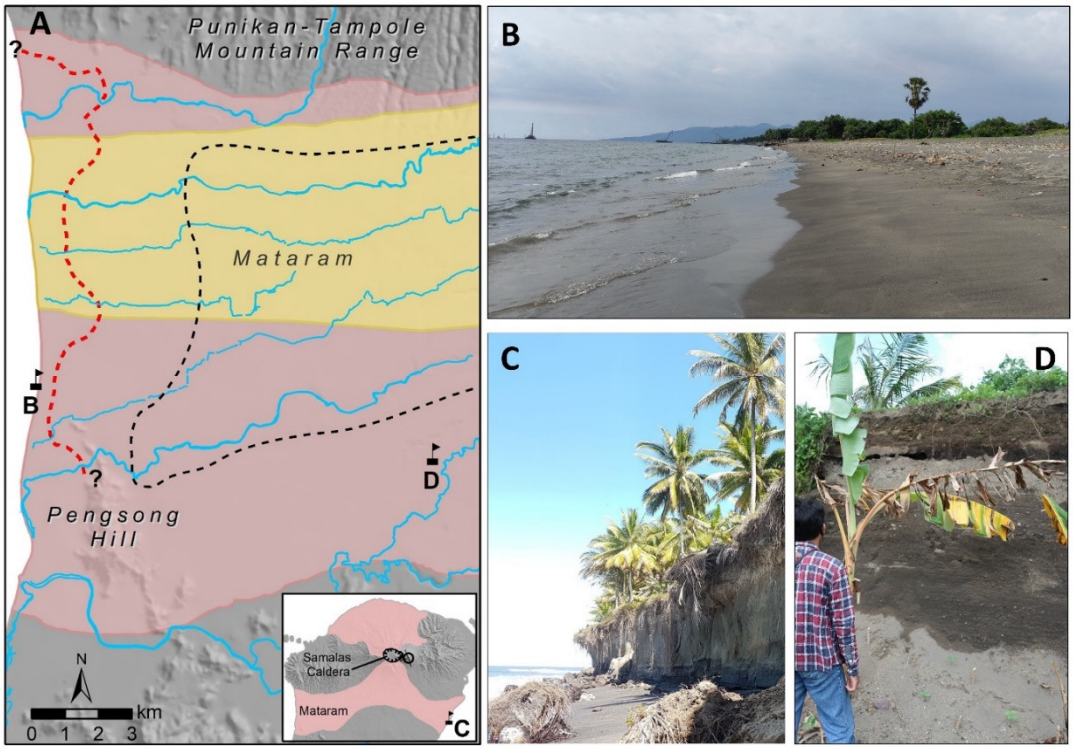

Figure 5.11. (A) Comparison of the PDC emplacement boundary in the Mataram Plain: pink area from Vidal et al. (2015), yellow area from Lavigne et al. (2013), and black-dashed line from this study. This delineation is based on the PDCs that are observable in the field. Paleo-shoreline delineation represented by red-dashed line. Beach morphology in the Mataram Plain indicates no evidence of PDC entrance to the sea (B), in contrast with Korleko (SE direction), the cliff-beach formed by the PDCs deposition (C). Laharic type is the common surface deposit in the Mataram Plain (D).

We also calculated the volume of deposit that buried the paleo-topography of the Mataram Plain due to the Samalas eruption. The total of preserved volume in the study area is 318 x 10^6 m^3, composed of two types: PDC that suddenly changes the topography (110 $\pm$ 3 x 10^6 m^3), and fluvio-laharic deposits that gradually deposited (208 $\pm$ 3 x 10^6

m^3). This total volume is only half of the total preserved volume in the SE direction. This is due to the fact that the average deposit thickness in the SE direction is 7.8 m with a maximum thickness of 30 m (Mutaqin et al., 2019), whereas in the study area these value are only 4.6 m and 14 m respectively.

To better understand the study area's sedimentation pattern and landscape evolution, we propose a schematic model that displays three phases of landscape evolution: the pre-eruption condition, the immediate post-eruption condition, and the development to the current condition (Figure 5.12). This model shows that the Mataram Plain has evolved due to the direct impact of volcanic eruption by a landscape-mantling process (Manville et al., 2009) (Figure 5.12B). The following process is landscape-modifying and –forming (Manville et al., 2009), which is significantly influenced by fluvial processes (Figure 5.12C). The PDC is considered to have been the main driving force responsible for the abrupt impact on the landscape (Aydin et al., 2013; Pierson et al., 1992; Vogel and Märker, 2013). At the same time, fluvial processes are also an influencing factor in many locations that experienced landscape changes (Gob et al., 2016; Hadmoko et al., 2018; Umbal and Rodolfo, 1996; Ville et al., 2015).

The schematic model in Figure 5.12 extends a similar model on the Lombok Island that describes the topographic evolution of this island from the Late Oligocene to the Holocene (Zubaidah, 2010). Although only focused on the western part (SW direction from caldera), our model further develops the previously proposed model yet with a higher resolution, especially the recent evolution over the last ~700 years. The exact timing of each phase of landscape evolution in Lombok has yet to be determined. However, the sediment remobilisation process in the study area can be described using an analog model of fluvial sediment transport through time in a disturbed basin due to eruption (Gran et al., 2011). In the first stage of post-eruptive condition (Figure 5.12B), the heavily impacted drainage basin in Lombok might be entered the first phase of fluvial system response (Gran et al., 2011). During this stage, erosion in the hillslope areas was initiated, new valleys were created, and river networks started to develop (Gran et al., 2011; Pierson and Major, 2014). Remobilised materials were then stored in the lowland areas unmantled by PDC (2-3 km from the paleo-shoreline). This stage may persist for an extended period with an estimated maximum duration of ~300 years. This duration is based on the indication of a shallow marine environment that remained undisturbed until

the 17th century. In the following stage (Figure 5.12C), Lombok entered the second phase of fluvial instability, where valley widening and erosion continued, resulting in continuous sediment transport until it reached equilibrium conditions (Gran et al., 2011; Pierson and Major, 2014). In this stage, aggradation in the shallow marine environment may have been initiated. Accelerated sedimentation due to anthropogenic influences may also have occurred when the Balinese kingdom started to occupy the Mataram Plain after the 17th century (van der Kraan, 1997).

Other paleo-topographic reconstructions also reveal the intensity of anthropogenic influence modifying the landscape (Lajczak et al., 2021; Pröschel and Lehmkuhl, 2019). However, this study only considers the direct volcanic influence and subsequent fluvial processes, although an anthropogenic layer is also found in several stratigraphic logs. The incidental discovery of ancient ruins on the SW slopes of Samalas at Aik Berik and Batukiliang, 17 and 21 km respectively from the caldera, is a signal that other ancient villages or cities may have existed in this location (Malawani et al., 2022). These two locations are on gentle slopes and are associated with rivers, which are identical to ancient-agricultural settlements found in several sites in Java (Gomez et al., 2010). The Mataram coast is adjacent to Bali and Java islands, implying a high potential as a significant ancient coastal city/village. Paleo-topographic reconstruction is essential as an initial reference in evaluating ancient cities, ancient landscapes, or archaeological heritages (Mozzi et al., 2017). Therefore, the PDEM is a valuable reference for exploring potential locations of ancient ruins, such as through analysis of settlement suitability (Canuto and Auld-Thomas, 2021). The PDEM may also be helpful for paleo-hazard analysis (Wronna et al., 2017). Lombok is adjacent to the active subduction zone with a high potential for tsunamis where the Indo-Australian plate moves to the north beneath the Indonesian (Eurasian) plate. Although no paleo-tsunami deposits have been identified at Mataram (Mutaqin et al., 2021; Pradjoko et al., 2015), this study may provide valuable information on the vulnerability of ancient civilizations to disasters.

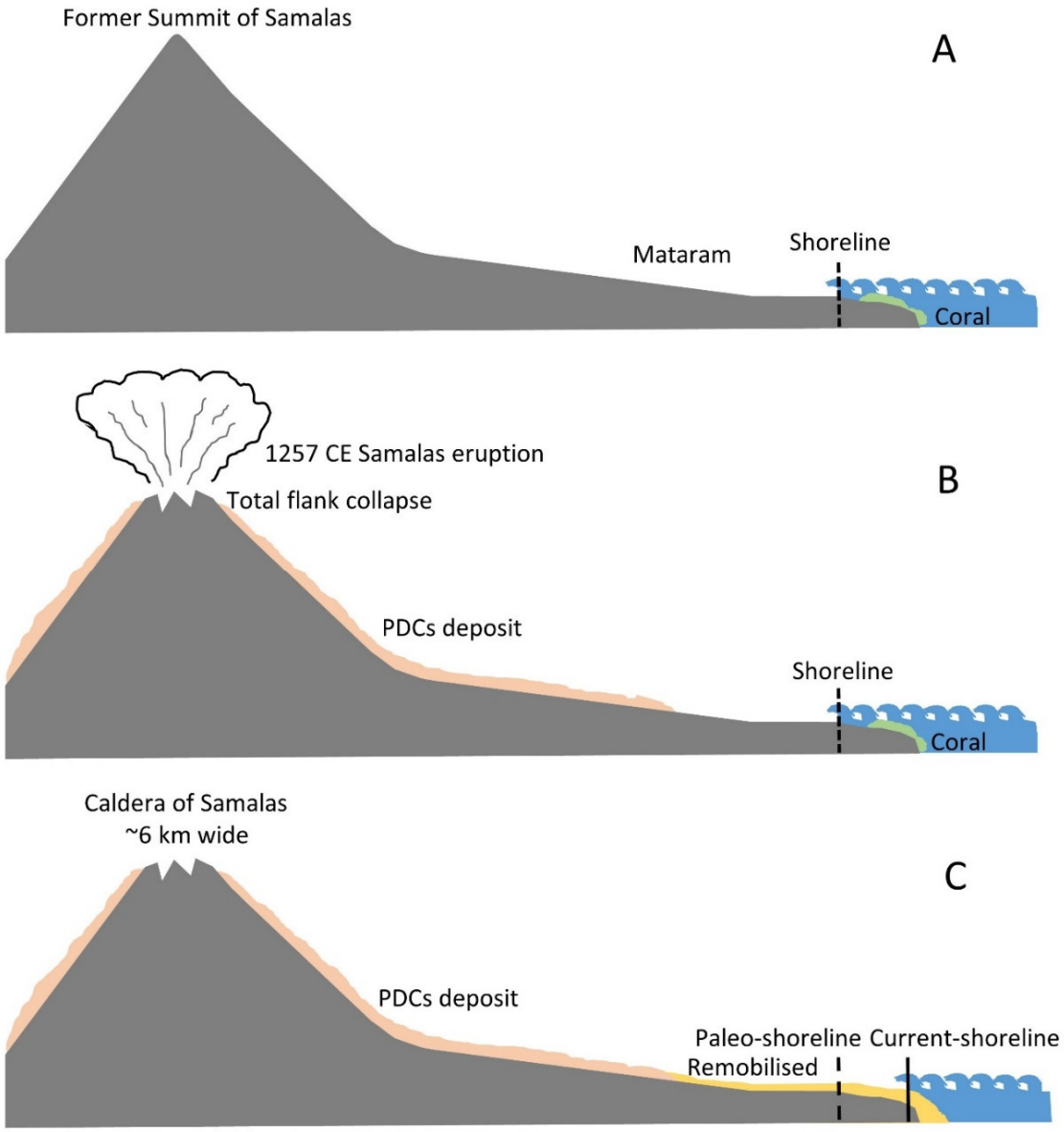

Figure 5.12. Illustration of the landscape evolution of the study area from pre-eruption condition (A), shortly after eruption of Samalas 1257 CE (B), and the further development up to the current condition (C). Figure description: Figure A: The Mataram Plain has a flat to gently sloping topography and is occupied by coral in the shallow marine environment; Figure B: Final phase of Samalas 1257 CE eruption ejected voluminous PDCs which mantled large areas of Lombok and caused the total collapse of Samalas volcano; Figure C: The deposits of Samalas 1257 CE eruption started to be reworked and remobilised across the study area sustained by several river networks, and the paleo-shoreline started to move westward into current condition.

5.6. Conclusions

Sedimentation patterns in western Lombok following the 1257 CE Samalas eruption have been successfully reconstructed through paleo-topography and paleo-hydrography analysis, employing various stratigraphic data sources and geophysical measurements. The result of the paleo-topographic model is considered valid with a relatively low error; thus, the hydrographic model based on PDEM data is also valid. Our results have good validity for the paleo-shoreline model because it is supported by the discovery of corals at several locations. Since the eruption of Samalas in 1257 CE, the study area has undergone both abrupt and gradual changes. The abrupt changes caused by PDC deposition occurred in the upstream of study area, whereas the downstream area experienced gradual change by post-eruptive lahar and fluvial sedimentation. The landscape evolution in the study area has occurred in three stages. The first stage is the pre-eruption condition when the coastal area of Mataram Plain consisted of bays and headlands that were locally occupied by the coral reef environments. The second stage is the eruption stage when the PDC partially covered the study area with a total volume of $110 \pm 3 \times 10^6$ m^3. In the last stage, there was progressive sedimentation by lahar and fluvial processes with a total volume of $208 \pm 3 \times 10^6$ m^3. As a result of this sedimentation, the shoreline has moved westward by an average of 1.6 km from its pre-eruptive position. In addition to modifying the estimated boundary of the PDC deposition from previous suggestions, our modeling results will be helpful for further investigation into the speculative ancient lost city that was buried by pyroclastic deposits of the Samalas eruption in 1257 CE.

CHAPTER 6

The previous chapter indicated that the topography of Mataram Plain was remarkably different before and after the 1257 CE Samalas eruption. It is also possible that Samalas deposits buried pre-eruption ancient villages. Indigenous written sources are available that can be used to illustrate the pre-eruption conditions. In addition to the Babad Lombok, which contains a complete narrative of the early history until ca. 17th century, two other babad, namely Babad Suwung and Babad Sembalun were likely compiled during the same period from the social memories of inhabitants. A detailed examination of these three documents is essential in assessing the social consequences of the eruption of Samalas in 1257 CE. The purpose of this chapter is to solve the enigma that surrounds the 1257 CE Samalas eruption on society, thus completing the previous chapter to explore the physical as well as social effects of a past major eruption in human history.

THE 1257 CE CATACLYSMIC ERUPTION OF SAMALAS VOLCANO REVEALED BY INDIGENOUS WRITTEN SOURCES

Abstract

Historical and archaeological findings have revealed that many human civilizations have been strongly affected by natural hazards, such as volcanic eruptions. An issue that still lacks attention is the response of ancient populations following eruptions as well as their resilience strategies. Three written sources from Lombok, Indonesia, provide descriptions of the ancient landscape of Lombok and the population's response to the Samalas volcano eruption in 1257 CE. The sources depict the conditions of Lombok and the surrounding areas during the pre-, onset-, and post-eruption phases of a catastrophic volcanic eruption with a volcanic explosivity index 7. Various responses of the inhabitants to the eruption are described in the sources, such as fleeing to the hills, avoiding hazards, and escaping to neighboring villages or islands. Several geographic features and toponyms are mentioned, allowing us to reconstruct the evacuation process during the crisis period. The sources also describe recovery strategies in the post-eruption period, including governance strategies, the rebuilding of cities and villages, and agriculture. The historical record suggests that Lombok may have taken up to a century to recover from the eruption and that new kingdoms and principalities became established by the fourteenth century. Disaster management related to the eruption is described in the texts from Lombok, but not in older written sources from Indonesia.

Keywords: Disaster recovery; emergency-response; large eruption; Samalas volcano; written source

This chapter corresponds to an article published in Journal of Volcanology and Geothermal Research, Vol. 432. No. 107688.

https://doi.org/10.1016/j.jvolgeores.2022.107688

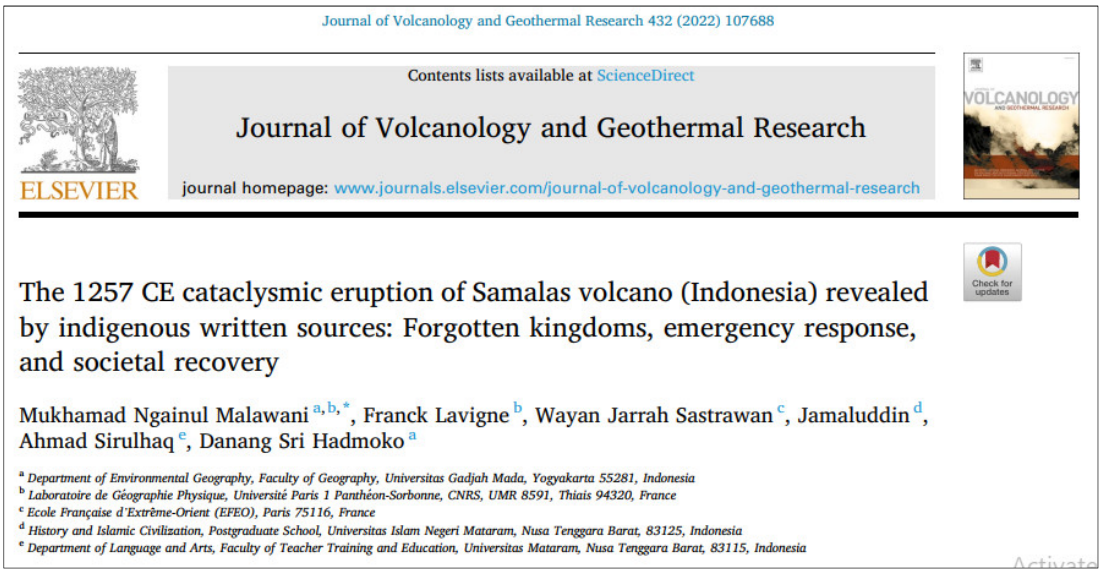

Journal of Volcanology and Geothermal Research 432 (2022) 107688

Contents lists available at ScienceDirect

Journal of Volcanology and Geothermal Research

journal homepage: www.journals.elsevier.com/journal-of-volcanology-and-geothermal-research

The 1257 CE cataclysmic eruption of Samalas volcano (Indonesia) revealed by indigenous written sources: Forgotten kingdoms, emergency response, and societal recovery

Mukhamad Ngainul Malawani [a,b,*], Franck Lavigne [b], Wayan Jarrah Sastrawan [c], Jamaluddin [d], Ahmad Sirulhaq [e], Danang Sri Hadmoko [a]

[a] Department of Environmental Geography, Faculty of Geography, Universitas Gadjah Mada, Yogyakarta 55281, Indonesia
[b] Laboratoire de Géographie Physique, Université Paris 1 Panthéon-Sorbonne, CNRS, UMR 8591, Thiais 94320, France
[c] Ecole Française d'Extrême-Orient (EFEO), Paris 75116, France
[d] History and Islamic Civilization, Postgraduate School, Universitas Islam Negeri Mataram, Nusa Tenggara Barat, 83125, Indonesia
[e] Department of Language and Arts, Faculty of Teacher Training and Education, Universitas Mataram, Nusa Tenggara Barat, 83115, Indonesia

6.1. Introduction

A mysterious volcanic eruption in 1257 CE has been associated with several volcanoes, but none have matched its magnitude, geochemistry, and eruption timing (Lowe and Higham, 1998; Palais et al., 1992). The polar ice cores data analyses suggest that this eruption had the highest sulfate aerosols spike in the last two millennia (Oppenheimer, 2003; Sigl et al., 2013). A multidisciplinary study subsequently confirmed that this eruption originated from a tropical volcano: the Samalas volcano on Lombok Island, part of Lesser Sunda Islands group in Indonesia (Lavigne et al., 2013). The Lesser Sunda Islands are a group of Miocene or younger islands located to the northwest of Australia and east of Java. This region is commonly divided into two zones due to magmatic processes, viz., the East Sunda Arc zone, which includes Bali, Lombok, and Sumbawa, and the Banda Arc zone, which includes other islands such as Flores, Timor, Alor, and Wetar (Hall, 2009). The Lesser Sunda Islands are home to three volcanoes that have experienced volcanic explosivity index (VEI) 7, including Batur volcano on Bali (34.6 ka), Samalas volcano (1257 CE), and Tambora volcano on Sumbawa (1815 CE) (De Maisonneuve and Bergal-Kuvikas, 2020).

The Samalas 1257 CE eruption's main characteristics have been determined, including ejecta volume and a model of the magmatic activity that provoked the eruption (Métrich et al., 2017; Vidal et al., 2015, 2016). This VEI 7 eruption occurred in four phases: initial Plinian phase, phreatomagmatic phase, explosive Plinian climax phase, and caldera formation phase that was accompanied by widespread pyroclastic density currents (PDCs) (Vidal et al., 2015). The total volume of ejected material was ~40 km^3 of dense rock equivalent (Vidal et al., 2015). This eruption led to a climatic disturbance worldwide in the thirteenth century. Climatic conditions of the Northern Hemisphere were severely disturbed for two years, especially in Europe, in the aftermath of the Samalas eruption (Guillet et al., 2017). These climatic disturbances presumably then provoked societal and political disruptions in European countries in the medieval era (Campbell, 2017; Stothers, 2000). The latest findings suggest that the Samalas eruption had a close connection to the climatic disruption that led to the apocalyptic plague: the Black Death (Fell et al., 2020). In the long term, the Samalas eruption in 1257 CE was one of the significant triggers that contributed to the Little Ice Age (Miller et al., 2012). Although its global impact has been widely discussed, its local impact remains little known, including its societal impact at

local and regional scales on Lombok and the neighboring islands of Bali and Sumbawa (Alloway et al., 2017; Reid, 2016). Through historical documents from Lombok, we attempt to address these issues.

Tracing the societal impact of a past eruption requires a search for historical documents. Historical documents generally reflect an author's own direct experiences as an eyewitness or those of third parties (Garrison et al., 2018; Principe et al., 2004; Trigo et al., 2010; Ulusoy et al., 2019). In the study of volcanic eruptions, the combination of historical sources and geological data provides a better understanding of past eruptions: volcanology yields the nature and timing of the eruption, while the historical sources describe the societal impacts that reflect the extent of the disturbance (Cashman and Giordano, 2008). Not all historical sources provide reliable evidence, and major questions are raised when only fragmented accounts are available (Guidoboni and Ciuccarelli, 2008). Access to archaeological data or eyewitness statements may also be limited, making the process more challenging (Tennant et al., 2021). However, addressing these issues in detail is crucial in preparing for future events (Cashman and Giordano, 2008; Martin, 2020; Pyle, 2017).

The first written source discovered from Lombok that mentions the Samalas eruption is *Babad Lombok* (Hägerdal, 2015; Jamaluddin, 2012; Lavigne et al., 2013; Marrison, 1997). A *babad* is a genre of historical writing found primarily in Java, Bali, and Lombok. *Babad* consist of a compilation of historical writings that describes the connections between various events, but also contains legendary elements (Ras, 1986; Paramartha, 2017). The accuracy of the content of different *babad* texts varies, but many can serve as valuable historical sources (Ricklefs, 1998; Ricklefs, 2008). The *Babad Lombok* mentions the collapse of a volcano during an undated eruption before the Selaparang Kingdom in Lombok (Lavigne et al., 2013; Marrison, 1999). A previous study by Lavigne et al. (2013) suggested that this event corresponds to the 1257 CE Samalas eruption; a mysterious eruption that had previously only been identified in the polar ice cores (Gao et al., 2007; Gao et al., 2008; Sigl et al., 2013). Many parts of the *Babad Lombok* provide invaluable information about the societal impacts of this eruption at the local and regional scales.

Another text that portrays an eruption is the *Babad Suwung*. This *babad* has been partly analysed by Mutaqin and Lavigne (2019). A new discovery by our team, the *Babad Sembalun*, is a once-forgotten document from Lombok that may also depict the account of the same event. These *babad* texts were written in relatively recent times (within the last three centuries), but they likely record oral and folk traditions of earlier times. Based on similar descriptions, we believe the narrative of volcanic eruptions in the three *babad* draws on memories of events from 1257 CE, even though no specific time is given for the eruptions described in the texts. Furthermore, the volcanological record indicates that, within the last 2500 years, only the Samalas eruption of 1257 CE had the sufficient magnitude to impact humans to the extent described in these texts (Lavigne et al., 2013; Métrich et al., 2017).

The local impact of the Samalas eruption can be traced in the three *babad* documents, especially the societal response. In this study, we provide an exegesis of the three sources that describe the situation during pre-eruption conditions, the emergency response, and the recovery strategies conducted by the inhabitants of Lombok amid the cataclysmic eruption of Samalas volcano. In addition, reconstruction of human migration following the Samalas eruption helps to trace the ancient lost kingdom of Pamatan, which was erased by the pyroclastic activity (Lavigne et al., 2013; Malawani et al., 2021). The experience of previous generations facing and surviving the Samalas eruption that was transmitted orally and documented in the *babad* texts may serve as a valuable lesson for future generations in dealing with natural hazards, especially those related to a volcano eruption.

6.2. Methods

6.2.1. Characteristics of Babad from Lombok

The lack of historic documents about eruptions is a crucial challenge for the volcanic history of Indonesia (Sastrawan 2022). The chief reason is the perishability of written documents in the archipelago. Although there is evidence of historical writing in Indonesia going back to at least the fourteenth century (e.g. the *Deśavarṇana* chronicle written in 1365 in the Javanese royal court of Majapahit), these early texts do not exist in their original physical forms. Rather, they have been copied from manuscript to manuscript over many centuries, with the original versions of these texts

long lost. In Lombok, as in neighbouring Bali, documents are traditionally written on palm leaves, including the *Babad Lombok*, *Babad Suwung*, and *Babad Sembalun.* Palm-leaf (*lontar*) manuscripts do not withstand the tropical climate for more than a few centuries, especially if they are frequently handled (van der Meij 2017). It is therefore extremely rare to encounter manuscripts older than 500 years anywhere in Indonesia. In Lombok, ancient texts survive only in recent copies—physically no older than a century or two. The texts concerning an eruption of Samalas, which we examine here, were written most likely within the last 300 years. They therefore represent a recent recording of what appears to have been older oral traditions.

The *Babad Lombok* and *Babad Sembalun* are written in Old Javanese, whereas the *Babad Suwung* is written in the Sasak language. Both languages are commonly used in the literature of Lombok's Sasak-speaking communities (Marrison, 1999; van der Meij, 2011). The *Babad Lombok* is the most familiar historic document of Lombok known to the wider public, and it is used as the chief reference in local studies of the history of Lombok (Marrison, 1997). In contrast, the content of the *Babad Suwung* was almost unknown before its recent exegeses (e.g., Mansyur, 2019; Mulyadi, 2014; Mutaqin and Lavigne, 2019). Although the original palm-leaf document is preserved in the Museum of Nusa Tenggara Barat (NTB), only a few historians are familiar with this written source and little has been published on it. *Babad Sembalun* contains accounts that are familiar to many people in the Sembalun valley, but are little recognized by people outside this area. According to the traditional custodians of the text, some of the narrations were sacred and kept secret from the broader community. There is still an oral tradition of *Babad Sembalun*, and the original palm-leaf document is well preserved in the village of Sembalun. *Babad Lombok*, *Babad Suwung*, and *Babad Sembalun* share similarities in depicting the ancient settlement landscape and portraying a major volcanic eruption that is likely the same event. These *babad* record the social memories of Lombok's inhabitants, including of a catastrophic volcanic eruption, even though they were written at least four centuries after the eruption (Hägerdal, 2015; Marrison, 1999).

Compared to other regions in eastern Indonesia, Lombok has a large number of historical manuscripts (van der Meij, 2011). Previous scholars have suggested that the original *Babad Lombok* may have been written around the fourteenth century,

based on the assumption that the writing tradition of the Sasak tribe began before the fourteenth century (Jamaludin, 2005). However, the majority of historical manuscripts in Lombok were recompiled and restructured since the arrival of the Islamic culture in Lombok around the sixteen and seventeen centuries as a strategy of Islamic diffusion (Jamaluddin, 2012). This is indicated by the existence of Islamic cultural patterns and symbols throughout the *babad* texts, including extensive narratives involving Qur'anic figures such as Nabi Nuh (the Prophet Noah) (Marrison, 1999; Suparman 1994).

We suspect that textual histories of the three *babad* are similar, i.e., they were compiled in the eighteenth or nineteenth century from long-standing oral traditions that originated in Lombok. The composition of these *babad*, in their current written form, can be dated approximately to the period 1700–1900 CE based on information contained within the text. The *Babad Lombok* and *Babad Suwung* both describe the Balinese capture of Selaparang in 1692 CE (Hägerdal, 2001), which means that they must have been written after this time. The *Babad Lombok* exists in several recensions. The particular version used in this study belongs to a group of texts called *Babad Lombok Adam*, the earliest of which was written before 1861 CE (Teeuw, 1958; Marrison, 1999). By contrast, the *Babad Suwung* and the *Babad Sembalun* may well have obtained their current forms in the early twentieth century. We therefore consider the three *babad* as repositories of second-hand information, which were recompiled, rewritten, and restructured from multiple sources. According to Berry et al. (2021), such sources are of mediocre reliability as evidence for historical fact. However, these relatively recent *babad* texts express the community's memories and describe events in the distant past, however exaggerated or inaccurate their later retellings may be.

6.2.2. Exegesis of written sources

Until present, only the *Babad Lombok* has been officially translated by the Center for Language Development of the Ministry of Education and Culture Republic Indonesia (Figure 6.1A). It was published twice; the first version was issued in 1979 by L. Wacana, and the revised version in 1994 by L. Suparman. These publications are based on a typed copy of a *lontar* manuscript belonging to the *Babad Lombok Adam* tradition. The official transliterated version of *Babad Lombok* (1994) is available in the online repository of the Ministry of Education and Culture, Indonesia

(https://repositori.kemdikbud.go.id/1487/). The translated version of the *Babad Suwung* (Figure 6.1B) was recovered from the National Museum of NTB at the request of our team. The translated version of the *Babad Sembalun* was also obtained during the same mission from the ancestral keeper in Sembalun village (Figure 6.1C). Neither of these two manuscripts had a standard numbering format, unlike the *Babad Lombok*. We have received the raw translated text of the *Babad Suwung* in local Sasak language and Indonesian from the Museum of NTB. Accordingly, we cannot provide clear references to the number of the verse we quote, in contrast to those in the *Babad Lombok*. The difference between *Babad Lombok* and the other two *babad* is that *Babad Lombok* contains many verses (1217 verses in total), whereas the others are narrative types of writing with fewer stanzas. The National Museum of NTB has yet not digitized the *Babad Suwung* and *Babad Sembalun* at the time of this writing. Since there is no official translated version of these manuscripts in the current Indonesian language, the upcoming official version may not be identical to ours. Therefore, we also provide the romanized transliteration of the *Babad Suwung* and *Babad Sembalun* in the Supplementary Material (selected verses). The full copy of these two *babad* can be accessed by visiting the Museum of NTB and Sembalun village.

Figure 6.1. Original palm leaves of the *Babad Lombok* from the Museum of NTB (A) and the official transliterated version of the *Babad Lombok* by L. Suparman (1994) (B). Interpreter of the *Babad Suwung* from the Museum of NTB (C) and recitation of the *Babad Suwung* (D). Ancestral keeper of *Babad Sembalun* (E) and discussion of the *babad* narrations (F). Photo courtesy F. Lavigne (2016).

The exegesis of *babad* texts was conducted from various perspectives, such as history, linguistics, and geography. A historical perspective was gained by confirming the chronological narratives with local historians of Lombok. We selected the narratives related to the issues of volcanic eruptions. We focused only on the chronology of volcanic eruptions for the period before the Islamic arrival in Lombok, which occurred in the early sixteenth century. We used a linguistic approach to confirm toponyms mentioned in the *babad*. We determined the literal meanings of toponyms to assist in locating it on the current map and to identify possible place name transformations. We used a geographic approach to map the flow and direction of the migrants described in the *babad*. In order to provide a chronological account of the Samalas eruption, we classified the texts into three periods related to the Samalas eruption, i.e., pre-, onset-, and post-eruption (Table 6.1). All of the sources contain information from these periods, but the level of detail differs.

Table 6.1. Variation of narrations in *babad* related to the story of volcano eruption.

Source	Pre-eruption	Onset-eruption	Post-eruption
Babad Lombok	a,b,g	c,d,e	f,g
Babad Suwung	a	c,e	g
Babad Sembalun	a,b	c,e	f,g
[a]Settlement condition; [b]natural landscape; [c]nature of eruption, [d]impact, [e]emergency response, [f]recovery, [g]cultural landscape			

6.2.3. Linking written sources and field evidence

Previous studies have proven that a large volcanic eruption occurred in Lombok in 1257 CE (e.g., Lavigne et al., 2013; Vidal et al., 2015, 2016; Métrich et al., 2017). Volcanic eruptions mentioned in the three *babad* most likely refer to this eruption. Field investigations to verify the accuracy of the historical documents were necessary (Lavigne et al. 2021). Deposits from the 1257 CE eruption are easy to find

in Lombok. The Samalas deposits maps and stratigraphic columns from Lavigne et al. (2013) and Vidal et al. (2015) both illustrate the magnitude of this eruption, which matches the one described in the *babad*. However, in Lombok, evidence of ancient settlements is limited. The archaeological site in Aikberik (West Lombok) is not available for further investigation because it has been developed for agriculture, making re-excavation impossible at this time. This site was accidentally found when conducting land clearing for rice fields. A lithic fragment, suspected to be a kitchen utensil, was recovered and is currently stored in the office of the Aikberik village head. Eyewitnesses have described archaeological remnants of a small village including ruins, suspected to a former granary and an armory. We also identified archaeological artifacts at the Museum of NTB that were catalogued (Ceramics Inventory First and Second Edition) in order to track the occurrence of ceramics older than the 1257 CE Samalas eruption. Another source of evidence is the existence of toponyms mentioned in the *babad*. Several sources were used to map the toponyms: a recent topographic map (Rupa Bumi Indonesia/RBI, 1:25,000) (retrieved from https://tanahair.indonesia.go.id/portal-web/) and the 1900s topographic maps from Dutch Colonial Maps KIT (retrieved from https://digitalcollections.universiteitleiden.nl/view/collection/kitmaps). The old map of Lombok is useful for identifying the potential name transformations of villages and other geographical features such as rivers, hills, and mountains.

6.3. Results

6.3.1. Ancient kingdoms and settlements in Lombok

According to the *Babad Lombok*, the oldest settlement was called Lae or Laeq, a name that means 'a very long ago'. This etymology suggests that Lae may not be a historically real settlement but rather a legendary "original city". Lae was later abandoned, and a new settlement called Pamatan was built. The exact location of these two settlements remains uncertain. Currently there is no archaeological evidence that could be ascribed to these settlements. The description in the *Babad Lombok* indicates that the city of Pamatan was located in the lowland area, in the distal zone of the volcano: "…all the inhabitants slept soundly at the foot of the mountain" (verse 226) (Table 6.2). According to this *babad*, Pamatan was the capital city of a strong kingdom

prior to the thirteenth century, with complete infrastructure, such as houses, city walls, a town hall, and boulevards. The majority of the inhabitants were involved in agriculture and fishery, as indicated by the cultivation of various fruits and vegetables and sea fishing. Some of them were merchants with commercial connections to traders from other islands, such as the Bajo Tribe from Sulawesi (Celebes Island). Pamatan was inhabited by nearly ten thousand people (verse 226). The Pamatan city was also considered a developed city: "the inhabitants of Pamatan were prosperous and wealthy; there was no scarcity" (verse 226).

Table 6.2. The description of Pamatan in the Babad Lombok (transliterated version by L. Suparman, 1994).

Verse	Old-Javanese	Indonesian translation	English translation
222	*Kewala wus medaling nagari, desa Lae' punika dan tinggal, sami tumedun wong ngakeh, hapindah saking riku, malih pada ngawe nagari, sireng bumi Pamatan, hakumpul hing riku, hanggawe kuta balumbang, wus sumapta, lalarenpo pada nginggil, wus kukuh kang nagara.*	*Asalkan sudah keluar, desa Lae itu ditinggalkan, semua turun si orang banyak, berpindah dari situ, lagi membuat desa di bumi Pamatan, berkumpul di situ, membuat benteng kota, sudah siap semua, pagar dan tembok tinggi, sudah kukuh kotanya*	They left the village, the village of Lae was abandoned, everyone came down, moved from there (Lae), they made a new village in Pamatan, they all gathered, they made fortresses, everything was completed: fences, high walls; the city was established.
223	*Wus ya karya humah haling dadi, lan papalen, raranggon pasebon, wus lajur lurunge, harame desa hagung, kebun hasrih ngidu nagari, tetanduran samapta, pisang gedang tebu*	*Sudah membuat rumah dan lumbung, dan dapur, balai peranginan dan balai pertemuan, jalan-jalan terbentang, ramai di desa besar itu, taman indah mengelilingi kota, taman lengkap, pisang pepaya*	Houses had been built, barns, kitchens, halls and town halls, the roads extended out, the ambiance of the village was lively, beautiful gardens surrounded the city; crops were complete: bananas,

Verse	Old-Javanese	Indonesian translation	English translation
	saruh jambe lan jalima, gedang ngental, kalapa heran kasambi, tinggulun ladri dara.	*tebu, sirih pinang dan delima, pepaya, rontal, kelapa heran kusambi, tingguli seladri dara cina*	papayas, sugar cane, betel, areca and pomegranate, palm, coconut, celery, jujube.
226	*Kawarneha hing wong jero nagari, hing Pamatan, sami mukti suka, datan nana kurangane, wong dagang sami rawuh, lan wong bajo hakeh, kang prapti, salwir watangan hana ta halimbah hipun, wong Pamatan sajro katah, meh salaksa, pada sare kumalipit, ing gunung hitampiran.*	*Alkisah orang didalam negeri itu, di desa Pamatan, semua sejahtera makmur, tak ada kekurangannya, para pedagang datang, dan orang Bajo (Sulawesi) banyak yang datang, semua barang ada, diperjualbelikan, penduduk Pamatan banyak, hampir sepuluh ribu, semua tertidur nyenyak, di bawah kaki gunung*	It is told that the inhabitants of Pamatan were prosperous and wealthy, there was no scarcity, many traders came, and people from Bajo (Sulawesi), all goods were available and exchanged, the inhabitants of Pamatan were numerous, almost ten thousand, and all the inhabitants slept soundly at the foot of the mountain.

An additional ancient settlement in Lombok suspected to be older than Pamatan is described in the *Babad Sembalun*. This settlement is located in the northeastern part of Samalas volcano, i.e., the Sembalun valley and its surroundings. The *babad*'s story of Lombok's ancient settlement begins with several nomadic human groups living on the slopes of volcano, who eventually settled in the village of Beleq. Before that, they had lived at many places around the slopes of volcano, sheltered in the savannah of Lendang Goar, and established a permanent settlement on the slope of Anakdara hill, which was later called Beleq (Figure 6.2). This location was chosen because it is close to a lake (the former Sembalun Lake) and a spring. On the current topographic map, Beleq is located next to the Sembalun depression. They lived there for a long time until a major eruption of Samalas volcano, which we suggest was inspired by community memories of the 1257 CE event. It is uncertain how long they lived in Beleq.

According to oral traditions from Sembalun, the oldest ancestors of the local inhabitants had lived there since the ninth century. The eruption of Samalas in the thirteenth century forced them to migrate outside of the Sembalun valley.

The landscape of ancient settlements before the Samalas eruption is not clearly depicted in the *Babad Suwung*. An ancient kingdom named Suwung (meaning 'Emptiness') is mentioned, which then expanded by building new villages across Lombok. Similar to Lae, the symbolic name of Suwung may refer simply to a legendary original settlement. The toponyms of the ancient settlement before the eruption are given in the texts and are mappable on current topographic maps, including Bayan, Beleq, Sembalun, Pejanggik, Langko, Kuripan, Salut, Batukiliang, and Taliwang (Figure 6.2). Other toponyms are also available, but their locations are not found in current topographic maps. According to the *Babad Suwung*, the most developed settlement on Lombok was Selaparang. The representatives of Selaparang village were sent to support the development of Taliwang (on the neighbouring island of Sumbawa), but when they reached Taliwang, the volcanic eruption began. Based on these descriptions, the settlements developed by the Suwung kingdom were established before the Samalas eruption. Later in the text, the narrations recounting the eruption of Samalas reflect social memories of inter-island links across the Alas Strait.

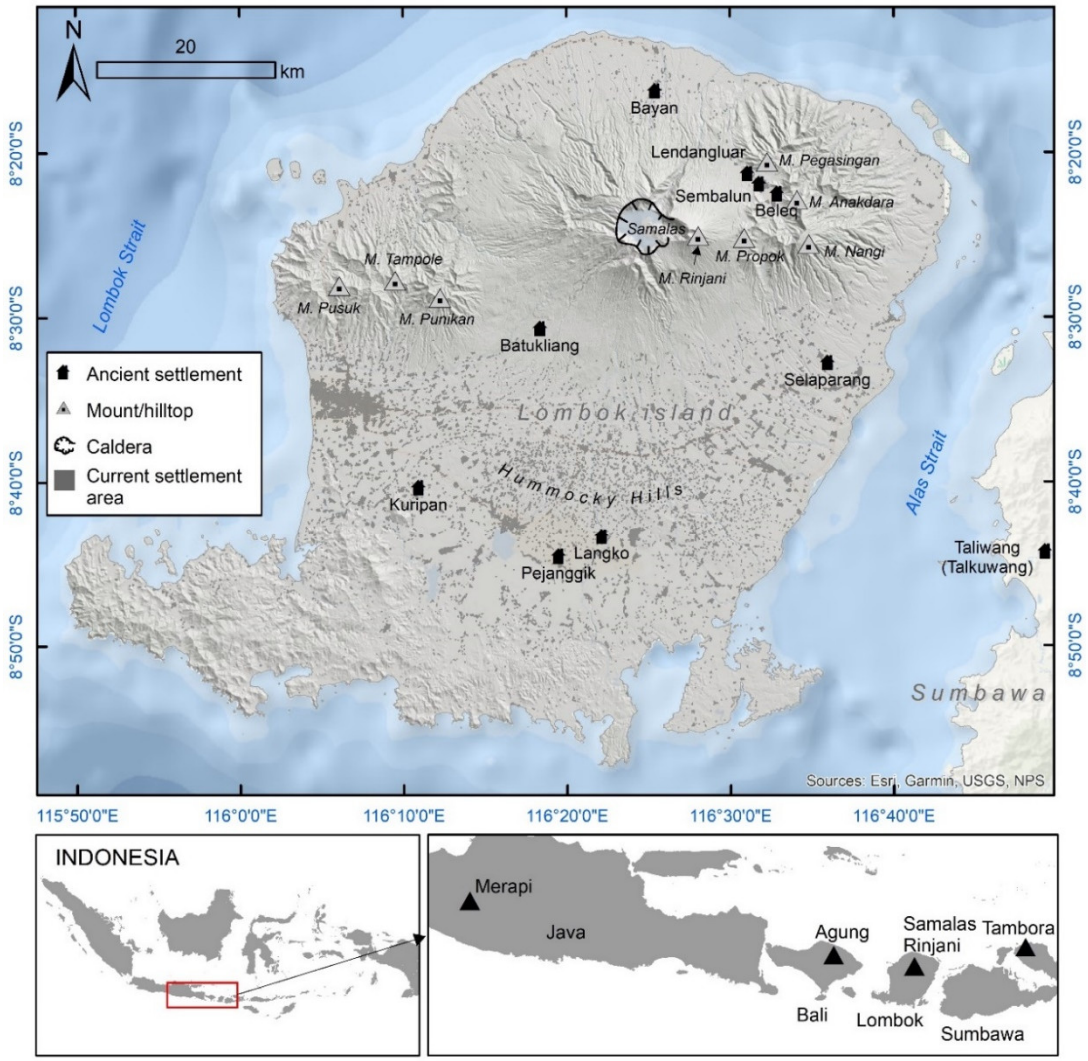

Figure 6.2. Comparison of the location of current settlements and ancient settlements in Lombok. The current settlement development may not always correspond to the ancient settlement locations before the 1257 CE Samalas eruption. The impact of the Samalas eruption and the subsequent recovery processes may have determined the current settlement distribution as delineated on the topographic map (RBI map, 1:25,000).

6.3.2. Narrative of the 1257 CE Samalas eruption in the written sources

The main eruption processes of Samalas are described in the *Babad Lombok* and *Babad Sembalun*. In the *Babad Lombok*, the eruption started at night and was preceded by rain and thunderstorms. The heavy rains may have triggered floods, landslides, and debris flows (Appendix C). The eruption is described as follows: "in the middle of the night there was rain and storms, wood and stones fell, avalanches came from the summit" (*tengah dalu rawuh hipun hudan nangin ributan sakweh kayu*

watu gunung pada rubuh gentuh batu halalabar dar saking luhur wukir; verse 273). In the *Babad Sembalun*, there is no information on the timing of the eruption (Appendix C), but the thickness of the clouds made it impossible to distinguish between day and night. The collapse of the Samalas volcano that formed the present Segara Anak caldera is indicated in the *Babad Lombok*: "Mount Rinjani had an avalanche and Mount Samalas collapsed, followed by large flows of debris accompanied by rumbling boulders" (*Gunung Renjani kularat miwah Gunung Samalas rakrak balabur watu gumuruh;* verse 274). A further relevant description of this process is indicated in *Babad Sembalun*: "Fire burned like molten tin, the slope of Rinjani collapsed completely" *api nyala ketia timah, hancur lebur lereng Rinjani*. These two sources appear to describe the same event, i.e., the eruption of Samalas and a consequent sector collapse in the western slope of Rinjani volcano, which displays a 2.5 km wide scarp clearly visible in the present topography. The text also indicates that the eyewitnesses saw the ejected materials during the eruption. In the *Babad Suwung*, a relevant passage refers to the description of the eruption by the communities of Talkuwang, the ancient name of Taliwang in Sumbawa Island, ~16 km east of Lombok Island (Appendix C). The inhabitants of Talkuwang noticed that "fire-rain fell from the sky" (*turun hudan geni haneng langit*) and "that hot wind burned everything in Talkuwang" (*hiku lantas binakur dese Takuwang)*. This description strongly suggests the occurrence of pyroclastic fallout at Talkuwang and dilute pyroclastic density currents (PDCs) that would have reached Sumbawa Island after crossing the Alas Strait, as previously interpreted by Mutaqin and Lavigne (2019).

6.3.3. Impacts of the eruption and societal responses

The extensive impact of the Samalas eruption on society is only described in the *Babad Lombok*, which may reflect social memories of Pamatan. The settlement at Pamatan was severely affected by pyroclastic surges, as indicated in the text: "These flows destroyed Pamatan. Houses were destroyed and swept away, floating into the sea, and many people died" (*tibeng desa Pamatan ya ta kanyut bale halang parubuh, kurambang ning sagara, wong ngipun halong kang mati*; verse 274). This suggests that Pamatan was a coastal city because a large portion of the settlement was dragged into the sea. In the *Babad Suwung*, it is also mentioned that voluminous ejected materials had reached the sea: "Formerly, it seemed like there was no sea between

Taliwang and Selaparang villages" (*Malik waktu sino iye laeq sopoq desa Taliwang dai Selaparang, ndeq naraq laut lalangne,*). Taliwang and Selaparang are separated by the Alas Strait, which is ~16 km long. The oral transmission may have exaggerated this description. It was likely a pumice raft along the Alas Strait that was perceived as a land bridge between Taliwang and Selaparang due to a massive influx of pumice fallout and PDCs. PDC deposits that today form beach-cliffs provide strong evidence for the formation of widespread pumice rafts (Figures 6.3A & 6.3B).

The thickest PDC deposit found in the eastern part of Lombok reaches ~30 m (25 km from caldera), in the northern part ~30 m (20 km from caldera), and in the western part ~40 m (25 km from caldera) (Mutaqin et al., 2019; Vidal et al., 2015). These voluminous flows undoubtedly devastated the majority of settlements in Lombok. Post-eruptive lahars also occurred, as depicted in the *Babad Lombok*: "Stranded in Leneng (Lenek), dragged by debris and floating boulders, all the inhabitants ran" (*hing Leneng hadampar hanerus maring batu dendeng kang hanyut wong ngipun kabeh hing paliya*; verse 275). At Samalas, post-eruptive lahars may occurred as evidenced in several outcrops, especially in Mataram in the West and Korleko in the East (Figure 6.3C). The *Babad Lombok* reports that the eruption lasted for seven days from beginning to end: "For seven days, the shocks struck the earth" (*pitung dina lami nira gentuh hiku hangebeki pertiwi*; verse 275). The oral tradition might have exaggerated this duration due to the chaotic situation in Lombok and Sumbawa, or it may refer to post-eruption tremors that lasted for approximately seven days after the main event. Seven days may also have been selected because it is a mythical number commonly used cross-culturally to describe the duration of a significant event (Alavijeh, 2013; Astakhova, 2020).

Figure 6.3. PDCs from the 1257 CE eruption were able to enter the sea, especially in the eastern (A) and northern (B) parts of Lombok. Above the PDC layer, lahar deposits are common, reaching ~10 meters (C). The PDC cliff is easily detected in the central part of the island, resulting from pumice quarrying activities. The open field is then turned into an agricultural area (D). Photo by F. Lavigne and M. Malawani taken in 2018 and 2020, respectively.

Narrations of the inhabitants' responses to the Samalas eruption are available in all three sources, but only the *Babad Lombok* records the whole event. According to this source, the first response of inhabitants was immediate and consisted of seeking safe places: "Some of them escaped to the hill" (*sawaneh munggah hing ngukir;* verse 275). This is similar to the *Babad Sembalun*, which describes survivors escaping to the hilly area: "They took refuge towards Ngenang Village, at the bottom of Batek Selak hill" (*warga milayu hanuju dasan ngenang, ring bawah bukit bantek selak)*. The subjects of these narrations are the inhabitants of Pamatan and Sembalun valley, respectively, whereas the *Babad Suwung* refers to the inhabitants of western Sumbawa: "All of the inhabitants are ran around in chaos" (*sedanging negere telas melayu)*.

There are reasons for the differences in responses of the inhabitants. In Lombok, the inhabitants are described as avoiding the "flood", "thunderstorm", and

"debris flow", whereas in Talkuwang (Sumbawa), the inhabitants avoid the "hot wind" and "fire rain". In Lombok, several hilly areas (e.g., Mount Pusuk, Punikan, and Tampole) are located in the western part, whereas the eastern part features locations, such as Mount Propok, Nangi, and Pegasingan. There is also a hummocky area in the south-central part of the island (Malawani et al., 2020) (see Figure 6.2). As mentioned in the texts, these hilly/mountainous areas were potential safe zones for evacuation to avoid hazards. Due to the chaotic situation described in the *Babad Suwung*, the direction of the movement of the displaced people is neither mentioned by toponymic name nor by geographic feature. The evacuation path of the inhabitants in Taliwang is thus difficult to trace.

In the *Babad Lombok* and the *Babad Sembalun*, the evacuation of inhabitants toward places for shelter is indicated by mentioning toponyms of settlements. In the *Babad Lombok*, the displaced royal family migrated to Jeringo: "The rest of the royal family fled and took shelter at Jeringo; they were gathered there" (*hing Jaringo hasingidan samiya ngungsi salon darak sangaji hakumpul hana ring riku*; verse 276). The toponym Jeringo can be found in both the western and eastern parts of the topographic map. Jeringo in the east is more appropriate for a shelter village than the one in the west part. Jeringo in the west is located in the hilly area of the Punikan and Tampole mountain range, which suffered from ~1 m thick pumice fall. Jeringo in the eastern part was less impacted by the pumice fall, and was safe from the PDCs. This may serve as a hint that the seat of the Pamatan Kingdom may have been situated in the eastern region adjacent to the royal's shelter village. Various toponyms are mentioned in the *Babad Lombok* (verse 276) as villages for shelter of evacuees, e.g., Samulia (Sambelia), Borok, Bandar, Pepumba, Pasalun, Serowok, Piling, Ranggi, Sembalun, Pajang, and Sapit. Not all of these village names are found on current topographic maps; those that are located in the eastern and southern parts of the island, outside the impacted area of PDCs (Figure 6.4). These locations are considered immediate sites for relocation, i.e., displacement sites during or immediately after the eruption. However, several shelter villages appear within the PDC area, especially in the western part. This condition may indicate three possibilities; the suggested PDC area from previous research might be inaccurate, or the original location shelter villages was not located in those areas due to name transformation, or considered as

intermediate displacement sites that were occupied several months or years after the eruption.

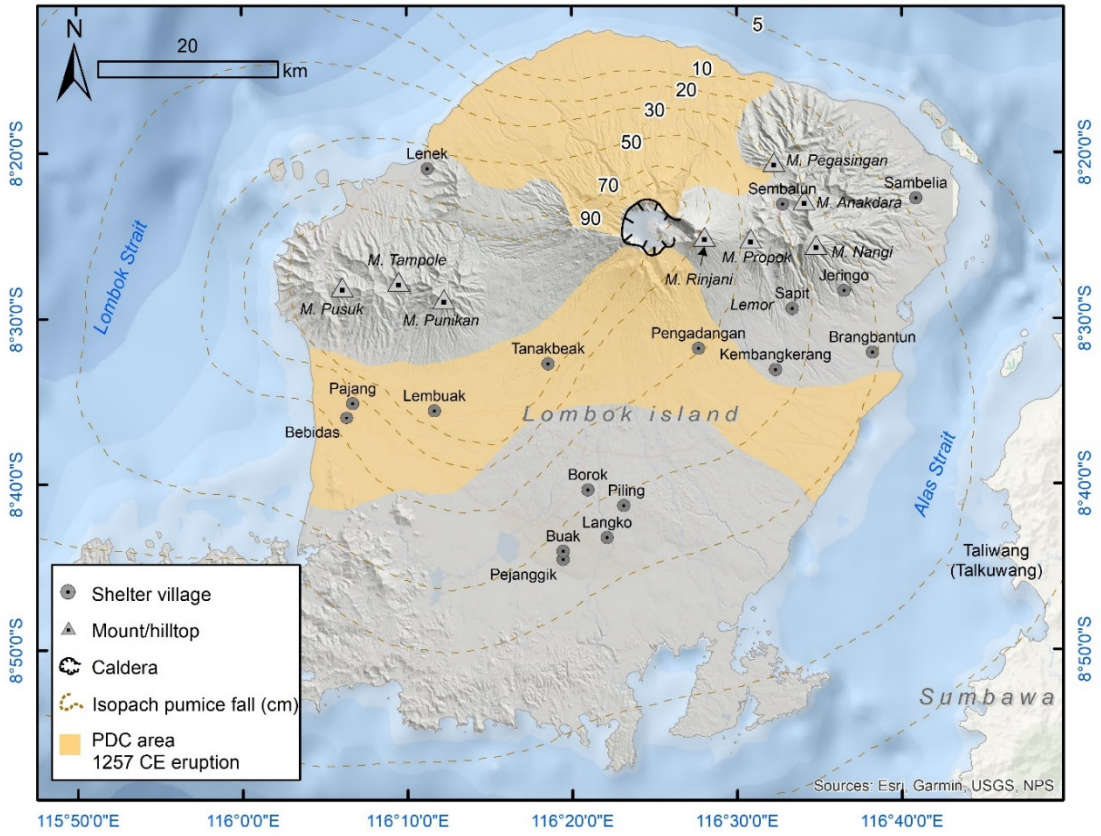

Figure 6.4. Distribution of shelter villages based on the narrations of the *Babad Lombok* and *Babad Sembalun*. The majority of shelter villages are in the southern and eastern parts of the island. Reconstruction of the PDC area is based on Vidal et al. (2015), and isopachs of pumice fall are based on Lavigne et al. (2013).

Several village names were also mentioned as evacuation places (villages for shelter): "There were those who went to Pundung, Buak Bekang, Tanak Beak, Lembuak, Bebidas. Several also escaped to the land of Kembang Kekrang, Pengadangan, Puka, Lungguh. Some of them made their way to Langko, Pejanggik" (*hana ring Pundung, Buwak Bakang, tana' Gadang Lembak Babidas hiki, sawenah hana halarut hing bumi Kembang Kekrang Pangadangan lawan Puka hatin lungguh saweneh malah kang tiba mara hing Langko Pajanggih*; verse 278). This verse indicates that the displaced people were not from a single location, i.e., Pamatan. They may have come from settlements around Pamatan. It is suggested that many villagers were displaced due to the impact of the eruption, even though the names of their

original settlements are not mentioned. Another village mentioned as a place of evacuation is Brang Batun. This toponym can be traced on the topographic map (current toponym: Brangbantun) and is located in the eastern part of the island. This village is said to have been founded by Prince Barang Bantun, as described in the *Babad Lombok*, in agreement with the *Babad Suwung*. Two other toponymic names are described to have been affected by the material ejected from Samalas: Nangan and Lemor. Only Lemor could be traced to its location on the current map: on the southeast slope of Samalas, approximately ~10 km from the present caldera. Due to its proximity to the volcano, Lemor was seriously affected by pyroclastic falls such as bombs and lapilli: "In Nangan and Palemoran (Lemor), large blocks of stone were piled up on the ground […] the stones fell in the middle [of the terrain]" (*yen Nange lan Palameran batu banda jejangkeh tanah* [...] *samalih tiba hing tengah;* verse 277).

Not all the villages for shelter could be traced to their locations on the current map because some toponyms may be based only on geographical memories of later generations. Another relevant process is the transformation of toponyms over time. Most of the shelter villages were predominantly in the eastern and southern parts of Lombok (Figure 6.4). This is most likely because other directions were seriously impacted by the eruption and were covered by thick deposits. It is also likely that those directions suffered extreme destruction and experienced a total loss of population. In addition, it should be noted that the displaced people were encouraged to evacuate by their respective leaders, which has become a crucial social mechanism for Lombok communities to recover from disasters.

The following narration describes more specifically the method used by the inhabitants to escape from hazards. It was not only an inland evacuation (i.e., running to hilly areas or places away from danger), but some also tried to leave the island by boat: an exodus to the neighboring island. "It is said that some of them embarked on boats, they all escaped with their former leaders" (*warnanen munggeng palowan sami larut lawan ratu hing nguni*; verse 279). This narration might support the notion that Pamatan was located in the eastern lowland coastal area and perhaps had a seaport. In all three *babad*, there is no description of the displaced people embarking to Bali, the adjacent island to the west. This strongly supports the idea that Pamatan, the most

prominent kingdom of Lombok in the thirteenth century, might have been located in the eastern part of the island.

6.3.4. Long-term post-eruptive recovery

According to the *Babad Lombok*, the survivors began to recover after seven days, which is implausible for such a large eruption. The initial recovery conducted by the survivors aimed to build new housing since the old settlements had been damaged and buried due to the volcanic eruption. The recovery process comprised of physical and social aspects: rebuilding a settlement and rearranging its governance. The physical recovery was performed by building palaces, forts, and roads, and creating permanent settlements. The *Babad Lombok* indicates that each of the new settlements was built in a new place led by a respective leader: Karang Bumbung, led by the chief minister (*adipati*); Tumbih Lalang, led by the headman (*penghulu*); Kembang Kuning, led by the governor (*papatih*); the officer (*raksa*) led the construction at Karang Melak, the harbormaster (*syahbandar*) took responsibility for coastal areas, whereas the chamberlain (*demang*) together with the king himself rebuilt a palace at Karang Lombok (verses 280-281). This division of new settlement construction worked effectively, resulting in a relatively quick physical recovery process. Other new settlements are also mentioned in verses 282-285, such as Brangabatun, Samulia, Pasalun, Kembangkerang, Pangadangan, Sukadona, Salondak, Buak Ketang, Bayan, Sokong, Kuripan, and Pejanggik. Not all new settlements can be traced on the current map (Figure 6.5). The most likely reason is due to name changes in the subsequent centuries. The recovery period culminated in a golden age, as described in the *Babad Lombok*: "The country of Lombok become glorious and prosperous" (*negareng Lombok kang lampah palamumbahara ketah hasuka sugih*; verse 286).

If the *Babad Lombok* primarily recounts the physical recovery, the *Babad Sembalun* describes social recovery; namely the governance recovery process. According to this account, Sembalun inhabitants (highlanders) were previously unfamiliar with any governance structure. After staying for shelter in Lendang Goar (Luar), Sembalun survivors rebuilt the Beleq village with new governance. They also further developed their agriculture by intensifying rice planting. This agricultural intensification conducted by survivors is also mentioned in the *Babad Lombok*: "Plenty

of clothes and food, gold, *ringgit*s and Chinese copper coins, with all kinds of buffalo, cow, horse, goat, chicken, duck, and much steamed rice" (*panganggo panganan wibuh mas ringgit picis muang sakadi kebo sampi jaran wadis ayam bebek danga* [recte *dangan*] *pakatah*; verse 286). These lines indicate that Lombok inhabitants started to advance their agriculture and farms to improve their economy. The recovery process of Sembalun highlanders might have taken a longer period than the recovery process conducted by lowlanders described in the *Babad Lombok*. Topographic bias may have influenced this recovery process. Sembalun inhabitants are highland people; hence, they might have been more isolated than the coastal lowland inhabitants described in the *Babad Lombok*.

None of the texts mention how long the recovery process took. However, information provided in the *Babad Lombok* may be helpful as a benchmark, e.g., a prince from the Javanese kingdom of Majapahit marrying a Pamatan princess could illustrate how long the recovery could have taken (verse 284). Majapahit travelers may have visited Lombok at the beginning of the fourteenth century. However, some caution is warranted when using the Majapahit reference to fix the chronology of the post-disaster recovery. Since these *babad* texts were written long after the eruption, later traditions concerning Majapahit influence in Lombok may have become incorporated into the account. Thankfully, there exists an original fourteenth century source from Java that gives insight into Lombok's post-eruption condition: the *Deśavarṇana* (also called the *Nagarakṛtāgama*), which was written in 1365 CE. In this text, Lombok is depicted as an independent and developed area (canto 14, verse 4) (Robson, 1995). According to the *Babad Lombok*, at the time of the Majapahit prince's arrival, Lombok had transformed into a major kingdom with several principalities. Based on these reports, whose reliability remains in doubt, the recovery process comprising the rebuilding of the city and creation of the new kingdom may have taken up to a century after the Samalas eruption.

6.4. Discussion

6.4.1. Limitations and relevance of the texts

Three written sources from Lombok provide useful insights into social memories of a volcanic eruption, its impact on the community and its behavior during the pre-, onset-, and post-eruption period in 1257 CE. However, in using these accounts, we are confronted with two limitations. The first limitation is insufficient corroboration between the texts and the limited archeological findings in Lombok to date. The catalog of the Museum of NTB contains no artifacts dated to the thirteenth century. The suspected ruins related to the Samalas eruption at Aikberik cannot clearly document the existence of major settlement in the thirteenth century as depicted in *babad* texts. The Airberik site has been severely damaged, and the missing artifacts have not yet been recovered. Although there is an Archaeological Office based in Bali, most of the investigations have only been conducted in Bali and Sumbawa. We hope that greater attention will be paid to the archaeology of Lombok. The second limitation is related to the characteristics of the three *babad*, namely, their nature as second-hand sources. As we mentioned, the *babad* are collections of oral traditions that were written several centuries after the time of occurrence. Modifications either by addition or subtraction are likely. Therefore, caution when interpreting these texts is required and consistency with scientific evidence needs to be established.

Concerning the texts' relevance, it is vital to corroborate content of the *babad* with field evidence. However, archaeological field evidence in Lombok that dates before the eruption in 1257 CE is scarce. Stratigraphic evidence demonstrates the occurrence of the Samalas eruption (Métrich et al., 2017; Vidal et al., 2015, 2016). In addition, an investigation in eastern Lombok provides an overview of Lombok's topography before the eruption (Mutaqin et al., 2019). Dendrochronological reconstruction and climate modeling from the Samalas eruption in the thirteenth century provide further evidence of a major eruption in Lombok (Guillet et al., 2017). The geographic identification and spatial distribution of toponyms mentioned in the manuscripts underscores their relevance. Several names mentioned in the sources correspond to toponyms used today, and their distribution is in agreement with Samalas's impact map provided by previous researchers (Lavigne et al., 2013; Vidal et al., 2015). Some might have experienced transformations or name duplications.

Javanese-patterned toponym names, which are partially mentioned in the manuscripts, are new villages that emerged after the recovery period or after the arrival of the Majapahit (Jamaluddin, 2012), making them less illustrative of pre-eruption conditions.

It is also challenging to prove specific facts about social and economic conditions, particularly the population size of the communities. However, in Indonesia or even worldwide, a city with ten thousand inhabitants was the normal size for a large city in the thirteenth century (Cesaretti et al., 2016; Tjandrasasmita, 2000). Interaction with the Bajo is plausible, given that this ethnic group is one of the most prominent nomadic maritime populations in Indonesia. Even today they are known to be experts in navigation and trade between islands in Indonesia. The majority of Bajo people are settled on various islands in Borneo (i.e., Kotabaru and Derawan Bajo) and Celebes/Sulawesi (i.e., Kendari Bajo) (Kusuma et al., 2017). Several descriptions in the text seem exaggerated, including claims that the eruption event lasted for seven days. Modeling from previous research shows that the eruption from its initial to final phases lasted less than ~48 hours (Vidal et al., 2015). During subsequent days post-eruption processes such as lahar floods might have occurred. Outcrop in Korleko (Figure 6.3C) records Samalas syn-eruption deposits covered directly by laharic deposits without an intercalated paleosol, indicating a short period between syn- and post-eruptive deposition.

Linguistic and stylistic comparison of written sources from Lombok with those of other Indonesian sources is also needed to further assess the Samalas eruption, e.g., indigenous vocabularies for eruption processes. The Old Javanese Rukam inscription (907 CE) in Central Java is the oldest known Indonesian source to document a volcanic eruption. This inscription provides information on how property was destroyed by an eruption of Sindoro volcano: "the demarcated land of the king's grandmother was lost in an eruption" *ilang dening guntur sīmān rakryān sañjīvana* (Sastrawan 2022). In Old Javanese, the word "guntur" means 'flood' or 'eruption', which in this case seems to have been associated with debris flows or pyroclastic flows from Sindoro volcano (Degroot, 2017). In Javanese texts, various terms are used to describe volcanic eruptions: "earthquake", "rain", "thunderstorm", "noise", "collapse" and "debris flow" (Cahyono, 2012). Another example is the Javanese royal chronicle *Pararaton*,

compiled in the early 1500s from older materials, which asserts that volcanoes in East Java erupted eight times during the fourteenth and fifteenth centuries. However, the complex textual transmission of the *Pararaton* casts doubt on the reliability of the dates ascribed to these eruption events (Sastrawan 2022). The *babad* from Lombok describes volcanic eruptions in similar ways, demonstrating that the pre-modern communities in Indonesia had a consistent vocabulary for describing volcanic eruptions.

6.4.2. The *babad* indicate the location of early kingdoms

The three *babad* that we analyzed, despite the methodological issues described above, offer essential information about the ancient societal landscape in Lombok, namely the existence of two ancient kingdoms that have remained disputable. These two kingdoms were Suwung and Pamatan. The Suwung Kingdom was investigated through interviews with local scholars from East Lombok: the possible location of Suwung was in the surrounding area of Sambelia and Sugian (Figure 6.5) (Mansyur, 2019). In contrast, according to Mulyadi (2014), Suwung was located in the northern part of Perigi. Although only Pamatan has been associated with the Samalas eruption, the narrative in *Babad Lombok* recalls the legacy of the Suwung Kingdom (Mansyur, 2019). Several settlements mentioned in *Babad Suwung* are also cited in *Babad Lombok* as locations of the Pamatan survivors' shelter. Therefore, we also provide a geographical illustration of the estimated location of Suwung to support the interpretation of where Pamatan may have been located.

Locations for Pamatan have been proposed previously, namely in Aikmel (Mulyadi, 2014) and in Sembalun (Mansyur, 2019). Considering this discrepancy, we attempted to investigate the possible location and existence of Pamatan. The direction of the Pamatan survivors' evacuation is helpful for tracing the potential location with the aid of toponyms and geographic analyses (Figure 6.5). The following geographical criteria can also be used as a reference for finding the possible location of Pamatan: 1) located on the PDC area; 2) on the lower slopes of the volcano; 3) in the proximity to the hilly areas suitable for evacuation; and 4) in the coastal area close to the sea, which allows evacuation by boats or ships.

In eastern Lombok, there is a village called Paok Motong. In the Sasak dialect, it is common for a long word to be said quickly and abbreviated to "Pakmotong" or "Pamotong," making the name sound almost identical to the word "Pamatan". Similarly, in the west, a small village named “Pamotan” is also similar to “Pamatan”. However, western Lombok toponyms are heavily influenced by the Javanese-Balinese tradition from the seventeenth and eighteenth centuries, e.g., Mataram, Singhasari, Kediri, Karangasem (van der Kraan, 1997; Hägerdal 2001). Pamotan is identical to a Javanese toponym that was probably transplanted to western Lombok under Balinese rule. The village of Paok Motong is not featured as part of the PDC area, therefore this location does not appear to have been buried by thick pyroclastic deposits. Since there are no toponyms that have a close correlation to Pamatan, we suggest that the ancient kingdom of Pamatan was located in the eastern part, adjacent to Selaparang, a village that emerged during the period of the Suwung kingdom. This geographic location fits with the narrations of *Babad Lombok*. Figure 6.5 indicates a possible location that might represent the location of this hitherto lost kingdom.

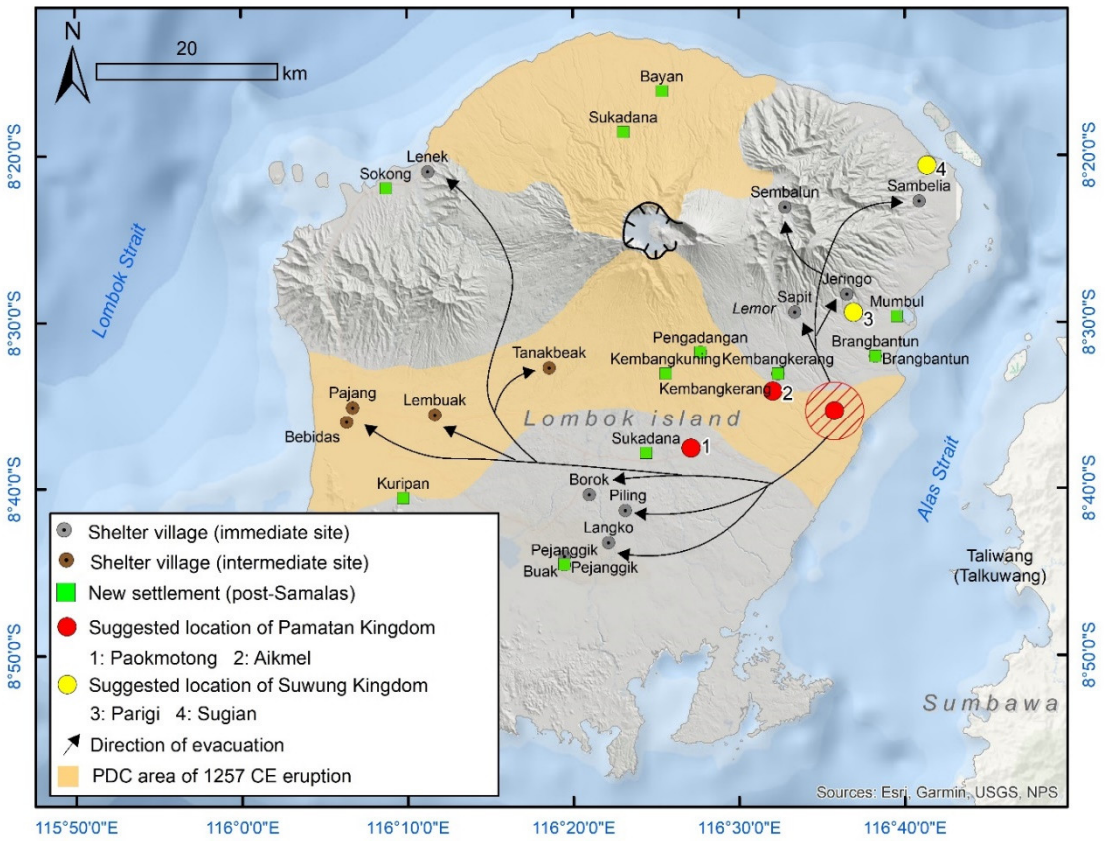

Figure 6.5. Reconstruction of the evacuation paths taken by Pamatan inhabitants toward shelter villages. The combination of evacuation direction (black arrows) and several other geographical criteria provides a proposed potential location of the Pamatan Kingdom (red circle). The proposed locations of the Pamatan and Suwung Kingdoms from Mansyur (2019) and Mulyadi (2014) are indicated by number 2, 3, and 4, respectively.

6.4.3. Valuable sources for reconstructing the human response to a large-scale eruption

Popular perceptions of Lombok inhabitants concerning threats may be crucial in conducting response and recovery from eruptions. The fatalistic perception of disasters being God's punishment have had a critical effect on Lombok inhabitants' response and recovery. This perception indicates a strong belief that disasters come from God because of human negligence. In Indonesia, three written sources from the nineteenth century also recount the risk perception towards volcanic eruptions as God's punishment (Sudibyo, 2019). The first is the *Syair Kerajaan Bima* manuscript from Sumbawa, which describes the Tambora eruption in 1815 CE as God's curse and anger. The next is the *Babad Betawi* manuscript from Java, which mentions that the Merapi eruption in 1822 CE is God's punishment due to human negligence. The last is the *Syair Lampung Karam* manuscript from Sumatera that tells the devastating story of the tsunamigenic eruption of Krakatoa in 1883 CE. Similar perceptions persist in several Indonesian communities (Bachri et al., 2015; Gianisa and Le De, 2018). It affects the responses and recovery process of disasters; therefore, various recovery strategies are applied to avoid God's punishment. A simple method that communities have conducted in Lombok is reconstructing the new villages beyond the affected ones. This method refers to relocation in contemporary disaster risk reduction strategies (Bowman and Henquinet, 2015).

The emergency response conducted by Samalas survivors was centered on immediate responses: avoiding hazards and seeking safe places. This is similar to the response by survivors of the 1669 CE Etna eruption in Italy, who also believed that the disaster was a punishment from God (Chester et al., 2012). It was comprised of evacuation, construction of new settlements, new harbors, and reestablishment of agriculture (Branca et al., 2015). Another example is in Java, where the interaction of religious beliefs shapes specific folklore that helps to improve hazard mitigation for

the local communities surrounding the volcano (Lavigne et al., 2008; Troll et al., 2015). In general, these practices were similar to those in Lombok following the 1257 CE eruption. In addition to religious influences, political (government) institutions highly contributed to the successful evacuation and recovery processes, for example in the case of the 1906 CE eruption of Vesuvius, Italy (Chester et al., 2015). The immediate or emergency response method was prevalent in Indonesian and global disaster management strategies up to the 1960s. It was then replaced by the reactive-proactive paradigm (1970-1990), with risk reduction being the latest paradigm (Hizbaron et al., 2016).

6.4.4 Useful information for volcanic disaster recovery

The three *babad* illustrate that the inhabitants of Lombok conducted a mass evacuation and exodus from affected villages and cities. Inhabitants from ancient settlements in other regions of the world also conducted massive exoduses due to natural hazards, such as the Maya and Mongolians (Fei and Zhou, 2006; Lentz et al., 2018; Nooren et al., 2017). A distinctive feature of Lombok's evacuation process was the division of the population into small groups and the leadership of each displaced group. This leadership style provided a strong foundation for achieving recovery and resilience by rearranging the governance and city planning. These kinds of recovery strategies are still practiced by today's global communities, especially for relocating communities in the forms of adaptive governance and planning (Bakkour et al., 2015; Djalante, 2012).

The post-disaster recovery process in Lombok was relatively slow. According to the sparse sources, it may have taken up to 100 years to complete the recovery process, marked by evidence of a new kingdom in the fourteenth century. We would say this is the maximum timeframe, since Lombok was already a well-developed region by the time the Javanese chronicle *Deśavarṇana* was written in 1365 CE. Figure 6.6 shows the sequential long-term recovery process that occurred in Lombok following the Samalas eruption in 1257 CE. When compared to the impact of Etna in 1669 CE, the duration of this recovery process was also almost the same, i.e., taking nearly a century. However, the area around Etna was aggravated by an earthquake in 1693 CE (Branca et al., 2015). Compared to the impact of the El Chichon eruption in

Mexico, the Maya-Tikal also experienced almost the same period of recovery (536–540 CE). It took more than a century for this society to rebound, marked around 650 CE by the discovery of new monuments such as Tikal, Calakmul, and Caracol (Dahlin and Chase, 2014; Nooren et al., 2017). Technological development and political influences undoubtedly play a significant role during the recovery period (Chester et al., 2015). Indonesia experienced a period of accelerated recovery after the modernizing processes triggered by Netherlands East Indies colonial rule. For example, after the eruption of Krakatoa in 1883 CE, it only took two decades for the population around Java (Banten and surrounding area) to recover from the effects of the eruption (Brata et al., 2013). Significant experience managing volcanic eruptions by a community became a very strong basis for dealing with future hazards. In Indonesia nowadays, positive trends have emerged in managing volcanic hazards.

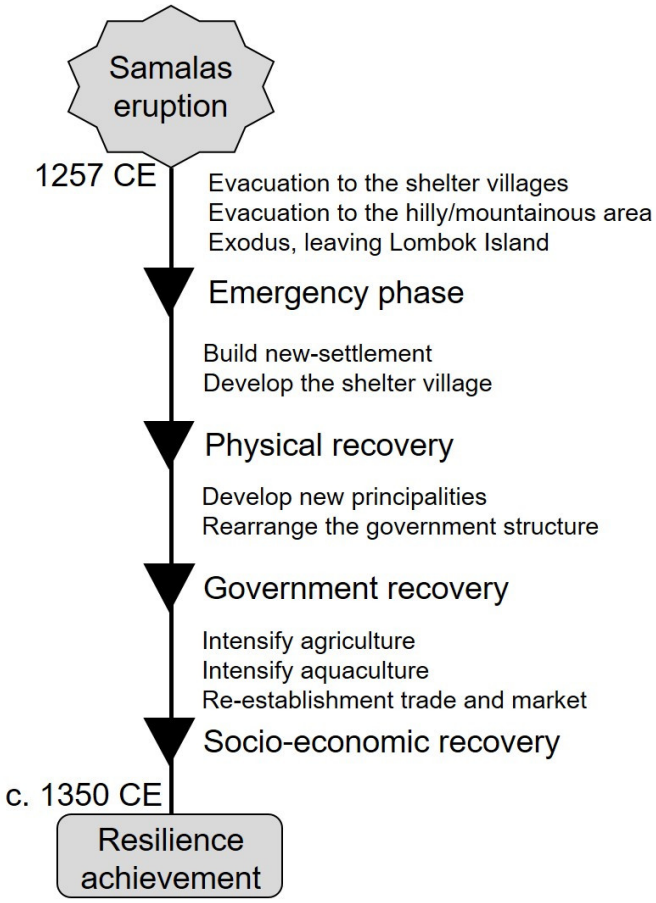

Figure 6.6. Illustration of emergency-recovery phase in Lombok following the 1257 CE Samalas eruption.

There have been no significant eruptions recorded on Lombok prior to the Samalas event, except between the fifth and sixth centuries (Métrich et al., 2017; Rachmat et al., 2016). Experiences of past generations in overcoming previous disasters provides a robust model in handling disasters. The legacy of adaptation strategies from previous generations may be reflected in myths and legends (Troll et al., 2015; Donovan et al., 2012) For example, in Sumbawa, after the Samalas and Tambora eruptions, the coastal area of Sumbawa (the western part) was considered a forbidden place due to legends prohibiting people from living there (Mutaqin and Lavigne, 2019). Lombok does not have such notions, due to political turmoil and social conditions after the fifteenth century (Hägerdal 2001; Ediyono and Ridwan, 2018). This cultural tradition would be a valuable foundation for disaster-risk reduction issues if preserved among communities in Lombok. We suggest that the story of the 1257 CE eruption was not forgotten in the subsequent centuries after eruption, but simply that the memories were incorporated into stories that are otherwise focused more on political conditions. Thanks to the local Sasak community that was willing to compile the fragmented oral stories into a unified chronicle in the form of *babad* as valuable written sources. Hopefully, these reconstructions of oral tradition from *babad* will serve as valuable information for strengthening preparedness and recovery strategies for a volcanic eruption to the Lombok and larger community.

We suggest that the earlier claim that the *Babad Lombok* is the oldest written source documenting a significant volcanic eruption in Southeast Asia (Mutaqin and Lavigne, 2019) might be revised and updated, because the *babad* texts were recompiled and were not first-hand written sources, unlike Pliny the Younger's, account of the 79 CE Vesuvius eruption. The *Babad Lombok* may reflect later versions of old historical traditions that evoke social memories of the Samalas eruption and its consequences. Compared to other historical texts from Indonesia, such as the *Deśavarṇana*, the *Pararaton*, or the Rukam inscription, the *Babad Lombok* is more recent, but its depictions of the volcanic eruption are more detailed. A Balinese source about the 1710–11 eruption of Agung volcano in Bali provides a similarly detailed description of an eruption (Hägerdal 2006; Sastrawan 2022). However, texts from Lombok address the entire disaster management cycle, which is not reported in any early written sources from Indonesia or Southeast Asia.

6.5. Conclusion

Three written sources from Lombok (*Babad Lombok*, *Babad Suwung*, and *Babad Sembalun*) contain detailed societal memories from volcanic eruptions in Lombok, including information about the conditions before, during, and after the eruption. Based on similar descriptions, narrative chronology, and field evidence, we feel confident that the volcanic eruption mentioned in the *babad* corresponds to the Samalas eruption in 1257 CE. Although many of the descriptions seem exaggerated, we believe that these manuscripts are accurate in particular details and can be critically used as a reliable source related to the Samalas eruption.

The pre-Samalas narrative raises questions about the location of two early kingdoms. However, we are only able to trace the potential location of the Pamatan Kingdom using toponyms and geographic assessment. The population's response to the eruption is an essential element of these texts from Lombok, as they describe the detailed risk management from the emergency-crisis period to the recovery period. The *babad* from Lombok belong to a very small number of Indonesian texts that provide detailed descriptions of volcanic eruptions that were transmitted orally before being documented in written form. These narratives can be used as valuable lessons for reducing the risk associated with volcanic hazards in the future, both for communities in Lombok and more broadly, considering that the emergency response paradigms used by ancient populations in Lombok are also still practiced by communities today. The three *babad* from Lombok also provide useful knowledge related to the recovery processes from a volcanic eruption, which can be relevant to the modern world, such as physical recovery, governance, institutional recovery, and economic recovery.

CHAPTER 7

The results and discussions in this thesis have been outlined, and finally, the overall conclusion can be determined. This highlights the role of geomorphology in reconstructing past volcanic eruptions and their impacts on the landscape with the help of historical accounts. This chapter also provides limitations and outlooks for further development of the related studies on the same topic.

CONCLUDING REMARKS

7.1. Conclusions

Investigations of the physical and social impacts of a past volcanic eruption are relatively limited. Several limitations have led to the scarcity of this topic, such as access to field data and/or historical data if the eruption occurred several centuries ago. In this thesis, such research has been conducted comprehensively in Lombok Island, employing various geospatial data, field measurements, geographic modeling, and analysis of written sources. The impacts of two large eruptions of Samalas volcano that occurred in 1257 CE and 5000-2600 BCE are analyzed. These eruptions led to significant landscape evolution in both proximal and distal areas. Social memory documented in the written texts also provided a complete account of the emergency, migration, and recovery phases of a major caldera-forming eruption.

One of the Largest Debris Avalanche in Indonesia

Indonesia is one of the countries with a highest number of debris avalanches in the world, along with Japan. However, from 70 debris avalanches that have been identified, only 11 have had metrics calculations, and only four were successfully dated. With this number of events, Indonesia is supposed to be a natural laboratory related to the debris avalanche. This research presents a debris avalanche that has never been identified before, namely the Kalibabak debris avalanche from Samalas volcano. Basic geomorphologic approaches were successfully implemented to uncover this debris avalanche through morphology, structure, and chronology analysis.

The metrics of Kalibabak DAD show that it is the third largest among DADs in Indonesia and eighth among the large Holocene DADs worldwide. This fan-shaped DAD has a measured area of 535 km^2, and the calculated volume of 15.1 km^3. Although the pre-avalanche summit of Samalas volcano has been erased, the former topography of the edifice was reconstructed using ShapeVolc program. Before its sector collapse, the summit culminated at ~4200 m with a slope of 35%. The structure of DAD is dominated by andesitic breccia rock with sand matrix. Measured from outcrops, deep cores, and resistivity measurements, the thickest part of the DAD reaches 58 m with an average of

28 m. The runout flow of this non-cohesive debris avalanche reached 39 km from its source with a calculated velocity of ~65 m/s. Radiocarbon dating of paleosols beneath the DAD yields ages ranging from ~17,000 BCE (center part of the DAD) to 7,000 BCE (outermost hummocks). However, the oldest paleosol covering the DAD is 2,600 BCE. A significant eruptive event between 7,000 and 2,600 BCE may have triggered the Samalas debris avalanche. The only candidate that provoked this debris avalanche is a subplinian eruption with significant pumice dispersal (Propok pumice), which occurred between 5000 and 800 BCE (Nasution et al., 2004). It is also suggested that the Propok pumice be attributed to the Samalas volcano rather than a small Propok cone in the eastern part of Rinjani.

The dynamics of Kalibabak debris avalanche in Lombok illustrates that volcanic landform is susceptible to abrupt topographical changes. However, proximal activities might still influence the landscape transformation in the distal part. As it occurred in the coastal area of Mataram Plain, an eruption of Samalas volcano in 1257 CE caused significant landscape changes in this region, both during the syn-eruptive and pos-eruptive phases.

Paleo-topographic modeling

Paleotopographic modeling is a technique that can be utilized to determine the rate of eruption impact in modifying the landscape. The model can be constructed using simple or complex geometry. To examine the impact of the 1257 CE Samalas eruption on the distal area (Mataram Plain), a simple geometry was applied because of the presence of stratigraphic constraint in the subsurface layer. The white-coarse pumice marks the start of volcaniclastic sedimentation from the syn-eruptive deposits of the 1257 CE Samalas eruption. Without this stratigraphic marker, paleo-topographic reconstruction may be more challenging. The topographic changes between pre-eruptive and present-day can be measured by calculating the difference between present-day elevation and the limit depth of the pumiceous layer. This calculation was performed on each stratigraphic point and thus can be interpolated to produce a paleo-DEM. This paleo-DEM allows reconstructing pre-eruptive river courses and paleo-shoreline. Stratigraphic framework and radiocarbon dating help to provide the chronology of landscape evolution in the Mataram Plain.

The paleo-topographic modeling demonstrates that since the eruption of Samalas in 1257 CE, the study area has undergone abrupt changes in the upstream and gradual changes in the downstream area. The factors that led to these changes are PDC deposition, post-eruptive lahar, and fluvial sedimentation. The landscape evolution occurred as follows:

1. In the pre-eruption condition, the Mataram Plain coast consisted of bays and headlands occupied by the coral reef in some parts.
2. In the syn-eruptive stage, the Mataram plain was partially covered by PDC with a total volume of $110 \pm 3 \times 10^6$ m^3. During this stage, fluvial instabilities occurred. However, the river continued to erode the former river valley.
3. In the post-eruptive stage, lahar and fluvial processes transported the reworking materials ($208 \pm 3 \times 10^6$ m^3) to the downstream area of Mataram plain. During this stage, dominant channels are persisted, and smaller channels are abandoned. The persisted channels sustain the resedimentation of reworked material that caused the shoreline to move westward by ca. 1.6 km. In addition, the reconstruction of the topography and shoreline before 1257 CE can be helpful to constrain the investigation of speculative ancient villages/cities that were erased by pyroclastic deposition.

Exegesis of Indigenous Written Sources

Natural hazards that have occurred in human history are often preserved in folklores, legends, or local stories that are transmitted from generation to generation. However, if they are not preserved in written documents, the stories will have many biases from the original sources or eyewitnesses. In Lombok the local Sasak groups have documented fragmented local stories into thousands of written documents. Three of them, namely *Babad Lombok, Babad Suwung,* and *Babad Sembalun*, contain a story of volcanic eruption, starting from the pre-eruption phase, during the eruption, up to the post-eruption. They differ in format and content, but there is a nexus that connects them all, i.e., an undated eruption of Samalas volcano. Some facts described in these *babad* attest that this is the major eruption of 1257 CE (Lavigne et al., 2013). Interpretation of the text is complicated by using only a volcanological perspective. The help of local historians

and linguists is beneficial in verifying the *babad*'s story into a chronological narrative that is scientifically relevant.

The pre-eruption narratives help to trace the forgotten kingdoms in Lombok, i.e., the Pamatan Kingdom and Suwung Kingdom. The population's response to the eruption is the main interesting element of the texts. However, the emergency response paradigms used by ancient Lombok populations are still practiced by communities today. In addition, the texts describe the detailed risk management from the emergency-crisis up to the recovery period. The recovery processes practiced by the ancient society of Lombok are also relevant to the modern world. Therefore, these narratives are beneficial as valuable lessons for reducing the risk associated with volcanic hazards in the future, both for communities in Lombok and more broadly.

7.2. Limitations and Perspectives

Identifying the physical and social impacts of an ancient eruption is challenging but can be achieved with several approaches. There are some limitations and notes in this research, such as:

1. The first investigation of a DAD in Lombok only utilized limited numbers of structure/lithology data. Abundant lithology data enables the calculation of the deposit volume more precisely and improves the regional stratigraphic framework. Many examples of research on a single DAD have resulted in various types and titles of research. Hopefully, the results of this research will stimulate geological and volcanological communities to explore the large DAD in Lombok.
2. Archival or legacy stratigraphic data from geological exploration in Lombok is limited. Derived data from geological exploration is also minimal, such as grainsize, geochemical, or other geotechnical data. These data would have been valuable in this research and enabled the development of a better stratigraphic framework than that already established.
3. The analysis of historical documents was only conducted on three documents. Many other documents may contain the same nexus event, which is the eruption of the 1257 CE Samalas volcano. Other natural hazards may also be depicted in the written sources from Lombok. Currently, the digitalization of old documents

in Lombok is being carried out to ensure a more comprehensive catalog and accessible data for a wider audience.

Lombok has great potential as a natural laboratory of Holocene volcanoes with potential geosites and geoheritages. Since 2013, the 1257 CE Samalas eruption has attracted the geology and volcanology societies to conduct research in Lombok. However, the large DAD that have analyzed in this region will also be a new interest for geological and volcanological studies in Lombok. Given the impact of these two events on shaping the landscape of Lombok, studies on the topic of land and water resources will also be of great interest. Materials from the eruptions were the primary material for soil formation, and its deposition affected the aquifer structure below the surface. Historical and archaeological topics are also highly suggested to be explored in Lombok. Only a few artifacts or ruins have been found in Lombok. Ruin of ancient villages buried underground are possible to be discovered. This thesis presents the preliminary results for further exploration of these speculative ancient villages.

REFERENCE

A

Abdul-Jabbar, G., Rachmat, H., & Nakagawa, M. (2019). Temporal change of Barujari Volcano magmatic process: Inferred from petrological study of erupted products since AD 1944. Journal of Physics: Conference Series, 1363(1). https://doi.org/10.1088/1742-6596/1363/1/012030

Abrams, L. J., & Sigurdsson, H. (2007). Characterization of pyroclastic fall and flow deposits from the 1815 eruption of Tambora volcano, Indonesia using ground-penetrating radar. Journal of Volcanology and Geothermal Research, 161(4), 352–361. https://doi.org/10.1016/j.jvolgeores.2006.11.008

Alavijeh, A. Z. 2013. A comparative study on the signification of number seven in different social and religious contexts. Asian journal of social sciences & humanities, 2(4), 301-309

Alloway, B. V., Andreastuti, S., Setiawan, R., Miksic, J., & Hua, Q. (2017). Archaeological implications of a widespread 13th Century tephra marker across the central Indonesian Archipelago. Quaternary Science Reviews, 155, 86–99. https://doi.org/10.1016/j.quascirev.2016.11.020

Amorosi, A., Pacifico, A., Rossi, V., & Ruberti, D. (2012). Late Quaternary incision and deposition in an active volcanic setting: The Volturno valley fill, southern Italy. Sedimentary Geology, 282, 307–320. https://doi.org/10.1016/j.sedgeo.2012.10.003

Andrade, S. D., & van Wyk de Vries, B. (2010). Structural analysis of the early stages of catastrophic stratovolcano flank-collapse using analogue models. Bulletin of Volcanology, 72(7), 771–789. https://doi.org/10.1007/s00445-010-0363-x

Andreastuti, S. (2006). Menelusuri kebenaran letusan Gunung Merapi 1006. Indonesian Journal on Geoscience, 1(4), 201–207. https://doi.org/10.17014/ijog.vol1no4.20064

Argote-Espino, D. L., López-García, P. A., & Tejero-Andrade, A. (2016). 3D-ERT geophysical prospecting for the investigation of two terraces of an archaeological site northeast of Tlaxcala state, Mexico. Journal of Archaeological Science: Reports, 8, 406–415. https://doi.org/10.1016/j.jasrep.2016.06.047

Astakhova, E. 2020. Architectural symbolism in tradition and modernity. IOP Conference Series: Materials Science and Engineering, 913(3), 32024. https://doi.org/10.1088/1757-899x/913/3/032024

Aydin, F., Midilli, A., & Dincer, I. (2013). Environmental Impact Assessment of Explosive Volcanoes: A Case Study. In I. et al Dincer (Ed.), Causes, Impacts and

Solutions to Global Warming (pp. 261–290). https://doi.org/DOI 10.1007/978-1-4614-7588-0_17

B

Bachri, S., Stötter, J., Monreal, M., & Sartohadi, J. (2015). The calamity of eruptions, or an eruption of benefits? Mt. Bromo human-volcano system a case study of an open-risk perception. Natural Hazards and Earth System Sciences, 15(2), 277–290. https://doi.org/10.5194/nhess-15-277-2015

Bakkour, D., Enjolras, G., Thouret, J. C., Kast, R., Mei, E. T. W., & Prihatminingtyas, B. (2015). The adaptive governance of natural disaster systems: Insights from the 2010 mount Merapi eruption in Indonesia. International Journal of Disaster Risk Reduction, 13, 167–188. https://doi.org/10.1016/j.ijdrr.2015.05.006

Belousov, A., Belousova, M. & Voight, B. Multiple edifice failures, debris avalanches and associated eruptions in the Holocene history of Shiveluch volcano, Kamchatka, Russia. Bull Volcanol 61, 324–342 (1999). https://doi-org.ezproxy.ugm.ac.id/10.1007/s004450050300

Belousov, A., Voight, B., & Belousova, M. (2007). Directed blasts and blast-generated pyroclastic density currents : a comparison of the Bezymianny 1956 , Mount St Helens 1980 , and Soufrière Hills , Montserrat 1997 eruptions and deposits. Bull Volcanol, (69), 701–740. https://doi.org/10.1007/s00445-006-0109-y

Bernard, B., Takarada, S., Andrade, S. D., & Dufresne, A. (2021). Terminology and Strategy to Describe Large Volcanic Landslides and Debris Avalanches BT - Volcanic Debris Avalanches: From Collapse to Hazard (Matteo Roverato, A. Dufresne, & J. Procter, Eds.). https://doi.org/10.1007/978-3-030-57411-6_3

Bernard, B., van Wyk de Vries, B., & Leyrit, H. (2009). Distinguishing volcanic debris avalanche deposits from their reworked products: the Perrier sequence (French Massif Central). Bulletin of Volcanology, 71(9), 1041. https://doi.org/10.1007/s00445-009-0285-7

Bernard, K., Vries, B. V. W. De, & Thouret, J. (2019). Fault textures in volcanic debris-avalanche deposits and transformations into lahars : The Pichu Pichu thrust lobes in south Peru compared to worldwide avalanche deposits. J. Volcanol. Geotherm. Res, 371, 116–136.

Berry, H. C., Cashman, K. V., & Williams, C. A. (2021). The 1902 Plinian eruption of Santa María volcano, Guatemala: A new assessment of magnitude and impact using historical sources. Journal of Volcanology and Geothermal Research, 414. https://doi.org/10.1016/j.jvolgeores.2020.107167

Bertrand, C., Van Ypersele, J. P., & Berger, A. (1999). Volcanic and solar impacts on climate since 1700. Climate Dynamics, 15(5), 355–367. https://doi.org/10.1007/s003820050287

Bi, N., Wang, H., Wu, X., Saito, Y., Xu, C., & Yang, Z. (2021). Phase change in evolution of the modern Huanghe (Yellow River) Delta: Process, pattern, and mechanisms. Marine Geology, 437(March 2020). https://doi.org/10.1016/j.margeo.2021.106516

Biass, S., Todde, A., Cioni, R., Pistolesi, M., Geshi, N., & Bonadonna, C. (2017). Potential impacts of tephra fallout from a large-scale explosive eruption at Sakurajima volcano, Japan. Bulletin of Volcanology, 79(10). https://doi.org/10.1007/s00445-017-1153-5

Blong, R. J., & Kurbatov, A. V. (2020). Steps and missteps on the path to a 1665–1668 CE date for the VEI 6 eruption of Long Island, Papua New Guinea. Journal of Volcanology and Geothermal Research, 395, 106828. https://doi.org/10.1016/j.jvolgeores.2020.106828

Bowman, L. J., & Henquinet, K. B. (2015). Disaster risk reduction and resettlement efforts at San Vicente (Chichontepec) Volcano, El Salvador: Toward understanding social and geophysical vulnerability. Journal of Applied Volcanology, 4(1). https://doi.org/10.1186/s13617-015-0031-0

Branca, S., Azzaro, R., De Beni, E., Chester, D., & Duncan, A. (2015). Impacts of the 1669 eruption and the 1693 earthquakes on the Etna Region (Eastern Sicily, Italy): An example of recovery and response of a small area to extreme events. Journal of Volcanology and Geothermal Research, 303, 25–40. https://doi.org/10.1016/j.jvolgeores.2015.07.020

Branca, S., & Vigliotti, L. (2015). Finding of an historical document describing an eruption in the NW flank of Etna in July 1643 AD: timing, location and volcanic products. Bulletin of Volcanology, 77(11). https://doi.org/10.1007/s00445-015-0979-y

Brata, A. G., Rietveld, P., de Groot, H. L. F., & Zant, W. (2013). The Krakatau Eruption in 1883: Its Implications for the Spatial Distribution of Population in Java. Economic History of Developing Regions, 28(2), 27–55. https://doi.org/10.1080/20780389.2013.866381

Brönnimann, S., & Krämer, D. (2016). Tambora and the "Year Without a Summer" of 1816. A Perspective on Earth and Human Systems Science. In Geographica Bernensia (Vol. G90). https://doi.org/10.4480/GB2016.G90.01

Bronto, S, Ratdomopurbo, A., Asmoro, P., & Adityarani, M. (2014). Longsoran Raksasa Gunung Api Merapi Yogyakarta – Jawa Tengah (Giant landslide in Merapi volcano

Yogyakarta-Central Java). Jurnal Geologi Dan Sumberdaya Mineral, 15(5), 165–183. Retrieved from http://dx.doi.org/10.33332/jgsm.geologi.v15i4

Bronto, Sutikno. (1989). Volcanic geology of Galunggung, West Java, Indonesia. 511. Retrieved from http://ir.canterbury.ac.nz/handle/10092/5667

Brown, S. K., Jenkins, S. F., Sparks, R. S. J., Odbert, H., & Auker, M. R. (2017). Volcanic fatalities database: analysis of volcanic threat with distance and victim classification. Journal of Applied Volcanology, 6(1). https://doi.org/10.1186/s13617-017-0067-4

Brugnatelli, V., & Tibaldi, A. (2020). Effects in North Africa of the 934–940 CE Eldgjá and 1783–1784 CE Laki eruptions (Iceland) revealed by previously unrecognized written sources. Bulletin of Volcanology, 82(11). https://doi.org/10.1007/s00445-020-01409-0

C

Cahyono, M. D. (2012). Volkano-historis Kelud: Dinamika hubugan manusia-gunungapi (Volcano-hitory of Kelud: Dynamics relation between human and volcano). Kalpataru: Majalah Arkeologi, 21(20), 85–102.

Campbell, B. B. M. S. (2017). Global climates, the 1257 mega-eruption of samalas volcano , indonesia , and the english food crisis of 1258. Transactions of the RHS, 27, 87–121.

Camus, G., Diament, M., & Gloaguen, M. (1992). Emplacement of a Debris Avalanche during the 1883 Eruption of Krakatau Emplacement of a Debris Avalanche during the 1883 Eruption of Krakatau (Sunda Straits , Indonesia). GeoJournal, (September). https://doi.org/10.1007/BF00177224

Canuto, M. A., & Auld-Thomas, L. (2021). Taking the high ground: A model for lowland Maya settlement patterns. Journal of Anthropological Archaeology, 64(101349). https://doi.org/10.1016/j.jaa.2021.101349

Capra, L., Macías, J. L., Scott, K. M., Abrams, M., & Garduño-Monroy, V. H. (2002). Debris avalanches and debris flows transformed from collapses in the Trans-Mexican Volcanic Belt, Mexico – behavior, and implications for hazard assessment. Journal of Volcanology and Geothermal Research, 113(1), 81–110. https://doi.org/https://doi.org/10.1016/S0377-0273(01)00252-9

Cashman, K. V., & Giordano, G. (2008). Volcanoes and human history. Journal of Volcanology and Geothermal Research, 176(3), 325–329. https://doi.org/10.1016/j.jvolgeores.2008.01.036

Cesaretti, R., Lobo, J., Bettencourt, M. A., Ortman, S. G., & Smith, M. E. 2016. Population-Area Relationship for Medieval European Cities. PLOS ONE, 11(10), e0162678. https://doi.org/10.1371/journal.pone.0162678

Chester, D., Duncan, A., Kilburn, C., Sangster, H., & Solana, C. (2015). Human responses to the 1906 eruption of Vesuvius, southern Italy. Journal of Volcanology and Geothermal Research, 296, 1–18. https://doi.org/10.1016/j.jvolgeores.2015.03.004

Chester, D. K., Duncan, A. M., & Sangster, H. (2012). Human responses to eruptions of Etna (Sicily) during the late-Pre-Industrial Era and their implications for present-day disaster planning. Journal of Volcanology and Geothermal Research, 225–226, 65–80. https://doi.org/10.1016/j.jvolgeores.2012.02.017

Cooper, C. L., Swindles, G. T., Savov, I. P., Schmidt, A., & Bacon, K. L. (2018). Evaluating the relationship between climate change and volcanism. Earth-Science Reviews, 177(March 2017), 238–247. https://doi.org/10.1016/j.earscirev.2017.11.009

Cortés, A., Macías, J. L., Capra, L., & Garduño-monroy, V. H. (2010). Sector collapse of the SW fl ank of Volcán de Colima , México The 3600 yr BP La Lumbre – Los Ganchos debris avalanche and associated debris fl ows. Journal of Volcanology and Geothermal Research, 197, 52–66. https://doi.org/10.1016/j.jvolgeores.2009.11.013

D

D'Addabbo, M., Sulpizio, R., Guidi, M., Capitani, G., Mantecca, P., & Zanchetta, G. (2015). Ash leachates from some recent eruptions of Mount Etna (Italy) and Popocatepetl (Mexico) volcanoes and their impact on amphibian living freshwater organisms. Biogeosciences, 12(23), 7087–7106. https://doi.org/10.5194/bg-12-7087-2015

Dahlin, B. H., & Chase, A. F. (2014). A Tale of Three Cities: Effects of the A.D. 536 Event in the Lowland Maya Heartland. In The Great Maya Droughts in Cultural Context: Case Studies in Resilience and Vulnerability (Iannone, G, pp. 127–155). Retrieved from https://books.google.fr/books?id=tozgCwAAQBAJ&hl=fr

Darmawan, H., Walter, T. R., Brotopuspito, K. S., Subandriyo, & I Gusti Made Agung Nandaka. (2018a). Morphological and structural changes at the Merapi lava dome monitored in 2012–15 using unmanned aerial vehicles (UAVs). Journal of Volcanology and Geothermal Research, 349, 256–267. https://doi.org/10.1016/j.jvolgeores.2017.11.006

Darmawan, H., Walter, T. R., Troll, V. R., & Budi-Santoso, A. (2018b). Dome instability at Merapi volcano identified by drone photogrammetry and numerical modeling.

Natural Hazards and Earth System Sciences Discussions, (May), 1–27. https://doi.org/10.5194/nhess-2018-120

Davies, T. R., McSaveney, M. J., & Hodgson, K. A. (1999). A fragmentation-spreading model for long-runout rock avalanches. Canadian Geotechnical Journal, 36(6), 1096–1110. https://doi.org/10.1139/t99-067

Davies, T., McSaveney, M., & Kelfoun, K. (2010). Runout of the Socompa volcanic debris avalanche, Chile: A mechanical explanation for low basal shear resistance. Bulletin of Volcanology, 72(8), 933–944. https://doi.org/10.1007/s00445-010-0372-9

De Maisonneuve, C. B., & Bergal-Kuvikas, O. (2020). Timing, magnitude and geochemistry of major Southeast Asian volcanic eruptions: identifying tephrochronologic markers. Journal of Quaternary Science, 35(1–2), 272–287. https://doi.org/10.1002/jqs.3181

de Silva, S., & Lindsay, J. M. (2015). Chapter 15 - Primary Volcanic Landforms (H. B. T.-T. E. of V. (Second E. Sigurdsson, Ed.). https://doi.org/https://doi.org/10.1016/B978-0-12-385938-9.00015-8

Degroot, V. (2017). The Liangan Temple Site in Central Java. Archipel, (94), 191–209. https://doi.org/10.4000/archipel.456

Delcamp, A., Kervyn, M., Benbakkar, M., Kwelwa, S., & Peter, D. (2017). Large volcanic landslide and debris avalanche deposit at Meru , Tanzania. Landslides, (September 2016), 833–847. https://doi.org/10.1007/s10346-016-0757-8

Dibacto, S., Lahitte, P., Karátson, D., Hencz, M., Szakács, A., Biró, T., … Veres, D. (2020). Growth and erosion rates of the East Carpathians volcanoes constrained by numerical models: Tectonic and climatic implications. Geomorphology, 368, 107352. https://doi.org/https://doi.org/10.1016/j.geomorph.2020.107352

Djalante, R. (2012). Review Article: Adaptive governance and resilience: The role of multi-stakeholder platforms in disaster risk reduction. Nat. Hazards Earth Syst. Sci., 12(9), 2923–2942. https://doi.org/10.5194/nhess-12-2923-2012

Donovan, K., Suryanto, A., & Utami, P. (2012). Mapping cultural vulnerability in volcanic regions: The practical application of social volcanology at Mt Merapi, Indonesia. Environmental Hazards, 11(4), 303–323. https://doi.org/10.1080/17477891.2012.689252

Druitt, T. H. (1998). Pyroclastic density currents. Geological Society, London, Special Publications, 145(1), 145–182. https://doi.org/10.1144/GSL.SP.1996.145.01.08

Dufresne, A., & Davies, T. R. (2009). Longitudinal ridges in mass movement deposits. Geomorphology, 105(3–4), 171–181. https://doi.org/10.1016/j.geomorph.2008.09.009

Dufresne, Anja, Siebert, L., & Bernard, B. (2021). Distribution and Geometric Parameters of Volcanic Debris Avalanche Deposits BT - Volcanic Debris Avalanches: From Collapse to Hazard (Matteo Roverato, A. Dufresne, & J. Procter, Eds.). https://doi.org/10.1007/978-3-030-57411-6_4

E

Ediyono, S., & Ridwan, M. (2018). Cross-Cultural Communication in Lombok Society ' s Writing Tradition : Babad Lombok Manuscript. Advances in Social Science, Education and Humanities Research, 280, 548–552.

Elez, J., Silva, P. G., Huerta, P., Perucha, M. Á., Civis, J., Roquero, E., … Martínez-Graña, A. (2016). Quantitative paleotopography and paleogeography around the Gibraltar Arc (South Spain) during the Messinian Salinity Crisis. Geomorphology, 275, 26–45. https://doi.org/10.1016/j.geomorph.2016.09.023

F

Faral, A., Lavigne, F., Mutaqin, B. W., Mokadem, F., Achmad, R., Ningrum, R. W., … Mei, E. T. W. (2022). A 22,000-year tephrostratigraphy record of unidentified volcanic eruptions from Ternate and Tidore islands (North Maluku, Indonesia). Journal of Volcanology and Geothermal Research, 423, 107474. https://doi.org/https://doi.org/10.1016/j.jvolgeores.2022.107474

Fei, J., & Zhou, J. (2006). The possible climatic impact in China of Iceland's Eldgjá eruption inferred from historical sources. Climatic Change, 76(3–4), 443–457. https://doi.org/10.1007/s10584-005-9012-3

Fei, J., Zhou, J., & Hou, Y. (2007). Circa A.D. 626 volcanic eruption, climatic cooling, and the collapse of the Eastern Turkic Empire. Climatic Change, 81(3–4), 469–475. https://doi.org/10.1007/s10584-006-9199-y

Fell, H. G., Baldini, J. U. L., Dodds, B., & Sharples, G. J. (2020). Volcanism and global plague pandemics: Towards an interdisciplinary synthesis. Journal of Historical Geography, 70, 36–46. https://doi.org/10.1016/j.jhg.2020.10.001

Ferrario, M. F. (2019). Landslides triggered by multiple earthquakes: insights from the 2018 Lombok (Indonesia) events. Natural Hazards, 98(2), 575–592. https://doi.org/10.1007/s11069-019-03718-w

G

Gao, C., Oman, L., Robock, A., & Stenchikov, G. L. (2007). Atmospheric volcanic loading derived from bipolar ice cores: Accounting for the spatial distribution of

volcanic deposition. Journal of Geophysical Research Atmospheres, 112(9). https://doi.org/10.1029/2006JD007461

Gao, C., Robock, A., & Ammann, C. (2008). Volcanic forcing of climate over the past 1500 years: An improved ice core-based index for climate models. Journal of Geophysical Research Atmospheres, 113(23), 1–15. https://doi.org/10.1029/2008JD010239

Garajeh, M. K., Feizizadeh, B., Blaschke, T., & Lakes, T. (2022). Detecting and mapping karst landforms using object-based image analysis: Case study: Takht-Soleiman and Parava Mountains, Iran. Egyptian Journal of Remote Sensing and Space Science, 25(2), 473–489. https://doi.org/10.1016/j.ejrs.2022.03.009

Garrison, C. S., Kilburn, C. R. J., & Edwards, S. J. (2018). The 1831 eruption of Babuyan Claro that never happened: Has the source of the one of the largest volcanic climate forcing events of the nineteenth century been misattributed? Journal of Applied Volcanology, 7(1). https://doi.org/10.1186/s13617-018-0078-9

Gertisser, R., Cassidy, N. J., Charbonnier, S. J., Nuzzo, L., & Preece, K. (2012). Overbank block-and-ash flow deposits and the impact of valley-derived, unconfined flows on populated areas at Merapi volcano, Java, Indonesia. Natural Hazards, 60(2), 623–648. https://doi.org/10.1007/s11069-011-0044-x

Giachetti, T., Paris, R., Kelfoun, K., & Ontowirjo, B. (2012). Tsunami hazard related to a flank collapse of Anak Krakatau Volcano, Sunda Strait, Indonesia. Geological Society Special Publication, 361(1), 79–90. https://doi.org/10.1144/SP361.7

Gianisa, A., & Le De, L. (2018). The role of religious beliefs and practices in disaster. Disaster Prevention and Management, 27(1), 74–86. https://doi.org/10.1108/DPM-10-2017-0238

Gislason, S. R., Alfredsson, H. A., Eiriksdottir, E. S., Hassenkam, T., & Stipp, S. L. S. (2011). Volcanic ash from the 2010 Eyjafjallajökull eruption. Applied Geochemistry, 26(SUPPL.), 2010–2012. https://doi.org/10.1016/j.apgeochem.2011.03.100

Glicken, H. (1996). Rockslide-debris avalanche of May 18, 1980, Mount St. Helens volcano, Washington.

Gob, F., Gautier, E., Virmoux, C., Grancher, D., Tamisier, V., Primanda, K. W., … Lavigne, F. (2016). River responses to the 2010 major eruption of the Merapi volcano, central Java, Indonesia. Geomorphology, 273, 244–257. https://doi.org/10.1016/j.geomorph.2016.08.025

Gomez, C, Janin, M., Lavigne, F., Gertisser, R., Charbonnier, S., Lahitte, P., … Murwanto, H. (2010). Borobudur , a basin under volcanic in fl uence : 361 , 000

years BP to present. Journal of Volcanology and Geothermal Research, 196(3–4), 245–264. https://doi.org/10.1016/j.jvolgeores.2010.08.001

Gomez, Christopher, Shinohara, Y., Tsunetaka, H., Hotta, N., Bradak, B., & Sakai, Y. (2021). Twenty-Five Years of Geomorphological Evolution in the Gokurakudani Gully (Unzen Volcano): Topography, Subsurface Geophysics and Sediment Analysis. Geosciences, Vol. 11. https://doi.org/10.3390/geosciences11110457

Goto, Y., Danhara, T., & Tomiya, A. (2019). Catastrophic sector collapse at Usu volcano, Hokkaido, Japan: failure of a young edifice built on soft substratum. Bulletin of Volcanology, 81(6). https://doi.org/10.1007/s00445-019-1293-x

Gran, K. B., Montgomery, D. R., & Halbur, J. C. (2011). Long-term elevated post-eruption sedimentation at Mount Pinatubo, Philippines. Geology, 39(4), 367–370. https://doi.org/10.1130/G31682.1

Grilli, S. T., Tappin, D. R., Carey, S., Watt, S. F. L., Ward, S. N., Grilli, A. R., … Muin, M. (2019). Modelling of the tsunami from the December 22, 2018 lateral collapse of Anak Krakatau volcano in the Sunda Straits, Indonesia. Scientific Reports, 9(1), 11946. https://doi.org/10.1038/s41598-019-48327-6

Grishin, S. Y. (2009). Forest die-off under the impact of burning pyroclastic surge on the Shiveluch Volcano (Kamchatka, 2005). Russian Journal of Ecology, 40(2), 146–148. https://doi.org/10.1134/S106741360902012X

Grishin, S. Y. (2011). Environmental impact of the powerful eruption of Sarychev Peak volcano (Kuril Islands, 2009) according to satellite imagery. Izvestiya - Atmospheric and Ocean Physics, 47(9), 1028–1031. https://doi.org/10.1134/S0001433811090064

Grosse, P., Danišík, M., Apaza, F. D., Guzmán, S. R., Lahitte, P., Quidelleur, X., … Bachmann, O. (2022). Holocene collapse of Socompa volcano and pre- and post-collapse growth rates constrained by multi-system geochronology. Bulletin of Volcanology, 84(9), 1–18. https://doi.org/10.1007/s00445-022-01594-0

Guidoboni, E., & Ciuccarelli, C. (2008). First historical evidence of a signi fi cant Mt . Etna eruption in 1224. Journal of Volcanology and Geothermal Research, 178(4), 693–700. https://doi.org/10.1016/j.jvolgeores.2008.08.009

Guillet, S., Corona, C., Stoffel, M., Khodri, M., Lavigne, F., Ortega, P., … Oppenheimer, C. (2017). Climate response to the Samalas volcanic eruption in 1257 revealed by proxy records. Nature Geoscience, 10(2), 123–128. https://doi.org/10.1038/ngeo2875

Gunkel, G., Beulker, C., Grupe, B., & Viteri, F. (2008). Hazards of volcanic lakes: Analysis of Lakes Quilotoa and Cuicocha, Ecuador. Advances in Geosciences, 14, 29–33. https://doi.org/10.5194/adgeo-14-29-2008

H

Hadi, M. N., Yushantarti, A., Suhanto, E., & Sundhoro, H. (2007). Survei panas bumi terpadu (geologi, geokimia dan geofisika) daerah sembalun, kabupaten lombok timur - NTB (Integrated geothermal survey in Sembalun, East Lombok - NTB). Proceeding Pemaparan Hasil Kegiatan Lapangan Dan Non Lapangan. Bandung: Pusat Sumber Daya Geologi.

Hadmoko, D. S., de Belizal, E., Mutaqin, B. W., Dipayana, G. A., Marfai, M. A., Lavigne, F., … Gomez, C. (2018). Post-eruptive lahars at Kali Putih following the 2010 eruption of Merapi volcano, Indonesia: occurrences and impacts. Natural Hazards, 94(1), 419–444. https://doi.org/10.1007/s11069-018-3396-7

Hägerdal, H. 2001. Hindu Rulers, Muslim Subjects: Lombok and Bali in the Seventeenth and Eighteenth Centuries. Bangkok: White Lotus Press.

Hägerdal, H. (2015). Eastern Indonesia and the Writing of History. Archipel, 90, 75–97. https://doi.org/10.4000/archipel.369

Hall, R. (2009). Indonesia, Geology. In R. Gillespie & D. Clague (Eds.), Encyclopedia of Islands (pp. 454–460). Berkeley, California: University of California Pres.

Hall, R. (2012). Late Jurassic–Cenozoic reconstructions of the Indonesian region and the Indian Ocean. Tectonophysics, 570–571, 1–41. https://doi.org/https://doi.org/10.1016/j.tecto.2012.04.021

Harsuko, M. R. C., Zulfakriza, Z., Nugraha, A. D., Sarjan, A. F. N., Widiyantoro, S., Rosalia, S., … Sahara, D. . (2020). Investigation of Hilbert – Huang Transform and Fourier Transform for Horizontal-to-Vertical Spectral Ratio Analysis : Understanding the Shallow Structure in Mataram City , Lombok , Indonesia. Front. Earth Sci., 8(334). https://doi.org/10.3389/feart.2020.00334

Hart, K., Carey, S., Sigurdsson, H., Sparks, R. S. J., & Robertson, R. E. A. (2004). Discharge of pyroclastic flows into the sea during the 1996-1998 eruptions of the Soufrière Hills volcano, Montserrat. Bulletin of Volcanology, 66(7), 599–614. https://doi.org/10.1007/s00445-004-0342-1

Hayakawa, Y. S., Yoshida, H., Obanawa, H., Naruhashi, R., Okumura, K., Zaiki, M., & Kontani, R. (2018). Characteristics of debris avalanche deposits inferred from source volume estimate and hummock morphology around Mt. Erciyes, central Turkey. Natural Hazards and Earth System Sciences, 18(2), 429–444. https://doi.org/10.5194/nhess-18-429-2018

Heaton, T. J., Köhler, P., Butzin, M., Bard, E., Reimer, R. W., Austin, W. E. N., … Skinner, L. C. (2020). Marine20—The Marine Radiocarbon Age Calibration Curve (0–55,000 cal BP). Radiocarbon, 62(4), 779–820. https://doi.org/DOI: 10.1017/RDC.2020.68

Hickson, C. J., Spurgeon, T. C., & Tilling, R. I. (2013). Eruption Types (Volcanic Eruptions). In P. T. Bobrowsky (Ed.), Encyclopedia of Natural Hazards (pp. 290–293). https://doi.org/10.1007/978-1-4020-4399-4_122

Hickson, C., Spurgeon, T., Tilling, R., & Adam, P. (2013). Factors influencing volcanic hazards and the morphology of volcanic landforms. In J. Shroder, L. . James, C. . Harden, & J. . Clague (Eds.), Treatise on Geomorphology (pp. 219–242). https://doi.org/10.1007/978-1-4020-4399-4

Hiden, H., Brotopuspito, K. S., Hadmoko, D. S., Lavigne, F., Airaksinen, K. B., Mutaqin, B. W., … Suryanto, W. (2017). The isopach mapping of volcanic deposits of mount samalas 1257 AD based on the values of resistivity and physical properties. Geosciences (Switzerland), 7(67). https://doi.org/10.3390/geosciences7030067

Hizbaron, D. R., Iffani, M., Wijayanti, H., & Wicaksono, G. N. (2016). Disaster Management Practice Towards Diverse Vulnerable Groups in Yogyakarta. Proceedings of the 1st International Conference on Geography and Education (ICGE 2016), 7–12. https://doi.org/https://doi.org/10.2991/icge-16.2017.2

Hogg, A. G., Heaton, T. J., Hua, Q., Palmer, J. G., Turney, C. S. M., Southon, J., … Wacker, L. (2020). SHCal20 Southern Hemisphere Calibration, 0–55,000 Years cal BP. Radiocarbon, 62(4), 759–778. https://doi.org/DOI: 10.1017/RDC.2020.59

Hunt, J. E., Cassidy, M., & Talling, P. J. (2018). Multi-stage volcanic island flank collapses with coeval explosive caldera-forming eruptions. Scientific Reports, 8(1), 1–11. https://doi.org/10.1038/s41598-018-19285-2

J

Jamaluddin. (2012). Kerajaan dan Perkembangan Peradaban Islam: Telaah terhadap Peran Istana dalam Tradisi Per- naskahan di Lombok. Jurnal Manassa Manuskripta, 2(1), 181–200.

Jamaluddin, J. (2005). Sejarah Tradisi Tulis Dalam Masyarakat Sasak Lombok. Ulumuna, 9(2), 369–384. https://doi.org/10.20414/ujis.v9i2.493

Jeffery, A. J., Gertisser, R., Troll, V. R., Jolis, E. M., Dahren, B., Harris, C., … Chadwick, J. P. (2013). The pre-eruptive magma plumbing system of the 2007-2008 dome-forming eruption of Kelut volcano, East Java, Indonesia. Contributions to Mineralogy and Petrology, 166(1), 275–308. https://doi.org/10.1007/s00410-013-0875-4

Jenkins, S. F., Phua, M., Warren, J. F., Biass, S., Bouvet, C., & Maisonneuve, D. (2020). Reconstructing eruptions from historical accounts : Makaturing c . Journal of Volcanology and Geothermal Research, 404, 107022. https://doi.org/10.1016/j.jvolgeores.2020.107022

K

Kasbani, Gunawan, H., McCausland, W., Pallister, J., Iguchi, M., & Nakada, S. (2019). The eruptions of Sinabung and Kelud volcanoes, Indonesia. Journal of Volcanology and Geothermal Research, 382(October), 1–5. https://doi.org/10.1016/j.jvolgeores.2019.07.008

Kelfoun, K., & Druitt, T. H. (2005). Numerical modeling of the emplacement of Socompa rock avalanche, Chile. Journal of Geophysical Research: Solid Earth, 110(12), 1–13. https://doi.org/10.1029/2005JB003758

Kelfoun, K., Giachetti, T., and Labazuy, P. (2010), Landslide-generated tsunamis at Réunion Island, J. Geophys. Res., 115, F04012, doi:10.1029/2009JF001381.

Kelfoun, K. (2011). Suitability of simple rheological laws for the numerical simulation of dense pyroclastic flows and long-runout volcanic avalanches. Journal of Geophysical Research: Solid Earth, 116(8). https://doi.org/10.1029/2010JB007622

Kirchner, A., Zielhofer, C., Werther, L., Schneider, M., Linzen, S., Wilken, D., … Ettel, P. (2018). A multidisciplinary approach in wetland geoarchaeology: Survey of the missing southern canal connection of the Fossa Carolina (SW Germany). Quaternary International, 473, 3–20. https://doi.org/https://doi.org/10.1016/j.quaint.2017.12.021

Kusuma, P., Brucato, N., Cox, M. P., Letellier, T., Manan, A., Nuraini, C., … Ricaut, F. X. (2017). The last sea nomads of the Indonesian archipelago: Genomic origins and dispersal. European Journal of Human Genetics, 25(8), 1004–1010. https://doi.org/10.1038/ejhg.2017.88

L

Lahitte, P., Samper, A., & Quidelleur, X. (2012). DEM-based reconstruction of southern Basse-Terre volcanoes (Guadeloupe archipelago, FWI): Contribution to the Lesser Antilles Arc construction rates and magma production. Geomorphology, 136(1), 148–164. https://doi.org/10.1016/j.geomorph.2011.04.008

Łajczak, A., Zarychta, R., & Wałek, G. (2020). Changes in the topography of Krakow city centre Poland during the last millennium. Journal of Maps. https://doi.org/10.1080/17445647.2020.1823253

Łajczak, A., Zarychta, R., & Wałek, G. (2021). Quantitative Assessment of Changes in Topography of Town Caused by Human Impact, Krakow City Centre, Southern Poland. Remote Sens. 13, 2286. https://doi.org/10.3390/rs13122286

Lavigne, F., De Coster, B., Juvin, N., Flohic, F., Gaillard, J. C., Texier, P., … Sartohadi, J. (2008). People's behaviour in the face of volcanic hazards: Perspectives from

Javanese communities, Indonesia. Journal of Volcanology and Geothermal Research, 172(3–4), 273–287. https://doi.org/10.1016/j.jvolgeores.2007.12.013

Lavigne, F., Degeai, J. P., Komorowski, J. C., Guillet, S., Robert, V., Lahitte, P., … De Belizal, E. (2013). Source of the great A.D. 1257 mystery eruption unveiled, Samalas volcano, Rinjani Volcanic Complex, Indonesia. Proceedings of the National Academy of Sciences of the United States of America, 110(42), 16742–16747. https://doi.org/10.1073/pnas.1307520110

Lavigne, F., Morin, J., Wassmer, P., Weller, O., Kula, T., Maea, A. V, … Gomez, C. (2021). Bridging Legends and Science: Field Evidence of a Large Tsunami that Affected the Kingdom of Tonga in the 15th Century. Frontiers in Earth Science, 9, 748755. https://doi.org/10.3389/feart.2021.748755

Lechner, P., Tupper, A., Guffanti, M., Loughlin, S., & Casadevall, T. (2018). Volcanic Ash and Aviation—The Challenges of Real-Time, Global Communication of a Natural Hazard. Advances in Volcanology, (June 2017), 51–64. https://doi.org/10.1007/11157_2016_49

Lee, K. H., Kim, S. W., & Kim, S. H. (2018). Simulating floods triggered by volcanic activities in the Cheon-ji caldera lake for hazards and risk analysis. Journal of Flood Risk Management, 11, 479–488.

Lentz, D. L., Dunning, N. P., Scarborough, V. L., & Grazioso, L. (2018). Imperial resource management at the ancient Maya city of Tikal: A resilience model of sustainability and collapse. Journal of Anthropological Archaeology, 52(July), 113–122. https://doi.org/10.1016/j.jaa.2018.08.005

Leopold, L. B., Wolman, M., G., & Miller, J. P. (1995). Fluvial Processes in Geomorphology. New York: Dover Publication, Inc.

Lomoschitz, A., Hervás, J., Yepes, J., & Meco, J. (2008). Characterisation of a pleistocene debris-avalanche deposit in the Tenteniguada Basin, Gran Canaria Island, Spain. Landslides, 5(2), 227–234. https://doi.org/10.1007/s10346-008-0115-6

Lowe, D. J., Higham, T. F. G. 1998. Hit-or-myth? Linking a 1259 AD acid spike with an Okataina eruption. Antiquity, 72(276), 427–432. https://doi.org/DOI: 10.1017/S0003598X00086737

Luberti, G. M. (2018). Computation of modern anthropogenic-deposit thicknesses in urban areas: A case study in Rome, Italy. Anthropocene Review, 5(1), 2–27. https://doi.org/10.1177/2053019618757252

Lucchi, F. (2019). On the use of unconformities in volcanic stratigraphy and mapping: Insights from the Aeolian Islands (southern Italy). Journal of Volcanology and Geothermal Research, 385, 3–26. https://doi.org/https://doi.org/10.1016/j.jvolgeores.2019.01.014

M

MacLeod, N. (1989). Sector-failure eruptions in Indonesian volcanoes. Geol Indonesia, 12, 563–601.

Madden-Nadeau, A. L., Cassidy, M., Pyle, D. M., Mather, T. A., Watt, S. F. L., Engwell, S. L., … Ismail, T. (2021). The magmatic and eruptive evolution of the 1883 caldera-forming eruption of Krakatau: Integrating field- to crystal-scale observations. Journal of Volcanology and Geothermal Research, 411. https://doi.org/10.1016/j.jvolgeores.2021.107176

Malawani, Mukhamad N., Lavigne, F., Gomez, C., Mutaqin, B. W., & Hadmoko, D. S. (2021). Review of local and global impacts of volcanic eruptions and disaster management practices: The Indonesian example. Geosciences (Switzerland), 11(3)(109). https://doi.org/10.3390/geosciences11030109

Malawani, Mukhamad N, Lavigne, F., Hadmoko, D. S., Marfai, M. A., & Mutaqin, B. W. (2020). Hummocky terrain of the Kalibabak debris avalanche deposit , Lombok Island , Indonesia. E3S Web of Conferences, 200(02015). https://doi.org/https://doi.org/10.1051/e3sconf/202020002015

Malawani, Mukhamad Ngainul, Lavigne, F., Sastrawan, W. J., Jamaluddin, Sirulhaq, A., & Hadmoko, D. S. (2022). The 1257 CE cataclysmic eruption of Samalas volcano (Indonesia) revealed by indigenous written sources: Forgotten kingdoms, emergency response, and societal recovery. Journal of Volcanology and Geothermal Research, 432(September), 107688. https://doi.org/10.1016/j.jvolgeores.2022.107688

Mangga, S., Atmawinata, S., Hermanto, B., Setyogroho, B., & Amin, T. (1994). Geological Map of the Lombok Sheet, West Nusatenggara. Bandung: Geological Reseracg and Development Centre.

Mansyur, Z. (2019). Social wisdom of Sasak Tribe-Lombok in the local tradition (Kearifan Sosial Masyarakat Sasak-Lombok dalam Tradisi Lokal). Mataram: Sanabil.

Manville, V., Segschneider, B., Newton, E., White, J. D. L., Houghton, B. F., & Wilson, C. J. N. (2009). Environmental impact of the 1 . 8 ka Taupo eruption , New Zealand : Landscape responses to a large-scale explosive rhyolite eruption. Sedimentary Geology, 220(3–4), 318–336. https://doi.org/10.1016/j.sedgeo.2009.04.017

Marrison, G. E. (1997). The literature of Lombok : Sasak, Balinese , and Javanese. Indonesia and the Malay World, 25(37), 221–234. https://doi.org/10.1080/13639819708729901

Marrison, G. E. (1999). Sasak and Javanese Literature of Lombok. Leiden: KITLV Press.

Martí, J., Groppelli, G., & Brum da Silveira, A. (2018). Volcanic stratigraphy: A review. Journal of Volcanology and Geothermal Research, 357, 68–91. https://doi.org/https://doi.org/10.1016/j.jvolgeores.2018.04.006

Martin, S. C. (2020). Past eruptions and future predictions : Analyzing ancient responses to Mount Vesuvius for use in modern risk management. Journal of Volcanology and Geothermal Research, 396, 106851. https://doi.org/10.1016/j.jvolgeores.2020.106851

Maryanto, S, Hasan, R., & Siregar, D. . (2009). Mineralogi matriks breksi gunung api plistosen akhir – kuarter berdasarkan data XRD di daerah lombok timur, nusa tenggara barat. Jurnal Geologi Dan Sumberdaya Mineral, 19(1).

Maryanto, Sigit. (2009). Distribusi ukuran butir matriks breksi gunungapi di daerah Lombok Timur, Nusa Tenggara Barat. Bulletin of Scientific Contribution, 7(1), 49–71. https://doi.org/https://doi.org/10.24198/bsc%20geology.v7i1.8233

Mayr, C., Smith, R. E., García, M. L., Massaferro, J., Lücke, A., Dubois, N., … Zolitschka, B. (2019). Historical eruptions of Lautaro Volcano and their impacts on lacustrine ecosystems in southern Argentina. Journal of Paleolimnology, 62(2), 205–221. https://doi.org/10.1007/s10933-019-00088-y

Métrich, N., Vidal, C. M., Komorowski, J. C., Pratomo, I., Michel, A., Kartadinata, N., … Surono. (2017). New insights into magma differentiation and storage in holocene crustal reservoirs of the lesser sunda arc: The Rinjani-Samalas volcanic complex (Lombok, Indonesia). Journal of Petrology, 58(11), 2257–2284. https://doi.org/10.1093/petrology/egy006

Meulen, B. Van Der, Cohen, K. M., Pierik, H. J., Zinsmeister, J. J., & Middelkoop, H. (2020). Geomorphology LiDAR-derived high-resolution palaeo-DEM construction work fl ow and application to the early medieval Lower Rhine valley and upper delta. Geomorphology, 370, 107370. https://doi.org/10.1016/j.geomorph.2020.107370

Miller, G. H., Geirsdóttir, Á., Zhong, Y., Larsen, D. J., Otto-bliesner, B. L., Holland, M. M., … Björnsson, H. (2012). Abrupt onset of the Little Ice Age triggered by volcanism and sustained by sea- ice/ocean feedbacks. Geophysical Research Letters, 39(January). https://doi.org/10.1029/2011GL050168

Minimo, L. G., & Lagmay, A. M. F. A. (2016). 3D modeling of the Buhi debris avalanche deposit of Iriga Volcano, Philippines by integrating shallow-seismic reflection and geological data. Journal of Volcanology and Geothermal Research, 319, 106–123. https://doi.org/10.1016/j.jvolgeores.2016.03.002

Moktikanana, M. L. A., Wibowo, H. E., Rahayu, E., & Harijoko, A. (2021). Hummock size and alignment in Gadung debris avalanche deposit, Raung Volcanic Complex,

East Java, Indonesia. IOP Conference Series: Earth and Environmental Science, 851(1), 012037. https://doi.org/10.1088/1755-1315/851/1/012037

Mothes, P. A., & Vallance, J. W. (2015). Chapter 6 - Lahars at Cotopaxi and Tungurahua Volcanoes, Ecuador: Highlights from Stratigraphy and Observational Records and Related Downstream Hazards. In J. F. Shroder & P. B. T.-V. H. Papale Risks and Disasters (Eds.), Hazards and Disasters Series (pp. 141–168). https://doi.org/https://doi.org/10.1016/B978-0-12-396453-3.00006-X

Mozzi, P., Ferrarese, F., Zangrando, D., Gamba, M., Vigoni, A., Sainati, C., … Veronese, F. (2017). The modeling of archaeological and geomorphic surfaces in a multistratified urban site in Padua, Italy. Geoarchaeology, 33(1), 67–84. https://doi.org/10.1002/gea.21641

Mulyadi, L. (2014). History of Sasak World Lombok (Sejarah Gumi Sasak Lombok). Malang: Faculty of Civil Engeneering and Planning ITN.

Mutaqin, B. W., Lavigne, F., Hadmoko, D. S., & Ngalawani, M. N. (2019). Volcanic Eruption-Induced Tsunami in Indonesia: A Review. IOP Conference Series: Earth and Environmental Science, 256(1). https://doi.org/10.1088/1755-1315/256/1/012023

Mutaqin, Bachtiar W., & Lavigne, F. (2019). Oldest description of a caldera-forming eruption in Southeast Asia unveiled in forgotten written sources. GeoJournal, 5. https://doi.org/10.1007/s10708-019-10083-5

Mutaqin, Bachtiar W., Lavigne, F., Sudrajat, Y., Handayani, L., Lahitte, P., Virmoux, C., … Boillot-Airaksinen, K. (2019). Landscape evolution on the eastern part of Lombok (Indonesia) related to the 1257 CE eruption of the Samalas Volcano. Geomorphology, 327, 338–350. https://doi.org/10.1016/j.geomorph.2018.11.010

N

Naranjo, J. A., & Francis, P. (1987). High velocity debris avalanche at Lastarria volcano in the north Chilean Andes. Bulletin of Volcanology, 49(2), 509–514. https://doi.org/10.1007/BF01245476

Nasution, A., Takada, A., & Rosgandika, M. (2004). The volcanic activity of Rinjani, Lombok Island, Indonesia, during the last thousand years, viewed from 14C datings. The 33rd Annual Convention & Exhibition. Bandung 29–30 November 2004.

Nasution, Asnawir, Takada, A., Udiwibowo, Widarto, D., & Hutasoit, L. (2010). Rinjani and Propok Volcanics as a Heat Sources of Geothermal Prospects from Eastern Lombok, Indonesia. Jurnal Geoaplika, 5(1), 1–9. Retrieved from https://www.researchgate.net/publication/261177243

Németh, K., & Kósik, S. (2020). Review of Explosive Hydrovolcanism. Geosciences, Vol. 10. https://doi.org/10.3390/geosciences10020044

Németh, K., & Palmer, J. (2019). Geological mapping of volcanic terrains: Discussion on concepts, facies models, scales, and resolutions from New Zealand perspective. Journal of Volcanology and Geothermal Research, 385, 27–45. https://doi.org/10.1016/j.jvolgeores.2018.11.028

Newhall, C., Self, S., & Robock, A. (2018). Anticipating future Volcanic Explosivity Index (VEI) 7 eruptions and their chilling impacts. Geosphere, 14(2), 572–603. https://doi.org/10.1130/GES01513.1

Newhall, G., & Self, S. (1982). The Volcanic Explosivity Index (VEI): An Estimate of Explosive Magnitude for Historical Volcanism. Journal of Geophysical Research Atmospheres, 87, 1231–1238. https://doi.org/10.1029/JC087iC02p01231

Nooren, K., Hoek, W. Z., van der Plicht, H., Sigl, M., van Bergen, M. J., Galop, D., … Middelkoop, H. (2017). Explosive eruption of El Chichon volcano (Mexico) disrupted 6th century Maya civilization and contributed to global cooling. Geology, 45(2), 175–178. https://doi.org/10.1130/G38739.1

Norini, G., Bustos, E., Arnosio, M., Baez, W., Zuluaga, M. C., & Roverato, M. (2020). Unusual volcanic instability and sector collapse configuration at Chimpa volcano, central Andes. Journal of Volcanology and Geothermal Research, 393. https://doi.org/10.1016/j.jvolgeores.2020.106807

Novikova, T., Papadopoulos, G. A., & McCoy, F. W. (2011). Modelling of tsunami generated by the giant Late Bronze Age eruption of Thera, South Aegean Sea, Greece. Geophysical Journal International, 186(2), 665–680. Retrieved from https://doi.org/10.1111/j.1365-246X.2011.05062.x

Nursalim, A., Sulaksana, N., & Sukiyah, E. (2016). Peran aspek geomorfologi dalam menentukan karakteristik endapan debris. Bulletin of Scientific Contribution, 14(April), 45–54.

O

Ogburn, S. E., Loughlin, S. C., & Calder, E. S. (2015). The association of lava dome growth with major explosive activity (VEI ≥ 4): DomeHaz, a global dataset. Bulletin of Volcanology, 77(5). https://doi.org/10.1007/s00445-015-0919-x

Oppenheimer, C. (2003). Climatic, environmental and human con sequences of the largest known historic eruption: Tambora volcano (Indonesia) 1815. Progress in Physical Geography, 27(2), 230–259. https://doi.org/10.1191/0309133303pp379ra

Oppenheimer, C., Orchard, A., Stoffel, M., Newfield, T. P., Guillet, S., Corona, C., … Büntgen, U. (2018). The Eldgjá eruption: timing, long-range impacts and influence

on the Christianisation of Iceland. Climatic Change, 147(3–4), 369–381. https://doi.org/10.1007/s10584-018-2171-9

Özdemir, Y., Akkaya, İ., Oyan, V., & Kelfoun, K. (2016). A debris avalanche at Süphan stratovolcano (Turkey) and implications for hazard evaluation. Bulletin of Volcanology, 78(2), 1–13. https://doi.org/10.1007/s00445-016-1007-6

P

Paguican, E. M. R., van Wyk de Vries, B., & Lagmay, A. M. F. (2014). Hummocks: how they form and how they evolve in rockslide-debris avalanches. Landslides, 11(1), 67–80. https://doi.org/10.1007/s10346-012-0368-y

Palais, J. M., Germani, M. S., Zielinski, G. A. 1992. Inter-hemispheric Transport of Volcanic Ash from a 1259 A.D. Volcanic Eruption to the Greenland and Antarctic Ice Sheets. Geophysical Research Letters, 19(8), 801–804. https://doi.org/https://doi.org/10.1029/92GL00240

Paramartha, K. (2017). Mitos dan Legenda dalam Babad Pulesari (Myth and Legend in the Babad Pulesari). Denpasar: Faculty of Language and Culture, Udayana University.

Pardo, N., Pulgarín, B., Betancourt, V., Lucchi, F., & Valencia, L. J. (2019). Facing geological mapping at low-latitude volcanoes: The Doña Juana Volcanic Complex study-case, SW-Colombia. Journal of Volcanology and Geothermal Research, 385, 46–67. https://doi.org/https://doi.org/10.1016/j.jvolgeores.2018.04.016

Paris, R., Wassmer, P., Lavigne, F., Belousov, A., Belousova, M., Iskandarsyah, Y., … Mazzoni, N. (2014). Coupling eruption and tsunami records: the Krakatau 1883 case-study, Indonesia. Bulletin of Volcanology, 76(814). Retrieved from https://doi.org/10.1007/s00445-014-%0A0814-x.

Paris, R., Bravo, J. J. C., González, M. E. M., Kelfoun, K., & Nauret, F. (2017). Explosive eruption, flank collapse and megatsunami at Tenerife ca. 170 ka. Nature Communications, 8(May 2016), 1–8. https://doi.org/10.1038/ncomms15246

Petterson, M., Cronin, S., Taylor, P., Tolia, D., Papabatu, A., Toba, T., & Qopoto, C. (2003). The eruptive history and volcanic hazards of Savo, Solomon Islands. Bulletin of Volcanology, 65(2), 165–181. https://doi.org/10.1007/s00445-002-0251-0

Picquout, A., Lavigne, F., Mei, E. T. W., Grancher, D., Noer, C., Vidal, C. M., & Hadmoko, D. S. (2013). Air traffic disturbance due to the 2010 Merapi volcano eruption. Journal of Volcanology and Geothermal Research, 261, 366–375. https://doi.org/10.1016/j.jvolgeores.2013.04.005

Pierik, H. J., Cohen, K. M., & Stouthamer, E. (2016). Geomorphology A new GIS approach for reconstructing and mapping dynamic late Holocene coastal plain palaeogeography. 270, 55–70.

Pierik, H. J., Stouthamer, E., & Cohen, K. M. (2017). Geomorphology Natural levee evolution in the Rhine-Meuse delta , the Netherlands , during the fi rst millennium CE. Geomorphology, 295(February), 215–234. https://doi.org/10.1016/j.geomorph.2017.07.003

Pierson, T.C., Janda, R. J., Umbal, J. V., & Daag, A. S. (1992). Immediate and long-term hazards from lahars and excess sedimentation in rivers draining Mount Pinatubo, Philippines. Retrieved from https://doi.org/10.3133/wri924039

Pierson, Thomas C, & Major, J. J. (2014). Hydrogeomorphic Effects of Explosive Volcanic Eruptions on Drainage Basins. Annual Review of Earth and Planetary Sciences, 42(1), 469–507. https://doi.org/10.1146/annurev-earth-060313-054913

Ponomareva, V., Pevzner, M. & Melekestsev, I. Large debris avalanches and associated eruptions in the Holocene eruptive history of Shiveluch Volcano, Kamchatka, Russia. Bull Volcanol 59, 490–505 (1998). https://doi-org.ezproxy.ugm.ac.id/10.1007/s004450050206

Pradjoko, E., Kusuma, T., Setyandito, O., Suroso, A., & Harianto, B. (2015). The Tsunami Run-up Assesment of 1977 Sumba Earthquake in Kuta, Center of Lombok, Indonesia. Procedia Earth and Planetary Science, 14, 9–16. https://doi.org/10.1016/j.proeps.2015.07.079

Pratomo, I. (2006). Klasifikasi Gunung Api Aktif Indonesia, Studi Kasus Dari Beberapa Letusan Gunung Api Dalam Sejarah (Classification of Indonesian active volcano" case study from several historic eruptions). Indonesian Journal on Geoscience, 1(4), 209–227. https://doi.org/10.17014/ijog.1.4.209-227

Principe, C., Tanguy, J. C., Arrighi, S., Paiotti, A., Goff, M. Le, & Zoppi, U. (2004). Chronology of Vesuvius' activity from A.D. 79 to 1631 based on archeomagnetism of lavas and historical sources. Bulletin of Volcanology, 66(8), 703–724. https://doi.org/10.1007/s00445-004-0348-8

Procter, J. N., Zernack, A. V, & Cronin, S. J. (2021). Computer Simulation of a Volcanic Debris Avalanche from Mt. Taranaki, New Zealand BT - Volcanic Debris Avalanches: From Collapse to Hazard (Matteo Roverato, A. Dufresne, & J. Procter, Eds.). https://doi.org/10.1007/978-3-030-57411-6_11

Pröschel, B., & Lehmkuhl, F. (2019). Paleotopography and anthropogenic deposition thickness of the city of Aachen , Germany. 15(2), 269–277. https://doi.org/10.1080/17445647.2019.1590248

Pyle, D. M. (2017). What Can We Learn from Records of Past Eruptions to Better Prepare for the Future? In Advances in Volcanology (pp. 445–462). https://doi.org/10.1007/11157_2017_5

R

Rachmat, H., Rosana, M., Wirakusumah, A. D., & Jabbar, G. A. (2016). Petrogenesis of Rinjani post-1257 caldera-forming -eruption lava flows. Indonesian Journal of Geoscience, 3(2), 107–126. https://doi.org/10.17014/ijog.3.2.107-126

Ras, J. J. 1986. The Babad Tanah Jawi and its Reliability: Questions of Content, Structure and Function. In C. D. Grijns, S. O. Robson (Eds.), Cultural Contact and Textual Interpretation. Dordrecht & Cinnaminson: Foris Publications, pp: 246–273. https://doi.org/10.1163/9789004454170_019

Reid, Anthony. (2016). Revisiting Southeast Asian History with Geology: Some Demographic Consequences of a Dangerous Environment. In G. Bankoff & J. Christensen (Eds.), Natural Hazards and Peoples in the Indian Ocean World (Palgrave S, pp. 31–53). https://doi.org/10.1057/978-1-349-94857-4_2

Reid, M. E., Keith, T. E. C., Kayen, R. E., Iverson, N. R., Iverson, R. M., & Brien, D. L. (2010). Volcano collapse promoted by progressive strength reduction: New data from Mount St. Helens. Bulletin of Volcanology, 72(6), 761–766. https://doi.org/10.1007/s00445-010-0377-4

Retief, F. P., & Cilliers, L. (2005). The eruption of Vesuvius in AD 79 and the Death of Gaius Plinius Secundus. Acta Theologica, (SUPPL. 7), 107–114. https://doi.org/10.7445/42-2-190

Ricklefs, M. C. (2008). A History of Modern Indonesia Since c. 1200 (Fourth Edi). Palgrave Macmillan.

Ricklefs, M. C. (1998). Babad Sangkala and the Javanese Sense of History. Archipel, 55, 125–140. https//doi.org/10.3406/arch.1998.3445

Riede, F. (2019). Doing palaeo-social volcanology : Developing a framework for systematically investigating the impacts of past volcanic eruptions on human societies using archaeological datasets. Quaternary International, 499, 266–277. https://doi.org/10.1016/j.quaint.2018.01.027

Robson, S. O. (1995). Deśawarṇana by Prapañca (Mpu) (transl.). Leiden: KITLV Press.

Romero, J. E., Moreno, H., Polacci, M., Burton, M., & Guzmán, D. (2022). Mid-Holocene lateral collapse of Antuco volcano (Chile): debris avalanche deposit features, emplacement dynamics, and impacts. Landslides, 19(6), 1321–1338. https://doi.org/10.1007/s10346-022-01865-z

Roverato, M., Capra, L., Sulpizio, R., & Norini, G. (2011). Stratigraphic reconstruction of two debris avalanche deposits at Colima Volcano (Mexico): Insights into pre-failure conditions and climate influence. Journal of Volcanology and Geothermal Research, 207(1–2), 33–46. https://doi.org/10.1016/j.jvolgeores.2011.07.003

S

Salinas, S., & López-Blanco, J. (2010). Geomorphic assessment of the debris avalanche deposit from the Jocotitlán volcano, Central Mexico. Geomorphology, 123(1–2), 142–153. https://doi.org/10.1016/j.geomorph.2010.07.006

Sastrawan, W. J. (2022). Portents of Power: Natural Disasters throughout Indonesian History. Indonesia, 113, 9–32.

Schaefer, L. N., Kennedy, B. M., Villeneuve, M. C., Cook, S. C. W., Jolly, A. D., Keys, H. J. R., & Lenoard, G. S. (2018). Stability assessment of the Crater Lake Te Wai-a-moe channel at Mt. Ruapehu (New Zealand), and implications for volcanic lake break-out triggers. Journal of Volcanology and Geothermal Research, 358, 31–44.

Schmidt, J., Werther, L., & Zielhofer, C. (2018). Shaping pre-modern digital terrain models : The former topography at Charlemagne ' s canal construction site. PLoS ONE, 13(7), e0200167. Retrieved from https://doi.org/10.1371/journal.pone.0200167

Selles, A., Deffontaines, B., Hendrayana, H., & Violette, S. (2015). Journal of Asian Earth Sciences The eastern flank of the Merapi volcano (Central Java , Indonesia): Architecture and implications of volcaniclastic deposits. Journal of Asian Earth Sciences, 108, 33–47. https://doi.org/10.1016/j.jseaes.2015.04.026

Shea, T., van Wyk de Vries, B., & Pilato, M. (2008). Emplacement mechanisms of contrasting debris avalanches at Volcán Mombacho (Nicaragua), provided by structural and facies analysis. Bulletin of Volcanology, 70(8), 899–921. https://doi.org/10.1007/s00445-007-0177-7

Siebert, L. (2002). Landslide resulting from structural failure of volcanoes. In S. Evans & J. De Graff (Eds.), Catastrophic landslide: effects, occurrence, and mechanisms (pp. 209–235). Colorado: Geological Society of America Reviews in Engineering Geology.

Siebert, L. (1984). Large volcanic debris avalanches: Characteristics of source areas, deposits, and associated eruptions. Journal of Volcanology and Geothermal Research, 22(3–4), 163–197. https://doi.org/10.1016/0377-0273(84)90002-7

Siebert, L., Beget, J. E., & Glicken, H. (1995). The 1883 and late-prehistoric eruptions of Augustine volcano, Alaska. Journal of Volcanology and Geothermal Research, 66, 367–395.

Siebert, L., Cottrell, E., Venzke, E., & Edwards, B. (2015). Catalog of Earth's Documented Holocene Eruptions. In The Encyclopedia of Volcanoes (Second Edi). https://doi.org/10.1016/b978-0-12-385938-9.15002-3

Siebert, L., Glicken, H., & Ui, T. (1987). Volcanic hazards from Bezymianny- and Bandai-type eruptions. Bulletin of Volcanology, 49(1), 435–459. https://doi.org/10.1007/BF01046635

Siebert, L., & Roverato, M. (2021). A Historical Perspective on Lateral Collapse and Volcanic Debris Avalanches. In Matteo Roverato, A. Dufresne, & J. Procter (Eds.), Volcanic Debris Avalanches: From Collapse to Hazard (pp. 11–50). https://doi.org/10.1007/978-3-030-57411-6_2

Sigl, M., Winstrup, M., McConnell, J. R., Welten, K. C., Plunkett, G., Ludlow, F., … Woodruff, T. E. (2015). Timing and climate forcing of volcanic eruptions for the past 2,500 years. Nature, 523(7562), 543–549. https://doi.org/10.1038/nature14565

Sigl, M., McConnell, J. R., Layman, L., Maselli, O., McGwire, K., Pasteris, D., … Kipfstuhl, S. (2013). A new bipolar ice core record of volcanism from WAIS Divide and NEEM and implications for climate forcing of the last 2000 years. Journal of Geophysical Research Atmospheres, 118(3), 1151–1169. https://doi.org/10.1029/2012JD018603

Sigurdsson, H., Cashdollar, S., & Sparks, S. R. J. (1982). The Eruption of Vesuvius in A. D. 79: Reconstruction from Historical and Volcanological Evidence. American Journal of Archaeology, 86(1), 39. https://doi.org/10.2307/504292

Silva, P. G., López-Recio, M., Tapias, F., Roquero, E., Morín, J., Rus, I., … Pérez-López, R. (2013). Stratigraphy of the Arriaga Palaeolithic sites. Implications for the geomorphological evolution recorded by thickened fluvial sequences within the Manzanares River valley (Madrid Neogene Basin, Central Spain). Geomorphology, 196, 138–161. https://doi.org/10.1016/j.geomorph.2012.10.019

Solikhin, A., Kunrat, S., Barbier, B., & Campion, R. (2010). Geochemical and Thermodinamic Modeling of Segara Anak Lake and the 2009 Eruption of Rinjani Volcano , Lombok , Indonesia. Jurnal Geologi Indonesia, 5(4), 227–239.

Statistics. (2020). Nusa Tenggara Barat in Figures. Mataram: Bureau of Statistics.

Statistics. (2022). Mataram Municipality in Figures. Mataram: Bureau of Statistics (BPS).

Stothers, R. B. (2000). Climatic and demographic consequences of the massive volcanic eruption of 1258. Climatic Change, 45, 361–374.

Stuiver, M., Reimer, P. J., & Reimer, R. W. (2022). CALIB 8.2 [WWW program]. Retrieved from http://calib.org website: http://calib.org

Sudarmadji, S., Suprayogi, S., Lestari, S., & Malawani, M. N. (2019). Water quality and sustainability of Merdada Lake, Dieng, Indonesia. E3S Web of Conferences, 76. https://doi.org/10.1051/e3sconf/20197602003

Sudibyo. (2019). Letusan Gunung dan Persepsi Sang Pujangga: Kesaksian Teks Bima, Jawa, dan Melayu Abad ke-19 (Volcano eruption and poet perception: Eyewitness account from Bima, Java, and Malay Text in 19th century). Manuskripta, 9(1), 97–111.

Suhendro, I., Mutaqin, B. W., Sobaruddin, D. P., Agustiningtyas, L., Humaida, H., Marfai, M. A., & Hadmoko, D. S. (2022). Dynamics of Two Caldera-Forming Eruptions (Banda Besar and Naira) in the Marine Conservation Zone of Banda, Maluku, Indonesia. Geosciences, Vol. 12. https://doi.org/10.3390/geosciences12110428

Sukandi. (2017). Resistivity measurement for mapping groundwater potential at praya regional general hospital (in bahasa). Sangkareang, 3(3), 66–71.

Sumita, M., & Schmincke, H. U. (2013). Impact of volcanism on the evolution of Lake Van I: Evolution of explosive volcanism of Nemrut Volcano (eastern Anatolia) during the past >400,000 years. Bulletin of Volcanology, 75(5), 1–32. https://doi.org/10.1007/s00445-013-0714-5

Suparman, L. G. (1994). Babad Lombok. Jakarta: Department of Education and Culture.

Syifa, M., Kadavi, P. R., Lee, C. W., & Pradhan, B. (2018). Landsat images and artificial intelligence techniques used to map volcanic ashfall and pyroclastic material following the eruption of Mount Agung, Indonesia. Arabian Journal of Geosciences, 13(133).

T

Tagawa, H. (1992). Primary succession and the effect of first arrivals on subsequent development of forest types. GeoJournal, 28, 175–183. Retrieved from https://doi.org/10.1007/BF00177231

Tang, M., Liu-Zeng, J., Hoke, G. D., Xu, Q., Wang, W., Li, Z., … Wang, W. (2017). Paleoelevation reconstruction of the Paleocene-Eocene Gonjo basin, SE-central Tibet. Tectonophysics, 712–713, 170–181. https://doi.org/10.1016/j.tecto.2017.05.018

Teltscher, K., & Fassnacht, F. E. (2018). Using multispectral landsat and sentinel-2 satellite data to investigate vegetation change at Mount St. Helens since the great volcanic eruption in 1980. Journal of Mountain Science, 15(9), 1851–1867. https://doi.org/10.1007/s11629-018-4869-6

Temme, A. J. A. M., Armitage, J., Attal, M., van Gorp, W., Coulthard, T. J., & Schoorl, J. M. (2017). Developing, choosing and using landscape evolution models to inform field-based landscape reconstruction studies. Earth Surface Processes and Landforms, 42(13), 2167–2183. https://doi.org/https://doi.org/10.1002/esp.4162

Temme, A. J. A. M., Peeters, I., Buis, E., Veldkamp, A., & Govers, G. (2011). Comparing landscape evolution models with quantitative field data at the millennial time scale in the Belgian loess belt. Earth Surface Processes and Landforms, 36(10), 1300–1312. https://doi.org/https://doi.org/10.1002/esp.2152

Teeuw, A. 1958. Lombok: Een Dialect-Geografische Studie. 'S-Gravenhage: Martinus Nijhoff

Tennant, E., Jenkins, S. F., Winson, A., Widiwijayanti, C., Gunawan, H., Haerani, N., … Triastuti, H. (2021). Reconstructing eruptions at a data limited volcano: A case study at Gede (West Java). Journal of Volcanology and Geothermal Research, 107325. https://doi.org/https://doi.org/10.1016/j.jvolgeores.2021.107325

Thouret, J. C., & Lavigne, F. (2000). Lahars: occurrence, deposits and behaviour of volcano- hydrologic flows. In H. Leyrit & C. Montenat (Eds.), Volcaniclastic rocks from magmas to sediments (pp. 151–174). Gordon and Breach Science Publishers.

Thouret, Jean Claude, Oehler, J. F., Gupta, A., Solikhin, A., & Procter, J. N. (2014). Erosion and aggradation on persistently active volcanoes—a case study from Semeru Volcano, Indonesia. Bulletin of Volcanology, 76(10). https://doi.org/10.1007/s00445-014-0857-z

Tjandrasasmita, U. (2000). Development of the moslem cities in Indonesia from the thirteenth to eighteenth centuries. (Pertumbuhan dan perkembangan kota-kota muslim di Indonesia dari abad XIII sampai XVIII Masehi). Kudus: Menara Kudus (in Indonesian)

Tibaldi, A. (2001). Multiple sector collapses at Stromboli volcano, Italy: How they work. Bulletin of Volcanology, 63(2–3), 112–125. https://doi.org/10.1007/s004450100129

Todesco, M., & Todini, E. (2004). Volcanic eruption induced floods. A rainfall-runoff model applied to the Vesuvian Region (Italy). Natural Hazards, 33(2), 223–245. https://doi.org/10.1023/B:NHAZ.0000037039.35228.c0

Toy, T. J., & Chuse, W. R. (2005). Topographic reconstruction: a geomorphic approach. Ecological Engineering, 24(1), 29–35. https://doi.org/https://doi.org/10.1016/j.ecoleng.2004.12.014

Trigo, R. M., Vaquero, J. M., & Stothers, R. B. (2010). Witnessing the impact of the 1783-1784 Laki eruption in the Southern Hemisphere. Climatic Change, 99(3), 535–546. https://doi.org/10.1007/s10584-009-9676-1

Troll, V. R., Deegan, F. M., Jolis, E. M., Budd, D. A., Dahren, B., & Schwarzkopf, L. M. (2015). Ancient oral tradition describes volcano–earthquake interaction at merapi volcano, indonesia. Geografiska Annaler: Series A, Physical Geography, 97(1), 137–166. https://doi.org/10.1111/geoa.12099

Tsuyuzaki, S. (2019). Vegetation changes from 1984 to 2008 on Mount Usu, northern Japan, after the 1977–1978 eruptions. Ecological Research, 34(6), 813–820. https://doi.org/10.1111/1440-1703.12045

U

Ui, T. (1989). Discrimination Between Debris Avalanches and Other Volcaniclastic Deposits. In J. H. Letter (Ed.), AVCEI Proceedings in Volcanology. Springer-Verlag Berlin Heidelberg .

Ui, Tadahide, Yamamoto, H., & Suzuki-Kamata, K. (1986). Characterization of debris avalanche deposits in Japan. Journal of Volcanology and Geothermal Research, 29, 231–243.

Ullmann, T., Lange-Athinodorou, E., Göbel, A., Büdel, C., & Baumhauer, R. (2019). Preliminary results on the paleo-landscape of Tell Basta /Bubastis (eastern Nile delta): An integrated approach combining GIS-Based spatial analysis, geophysical and archaeological investigations. Quaternary International, 511, 185–199. https://doi.org/10.1016/j.quaint.2017.12.053

Ulusoy, İ., Sarıkaya, M. A., Schmitt, A. K., Şen, E., Danišík, M., & Gümüş, E. (2019). Volcanic eruption eye-witnessed and recorded by prehistoric humans. Quaternary Science Reviews, 212, 187–198. https://doi.org/10.1016/j.quascirev.2019.03.030

V

Valverde, V., Mothes, P. A., Beate, B., & Bernard, J. (2021). Enormous and far-reaching debris avalanche deposits from Sangay volcano (Ecuador): Multidisciplinary study and modeling the 30 ka sector collapse. 411.

van der Kraan, A. (1997). Lombok under the Mataram Dynasty, 1839–94. In A. Reid (Ed.), The Last Stand of Asian Autonomies. Studies in the Economies of East and South-East Asia. Retrieved from https://doi.org/10.1007/978-1-349-25760-7_16

Van Der Meij, D. (2011). Satra Sasak Selayang Pandang. Jurnal Manassa Manuskripta, 1(1), 17–45.

van der Meij, D. (2017). Indonesian Manuscripts from the Islands of Java, Madura, Bali and Lombok. Leiden, The Netherlands: Brill. https://doi.org/10.1163/9789004348110

van der Meij, M., Temme, A. J. A. M., Wallinga, J., & Sommer, M. (2020). change on soil and landscape patterns Modeling soil and landscape evolution – the effect of

rainfall and land-use change on soil and landscape patterns. Soil, 6, 337–358. https://doi.org/10.5194/soil-6-337-2020

van der Meij, W. M., Temme, A. J. A. M., Wallinga, J., Hierold, W., & Sommer, M. (2017). Topography reconstruction of eroding landscapes – A case study from a hummocky ground moraine (CarboZALF-D). Geomorphology, 295, 758–772. https://doi.org/https://doi.org/10.1016/j.geomorph.2017.08.015

van Wyk de Vries, B., & Davies, T. (2015). Chapter 38 - Landslides, Debris Avalanches, and Volcanic Gravitational Deformation. In H. Sigurdsson (Ed.), The Encyclopedia of Volcanoes (Second Edition) (pp. 665–685). https://doi.org/https://doi.org/10.1016/B978-0-12-385938-9.00038-9

Verbeek, R. D. M. (1884). The Krakatoa Eruption. Nature, 30(757), 10–15. https://doi.org/10.1038/030010a0

Vermeer, J. A. M., Finke, P. A., Zwertvaegher, A., Gelorini, V., Bats, M., Antrop, M., … Crombé, P. (2014). Reconstructing a prehistoric topography using legacy point data in a depositional environment. 645(September 2013), 632–645. https://doi.org/10.1002/esp.3472

Vezzoli, L., Apuani, T., Corazzato, C., & Uttini, A. (2017). Geological and geotechnical characterization of the debris avalanche and pyroclastic deposits of Cotopaxi Volcano (Ecuador). A contribute to instability-related hazard studies. Journal of Volcanology and Geothermal Research, 332, 51–70. https://doi.org/10.1016/j.jvolgeores.2017.01.004

Vidal, C. M., Komorowski, J. C., Métrich, N., Pratomo, I., Kartadinata, N., Prambada, O., … Surono. (2015). Dynamics of the major plinian eruption of Samalas in 1257 A.D. (Lombok, Indonesia). Bulletin of Volcanology, 77(9). https://doi.org/10.1007/s00445-015-0960-9

Vidal, C. M., Métrich, N., Komorowski, J. C., Pratomo, I., Michel, A., Kartadinata, N., … Lavigne, F. (2016). The 1257 Samalas eruption (Lombok, Indonesia): The single greatest stratospheric gas release of the Common Era. Scientific Reports, 6(October). https://doi.org/10.1038/srep34868

Ville, A., Lavigne, F., Virmoux, C., Brunstein, D., De Bélizal, E., Wibowo, S. B., & Hadmoko, D. S. (2015). Evolution géomorphologique de la vallée de la Gendol à la suite de l'éruption d'octobre 2010 du volcan Merapi (Java, Indonésie). Geomorphologie: Relief, Processus, Environnement, 21(3), 235–250. https://doi.org/10.4000/geomorphologie.11073

Vogel, S., & Märker, M. (2010). Reconstructing the Roman topography and environmental features of the Sarno River Plain (Italy) before the AD 79 eruption

of Somma-Vesuvius. Geomorphology, 115(1–2), 67–77. https://doi.org/10.1016/j.geomorph.2009.09.031

Vogel, S., & Märker, M. (2011). Characterization of the pre-AD 79 Roman paleosol south of Pompeii (Italy): Correlation between soil parameter values and paleo-topography. Geoderma, 160(3–4), 548–558. https://doi.org/10.1016/j.geoderma.2010.11.003

Vogel, S., & Märker, M. (2012). Comparison of pre-AD 79 Roman paleosols in two contrasting paleo-topographical situations around Pompeii (Italy). Geografia Fisica e Dinamica Quaternaria, 35(2), 199–209. https://doi.org/10.4461/GFDQ.2012.35.18

Vogel, S., & Märker, M. (2013). Modeling the spatial distribution of AD 79 pumice fallout and pyroclastic density current and derived deposits of Somma-Vesuvius (Campania, Italy) integrating primary deposition and secondary redistribution. Bulletin of Volcanology, 75(12), 1–15. https://doi.org/10.1007/s00445-013-0778-2

Vogel, S., Märker, M., & Seiler, F. (2011). Revised modelling of the post-AD 79 volcanic deposits of Somma-Vesuvius to reconstruct the pre-AD 79 topography of the Sarno River plain (Italy). Geologica Carpathica, 62(1), 5–16. https://doi.org/10.2478/v10096-011-0001-3

Voight, B., Janda, R. J., & Glicken, H. (1983). Nature and mechanics of the mount St Helens rockslide avalanche of 18 May 1980. Geotechnique, 33(3), 243–273. https://doi.org/10.1016/0148-9062(83)90666-6

Voight, B., Janda, R. J., H, & Glicken†, and P. M. D. (1985). Nature and mechanics of the Mount St Helens rockslide-avalanche of 18 May 1980. Geotechnique, 35(3), 357–368. https://doi.org/10.1680/geot.1985.35.3.357

W

Warsini, S., Buettner, P., Mills, J., West, C., & Usher, K. (2014). The Psychosocial Impact of the Environmental Damage Caused by the MT Merapi Eruption on Survivors in Indonesia. EcoHealth, 11(4), 491–501. https://doi.org/10.1007/s10393-014-0937-8

Waythomas, C. F. (2015). Geomorphic consequences of volcanic eruptions in Alaska: A review. Geomorphology, 246, 123–145. https://doi.org/10.1016/j.geomorph.2015.06.004

Waythomas, C. F., & Neal, C. A. (1998). Tsunami generation by pyroclastic flow during the 3500-year B.P. caldera-forming eruption of Aniakchak volcano, Alaska. Bulletin of Volcanology, 60(2), 110–124. https://doi.org/10.1007/s004450050220

Werbrouck, I., Antrop, M., Van Eetvelde, V., Stal, C., De Maeyer, P., Bats, M., … Zwertvaegher, A. (2011). Digital Elevation Model generation for historical

landscape analysis based on LiDAR data, a case study in Flanders (Belgium). Expert Systems with Applications, 38(7), 8178–8185. https://doi.org/10.1016/j.eswa.2010.12.162

Wibowo, S. B., Hadmoko, D. S., Isnaeni, Y., Farda, N. M., Febri, A., Putri, S., … Supangkat, S. H. (2021). Spatio-Temporal Distribution of Ground Deformation Due to 2018 Lombok Earthquake Series.

Wiranata, A., Soekarno, S., & Suroso, A. (2018). Estimation Of Groundwater Potential With Geoelectric Method In Central Lombok Regency (in Bahasa). In Artikel Ilmiah (Unpublished thesis). Mataram: Civil Engineering, Universitas Mataram.

Wronna, M., Baptista, M. A., & Götz, J. (2017). On the construction and use of a Paleo-DEM to reproduce tsunami inundation in a historical urban environment–the case of the 1755 Lisbon tsunami in Cascais. Geomatics, Natural Hazards and Risk, 8(2), 841–862. https://doi.org/10.1080/19475705.2016.1271832

Y

Yamamoto, T., Nakamura, Y., & Glicken, H. (1999). Pyroclastic density current from the 1888 phreatic eruption of Bandai volcano, NE Japan. Journal of Volcanology and Geothermal Research, 90(3–4), 191–207. https://doi.org/10.1016/S0377-0273(99)00025-6

Yoshida, H. (2013). Decrease of size of hummocks with downstream distance in the rockslide-debris avalanche deposit at Iriga volcano, Philippines: Similarities with Japanese avalanches. Landslides, 10(5), 665–672. https://doi.org/10.1007/s10346-013-0414-4

Yoshida, H. (2014). Hummock alignment in Japanese volcanic debris avalanches controlled by pre-avalanche slope of depositional area. Geomorphology, 223, 67–80. https://doi.org/10.1016/j.geomorph.2014.06.024

Yoshida, H., Sugai, T., & Ohmori, H. (2012). Geomorphology Size – distance relationships for hummocks on volcanic rockslide-debris avalanche deposits in Japan. Geomorphology, 136(1), 76–87. https://doi.org/10.1016/j.geomorph.2011.04.044

Z

Zaennudin, A. (2010). The characteristic of eruption of indonesian active volcanos in the last four decades. Jurnal Ling. Dan Benc. Geol., 1(2), 113–129.

Zubaidah, T. (2010). Spatio-temporal characteristics of the geomagnetic field over the Lombok Island, the Lesser Sunda Islands region: New geological, tectonic, and seismo-electromagnetic insights along the Sunda-Banda Arcs transition (Deutsche

GeoForschungsZentrum GFZ). Retrieved from https://doi.org/10.2312/GFZ.b103-10079

Zubaidah, Teti, Korte, M., Mandea, M., & Hamoudi, M. (2014). New insights into regional tectonics of the Sunda – Banda Arcs region from integrated magnetic and gravity modelling. Journal of Asian Earth Sciences, 80, 172–184. https://doi.org/10.1016/j.jseaes.2013.11.013

LIST OF FIGURES

LIST OF TABLES

APPENDIX A

Table A.1. Inverted resistivity cross-sections of the debris avalanche deposit

Location	Resistivity Cross-section
Jenggik 1 Interpretation: DAD formed a stratum at a depth of >8 m, overlain by reworked material.	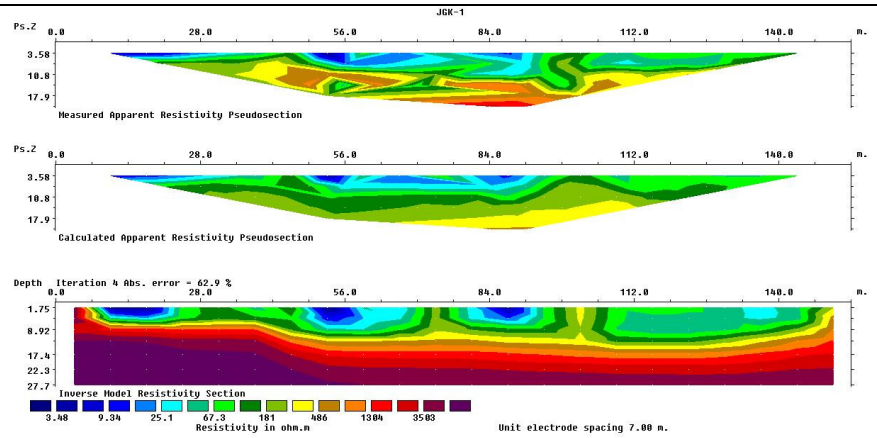
Jenggik 2 Interpretation: DAD contain water (low resistivity). This is typical of intra-hummock bedding.	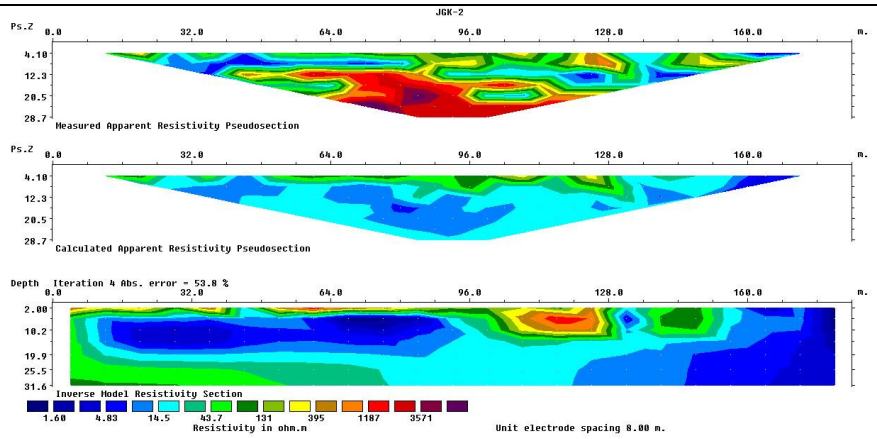
Jenggik 3 Interpretation: The boundary between hummock and intra-hummock is visible on this line. Intra-hummock has a lower resistivity due to water content.	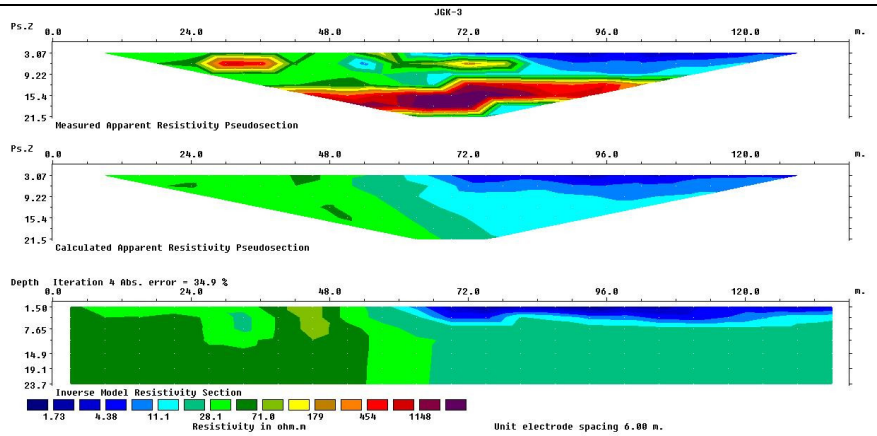

Location	Resistivity Cross-section
Janapria 1 Interpretation: DAD formed a stratum at a depth of >12 m, overlain by reworked material.	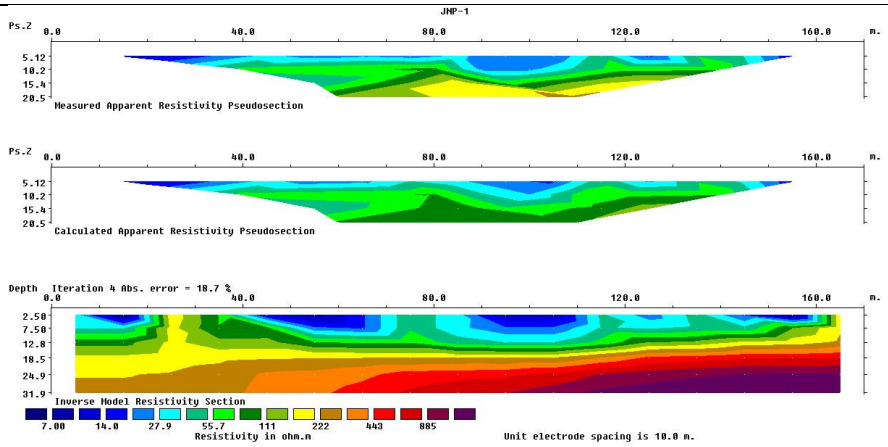
Janapria 2 Interpretation: DAD formed a stratum at a depth of >10 m, overlain by reworked material.	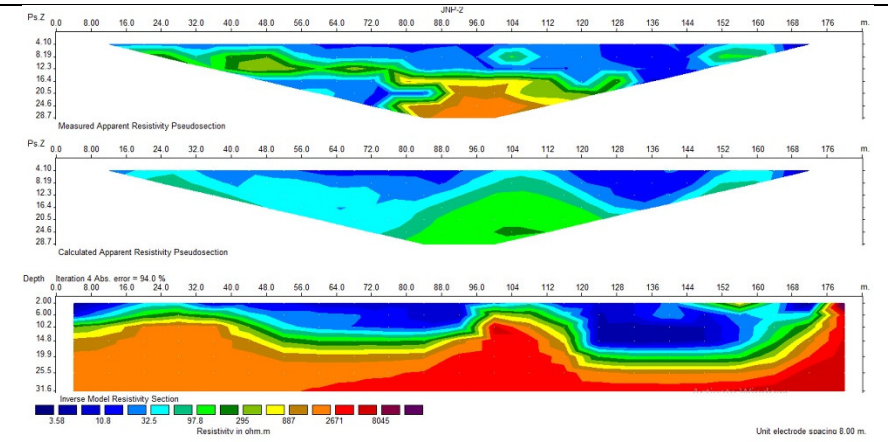
Janapria 3 Interpretation: The boundary of the DAD layer is at a depth of ~20 m. This region is close to the front of the DAD and thus the thickness is decreased.	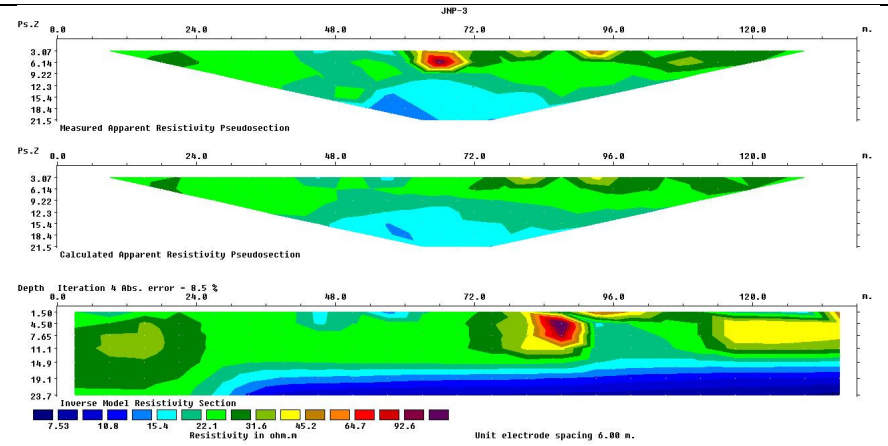

Location	Resistivity Cross-section
Kwang Wai 1 Interpretation: The hummock has a unique resistivity profile. Hummock at this location is up to 25 m thick.	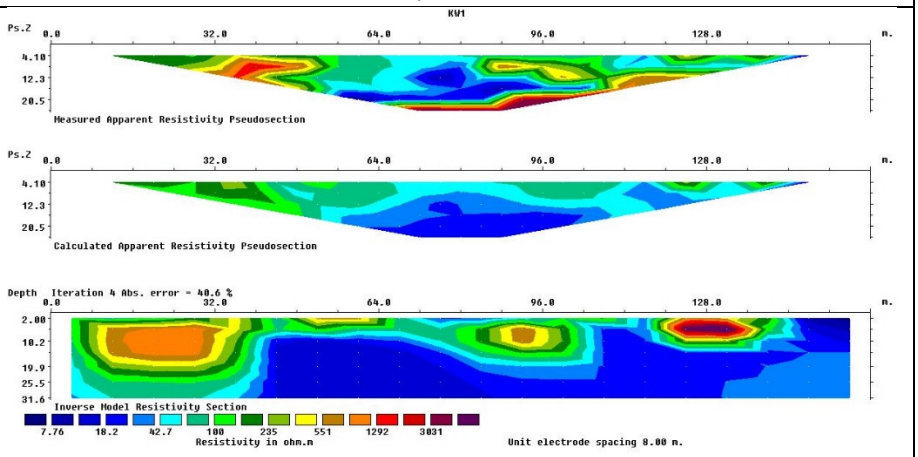
Kwang Wai 2 Interpretation: Because it is located in a very distal part, the DAD layer is obscured and mixed with other materials as it is affected by marine and fluvial processes.	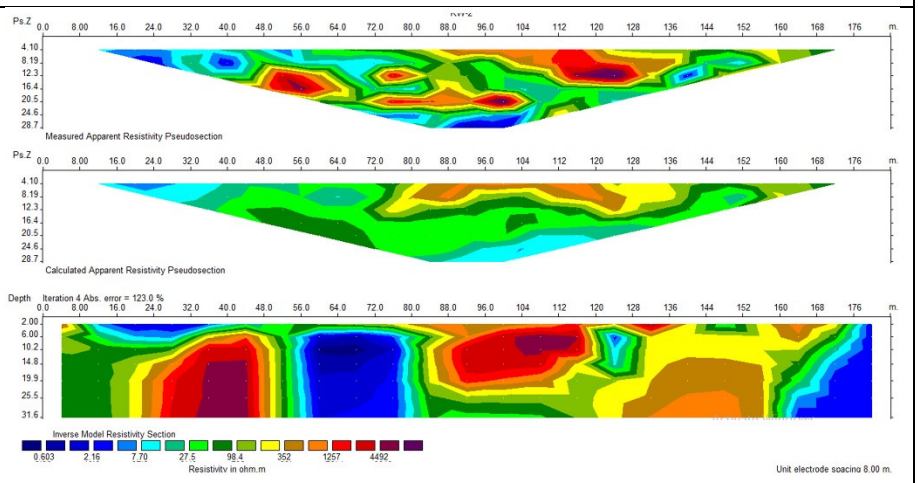

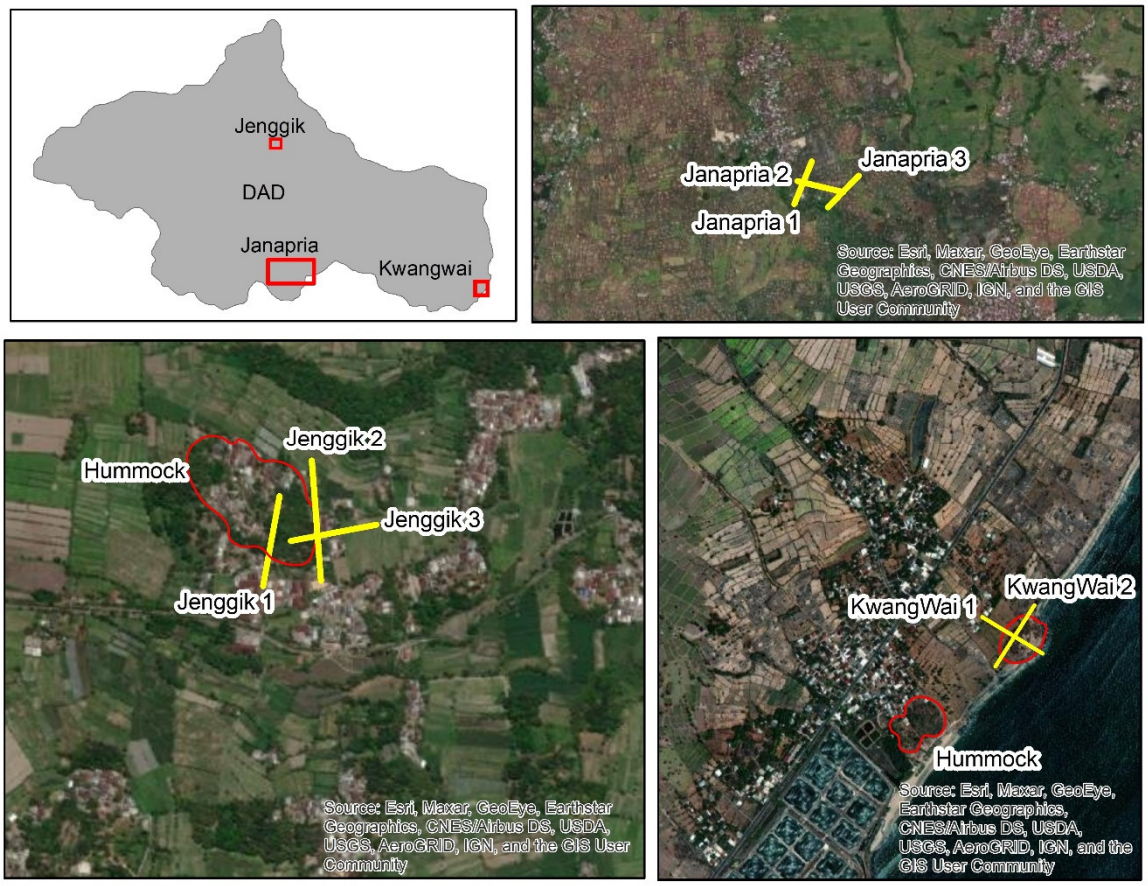

Figure A.1. Map of resistivity measurements

Table A.2. VolcFlow Simulation (performed by K. Kelfoun)

No	Result (snapshot and video)
1	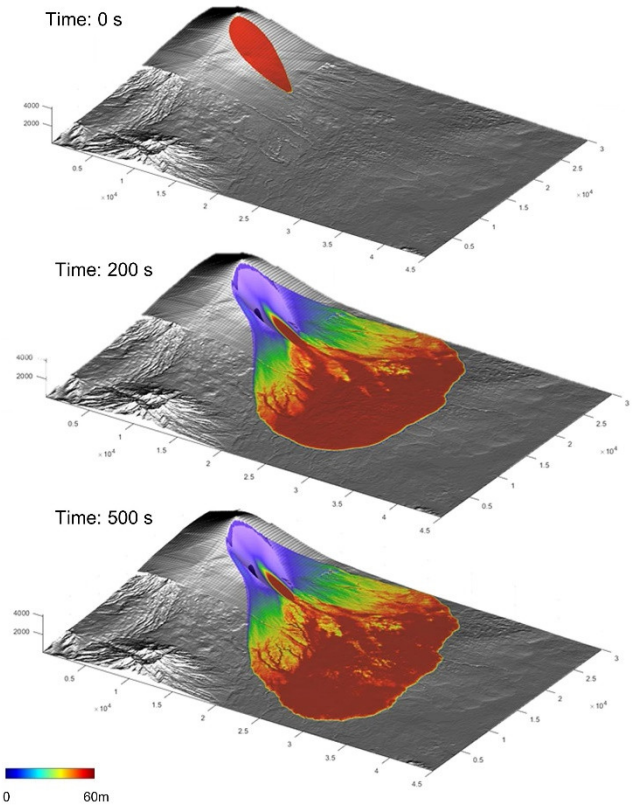 Link to video: https://drive.google.com/file/d/1mZvaUVEUJDY6YQLPrLf-9Grv-a7hzlKH/view?usp=share_link
2	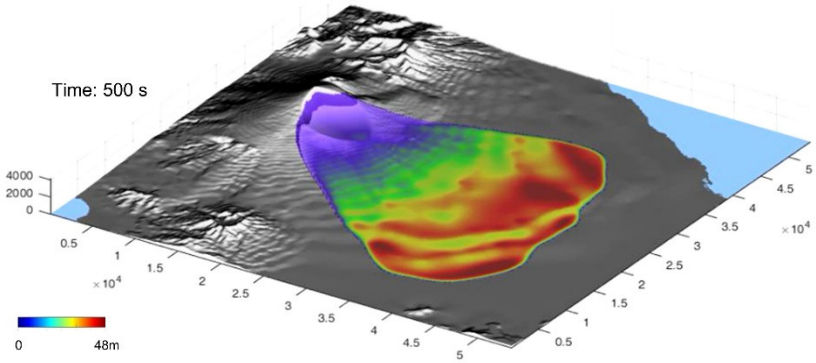 Link to video: https://drive.google.com/file/d/1q0d2XJdDBlfZfvswnQfUkBM12OKacVVa/view?usp=share_link

No	Result (snapshot and video)
3	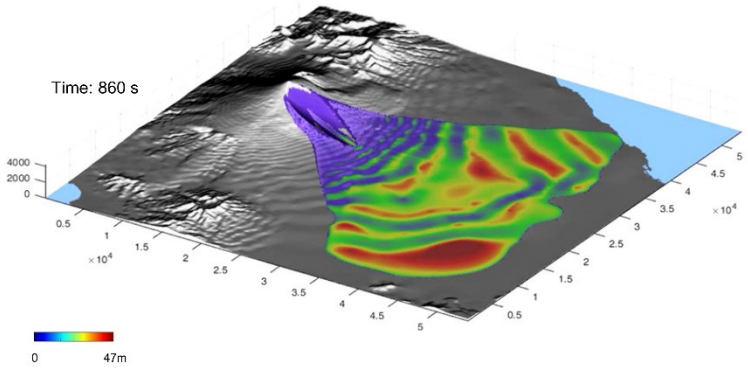 Link to video: https://drive.google.com/file/d/17LAi5-UnrZtLf9YN0A58WQ7uMW8UjhKz/view?usp=share_link
4	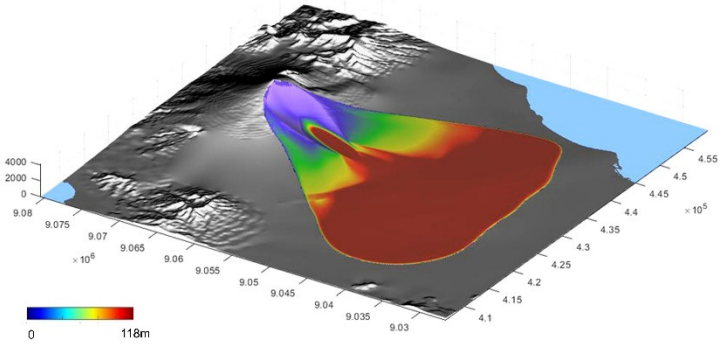 Link to video: https://drive.google.com/file/d/1pNK32KJJ1UvjxIeA6M4a5uN78ADWhjdb/view?usp=sharing

Table A.3. Calculation of debris avalanche velocity

Equation 1	Equation 2
$F = 100\ [1 - \left(\frac{h}{H}\right)^{0.5}\ ]$ $F = 100[1 - \left(\frac{28}{1700}\right)^{0.5}\ ]$ $F = 100[0.87]$ $F = 87$	$v\ = 10. \sqrt{\frac{2gh}{100 - F}}$ $v\ = 10. \sqrt{\frac{548}{13}}$ $v\ = 65\ m/s$

Table A4. Calibration of the radiocarbon ages

Paleosols and Sediments under DAD			
KW1 TOC Lab Code Description Radiocarbon Age BP 8620 +/- 330 Calibration data set: shcal20.14c # Hogg et al. 2020			
% area enclosed	cal AD age ranges		relative area under probability distribution
68.3 (1 sigma)	cal BC	8201- 8107	0.092
		8099- 8033	0.063
		8018- 7325	0.834
		7217- 7204	0.011
95.4 (2 sigma)	cal BC	8535- 8516	0.003
		8467- 6772	0.996
		6717- 6706	0.002
Median Probability: -7675			
KW2 Lab Code Description Radiocarbon Age BP 10380 +/- 300 Calibration data set: shcal20.14c # Hogg et al. 2020			
% area enclosed	cal AD age ranges		relative area under probability distribution
68.3 (1 sigma)	cal BC	10672- 9767	0.989
		9709- 9696	0.011
95.4 (2 sigma)	cal BC	10877- 10870	0.001
		10830- 9253	0.999
Median Probability:-10133			
KW3 Lab Code Description Radiocarbon Age BP 8070 +/- 500 Calibration data set: shcal20.14c # Hogg et al. 2020			
% area enclosed	cal AD age ranges		relative area under probability distribution
68.3 (1 sigma)	cal BC	7575- 7561	0.009
		7543- 6436	0.991
95.4 (2 sigma)	cal BC	8242- 5983	0.999
		5938- 5930	0.001
Median Probability: -7009			
KW3 TOC Lab Code Description Radiocarbon Age BP 13610 +/- 90			

```
 Calibration data set: shcal20.14c                  # Hogg et al.
2020
   % area enclosed       cal AD age ranges             relative area
under
                                                      probability
distribution
   68.3 (1 sigma)     cal BC 14586- 14298                    1.000
   95.4 (2 sigma)     cal BC 14739- 14124                    1.000
   Median Probability:-14439
```

```
KD
 Lab Code
 Description
 Radiocarbon Age BP  14940 +/-   90
 Calibration data set: shcal20.14c                  # Hogg et al.
2020
   % area enclosed       cal AD age ranges             relative area
under
                                                      probability
distribution
   68.3 (1 sigma)     cal BC 16336- 16167                    1.000
   95.4 (2 sigma)     cal BC 16660- 16545                    0.106
                             16362- 16005                    0.894
   Median Probability:-16264
```

```
KD TOC
 Lab Code
 Description
 Radiocarbon Age BP  13020 +/-   60
 Calibration data set: shcal20.14c                  # Hogg et al.
2020
   % area enclosed       cal AD age ranges             relative area
under
                                                      probability
distribution
   68.3 (1 sigma)     cal BC 13705- 13468                    1.000
   95.4 (2 sigma)     cal BC 13787- 13357                    1.000
   Median Probability:-13588
```

```
KP
 Lab Code
 Description
 Radiocarbon Age BP  11580 +/-  230
 Calibration data set: shcal20.14c                  # Hogg et al.
2020
   % area enclosed       cal AD age ranges             relative area
under
                                                      probability
distribution
   68.3 (1 sigma)     cal BC 11776- 11775                    0.001
                             11657- 11225                    0.999
   95.4 (2 sigma)     cal BC 12058- 11980                    0.020
                             11919- 11108                    0.968
                             11093- 11054                    0.009
                             11041- 11026                    0.003
   Median Probability:-11480
```

```
KP TOC
 Lab Code
 Description
 Radiocarbon Age BP  14750 +/-  130
```

Calibration data set: shcal20.14c # Hogg et al. 2020 % area enclosed cal AD age ranges relative area under probability distribution 68.3 (1 sigma) cal BC 16249- 15928 1.000 95.4 (2 sigma) cal BC 16302- 15587 1.000 Median Probability:-16052
KD 2017 Lab Code Description Radiocarbon Age BP 16490 +/- 50 Calibration data set: shcal20.14c # Hogg et al. 2020 % area enclosed cal AD age ranges relative area under probability distribution 68.3 (1 sigma) cal BC 18006- 17859 0.705 17767- 17683 0.295 95.4 (2 sigma) cal BC 18090- 17655 1.000 Median Probability:-17903
Paleosols above DAD
DAD1 Lab Code Description Radiocarbon Age BP 3080 +/- 30 Calibration data set: shcal20.14c # Hogg et al. 2020 % area enclosed cal AD age ranges relative area under probability distribution 68.3 (1 sigma) cal BC 1384- 1339 0.383 1317- 1258 0.512 1245- 1229 0.105 95.4 (2 sigma) cal BC 1412- 1199 0.990 1170- 1166 0.003 1140- 1133 0.007 Median Probability: -1300 DAD2 Lab Code Description Radiocarbon Age BP 4100 +/- 50 Calibration data set: shcal20.14c # Hogg et al. 2020 % area enclosed cal AD age ranges relative area under probability distribution 68.3 (1 sigma) cal BC 2842- 2814 0.125 2672- 2557 0.609 2541- 2490 0.259 2479- 2476 0.007 95.4 (2 sigma) cal BC 2866- 2803 0.143 2767- 2716 0.082

```
                              2706- 2468                        0.775
   Median Probability: -2616


DAD3
 Lab Code
 Description
 Radiocarbon Age BP   3120 +/-   50
 Calibration data set: shcal20.14c                  # Hogg et al.
2020
   % area enclosed       cal AD age ranges             relative area
under
                                                     probability
distribution
   68.3 (1 sigma)     cal BC 1413- 1280                         1.000
   95.4 (2 sigma)     cal BC 1490- 1484                         0.004
                             1451- 1200                         0.990
                             1169- 1166                         0.002
                             1140- 1133                         0.004
   Median Probability: -1336



DAD4
 Lab Code
 Description
 Radiocarbon Age BP   1635 +/-   30
 Calibration data set: shcal20.14c                  # Hogg et al.
2020
   % area enclosed       cal AD age ranges             relative area
under
                                                     probability
distribution
   68.3 (1 sigma)     cal AD 421- 479                           0.693
                             485- 498                           0.142
                             508- 523                           0.164
   95.4 (2 sigma)     cal AD 390- 399                           0.017
                             410- 542                           0.972
                             564- 571                           0.011
   Median Probability:   470
```

APPENDIX B

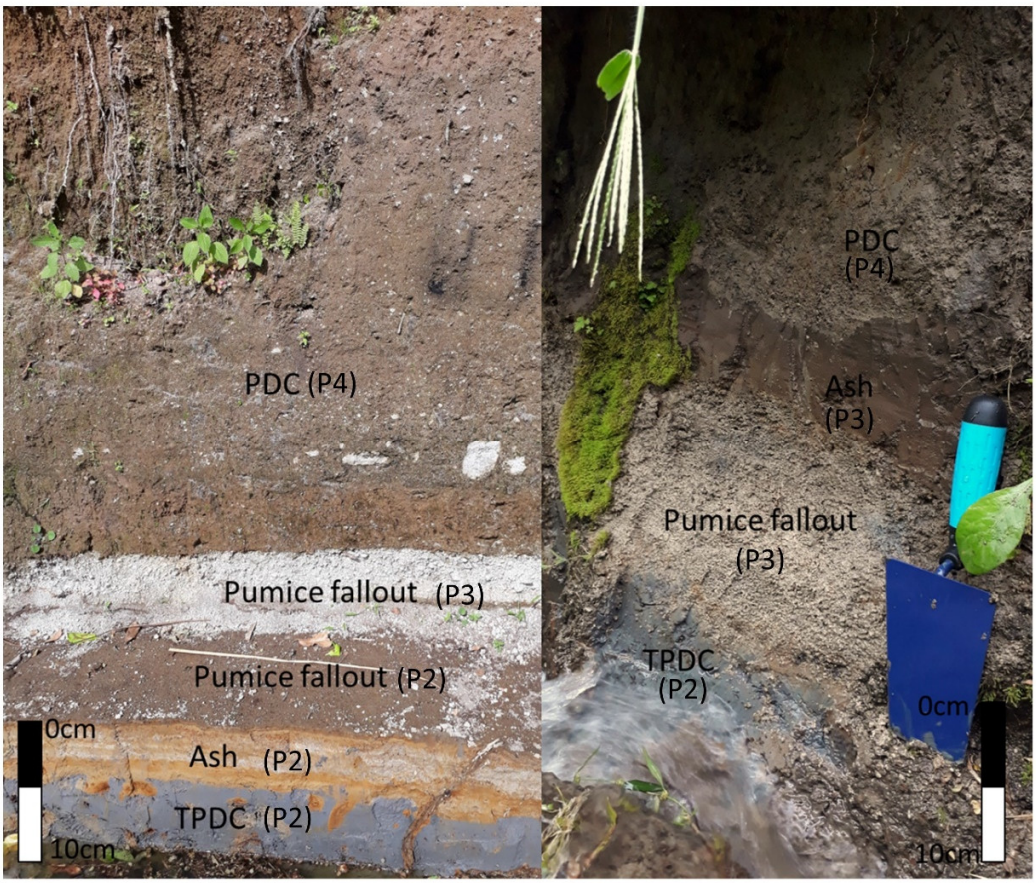

Figure B.1. (Left) Outcrop in Batukiliang near Babak river (middle-stream area) and (right) outcrop in Sandubaya near Jangkok river.

Table B.1. Inverted resistivity cross-sections of the Mataram Plain on the N-S and W-E direction.

Inverted resistivity cross-section in the N-S direction	
Sriwedari site	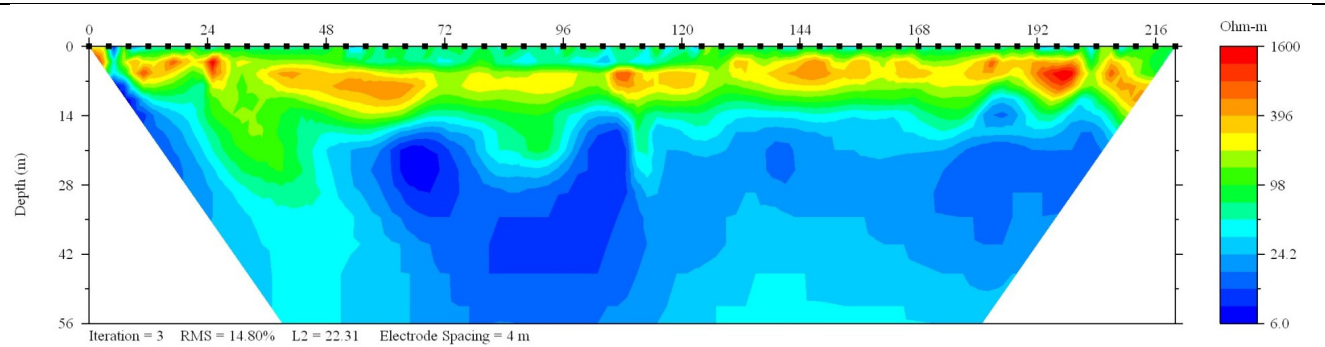
Rajawali site	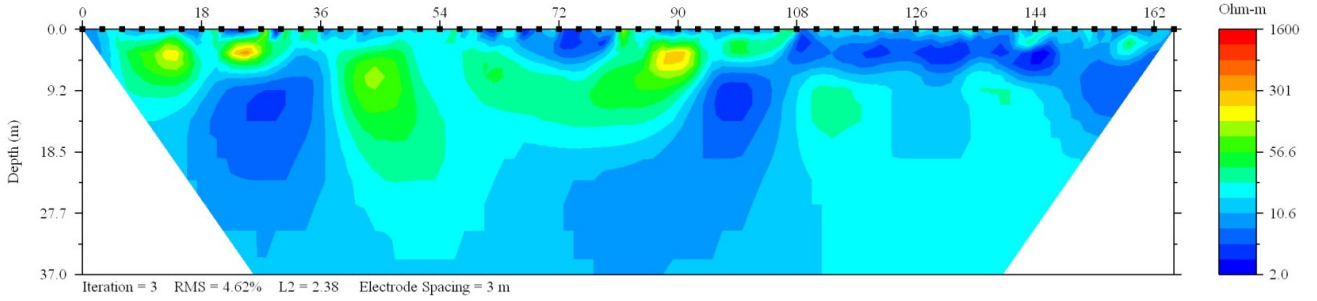

Umarmadi site	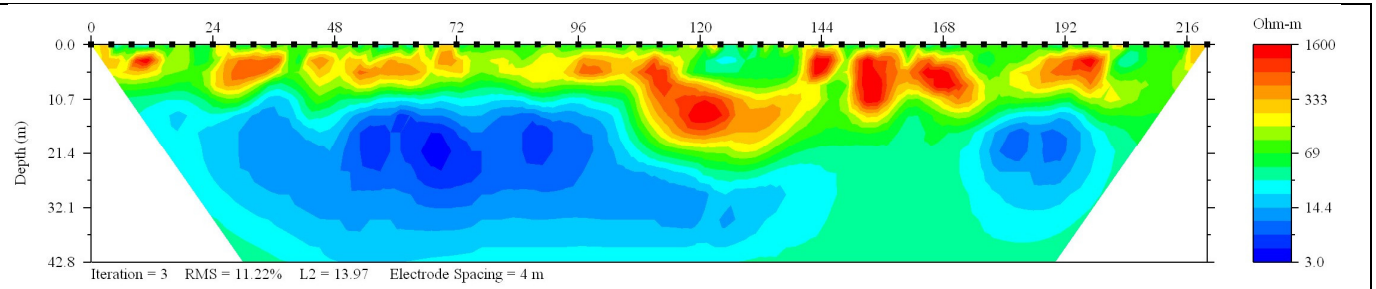
Prambanan site	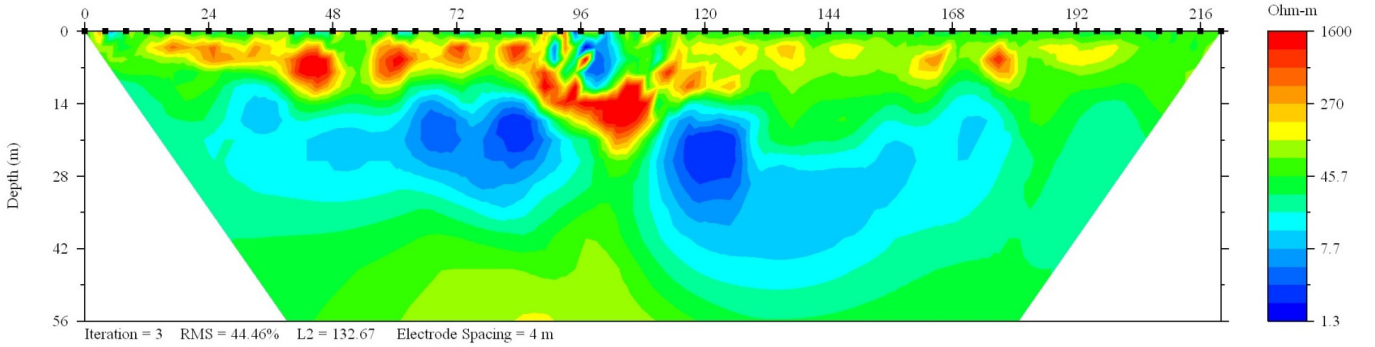
Selaparang NS	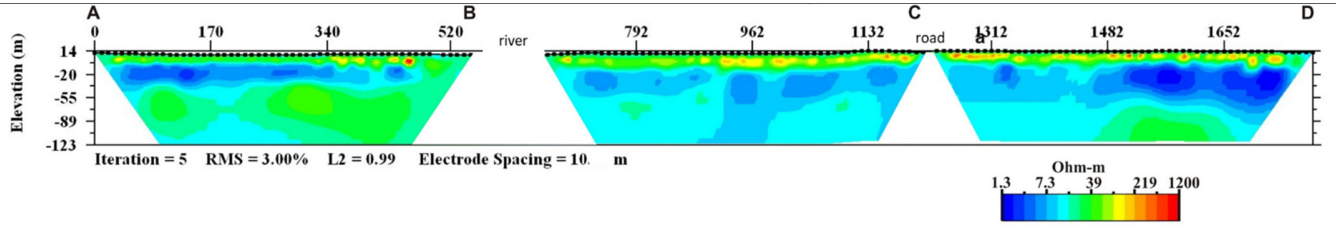

Monjok site	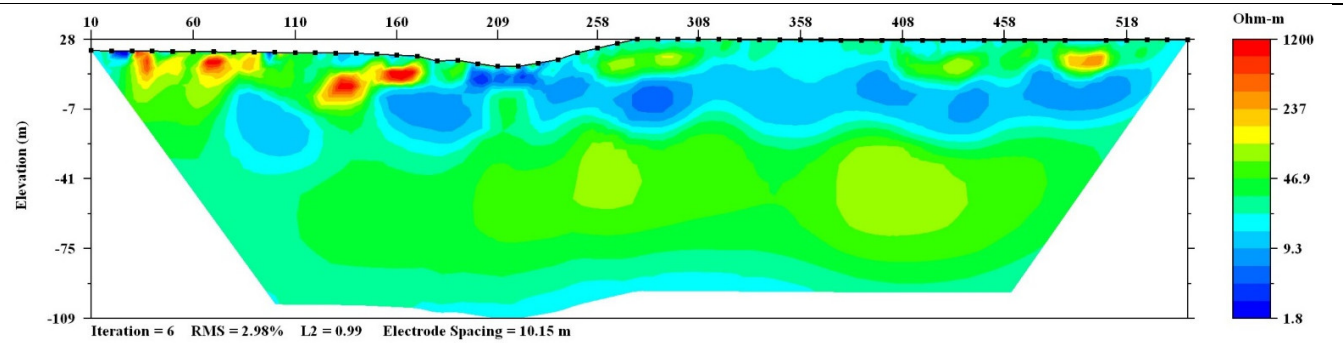
Inverted resistivity cross-section in the W-E direction	
Batudehe site	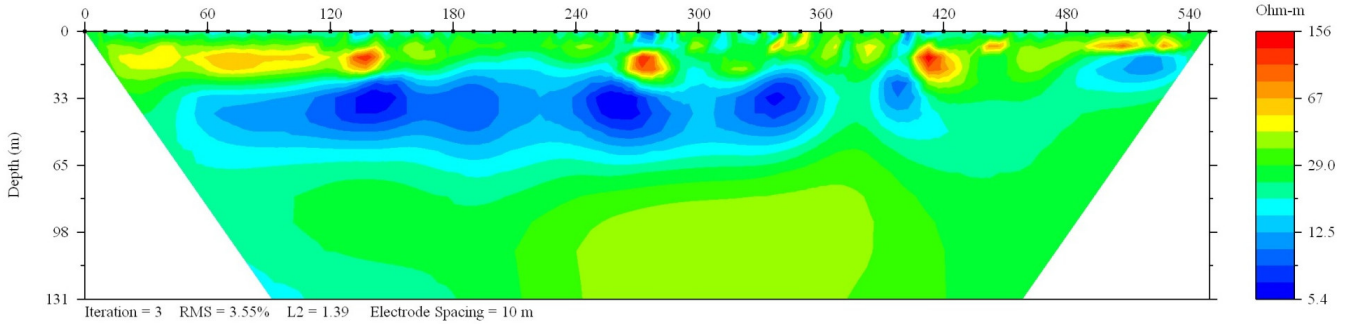

Lalumesir site	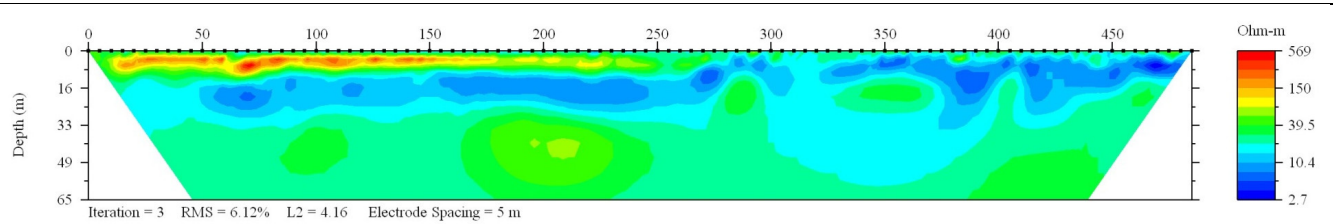

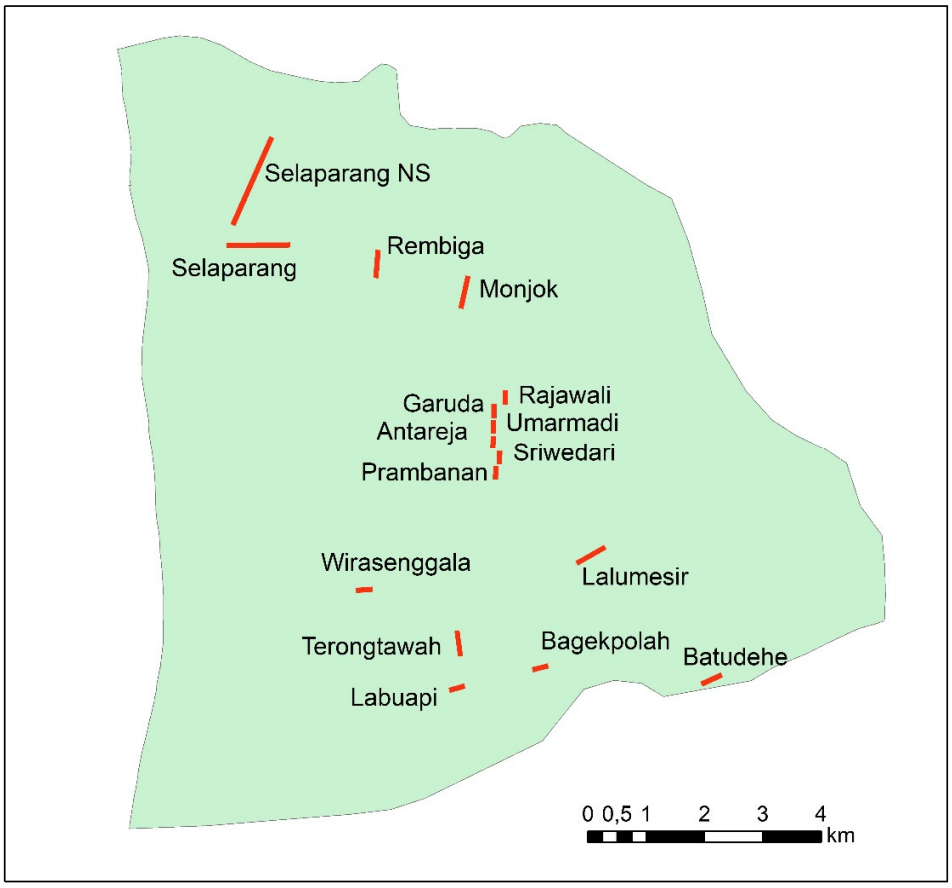

Figure B.2. Map of ERT measurements in the study area

Table B.2. Paleo-topographic points

X	Y	Present Elevation	Delta high	Paleo-elevation	Source	Name
407493	9050244	57,0	1,7	55,3	hand auger	Bertais
409277	9050045	86,0	2,1	83,9	hand auger	Kembangkuning
406433	9050940	44,0	2,4	41,6	hand auger	Pertanian
404315	9052360	34,1	0,6	33,5	coring	Jangkok
406707	9049350	40,0	0,8	39,2	coring	Mandalika
406144	9051609	50,0	5,0	45,0	coring	RS Harapan Keluarga
401810	9051248	15,7	5,6	10,1	coring	Hotel Santika
401129	9051474	12,7	9,0	3,7	coring	Islamic center
401848	9056638	37,0	1,6	35,4	outcorp	OC-3
401532	9056343	27,0	2,0	25,0	outcorp	OC-2
402213	9044501	14,5	2,5	12,0	outcorp	OC-1
404086	9054545	23,0	3,0	20,0	outcorp	OC-4
401585	9053513	15,8	6,7	9,1	outcorp	OC-5
403167	9052419	12,0	4,0	8,0	outcorp	OC-7
402276	9052938	12,5	5,0	7,5	outcorp	OC-6
406460	9050748	37,5	2,2	35,4	outcorp	OC-8
405669	9052196	37,0	2,3	34,8	outcorp	OC-9
402634	9054095	21,0	5,0	16,0	outcorp	OC-10
402534	9044512	17,1	6,0	11,1	outcorp	OC-11
401553	9044625	14,5	3,0	11,5	outcorp	OC-12
401782	9044509	14,0	3,5	10,5	outcorp	OC-13
402054	9052921	9,5	5,0	4,5	water-well	S01
400148	9048543	6,0	8,0	-2,0	drilling	BOR-1
401183	9045065	13,0	8,0	5,0	drilling	BOR-2
399109	9054755	5,3	10,7	-5,4	drilling	BOR-3
404884	9050574	31,0	4,3	26,7	water-well	S02
401966	9055570	12,0	1,0	11,0	water-well	P45
403711	9053693	27,0	1,0	26,0	water-well	P84
399942	9046744	5,5	1,0	4,5	water-well	P574
398706	9046636	2,5	1,0	1,5	water-well	P602
405049	9049862	34,3	1,0	33,3	water-well	P2104-18
402605	9045792	18,9	1,0	17,9	water-well	P2103-47
398573	9046909	2,2	1,5	0,7	water-well	P571
405740	9048414	25,5	1,5	24,0	water-well	P478
405024	9055209	34,5	1,5	33,0	water-well	S-1
404746	9055281	25,5	1,5	24,0	water-well	S-4
404512	9055627	31,5	1,5	30,0	water-well	S-5
406042	9050888	43,2	1,5	41,7	water-well	P2104-3

399145	9046844	6,3	1,5	4,8	water-well	P2103-52
399433	9054436	4,0	2,0	2,0	water-well	P57
402015	9054376	17,0	2,0	15,0	water-well	P62
401916	9056121	12,0	2,0	10,0	water-well	P21
403672	9055421	21,0	2,0	19,0	water-well	P34
402999	9054613	21,0	2,0	19,0	water-well	P64
405579	9054386	50,3	2,0	48,3	water-well	P69
403333	9053184	24,0	2,0	22,0	water-well	P115b
398274	9054768	3,0	2,0	1,0	water-well	P37
404595	9052895	36,0	2,0	34,0	water-well	P152
399734	9046603	6,8	2,0	4,8	water-well	P604
398861	9046206	4,5	2,0	2,5	water-well	P603
398336	9046631	2,3	2,0	0,3	water-well	P601
398215	9045749	3,5	2,0	1,5	water-well	P629
399619	9046007	6,0	2,0	4,0	water-well	P632
404477	9045729	21,0	2,0	19,0	water-well	P684
406940	9052132	62,0	2,0	60,0	water-well	P229
406692	9051020	50,0	2,0	48,0	water-well	P300
405633	9050521	32,0	2,0	30,0	water-well	P334
406615	9048353	37,0	2,0	35,0	water-well	P480
405553	9049830	36,5	2,0	34,5	water-well	P2104-19
405241	9049156	33,7	2,0	31,7	water-well	P2104-26
404557	9053111	40,2	2,0	38,2	water-well	P2104-39
403563	9050665	24,3	2,0	22,3	water-well	P2104-47
406282	9047552	34,9	2,0	32,9	water-well	P2104-58
402449	9048460	15,7	2,0	13,7	water-well	P2104-69
401616	9052436	10,9	2,0	8,9	water-well	P2103-12
399197	9051207	5,1	2,0	3,1	water-well	P2103-18
398522	9050829	4,0	2,0	2,0	water-well	P2103-19
400649	9048662	8,2	2,0	6,2	water-well	P2103-29
404018	9052705	27,4	2,0	25,4	water-well	P2103-40
401851	9046758	16,9	2,0	14,9	water-well	P2103-48
400855	9052248	8,9	2,0	6,9	water-well	P2103-9
406026	9051304	43,7	2,4	41,3	water-well	P2104-2
404856	9051288	35,2	2,4	32,8	water-well	P2104-8
399004	9054458	3,0	2,5	0,5	water-well	P56
398597	9054453	3,0	2,5	0,5	water-well	P55
402021	9055126	13,5	2,5	11,0	water-well	P31
403766	9053298	27,5	2,5	25,0	water-well	P115
403096	9053944	22,5	2,5	20,0	water-well	P83
404062	9053968	34,1	2,5	31,6	water-well	P85

399949	9045964	6,0	2,5	3,5	water-well	P633
405709	9054692	49,4	2,5	46,9	water-well	S-3
398774	9051670	4,6	2,5	2,1	water-well	P2103-16
399254	9055096	7,3	2,5	4,8	water-well	P2103-42
401844	9046156	15,1	2,5	12,6	water-well	P2103-50
399711	9051785	6,9	2,5	4,4	water-well	P2103-7
398673	9052340	3,7	3,0	0,7	water-well	P176
401535	9051382	13,7	3,0	10,7	water-well	P234
400044	9051419	8,1	3,0	5,1	water-well	P215
397674	9054250	1,0	3,0	-2,0	water-well	P53
397683	9056912	4,4	3,0	1,4	water-well	P0
400646	9054356	7,0	3,0	4,0	water-well	P59
404514	9051704	33,0	3,0	30,0	water-well	P224
404068	9051323	26,0	3,0	23,0	water-well	P259
398576	9045752	4,0	3,0	1,0	water-well	P630
407501	9050808	53,0	3,0	50,0	water-well	P302
405688	9050765	35,0	3,0	32,0	water-well	P298
407561	9050446	56,0	3,0	53,0	water-well	P338
407702	9049886	60,0	3,0	57,0	water-well	P374
407169	9048892	50,0	3,0	47,0	water-well	P445
406878	9048595	39,0	3,0	36,0	water-well	P481
405924	9048523	30,0	3,0	27,0	water-well	P479
406007	9047310	34,0	3,0	31,0	water-well	P551
405653	9047475	26,0	3,0	23,0	water-well	P550
406173	9047159	34,0	3,0	31,0	water-well	P586
406447	9047060	33,0	3,0	30,0	water-well	P587
404549	9045789	22,0	3,0	19,0	water-well	P642
403825	9054966	23,0	3,0	20,0	water-well	S-2
400974	9052283	8,7	3,0	5,7	water-well	P181
401542	9051550	13,6	3,0	10,6	water-well	P254
406411	9050896	45,8	3,0	42,8	water-well	P2104-1
405097	9050182	34,5	3,0	31,5	water-well	P2104-17
404055	9050174	27,1	3,0	24,1	water-well	P2104-28
406219	9050495	40,4	3,0	37,4	water-well	P2104-37
404183	9053089	37,8	3,0	34,8	water-well	P2104-38
404284	9051262	29,7	3,0	26,7	water-well	P2104-42
405144	9051648	41,8	3,0	38,8	water-well	P2104-43
404166	9048625	20,2	3,0	17,2	water-well	P2104-52
404264	9047672	26,4	3,0	23,4	water-well	P2104-55
404157	9048305	21,4	3,0	18,4	water-well	P2104-62
403560	9049821	20,7	3,0	17,7	water-well	P2104-66

402986	9048030	19,5	3,0	16,5	water-well	P2104-72
406497	9050287	43,7	3,0	40,7	water-well	P2104-73
398625	9052894	3,0	3,0	0,0	water-well	P2103-1
398962	9050252	3,7	3,0	0,7	water-well	P2103-21
399597	9049508	9,1	3,0	6,1	water-well	P2103-26
399448	9047673	5,4	3,0	2,4	water-well	P2103-27
403354	9049863	19,6	3,0	16,6	water-well	P2103-38
403629	9052968	26,1	3,0	23,1	water-well	P2103-39
399120	9051945	4,5	3,0	1,5	water-well	P2103-45
403273	9047194	22,3	3,0	19,3	water-well	P2103-49
403286	9045342	21,4	3,0	18,4	water-well	P2103-53
399966	9052613	7,5	3,5	4,0	water-well	P142
399192	9052243	3,8	3,5	0,3	water-well	P177
404087	9049301	22,6	3,5	19,1	water-well	P2104-30
405978	9050383	43,6	3,5	40,1	water-well	P2104-31
404937	9053313	43,9	3,5	40,4	water-well	P2104-40
404766	9049642	33,5	3,5	30,0	water-well	P2104-77
399031	9049331	4,5	3,5	1,0	water-well	P2103-25
399540	9053832	7,7	3,5	4,2	water-well	P2103-43
398452	9051349	3,0	4,0	-1,0	water-well	P248
400743	9052698	9,8	4,0	5,8	water-well	P145
402365	9054987	15,0	4,0	11,0	water-well	P46
401804	9055207	13,6	4,0	9,6	water-well	P30
401043	9055243	9,0	4,0	5,0	water-well	P29
401633	9056001	13,0	4,0	9,0	water-well	P28
404694	9054466	36,5	4,0	32,5	water-well	P67
405098	9053772	40,0	4,0	36,0	water-well	P87
400340	9052264	6,5	4,0	2,5	water-well	P179
400488	9052661	9,0	4,0	5,0	water-well	P144
399775	9051942	6,5	4,0	2,5	water-well	P214
401309	9052037	7,6	4,0	3,6	water-well	P217
398451	9057095	6,5	4,0	2,5	water-well	P2
399003	9056948	7,0	4,0	3,0	water-well	P3
400726	9056012	12,0	4,0	8,0	water-well	P18
400725	9056351	12,0	4,0	8,0	water-well	P11
401996	9052903	9,0	4,0	5,0	water-well	P147
402373	9052261	11,0	4,0	7,0	water-well	P184
404498	9052525	37,0	4,0	33,0	water-well	P188a
404490	9052601	37,3	4,0	33,3	water-well	P188b
405168	9052587	42,0	4,0	38,0	water-well	P189
403509	9051401	22,0	4,0	18,0	water-well	P258

403492	9050176	19,9	4,0	15,9	water-well	P330
404431	9051035	25,0	4,0	21,0	water-well	P296
397948	9045401	4,1	4,0	0,1	water-well	P653
398471	9045487	4,5	4,0	0,5	water-well	P654
399172	9044881	5,0	4,0	1,0	water-well	P674
398258	9044610	3,4	4,0	-0,6	water-well	P688
399188	9044449	6,0	4,0	2,0	water-well	P690
400413	9044774	11,0	4,0	7,0	water-well	P677
400316	9044673	11,4	4,0	7,4	water-well	P692
405718	9052451	50,0	4,0	46,0	water-well	P190
406632	9052143	58,0	4,0	54,0	water-well	P228
406984	9050991	51,0	4,0	47,0	water-well	P301
404436	9048962	19,6	4,0	15,6	water-well	P440
403954	9047971	19,0	4,0	15,0	water-well	P511
399788	9050003	5,2	4,0	1,2	water-well	731p
399235	9050575	5,5	4,0	1,5	water-well	741p
401779	9046978	14,4	4,0	10,4	water-well	759p
405377	9049926	37,1	4,0	33,1	water-well	P2104-14
404401	9050022	26,2	4,0	22,2	water-well	P2104-46
402976	9049279	17,4	4,0	13,4	water-well	P2104-49
402619	9047190	18,0	4,0	14,0	water-well	P2104-54
405255	9047433	29,2	4,0	25,2	water-well	P2104-57
406903	9050466	44,0	4,0	40,0	water-well	P2104-74
404718	9052210	37,0	4,0	33,0	water-well	P2104-82
401250	9050978	13,5	4,0	9,5	water-well	P2103-15
401296	9050195	14,1	4,0	10,1	water-well	P2103-20
401496	9048742	11,7	4,0	7,7	water-well	P2103-32
402239	9047604	15,9	4,0	11,9	water-well	P2103-34
403623	9049497	19,9	4,0	15,9	water-well	P2103-36
403894	9052195	27,6	4,0	23,6	water-well	P2103-44
400306	9051996	7,9	4,0	3,9	water-well	P2103-8
404135	9051978	33,4	4,5	28,9	water-well	P2104-32
405077	9051089	35,3	4,5	30,8	water-well	P2104-44
402413	9048938	14,3	4,5	9,8	water-well	P2104-68
400512	9051704	8,6	4,6	4,0	water-well	P2103-6
400794	9053138	11,3	5,0	6,3	water-well	P144
406159	9054113	52,0	5,0	47,0	water-well	P89
399574	9052219	6,1	5,0	1,1	water-well	P178
397845	9053608	2,0	5,0	-3,0	water-well	P103
397916	9055415	3,3	5,0	-1,7	water-well	P23
399061	9055535	4,5	5,0	-0,5	water-well	P25

402075	9052474	11,8	5,0	6,8	water-well	P183
402991	9051570	21,0	5,0	16,0	water-well	P257
402696	9051562	20,0	5,0	15,0	water-well	P256
402762	9050772	19,0	5,0	14,0	water-well	P292
404879	9050745	32,0	5,0	27,0	water-well	P297
402692	9049622	16,0	5,0	11,0	water-well	P400
399004	9045419	5,3	5,0	0,3	water-well	P655
400536	9044339	12,0	5,0	7,0	water-well	P693
404488	9045500	23,0	5,0	18,0	water-well	P666
402365	9050416	16,1	5,0	11,1	water-well	703p
401468	9050588	14,4	5,0	9,4	water-well	716p
400065	9050169	5,4	5,0	0,4	water-well	728p
398323	9048249	3,1	5,0	-1,9	water-well	764p
400736	9047694	11,3	5,0	6,3	water-well	765p
407673	9047703	49,0	5,0	44,0	water-well	669p
407823	9047842	50,0	5,0	45,0	water-well	671p
408950	9047087	62,0	5,0	57,0	water-well	682p
408431	9050363	63,0	5,0	58,0	water-well	700p
399252	9052921	5,1	5,0	0,1	water-well	P141
405409	9050535	38,2	5,0	33,2	water-well	P2104-12
406163	9049477	38,6	5,0	33,6	water-well	P2104-22
404135	9051497	31,4	5,0	26,4	water-well	P2104-33
406509	9048090	30,2	5,0	25,2	water-well	P2104-59
405706	9051497	48,3	5,0	43,3	water-well	P2104-6
404181	9052520	28,7	5,0	23,7	water-well	P2104-79
398613	9053289	3,6	5,0	-1,4	water-well	P2103-2
402675	9049345	15,6	5,0	10,6	water-well	P2103-46
402624	9045151	18,3	5,0	13,3	water-well	P2103-51
402624	9051130	20,2	5,0	15,2	water-well	P2103-56
398102	9051292	3,7	6,0	-2,3	water-well	P247
399694	9054081	6,7	6,0	0,7	water-well	P76
404069	9054876	24,5	6,0	18,5	water-well	P49
403036	9054697	21,0	6,0	15,0	water-well	P47
402683	9051727	20,0	6,0	14,0	water-well	P220
402956	9052323	17,0	6,0	11,0	water-well	P185
404432	9049604	21,9	6,0	15,9	water-well	P404
405030	9050241	32,2	6,0	26,2	water-well	P333
401928	9044826	14,7	6,0	8,7	water-well	P680
401028	9044816	13,6	6,0	7,6	water-well	P678
401098	9046009	11,5	6,0	5,5	water-well	P635
402306	9047375	17,2	6,0	11,2	water-well	758p

408537	9047950	62,0	6,0	56,0	water-well	677p
409964	9047561	75,0	6,0	69,0	water-well	687p
409795	9047888	79,0	6,0	73,0	water-well	690p
409647	9050748	100,0	6,0	94,0	water-well	702p
404070	9052353	31,7	6,0	25,7	water-well	P187
404888	9049774	31,6	6,0	25,6	water-well	P2104-11
405417	9050295	38,4	6,0	32,4	water-well	P2104-13
405586	9050262	39,3	6,0	33,3	water-well	P2104-20
406002	9049870	41,3	6,0	35,3	water-well	P2104-21
404047	9049846	23,7	6,0	17,7	water-well	P2104-29
404880	9050415	33,4	6,0	27,4	water-well	P2104-9
398493	9049182	4,6	6,0	-1,4	water-well	P2103-23
399814	9048267	6,4	6,0	0,4	water-well	P2103-28
402296	9048868	12,9	6,0	6,9	water-well	P2103-31
402188	9050971	16,9	6,0	10,9	water-well	P2103-55
403403	9054828	21,0	7,0	14,0	water-well	P48
406194	9054169	53,0	7,0	46,0	water-well	P70
400063	9056446	9,5	7,0	2,5	water-well	P10
400265	9056075	10,0	7,0	3,0	water-well	P17
400259	9055458	8,0	7,0	1,0	water-well	P27
400437	9055587	8,6	7,0	1,6	water-well	P28
404994	9052680	42,0	7,0	35,0	water-well	P153
403247	9050311	19,6	7,0	12,6	water-well	P329
399879	9045088	8,5	7,0	1,5	water-well	P676
401059	9044552	13,5	7,0	6,5	water-well	P694
401534	9044761	14,5	7,0	7,5	water-well	P679
405903	9050764	34,0	7,0	27,0	water-well	P299
406185	9050029	37,0	7,0	30,0	water-well	P371
405170	9049495	26,2	7,0	19,2	water-well	P405
404025	9046241	24,0	7,0	17,0	water-well	P613
409473	9049234	79,0	7,0	72,0	water-well	S-6
405113	9050583	35,9	7,0	28,9	water-well	P2104-16
405650	9051064	42,0	7,0	35,0	water-well	P2104-4
403148	9049827	20,3	7,0	13,3	water-well	P2104-64
401479	9051796	12,5	7,0	5,5	water-well	P2103-10
400826	9051458	11,3	8,0	3,3	water-well	P216
404553	9054803	32,8	8,0	24,8	water-well	P50
406365	9054510	65,0	8,0	57,0	water-well	P71
403390	9051906	22,3	8,0	14,3	water-well	P222
400348	9045301	9,4	8,0	1,4	water-well	P657
401996	9044261	14,4	8,0	6,4	water-well	P696

406704	9050029	50,0	8,0	42,0	water-well	P372
404633	9048364	25,0	8,0	17,0	water-well	P476
404063	9050607	29,4	8,0	21,4	water-well	P2104-27
405542	9048257	27,6	8,0	19,6	water-well	P2104-61
402845	9050289	19,9	8,0	11,9	water-well	P2104-63
403930	9052293	25,7	8,0	17,7	water-well	P2104-80
404041	9049022	19,4	8,0	11,4	water-well	P2103-37
401008	9054418	12,9	9,0	3,9	water-well	P60
402557	9048054	18,0	9,0	9,0	water-well	P2104-70
407309	9050681	54,4	9,0	45,4	water-well	P2104-75
398646	9050375	3,5	10,0	-6,5	water-well	P320
401070	9050403	15,0	10,0	5,0	water-well	P328
406371	9053884	62,0	10,0	52,0	water-well	P90
398080	9056669	6,4	10,0	-3,6	water-well	P1
402888	9051779	23,0	10,0	13,0	water-well	P221
404808	9049100	26,9	10,0	16,9	water-well	P2104-25
400182	9053403	9,7	12,0	-2,3	water-well	P112
402145	9054035	19,5	12,0	7,5	water-well	P81
401734	9055067	13,0	12,0	1,0	water-well	P44
401573	9050314	13,7	2,0	11,7	drlling	Rampe
398741	9050975	3,6	3,0	0,6	drlling	Gatep
402486	9054420	21,0	3,0	18,0	drlling	Belencong
398304	9049850	2,8	3,0	-0,2	drlling	Tanjungkarang
399970	9047224	6,4	3,0	3,4	drlling	Mahkota
400484	9047732	6,0	4,0	2,0	drlling	Jempongbarat
401569	9052898	11,5	5,0	6,5	drlling	Rembiga
400876	9048011	6,0	5,0	1,0	drlling	Kodya asri
402861	9053391	22,0	5,0	17,0	drlling	Monjokdaye
402148	9047835	13,4	5,0	8,4	drlling	Pagutanpersak
402011	9050417	15,0	6,0	9,0	drlling	Karangbedil
402618	9049900	17,0	6,0	11,0	drlling	Bandaseraya
400940	9055817	12,0	6,0	6,0	drlling	Pakel
399438	9056641	7,0	6,0	1,0	drlling	Tatto
401554	9049065	9,6	6,0	3,6	drlling	Bebidas
402448	9046459	15,9	6,0	9,9	drlling	Lingkarasri
402297	9051420	20,0	7,0	13,0	drlling	Camara
400276	9048981	7,1	7,0	0,0	drlling	Pandemas
399266	9044119	6,3	7,0	-0,7	drlling	Bongor
400186	9048807	6,0	7,0	-1,0	drlling	BTNmerdeka
399610	9055319	5,5	7,0	-1,5	drlling	Remaniskeng
399600	9048498	6,1	7,0	-0,9	drlling	BTNalamanda

399688	9048827	6,0	8,0	-2,0	drlling	Baturinggit
400449	9046348	9,2	8,0	1,2	drlling	Pededodol
402736	9045500	16,9	8,0	8,9	drlling	Pengsong
399206	9056119	7,2	8,0	-0,8	drlling	BTNsandik
401039	9048727	8,3	8,0	0,3	drlling	Pabri
399524	9056050	9,2	9,0	0,2	drlling	Sandikindah
401804	9047973	14,6	9,0	5,6	drlling	UD rizley
399111	9049085	4,1	10,0	-5,9	drlling	Batudawe
401116	9048981	8,5	10,0	-1,5	drlling	Pertaminap
399327	9053191	5,7	10,0	-4,3	drlling	Tinggar
399295	9056558	10,2	11,0	-0,8	drlling	Tatodandila
400592	9049638	9,6	11,0	-1,4	drlling	Kekalik
401030	9049556	10,4	12,0	-1,6	drlling	Mumbul
403231	9051127	24,2	14,0	10,2	drlling	Karangkemong
403951	9050769	26,4	4,0	22,4	drilling	P295
403699	9050923	22,0	5,0	17,0	drilling	P294
404410	9050350	22,0	5,0	17,0	drilling	P332
404504	9046077	23,0	5,0	18,0	drilling	P641
400594	9054858	8,0	6,0	2,0	drilling	P42
403621	9050164	19,0	6,0	13,0	drilling	P366
400044	9054180	8,1	7,0	1,1	drilling	P58

APPENDIX C

Table C.1. Narrations related to the 1257 CE Eruption of Samalas volcano in *Babad Lombok*

Verse	Old Javanese text	Indonesian transliteration	English translation
Pre-Eruption			
222	*Kewala wus medaling nagari, desa Lae' punika dan tinggal, sami tumedun wong ngakeh, hapindah saking riku, malih pada ngawe nagari, sireng bumi Pamatan, hakumpul hing riku, hanggawe kuta balumbag, wus sumapta, lalrenpo pada nginggil, wus kukuh kang nagara.*	*Asalkan sudah keluar, desa Lae itu ditinggalkan, semua turun si orang banyak, berpindah dari situ, lagi membuat desa di bumi Pamatan, berkumpul di situ, membuat benteng kota, sudah siap semua, pagar dan tembok tinggi, sudah kukuh kotanya*	They left the village, the village of Lae was abandoned, everyone came down, moved from there (Lae), they made a new village in Pamatan, they all gathered, they made fortresses, everything was completed: fences, high walls, the city was established.
223	*Wus ya karya humah haling dadi, lan papalen, raranggon pasebon, wus lajur lurunge, harame desa hagung, kebun hasruh ngidu nigari, tetanduran samapta, pisang gedang tebu saruh jambe lan jalima, gedang ngental, kalapa haran kasambi, tinggulun ladri dara.*	*Sudah membuatrumah dan lumbung, dan dapur, baiai peranginandan balai pertemuan, jaian-jalan terbentang, ramai di desa besar itu, taman indah mengelilingi kota, taman lengkap, pisang pepaya tebu, sirih pinang dan delima, pepaya,rontal, kelapa heran kusambi, tingguli seladri dara cina*	Houses had been built, barns, kitchens, halls and town halls, the roads extended out, the ambiance of the village was lively, beautiful gardens surrounded the city, crops were complete: bananas, papayas, sugar cane, betel, areca and pomegranate, palm, coconut, celery, jujube.
226	*Kawarneha hing wong jero nigari, hing Pamatan, sami mukti suka, datan nana kurangane, wong dagang sami rawuh, lan wong bajo hakeh, kang prapti, salwit watangan hana ta halimbah*	*Alkisah orang didalam negeri itu, di desa Pamatan, semua sejahtera makmur, tak ada kekurangannya, para pedagang datang, danorang Bajo(Sulawesi) banyak yang datang, semua barang ada, diperjualbelikan, penduduk*	It is told that the inhabitants of Pamatan were prosperous and wealthy, there was no scarcity, many traders came, and people from Bajo (Sulawesi); all goods were available and exchanged. The inhabitants of Pamatan

Verse	Old Javanese text	Indonesian transliteration	English translation
	hipun, wong Pamatan sajro katah, meh salaksa, pada sare kumalipit, ing gunung hitampiran.	*Pamatan banyak, hampir sepuluh ribu, semua tertidur nyenyak, di bawah kaki gunung*	were numerous, almost ten thousand, and all the inhabitants slept soundly at the foot of the mountain.
Eruption process			
273	*Nalika hing mangsa hika, Sang Hyang Suksma murka hing makhluk neki, tengah dalu rawuh hipun, hudan nangin ributan, sakweh kayu watu gunung pada rubuh, gentuh batu halalabar, dar saking luhur wukir.*	*Tatkala zaman itu, Tuhan murka kepada makluk-Nya, tengah malam datangnya, hujan dan angin taufan, semua kayu dan batu gunung rubuh, longsoran batu membanjir, melanda dari puncak bukit.*	At that time, God was angry with His creatures. In the middle of the night, there was rain and storms, wood and stones fell, avalanches came from the summit.
274	*Gunung Rinjani kularat, Gunung Samalas rakrak, balabur watu gemuruh, tiben desa Pamatan, yata kayut bale haling parubuh, karambanging sagara, wong ngipun halong kalang mati.*	*Gunung Rinjani longsor, dan gunung Samalas runtuh, banjir batu gemuruh, jatuh di desa Pamatan, lalu hanyut rumah lumpur rubuh, terapung-apung di lautan, penduduknya banyak yang mati.*	Mount Rinjani had an avalanche, and Mount Samalas collapsed, followed by large flows of debris accompanied by rumbling boulders. These flows destroyed Pamatan. Houses were destroyed and swept away, floating onto the sea, and many people died.
275	*Pitung dina lami nira, gentuh hiku hangebeki pertiwi, hing leneng hadampar, hanerus maring batu dendeng kang hanyut, wong ngipun kabeh ing paliya, saweneh munggah hing ngukir.*	*Tujuh hari lamanya, gempa dahsyat meruyak bumi, terdampar di Leneng (Lenek), diseret oleh batu gunung yang hanyut, manusia berlari semua, sebahagian lagi naik ke bukit.*	For seven days long, the shocks struck the earth, stranded in Leneng (Lenek), dragged by debris and floating boulders, all the inhabitants ran, and some of them escaped to the hill.
Emergency Response			
276	*Hing Jeringo hasingidan, samiya ngungsi salon darak sangaji, hakumpul*	*Bersembunyi di Jeringo, semua mengungsi sisa*	The rest of the royal family fled and took shelter at Jeringo; they were gathered there.

Verse	Old Javanese text	Indonesian transliteration	English translation
	hana hing riku, weneh ngungsi Samuliya, Boroh Bandar Papundak lawan Pasalun, Sarowok Pili lan Rangginya, Sambalun Pajang lan Sapit.	*kerabat raja, berkumpul mereka disitu, ada yang mengungsi ke Samulia, Borok, Bandar, Pepumba, dan Pasalun, Serowok, Piling, dan Ranggi, Sembalun, Pajang, dan Sapit*	Others escaped to Samulia, Borok, Bandar, Pepumba, and Pasalun, Serowok, Piling, dan Ranggi, Sembalun, Pajang, and Sapit.
277	*Yen Nange lan Palemoran, batu banda jejangkeh tanah neki, duri harane menyan batu, saher kalawan balas, watu rentang watu cangku, samalih tiba hing tengah, Brang bantun gennira ngungsi.*	*Yeh nangan dan Palemoran (Lemor) batu besar gelundungan tanah, duri dan batu menyan, batu apung dan pasir, batu sediment, granit dan forjir, jatuh ditengah daratan, mereka mengungsi ke Brangbatun*	In Nangan and Palemoran (Lemor), large stone blocks were piled up on the ground: [There follow some terms for different sorts of rock that are not yet fully understood]. The stones fell in the middle of the terrain. The inhabitant escaped to Brangbatun.
278	*Hana ring Pundung Buwang Bakang, Tanak Gadang, Lembak, Babidas hiki, sawenah hana halarut hing bumi Kembang Kekrang, Pangadangan lawan Puka hatin lungguh, saweneh malah kang tiba, mara hing Langko Pajanggih*	*Ada ke Pundung, Buak Bekang, Tana' Bea', Lembuak, Bebidas, sebagian ada mengungsi ke bumi Kembang Kekrang, Pengadangan dan Puka hate hate Lungguh. Sebagian ada yang sampai ke Langko, Pejanggik.*	There were those who went to Pundung, Buak Bekang, Tanak Beak, Lembuak, Bebidas. Several also escaped to the land of Kembang Kekrang, Pengadangan, Puka, Lungguh. Some of them made their way to Langko, Pejanggik.
279	*Warnanen munggeng palowan, sami larut lawan ratu hing nguni, hasangidan ya riku, hing Lombo goku medah, genep pitung dina punang gentuh, nulih hangumah desa hing preneha siji-siji.*	*Arkian yang naik perahu. semua mengungsi dengan ratunya, berlindung mereka disitu, di Lombok tempatnya diam, genap tujuh hari gempa itu, lalu membangun desa di tempatnya masing-masing*	It is said that some embarked on boats, they all escaped with their former leaders. They took shelter in Lombok, where they felt safe after seven days of shocks. They built villages in their respective places.
Post Eruption-Recovery and Resilience			

Verse	Old Javanese text	Indonesian transliteration	English translation
280	*Hing Lombok hakarya kuta, desa Hagung pernah hira sang ngaji, hana sireng Karang Mumbul, prenah harya sanga Nata, hadipati hing Karang bungbang gemipun, Pangulu hing tumbih lalang, Papatih hing kembang kuning*	*Di Lombok dibuat negeri, desa besar tempat sang raja, terdapat di dekat Karang Mumbul, tempat Arianya sang Raja, Adipati di Karang Bumbung, Penghulu di Tumbih Lalang, Patihnya di Kembang Kuning.*	A new city was built on Lombok led by the King. There were those at Karang Mumbul, the place of the king's lords. The chief minister led at Karang Bumbung, the headman at Tumbih Lalang, the governor at Kembang Kuning.
281	*Raksa sireng karang melak, punang bandar hawumah hing pasisir, Demang kalawan Sang Prabu karang Lombok gennira, wus hakarya bale lan keraton hagung, sula lulurung marapat, wus ketah punang nagari.*	*Raksa di dekat Karang Melak, Syahbandar berumah di pantai, Demang bersama Sri baginda di karang Lombok tempatnya, sudah membangun Keraton besar, jalan besar segi empat, sudah besar kotanya.*	The officer led at Karang Melak, the harbormaster settled on the coast, the chamberlain was assisting the King at Karang Lombok. A grand palace and pavilions were constructed, with a dense square streets. The city was already established.
282	*Desa Barangbantun kocapa, sampun kukuh kang kutane hanginggil, ki demung ngabehi hing riku, dadi Mangku negara, miwah haneng Samuliya lawan pasalut, putra Dipati Manggala dadi muter ring nagari.*	*Alkisah desa Brangbantun sudah kukuh kota berbenteng, ki Demang menjadi pemerintahnya, dan juga di Samulia dan Pasalun, Putra Adipati Manggala menjadi penguasa di wilayahnya.*	It is said that the village of Brangbantun was already constructed, complete with a lofty fortress. The chamberlain became the city administrator, while in Samulia and Pasalun, the son of the chief minister Manggala became the ruler.
283	*Miwah kang nging Kembang karang, Pangadangan kalawan Sukatahun, Punggawa hana hing riku, dadi Mangku negera, nanging Salonda lan Buak Kateng hiku, Dipati*	*Yang di Kembang Kerang, Pengadangan dan Sukatahun (Sukadona), Punggawa ada disitu, menjadi penguasa wilayahnya, tetapi Salondak dan Buak Kateng, Adipati yang*	In Kembang Karang, Pengadangan, and Sukadona, the local lord became the administrator, while in Salondak and Buak Ketang, it was the chief minister who became the

Verse	Old Javanese text	Indonesian transliteration	English translation
	hiking ngangreka, dadi mangku hing nagari.	*mengatur, menjadi penguasa wilayah.*	adminstrator of the city.
284	*Wenten kang atibeng bayan, hatmajane susunan Majapahit, hakarya negara luhung, nenggeh hing desa bayan, lan Pejanggik hing Lombok haji sang Prabu, hakrame putri Pamatan, dadi Prabu nyakra wati.*	*Ada yang sampai Bayan, Putra Sri Baginda Majapahit, membangun negara besar bertempat di desa Bayan, dan Pejanggik di Lombok ayahandanya, beristri putri Pamatan menjadi raja besar*	The child of the King of Majapahit arrived in Bayan, and constructed big city. Indeed, in the village of Bayan and at Pejanggik in Lombok, he reigned as king. He married a Princess of Pamatan and became a great ruler.
285	*Hamuter ring bumi Sasak, Sokong Bayan Kuripan lan Pajanggi, halurah hamung Sang Prabu, Lombok kang Amangkurat, saban tahun teka hanobe Sang Prabu, hakarya kuta semana, lan karahos Seribupati.*	*Menjadi raja di bumi Sasak, Sokong Bayan Kuripan dan Pejanggik, beraja hanya pada sang Prabu, Lombok yang mengatur, setiap tahun menghadap raja, membangun kota dan terkenallah Sang Prabu.*	He became the King of Sasak. Sokong, Bayan, Kuripan, and Pejanggik were the regions that served the King of Lombok. They have gathered annually to present themselves to the king. The city grew and the King became famous.
286	*Negareng Lombok kang lampah, palamumbahara ketah hasuka sugih, panganggo panganan wibuh, mas ringgit picis muang, sakadi kebo sampi jaran wadis, ayam bebek danga pakatah, buron hulam hakeh sami.*	*Negeri Lombok yang masyhur, negeri makmur sejahtera, sandang pangan cukup, emas picis ringgit murah, juga macam kerbau sapi, kuda kambing, ayam bebek angsa banyak, binatang hutan ikan banyak semua.*	The country of Lombok became glorious and prosperous, with plenty of clothes and food, gold, *ringgit*s, and Chinese copper coins, with all kinds of buffalo, cow, horse, goat, chicken, duck, goose, and much steamed rice, and many other game animals.

Table C.2. Narrations related to the 1257 CE Eruption of Samalas volcano in *Babad Suwung*

Sasak text	Indonesian translation	English translation
Hingsung hangalih, maka sewuse jangkep limang dine pon, ngalih serte lan rakyat lan sekoweh anak putu nire, Talkuwang ngadek dadi baginde, saking takdiring hyang Sukseme lantas turun hudan geni haneng langit, hiku lantas binakur dese Takuwang, sedanging negere telas melayu, hikulah asal dese nare hingriku.	*Setelah sampai lima hari mereka pindah bersama rakyat dan anak cucunya. Kamudian atas Takdir Yang Maha Kuasa, turunlah hujan dan api dari langit membakar desa Talkuwang bersama dengan isinya, yang masih selamat berlari tunggang langgang.*	After five days, they moved away with their people and grandchildren. By the decree of the Almighty, fire-rain fell from the sky, and that hot wind burned everything in Talkuwang. All of the inhabitants ran around in chaos.
Tinurunan hudan geni haneng langit, hanggesengkan negare hiku lah asal kang karuhun.	*Hujan dan api turun dari langit membakar sampai habis desa kita.*	Fire-rain came down from the sky, burning the village completely.
Malik waktu sino iye laeq sopoq desa Taliwang dai Selaparang, ndeq naraq laut lalangne, Taliwang Selaparang.	*Dan dahulu antara desa Taliwang dengan Selaparang tidak ada laut menjadi batas Taliwang dengan Selaparang*	Formerly, it seemed like there was no sea between Taliwang and Selaparang villages

Table C.3. Narrations related to the 1257 CE Eruption of Samalas volcano in *Babad Sembalun*

Old Javanese text	Indonesian translation	English translation
Pre-Eruption		
Kocap malih nek islamin punika, Lumbar hunuju bukit selong lereng gunung anak dara….. Kumbang derek bebaris sumanar satung sang tuduh	*Diceritakan lagi nek islamin dengan keluarganya, Berjalan dari lendang goar menuju bukit Selong, lereng bukit Anak Dara namanya….. Bunga-bunga sangat indah ditepi telaga*	It is told that Mother Islamin with her family walked from Lendang Goar to Selong Hill, on the slopes of Anak Dara….. The flowers flourish by the edge of the lake.
Ri bawan kang aran bukit selong hana pancoran ring rika, Nek islamin mapondokan lembah punike, Nek islamin ngandika maring sesemak nike, Duh sanak sami bija sami, Ring ki gone mepradikan, Ring lembah selong kang aran desa belek	*Ada pancoran dibawah bukit selong itu, Nek islamin bertempat tinggal di lembah……. Disini kita mendirikan pondok, Dilembah selong ini namanya Desa Belek*	There was a spring below the Selong hill, where Mother Islamin resided in the valley. Mother Islamin said to all her children: "Oh my children and offspring, here is the place we will build houses, in this valley of Selong, in a village called Belek (Beleq)"
Eruption process		
Banjir bandang hangelanda bumi sambahulun, Telaga bedah gunung rusak, Siang dalu horana beda Bumi pesung saking asap, Api nyala ketia timah, Hancur lebur lereng rinjani, Gumi inggur siang dalu, Nika kina balak punika	*Banjir bandang melanda sembahulun, Telaga jebol dibarengi dengan bukit-bukit yang longsor, Siang malam tidak ada bedanya, Bumi diselimuti kabut tebal, Api membara, seperti timah meleleh yang di panaskan, Lereng rinjani dibuat hancur, Bumi bergoyang siang malam Penduduk berlarian menyelamatkan diri*	Flash floods struck the land of Sembalun, the lake collapsed, accompanied by landslides from the hills. There was no difference between day and night, covered by thick fog, fire burned like molten tin, the slope of Rinjani had an avalanche, the earth shook day and night, the inhabitants ran away
Tatkala Nek islamin ring desa blek, Peteng limut siang dalu ujan kalawan angin, Gerah gemuruh suara gunung punike, Kelawan kilat kelawan	*Tatkala nek islamin di desa belek, Gelap gulita di selimuti awan hitam dan hujan bercampur angin, Suara Ledakan gunung yang amat dahsyat,*	At that time Mother Islamin stayed in Desa Beleq. The darkness covered day and night, due to dark clouds and rainstorms, thundering

Old Javanese text	Indonesian translation	English translation
petir kadia, Kidang kancil samia lari, Kabut petak hirang kelawan merah, Peteng limut nora beda siang kelawan dalu	*Kilauan kilat dan petir meyambar, Hewan seperti kijang dan kancil berlarian, Kabut tebal hitam bercampur merah, Suasana gelap siang malam tidak ada beda*	noise was heard from the mountain, lightning strikes, deer and chavrotains ran away. There was a thick black-reddish fog, darkness covered everything, there was no difference between day and night
Post-Eruption		
Kawarnaha nek islamin iringan kadang, Warga milayu hanuju dasan ngenang, Ring bawah bukit bantek selak, Sitibang mepondaran ring bawah bukit punika, Denia hanyerekan urip lan pati, Maring tuhan pencipta alam, Lami nira ring dusun ngenang, Anging nira nana tahune pasti	*Kemudian nek islamin dan keluarga pergi mengungsi, Warga berlari menuju dusun Ngenang, Di bawah bukit bantek selak, Disana dia lama tinggal sambil menunggu amannya letusan rinjani, Mereka pasrah antara hidup dan mati, Menyerahkan diri pada Tuhan Pencipta Alam, Mereka tinggal didusun ngenang bertahun-tahun, Berapa tahun mereka tinggal disana tidak pasti*	Then Mother Islamin and her family took refuge together with the residents towards Ngenang Village, at the bottom of Bantek Selak hill. They wandered around the bottom of this mountain, surrendering to God their life and death. They were settled in Ngenang village many years, but it is uncertain exactly how many.
Sawuse mangkana kocap rinjani mende Hannyugulang asap lan api Bumi terang benderang, Anging kayune malih punike kembali mantuk aning lendang goar punike, Ring gon nira katemu lawan wong agung punike, Kawarnaha lumbar malih iringan kadang wargine sami, Kumpul malinggih ring lendang goar, Kocap raden punike rauh ring harapan nek punike, Sedek nek islamin malinggih sambil nira hangilingang rinjani	*Sesudah letusan rinjani itu reda, keadaan lereng rinjani pun kembali normal, semua keluarga kembali ke lendang goar, mereka kumpul kembali disana, Ada pemuda datang di tengah-tengah orang yang sedang berkumpul, Nek islamin melihat mereka datang dari lereng rinjani*	After that, it is said that Rinjani returned to normal activity. All inhabitant returned to Lendang Goar, at the place where they have gathered with their leaders. It is said that everyone's companions and family members were gathered together at Lendang Goar. It is said that two princes arrived to present themselves to Mother Islamin, who saw them coming from slope of Rinjani
Kocap rauh malik wong agung punike Raden Aria	*Diceritakan pemuda itu menamakan dirinya raden*	It is said that the young men were named Raden

Old Javanese text	Indonesian translation	English translation
Pati lawan Raden Aria Mangun Jaya, Gih wong sembahulun nike sira bibit padi merah lan putih lan iring, Kang dadi papanganan sira sami, Lan malik punika sira. Gigaman kang dadi pembela diri keris lan tombak…… *Ping empat ingsun kanini sira sami daster lan kampuh, Lan malik niki segera talak mantuk mepondokan ring desa blek, Ingsun sembek sira lan terima neh tugas sari sami, Nek Islamin Kang dadi Kyai, Nek Kerta Jaya kang dadi Pabekel, Nek Ratani Kang dadi Pemangku Adat, Nek Bagia kang dadi Pande, Mangkin sira sigrah kembali mantuk aning desa blek punike, lawan malik moga mogi keterima malik*	*hariapati dan raden haria mangun jaya, Kedua raden tersebut berkata, "hey orang sembalun kami memberikan bibit padi merah untuk menyambung hidup,* *Selain itu kami berikan kalian keris dan tumbak sebagai senjata untuk membela diri…."* *Saya berikan kalian pakaian dan selimut, Dan saya harap lagi kembali kedesa Belek di sana tempat menetap, Dan anda saya berikan tugas, Nek islamin menjadi kyai (urusan agama),* *Nek kerta jaya menjadi prabekel (pemerintahan),* *Nek ratni menjadi pemangku adat,* *Nek bagia menjadi pande,* *Sekarang kembali ke desa Belek dan jalankan tugas anda sekalian dengan sebaik-baiknya*	Hariapati and Haria Mangunjaya. They said: "Hey, people of Sembalun, we will give you seeds of red and white rice that will become a source of food for everyone. We also give you *keris* and spears as defensive weapons….. Fourth, we will give you all headscarves and waistcloths. Now return quickly to the settlement at the village of Beleq. We will give you all different tasks: Mother Islamin will become kyai (Islamic cleric), Kerta Jaya become *prabekel* (local administrator), Ratni become the customary priest, Bagia become the blacksmith. Now please return to Beleq village and execute the tasks as well as possible